

Resurrection of *Pleurospermum lecomteanum* H.Wolff (Apiaceae) based on molecular and morphological evidence

Jing Zhou¹, Junmei Niu¹, Xinyue Wang¹, Shilin Zhou¹, Zhenwen Liu^{2,3,4}

1 School of Pharmaceutical Science and Yunnan Key Laboratory of Pharmacology for Natural Products, Kunming Medical University, Kunming 650500, China **2** Yunnan Academy of Forestry and Grassland, Kunming 650201, China **3** Gaoligong Mountain, Forest Ecosystem, Observation and Research Station of Yunnan Province, Yunnan, China **4** Yunnan Key Laboratory of Biodiversity and Ecological Security of Gaoligong Mountain, Yunnan, China

Corresponding author: Zhenwen Liu (liuzw2021@163.com)

Academic editor: A. Sukhorukov | Received 31 August 2022 | Accepted 6 October 2022 | Published 24 October 2022

Citation: Zhou J, Niu J, Wang X, Zhou S, Liu Z (2022) Resurrection of *Pleurospermum lecomteanum* H. Wolff (Apiaceae) based on molecular and morphological evidence. *PhytoKeys* 212: 1–11. <https://doi.org/10.3897/phytokeys.212.94280>

Abstract

The taxonomic placement of *Pleurospermum lecomteanum*, previously synonymized with *Pleurospermum wilsonii*, was carefully examined using herbarium specimens and molecular evidence. The results showed that *Pleurospermum lecomteanum* is distinguished from *P. wilsonii* by several morphological characters. Its phylogenetic position is separate from *P. wilsonii* in the ML tree. Therefore, *Pleurospermum lecomteanum* should be restored as a distinct species.

Keywords

Apiaceae, *Pleurospermum*, resurrection, synonym, taxonomy

Introduction

Of the four major worldwide distribution centers of Apiaceae, China has the highest taxonomic diversity at the species level (614–657 species), and represents approximately 1/5 of all species recognized within the family (Sheh and Shu 1987; Sheh et al. 2005; Pimenov 2017). However, numerous species in Chinese Apiaceae remain rather

enigmatic and have not been investigated adequately, even morphologically, because of their remote distribution and inadequate number of collections (Zhou et al. 2008; Pimenov 2017). Therefore, in the past few years, large efforts have been devoted to field investigations and examination of herbarium specimens towards a comprehensive understanding of the species of Chinese Apiaceae.

Until recently, *Pleurospermum* Hoffm. was treated as comprising about 50 species widely distributed in northern Asia and East Europe, of which 39 were in China (Pan and Watson 2005). Taxonomic changes by Pimenov and Kljuykov (2000a, b), Pimenov (2017), Pimenov et al. (2000) and Zhou et al. (2020a, 2021), have reduced that number considerably. However, relationships among some synonymous species are still ambiguous.

This statement also belongs to the widely accepted *Pleurospermum wilsonii* H.de Boissieu. It was described by H.de Boissieu based on the collections from western China in 1906. In the past years, several taxa have been included within it, namely *Physospermopsis lalabhduriana* Farille & S.B.Malla, *Pleurospermum cnidiifolium* H.Wolff, *P. crassicaule* H.Wolff, *P. lecomteanum* H.Wolff, *P. tanacetifolium* H.Wolff and *P. thalictrifolium* H.Wolff (Shan and Sheh 1979; Pan and Watson 2005; Pimenov 2017). *Pleurospermum tanacetifolium* and *P. thalictrifolium* were later merged with *Pleurospermum davidii* Franch. and *Pleurospermum astrantioideum* (H.de Boissieu) K.T.Fu et Y.C.Ho, respectively (Pimenov 2017). Pimenov and Kljuykov (2000a) have since transferred *Pleurospermum wilsonii*, *P. davidii* and *P. astrantioideum* to *Hymenidium*, but these taxonomic novelties need further confirmation based on the extensive molecular analysis (Zhou et al. unpublished data).

During our fieldwork in western China, we discovered several populations with morphological characters that are different from *Pleurospermum wilsonii* (10–25 cm tall, stem sometimes shortened vs. 15–60 cm tall, stem elongated; 2–3-pinnatisect, ultimate segments narrowly ovate or lanceolate, entire or 2–3-lobed vs. 1-pinnate, or subbipinnatisect with ultimate segments ovate or suborbicular, base cuneate, margins irregularly serrate to deeply lobed; rays 8–15, unequal or equal vs. 10–25, subequal). After consulting the relevant protologues (Boissieu 1906; Wolff 1925, 1926, 1929; Farille et al. 1985) and type specimens for each of the names, we consider that the population from Chayu County, Tibet, is identical with *P. wilsonii*, while the populations from Sichuan and Qinghai provinces correspond to *P. lecomteanum*, based on the morphology. A further analysis of comparative DNA sequences is presented here to clarify the taxonomic relationships between *P. lecomteanum* and *P. wilsonii*, and to identify their potential close relatives within the molecular framework of Apiaceae subfamily Apioideae.

Materials and methods

Morphological analysis

Digital resources of CVH, GBIF and JSTOR Global Plants for the type specimens of *Pleurospermum wilsonii* (K000685336, P00834554) and its synonyms (*Physospermopsis lalabhduriana*, E00000214; *Pleurospermum cnidiifolium*, PE00033257; *Pleurospermum*

crassicaule, P00834555; *Pleurospermum lecomteanum*, P00834556, P00834557) were carefully examined (Figs 1, 2). The morphological characters of *P. lecomteanum* were examined based on the types and specimens we collected in the field. The fruit was studied using a stereo microscope. Morphological comparisons between *P. wilsonii* and *P. lecomteanum* are provided in Table 1.

Phylogenetic analysis

The new nrDNA ITS sequences for five accessions of *P. wilsonii* and four accessions of *P. lecomteanum* (Table 2) were generated with the protocols described by Zhou et al. (2008). The new sequences were then aligned with the matrix of Zhou et al. (2020b) using the BioEdit sequence alignment editor (Hall 1999). All sequences were used to infer phylogenetic relationships. A maximum likelihood (ML) analysis was conducted with RAxML v.8.2.4 (Stamatakis 2006), using the GTR +G substitution model with 1000 bootstrap replicates, with other parameters following the default settings.

Results and discussion

The phylogenetic results revealed that all accessions of *Pleurospermum wilsonii* allied together, and constituted a sister group relationship with the clade of *Hymenidium huzhibaoi* Pimenov & Kljuykov and *P. lecomteanum* (Fig. 3, the complete tree containing all sampled representatives is available upon request). The whole clade fell within the tribe Pleurospermeae, and showed close relationship with the clade of *Hymenidium lindleyanum* (Klotzsch) Pimenov & Kljuykov, *Hymenidium stellatum* (D. Don) Pimenov & Kljuykov and *Trachydium roylei* Lindley. The pairwise sequence divergence value between *P. wilsonii* and *P. lecomteanum* was 3.44%.

Recently, the circumscription of *Pleurospermum* was reduced to comprise only two species (the type species *P. austriacum* L., and *P. uralense* Hoffm.), while the other species were referred to *Aulacospermum*, *Hymenidium*, *Hymenolaena*, *Physospermopsis*, and *Pterocyclus* (Pimenov and Kljuykov 2000a, 2000b). However, only two of these

Table 1. Morphological comparison between *Pleurospermum wilsonii* and *P. lecomteanum*.

Character	<i>P. lecomteanum</i>	<i>P. wilsonii</i>
Stem	10–25 cm tall, sometimes shortened	15–60 cm tall, elongated
Leaf	Oblong in outline, 2–3-pinnatisect	Oblong-lanceolate in outline, 1-pinnate or subbipinnatisect
Pinnae	4–8 pairs, shortly petiolulate or sessile	5–9 pairs, sessile
Ultimate segment	Narrowly ovate or lanceolate, 3–5 × 1–1.5 mm, entire or 2–3-lobed	Ovate or suborbicular, 7–14 × 4–10 mm, base cuneate, margins irregularly serrate to deeply lobed
Ray	8–15, unequal or equal	10–25, subequal
Calyx	Triangular	Triangular-ovate
Vitta	1 in each furrow, 2 on commissure	1–2 in each furrow, 2 on commissure

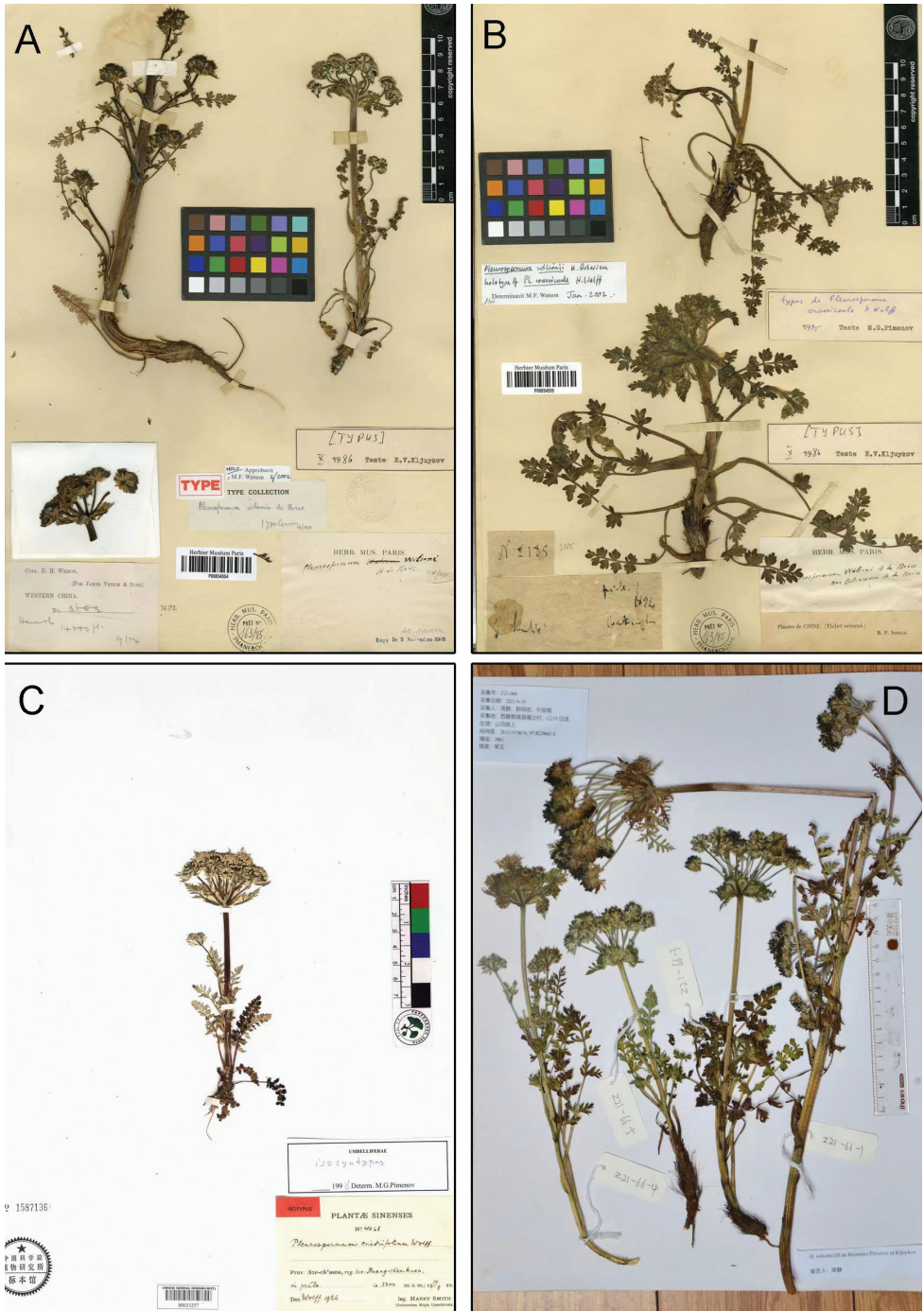


Figure 1. **A** lectotype of *Pleurosperrum wilsonii* from P (P00834554) **B** holotype of *Pleurosperrum crassicaule* from P (P00834555) **C** syntype of *Pleurosperrum cnidiifolium* from PE (PE00033257) **D** the voucher specimen of *Pleurosperrum wilsonii* from Z21-066.

Table 2. Voucher information and GenBank accession numbers for the five accessions of *Pleurospermum wilsonii* and four accessions of *P. lecomteanum* used in the phylogenetic analysis.

Taxa	Source/Voucher	GenBank number
<i>Pleurospermum wilsonii</i> H.de Boissieu	China, Xizang, Chayu, Z21-66-3 (KUN)	ON715443
	China, Xizang, Chayu, Z21-66-5 (KUN)	ON715444
	China, Xizang, Chayu, Z21-66-4 (KUN)	ON715445
	China, Xizang, Chayu, Z21-66-1 (KUN)	ON715446
	China, Xizang, Chayu, Z21-66-2 (KUN)	ON715447
<i>P. lecomteanum</i> H. Wolff	China, Qinghai, Jiuzhi, WG034 (KUN)	ON715451
	China, Qinghai, Jiuzhi, WG036 (KUN)	ON715450
	China, Qinghai, Jiuzhi, WG037 (KUN)	ON715449
	China, Qinghai, Jiuzhi, WG039 (KUN)	ON715448

genera, *Aulacospermum* and *Hymenolaena*, were supported as monophyletic groups in the molecular phylogenetic study by Valiejo-Roman et al. (2012). *Hymenidium* seems to be non-monophyletic, with its members assigned to the *Acronema* clade, the East-Asia clade, the *Sinodielsia* clade, the *Pleurospermopsis* clade and the Pleurospermeae (Zhou et al. 2009, 2020b; Wei 2020). Furthermore, the species of *Hymenidium* did not ally as monophyletic within three of the above clades. Pimenov & Kljuykov (2000a) indicated that *Hymenidium* in current circumscription is a genus with ambiguous taxonomy, and probably comprised several more distinct species groups. Recently, we conducted molecular phylogenetic studies for *Pleurospermum* and related genera, in which we sorted members of *Pleurospermum* into major clades of Apioideae, assessed relationships of these members to other apioid taxa within each of these major clades (Wei 2020), transferred *Pleurospermum bicolor* (Franch.) C.Norman ex Z.H.Pan & M.F.Watson into the genus *Pleurospermopsis* as *Pleurospermopsis bicolor* (Franch.) J.Zhou & J.Wei (Zhou et al. 2020a), confirmed the status of *Pterocyclus* as a separate genus with four species (*Pterocyclus angelicoides* (Wallich ex DC.) Klotzsch, *P. rotundatus* (DC.) Pimenov & Kljuykov, *P. forrestii* (Diels) Pimenov & Kljuykov, and a restored species, *P. wolffianus* Fedde ex H. Wolff; Zhou et al. 2021). All of these studies have enhanced our understanding of *Pleurospermum* and related genera, and brought us one step closer towards a more natural classification system.

Pleurospermum lecomteanum was described by H. Wolff based on collections from China in 1929. In Flora Reipublicae Popularis Sinicae, along with *P. cnidiifolium*, *P. tanacetifolium* and *P. thalictrifolium*, it was synonymized with *P. crassicaule* (Shan and Sheh 1979). All of the above species, plus *Physospermopsis lalabhduriana*, were included within *P. wilsonii* in the Flora of China (Pan and Watson 2005). After consulting the types of *P. tanacetifolium* (GB0048823) and *P. thalictrifolium* (GB0048825), we consider that it is reasonable to merge them with *P. davidii* and *P. astraintioideum*, respectively as proposed by Pimenov (2017). *Physospermopsis lalabhduriana* was described based on specimens from Nepal in 1985 (Farille et al. 1985). The morphology of the leaf and bracteoles of the isotype (E00000214) is different from that of *P. wilsonii*. It should be regarded as a distinct species that is not distributed in China (Pimenov 2017). Among the names treated as synonyms of *P. wilsonii*, *Pleurospermum crassicaule*

and *P. cnidiifolium* were each described by H. Wolff in 1925 and 1926, respectively. We have examined their type materials (holotype P00834555 for *P. crassicaule* and syntype PE00033257 for *P. cnidiifolium*), and consider that they cannot be separated from *P. wilsonii* and should be merged into a single species. However, we found a set of morphological characteristics, including the stem length, shape and division of leaves and pinnae, as well as the number and length of rays (Table 1), distinguished *P. lecomteanum* from *P. wilsonii*. In our field investigation in Qinghai and Sichuan provinces, we collected several specimens of *P. lecomteanum*, whose morphology is exactly the same as the type (P00834556 and P00834557), that led us to observe its morphology more carefully and reassess the status of this taxon. In our molecular analysis, the accessions of *P. lecomteanum* allied as monophyletic, and comprised a sister group relationship with *Hymenidium huzhibaoi*.

Hymenidium huzhibaoi was a species recently described by Pimenov and Kljuykov (Pimenov and Kljuykov 2004). It was distinguished from *P. lecomteanum* by being subcaulescent, umbellules compact, and apex of bracteoles 3–10-lobed, or rarely entire, and by its 1.23% nucleotide divergence. Therefore, both morphological and molecular evidence support recognition of *P. lecomteanum* as a distinct species. Since *Hymenidium* is a polyphyletic genus need to be further revision, and its type species (*H. brunonis* (DC.) Lindl.) does not fall into the Pleurospermeae to which *P. lecomteanum* belongs, so we here merely restore it as a distinct species without further taxonomic treatment.

Taxonomy

***Pleurospermum lecomteanum* H. Wolff, 1929, Repert. Spec. Nov. Regni Veg. 27: 116.**

Type. CHINA. Su-tchuen [Sichuan]: Bassin de Tongho (M. Thibet), Dzenla, roches metamorph., 3500 m, prairies alpines, 24 September 1911, *A.F. Legendre 1537* (lectotype P! barcode P00834556, designated by Pimenov, Kljuykov, 2000a: 550); Su-tchuen [Sichuan]: Bassin de Tong-ho (M. Thibet) Tse minuda, terrain schistos., 4500 m, 04 October 1911, *A.F. Legendre 1603* (syntype P! barcode P00834557); Sze-ch'uan [Sichuan]: reg. bor.-occid., Dalgang cia. 50 km VSV von Merge, 3500 m, 03 September 1922, *H. Smith 4313* (lectotype GB! barcode GB0048821; isolectotype UPS!).

Other specimens examined. CHINA. Qinghai: Jiuzhi, 4100 m, 20 August 2019, *J. Zhou, J. Wei & Y.Z. Gao G034, G036, G037, G039* (KUN); Sichuan: Hongyuan, 3600 m, 25 August 2005, *J. Zhou & L.Q. Fang ZJ0624* (KUN).

Description. Herbs perennial, 10–25 cm tall. Taproot long conic, simple. Stem erect, ribbed, sometimes shortened, bases with remnant sheaths. Basal and lower leaves petiolate; petioles 3–6 cm, petiole base sheathing, oblong, ca. 1.5–2 cm long; blade oblong in outline, 2–3-pinnatisect; pinnae 4–8 pairs, short petiolulate or subsessile; ultimate segment narrowly ovate or lanceolate, 3–5 × 1–1.5 mm, entire or 2–3-lobed. Upper leaves smaller and reduced, sheath prominent. Umbels compound,

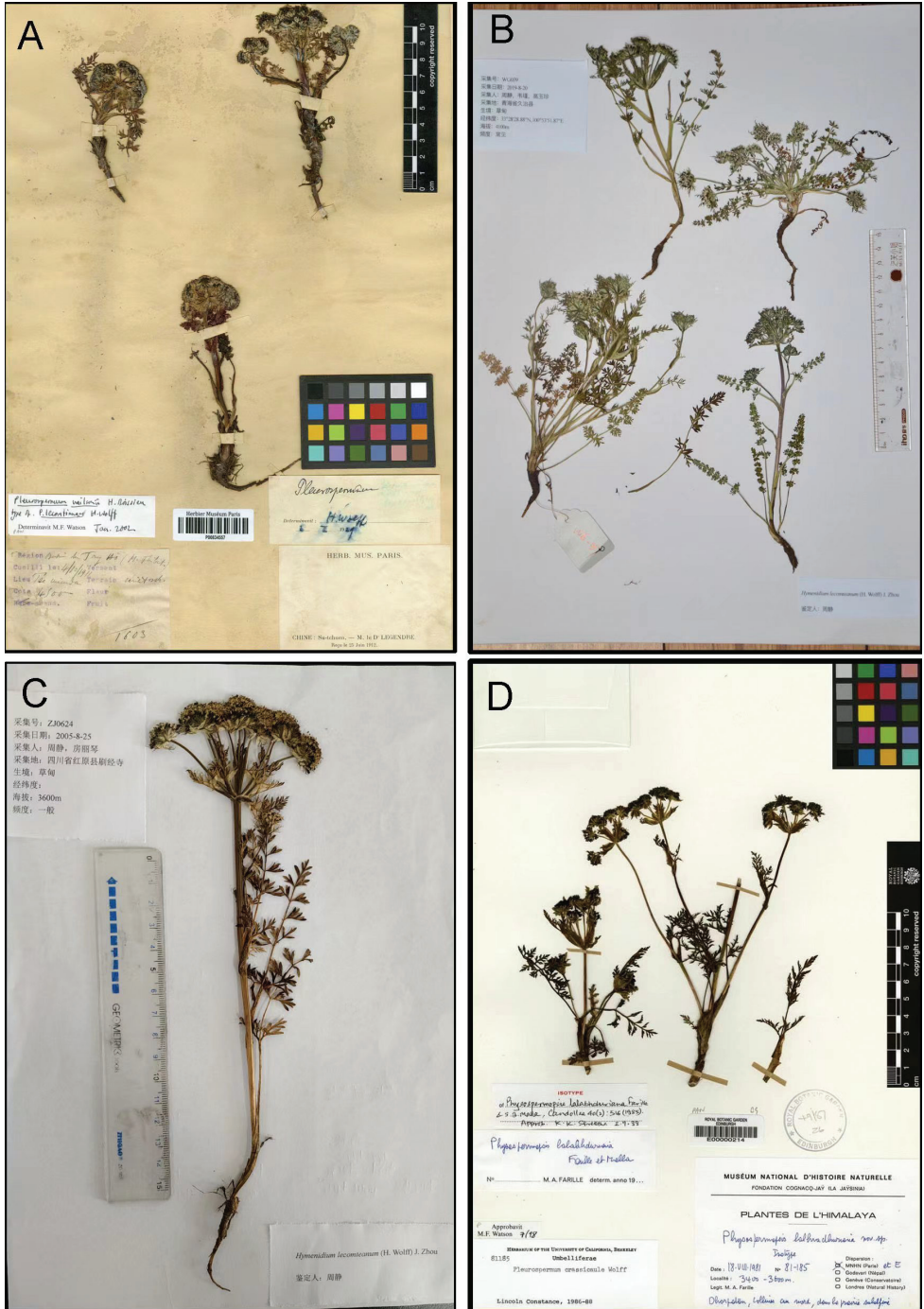


Figure 2. **A** syntype of *Pleurospermum lecomteanum* from P (P00834557) **B** the voucher specimen of *P. lecomteanum* from WG039 **C** the voucher specimen of *P. lecomteanum* from ZJ0624 **D** isotype of *Physospermopsis laballduriana* from E (E00000214).

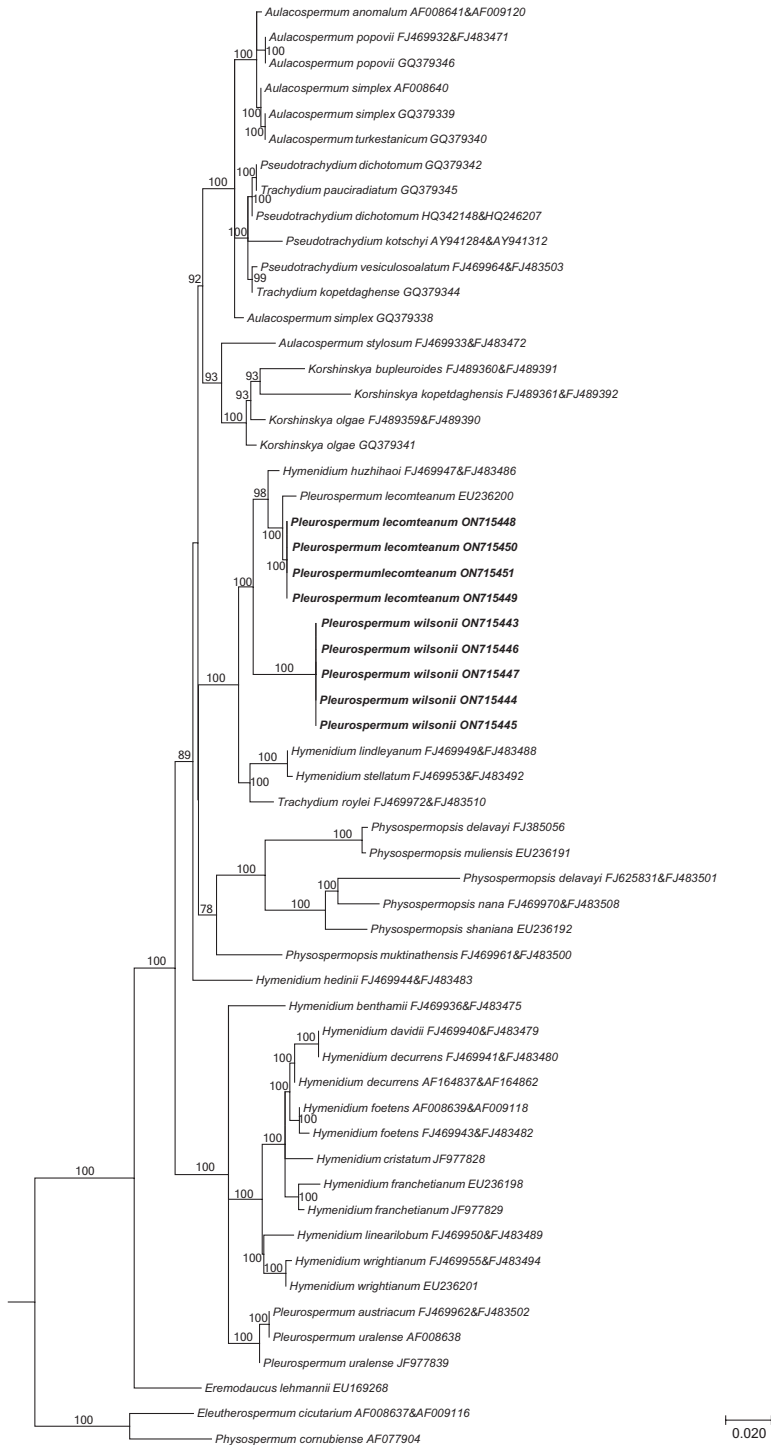


Figure 3. The consensus tree obtained from maximum likelihood analysis of 2920 nrDNA ITS sequences from Apiaceae subfamily Apioideae showing the tribe Pleurospermeae, with support values ($\geq 50\%$) provided next to the branches. The nine newly sampled accessions are shown in bold.

terminal or lateral; bracts 4–6, leaf-like, 2–6 cm long; rays 8–15, 1–7 cm long, unequal or equal; bracteoles 6–8, broadly ovate, similar to bracts, margin broadly white membranous, apex pinnate, longer than the flowers. Calyx teeth triangular, 0.5 mm long. Petals white, or purple, oblong-obovate, apex acute, short incurved. Stylopodium flat; styles longer than stylopodium. Fruit oblong, slightly compressed laterally; ribs prominent, broadly winged; vittae 1 in each furrow, 2 on commissure. Fl. Aug–Sep, fr. Sep–Oct.

Note. In flora of China, *Pleurospermum wilsonii* was described as 2–3-ternate-pinnate (Pan and Watson 2005). However, the type specimens and the protologues for it and its synonymous species, *P. crassicaule*, show that their leaf blades are “simpliciter pinnata” or “1- vel subbipinnatisecta” (Boissieu 1906; Wolff 1925). For *Pleurospermum cnidiifolium*, H. Wolff described its blades as “bi- vel subtripinnatipartita”, but the type has 1-pinnate (PE00033257), or 2-pinnatisect (GB0048821). After careful examination of GB0048821, we considered that its morphology was more similar to *P. lecomteanum*. That is, for *P. cnidiifolium*, the type PE00033257 should be selected, while GB0048821 should be put under *P. lecomteanum*. Our population in Chayu County of Tibet with variable leaf morphology (1-pinnate or subbipinnatisect) yielded identical ITS sequences. Therefore, with the resurrection of *P. lecomteanum*, the description for *P. wilsonii* should be revised as: blades 1-pinnate or subbipinnatisect, ultimate segments ovate or suborbicular, 7–14×4–10 mm, base cuneate, margins irregularly serrate to deeply lobed, rays 10–25, subequal. Furthermore, *Pleurospermum lecomteanum* occurs in the open grasslands in Yunnan, Sichuan, Gansu and Qinghai provinces of China, while *P. wilsonii* is on the south slope of mountains in Sichuan, Qinghai and Xizang provinces of China.

Key to *Pleurospermum wilsonii* and *P. lecomteanum*

- 1 Leaf blades 1-pinnate or subbipinnatisect, ultimate segments ovate or suborbicular, 7–14×4–10 mm, base cuneate, margins irregularly serrate to deeply lobed *P. wilsonii*
- Leaf blades 2–3-pinnatisect, ultimate segments narrowly ovate or lanceolate, 3–5× 1–1.5 mm, entire or 2–3-lobed.....*P. lecomteanum*

Acknowledgements

We are grateful to reviewers for helpful comments on the manuscript and thank David E. Boufford from Harvard University Herbaria for language polishing. This work was supported by the National Natural Science Foundation of China (no. 31960048 and 31872649), the Ten Thousand Talents Program of Yunnan (YNWRQNBj-2019-208), the department of Science and Technology of Yunnan Province (202201AT070118), the Hundred Talents Program of Kunming Medical University (no. 60118260127) and Gaoligong Mountain, Forest Ecosystem, Observation and Research Station of Yunnan Province (no. 202205AM070006).

References

- Boissieu H (1906) Note sur quelques Ombellifères de la Chine, d'après les collections du Muséum d'Histoire Naturelle de Paris. *Bulletin de la Société Botanique de France* 53(6): 418–437. <https://doi.org/10.1080/00378941.1906.10831189>
- Farille MA, Cauwet-Marc AM, Malla SB (1985) Apiaceae himalayenses III. *Candollea* 40(2): 509–562.
- Hall T (1999) BioEdit: biological sequence alignment editor for Win95/98/ NT/2K/ XP version 6.0.7. <http://www.mbio.ncsu.edu/BioEdit/bioedit.html>
- Pan ZH, Watson MF (2005) *Pleurospermum* Hoffm. In: Wu ZY, Peter HR, Hong DY (Eds) *Flora of China*, Vol. 14. Science Press & Missouri Botanical Garden Press, 23–35.
- Pimenov MG (2017) Updated checklist of Chinese Umbelliferae: Nomenclature, synonymy, typification, distribution. *Turczaninowia* 20(2): 106–239. <https://doi.org/10.14258/turczaninowia.20.2.9>
- Pimenov MG, Kljuykov EV (2000a) Taxonomic revision of *Pleurospermum* and related genera of the Umbelliferae. III. The genera *Physospermopsis* and *Hymenidium*. *Feddes Repertorium* 111(7–8): 535–552. <https://doi.org/10.1002/fedr.20001110719>
- Pimenov MG, Kljuykov EV (2000b) Taxonomic revision of *Pleurospermum* and related genera of the Umbelliferae. II. The genera *Pleurospermum*, *Pterocyclus*, *Trachydium*, *Keraymonia*, *Pseudotrachydium*, *Aulacospermum* and *Hymenolaena*. *Feddes Repertorium* 111(7–8): 517–534. <https://doi.org/10.1002/fedr.20001110718>
- Pimenov MG, Kljuykov EV (2004) *Hymenidium* (Umbelliferae) in China and India: The new species, a new combination and some corrections. *Botanicheskii Zhurnal* 89: 1652–1665.
- Pimenov MG, Kljuykov EV, Leonov MV (2000) Taxonomic revision of *Pleurospermum* and related genera of Umbelliferae. I. General part. *Feddes Repertorium* 111(7–8): 449–515. <https://doi.org/10.1002/fedr.20001110717>
- Shan RH, Sheh ML (1979) *Pleurospermum* Hoffm. In: Shan RH, Sheh ML (Eds) *Flora Reipublicae Popularis Sinicae*, vol. 55 (1). Science Press, Beijing, 133–184.
- Sheh ML, Shu P (1987) The floristic analysis of endemic genera in Chinese Umbelliferae. *Bulletin of Nanjing Botanical Garden Mem. Sun Yat-Sen*: 14–26.
- Sheh ML, Pu FD, Pan ZH, Watson MF, Cannon JFM, Holmes-Smith I, Kljuykov EV, Phillippe LR, Pimenov MG (2005) Apiaceae. In: Wu ZY, Raven PH, Hong DY (Eds) *Flora of China*, Vol. 14. Science Press & Missouri Botanical Garden Press, 1–205.
- Stamatakis A (2006) RAXML-VI-HPC: Maximum likelihood-based phylogenetic analyses with thousands of taxa and mixed models. *Bioinformatics* 22(21): 2688–2690. <https://doi.org/10.1093/bioinformatics/btl446>
- Valiejo-Roman CM, Terentieva EI, Pimenov MG, Kljuykov EV, Samigullin TH, Tilney PM (2012) Broad polyphyly in *Pleurospermum* s.l. (Umbelliferae-Apioideae) as inferred from nrDNA ITS and chloroplast sequences. *Systematic Botany* 37(2): 573–581. <https://doi.org/10.1600/036364412X635593>
- Wei J (2020) A phylogenetic study of *Pleurospermum* Hoffm. and related genera in China, and investigation of medicinal plants in Apiaceae. Master thesis, Kunming Medical University, China, 88 pp.

- Wolff H (1925) Neue Umbelliferen-Gattungen aus Ostasien. Notizblatt des Botanischen Gartens und Museums zu Berlin-Dahlem 9(84): 275–280. <https://doi.org/10.2307/3994550>
- Wolff H (1926) *Plantae sinenses a Dre. H. Smith annis 1921–22 lectae. XVI. Umbelliferae.* Acta Horti Gothoburgensis 2: 288–328.
- Wolff H (1929) Umbelliferae Asiaticae novae relictiae. I. Feddes Repertorium Specierum Novarum Regni Vegetabilis 27(1–8): 112–128. <https://doi.org/10.1002/fedr.4870270109>
- Zhou J, Peng H, Downie SR, Liu ZW, Gong X (2008) A molecular phylogeny of Chinese Apiaceae subfamily Apioideae inferred from nuclear ribosomal DNA internal transcribed spacer sequences. *Taxon* 57: 402–416. <https://doi.org/10.2307/25066012>
- Zhou J, Gong X, Downie SR, Peng H (2009) Towards a more robust molecular phylogeny of Chinese Apiaceae subfamily Apioideae: Additional evidence from nrDNA ITS and cp-DNA intron (rpl16 and rps16) sequences. *Molecular Phylogenetics and Evolution* 53(1): 56–68. <https://doi.org/10.1016/j.ympev.2009.05.029>
- Zhou J, Wei J, Liu ZW (2020a) An expanded circumscription for the previously monotypic *Pleurospermopsis* (Apiaceae) based on nrDNA ITS sequences and morphological evidence. *Phytotaxa* 460(2): 129–136. <https://doi.org/10.11646/phytotaxa.460.2.2>
- Zhou J, Gao YZ, Wei J, Liu ZW, Downie SR (2020b) Molecular phylogenetics of *Ligusticum* (Apiaceae) based on nrDNA ITS sequences: Rampant polyphyly, placement of the Chinese endemic species, and a much-reduced circumscription of the genus. *International Journal of Plant Sciences* 181(3): 306–323. <https://doi.org/10.1086/706851>
- Zhou J, Wei J, Niu JM, Liu XL, Liu ZW (2021) Molecular phylogenetics of *Pterocyclus* (Apiaceae) based on nrDNA ITS sequences: Revised circumscription with a restored species. *Phytotaxa* 498(2): 131–138. <https://doi.org/10.11646/phytotaxa.498.2.6>

Impatiens yunlingensis (Balsaminaceae), a new species from Yunnan, China

Jiang-Hong Yu^{1,2}, Wen-Di Zhang^{2,3}, Fei Qin^{2,3}, Chang-Ying Xia^{2,6,7}, Ying Qin^{8,9},
Ming-Tai An¹, Sudhindra R. Gadagkar^{4,5}, Sheng-Xiang Yu^{2,3}

1 College of Forestry, Guizhou University, Guiyang 550025, China **2** State Key Laboratory of Systematic and Evolutionary Botany, Institute of Botany, Chinese Academy of Sciences, Beijing 100093, China **3** University of Chinese Academy of Sciences, Beijing 100049, China **4** Biomedical Sciences, College of Graduate Studies, Midwestern University, Arizona 85308, USA **5** College of Veterinary Medicine, Midwestern University, Glendale, Arizona 85308, USA **6** School of Life Sciences, Southwest University, Chongqing 400715, China **7** Chongqing Key Laboratory of Plant Resource Conservation and Germplasm Innovation, Chongqing 400715, China **8** Guangxi Institute of Botany, Guangxi Zhuang Autonomous Region and the Chinese Academy of Sciences, Guilin 541006, China **9** College of Life Sciences, Guangxi Normal University, Guilin 541004, China

Corresponding authors: Sheng-Xiang Yu (yushengxiang@ibcas.ac.cn),
Sudhindra R. Gadagkar (sgadag@midwestern.edu),
Ming-Tai An (gdanmingtai@126.com)

Academic editor: W. A. Mustaqim | Received 21 June 2022 | Accepted 7 September 2022 | Published 27 October 2022

Citation: Yu J-H, Zhang W-D, Qin F, Xia C-Y, Qin Y, An M-T, Gadagkar SR, Yu S-X (2022) *Impatiens yunlingensis* (Balsaminaceae), a new species from Yunnan, China. *PhytoKeys* 212: 13–27. <https://doi.org/10.3897/phytokeys.212.89347>

Abstract

Impatiens yunlingensis S.X. Yu, Chang Y. Xia & J.H. Yu (Balsaminaceae), a species new to science discovered in Yunnan, China, is described and illustrated here, along with its phylogenetic position among other *Impatiens* species. Morphological, micro-morphological and molecular evidence is presented as an attestation of its novelty. *Impatiens yunlingensis* is similar to *I. delavayi* in having coarsely crenate leaf margins, bracts in the upper part, ca. $\frac{4}{5}$ length of the pedicels, saccate lower sepal with shallowly bifid spur, linear capsules, and elliptic-oblong, tuberculate seeds, but differs from *I. delavayi* with lateral sepals 4 (vs. 2), lateral united petal basal lobes subtriangular (vs. dolabriform), and seeds' surface equipped with tubercular ornamentation mostly covered with grain shaped appendages (vs. glabrous and without grain shaped appendages on the top).

Keywords

Morphology, phylogeny, pollen grains, seed micromorphology, taxonomy

Introduction

Impatiens L. (Balsaminaceae) is a large plant genus containing more than 1000 species, geographically distributed over a wide range, including tropical Africa, India, south-western Asia, southern China, and Japan, with a few species having radiated into Europe, Siberia, northern China, and North America (Grey-Wilson 1980; Fischer 2004; Yu et al. 2016). The greatest amount of diversification in this genus is seen in tropical Africa, Madagascar, the Himalayas and mainland tropical Asia (Song et al. 2003; Yuan et al. 2004). Of these, the latter two, located in southwest China, account for more than 270 species of *Impatiens* (Chen 2001; Chen et al. 2007; Yu 2012).

The genus *Impatiens* was recognized as a “notoriously” difficult group for taxonomical purposes more than a century ago (Hooker 1908), and it has continued to retain that status (Grey-Wilson 1980; Chen 2001). This reputation is largely because of the prolific diversification in this genus, which is exacerbated by the paucity of well-preserved specimens because of the rather ephemeral nature of the fleshy and succulent stems and the extremely delicate sepals and petals. Still, new species are constantly being discovered in this remarkable genus. Southwest China is one of the regions that has seen a surge, with six species added from the provinces of Sichuan and Yunnan in recent years – *I. maculifera* S.X. Yu & Chang Y. Xia (Xia et al. 2019), *I. baishaensis* B. Ding & H.P. Deng (Ding et al. 2017), *I. wawuensis* Bo Ding & S.X. Yu (Ding et al. 2016), *I. pandurata* Y.H. Tan & S.X. Yu (Tan et al. 2015), *I. shimianensis* Ge Chen Zhang & L.B. Zhang (Luo et al. 2015), and *I. xanthinoides* G.W. Hu (Cai et al. 2015). Unfortunately, the habitats of these mostly endemic species are being destroyed, or at the very least, fragmented, by increased tourism and the associated developments in infrastructure, underscoring the need to urgently investigate the presence of other *Impatiens* species and their distribution in this part of the country.

Our lab has made a concerted effort toward this end over the past few years by means of several expeditions into various regions of Southwest China, during which we discovered several species new to science of *Impatiens* (Bi et al. 2009; Yu et al. 2013; Tan et al. 2015; Ding et al. 2016; Xia et al. 2019). We now believe, based on a specimen collected from Northwest Yunnan in 2018, that we have found yet another species of *Impatiens* that is new to science. In the following, we describe its unique gross morphology and the micro-morphology of the pollen grains and seed coat, and discuss its relationships with its most closely related species (*I. delavayi* Franch., as determined by its phylogenetic position).

Materials and methods

Morphology

Morphological characters, such as leaves, inflorescences, flowers, and capsules, were carefully observed and measured in the field, followed by description and illustration in the lab, with meticulous attention to detail. In addition, we compared the specimen

with related species based on field notes and photographs taken during the expedition, as well as with FAA-fixed material and dried specimens from PE (abbreviation follows Thiers 2022).

Pollen grains and seeds

Mature, whole pollen grains and seeds collected from the field were observed directly and measured under magnification using an anatomical lens. Subsequently, they were mounted on double-sided adhesive tape and coated with a layer of gold before being photographed using a Hitachi S-4800 SEM. The micro-morphological characters were described following Wang and Wang (1983) and Lu (1991) for pollen grains, and Lu and Chen (1991), Liu et al. (2004), and Song et al. (2005) for seeds. The average size of pollen grains and seeds was calculated based on 20 of each.

Taxon sampling

We used a total of 152 species of *Impatiens* in this study, including three individuals of the putative new species, and three outgroup species: *Hydrocera triflora* (L.) Wight & Arn. (Balsaminaceae), *Marcgravia umbellata* L., and *Norantea guianensis* Aubl. (Marcgraviaceae) that were, included following Yuan et al. (2004), Janssens et al. (2006), and Yu et al. (2016). We downloaded DNA sequences for two molecular markers (see below) for all the species used, from GenBank except for the specimen under consideration, for which, they were newly generated for this study. Species names and GenBank accession numbers are listed in Suppl. material 1: Table S1.

DNA extraction, PCR amplification, and sequencing

We used two molecular markers in the study: ITS (ITS-1, 5.8S, and ITS-2) and *atpB-rbcL*. For the putative new species, we extracted total genomic DNA from silica gel-dried leaves using a CTAB protocol modified from that of Doyle and Doyle (1987). For the primers and PCR protocols for ITS and *atpB-rbcL*, we followed White et al. (1990) and Taberlet et al. (1991), respectively. Subsequently, we purified the PCR products using a GFXTMPCR DNA and Gel Band Purification Kit (Amersham Pharmacia Biotech, Piscataway, NJ, USA), and sequenced the markers using an ABI Prism BigDye Terminator Cycle Sequencing Kit (Applied Biosystems, Foster City, CA, USA), while analyzing the PCR products on an ABI3730xl automated DNA sequencer.

Phylogenetic analysis

Sequences were aligned using the default parameters in Clustal X v.1.83 (Thompson et al. 1997) and subsequently adjusted manually in BioEdit v.7.0 (Hall 1999). One difficult-to-align region in *atpB-rbcL* (encompassing 42 sites) was excluded from the analyses. Bayesian inference (BI) was used to analyze the ITS and plastid data sets, by means of MrBayes v.3.0b4 (Ronquist and Huelsenbeck 2003). Both regions

(ITS and *atpB-rbcL*) were assigned the GTR+I+G model of nucleotide substitution, as determined by the Akaike information criterion (AIC) in Modeltest v.3.06 (Posada and Crandall 1998).

Taxonomic treatment

Impatiens yunlingensis S.X. Yu, Chang Y. Xia & J.H. Yu, sp. nov.

urn:lsid:ipni.org:names:77307296-1

Figs 1, 2

Diagnosis. Similar to *I. delavayi* Franchet, in having coarsely crenate leaf margin, bracts in the upper part, ca. $\frac{4}{5}$ length of the pedicels, saccate lower sepal with shallowly bifid spur, but differs from *I. delavayi* with lateral sepals 4 (vs. 2) and lateral united petal basal lobes subtriangular (vs. dolabriform).

Type. CHINA. Yunnan: Dêqên County, Yunling Township, Yongzhi Village, understory and along river, alt. 1780 m, 28°11'N, 98°49'E, 07 Oct. 2018, Shengxiang Yu, Changying Xia, Xuexue Wu and Xiaxing Liu 9998 (holotype: PE, isotype: IBK).

Description. Annual herb, 50–70 cm tall. Stems slender, erect, branched, or simple, glabrous; inferior nodes swollen, glabrous. Leaves alternate; lower and middle leaves petiolate, upper leaves sessile or subsessile; petiole 2–3 cm long, slender, purplish or pale green, glabrous, glandless; leaf blade, 5–8 cm long, 3–5 cm wide, broadly ovate or ovate-orbicular, base cordate, apex obtuse, margin coarsely crenate, thinly membranous, glabrous; lateral vein 5–7 pairs; margin coarsely crenate. Lower and middle leaves petiolate; petiole 2–3 cm long, glabrous, purplish, slender; Racemes in upper axils, 2–3-flowered; peduncles 2–4 cm long, slender. Pedicels 1–3 cm long, glabrous, purplish, bracteate below flowers; bracts ovate, in the upper part, ca. $\frac{4}{5}$ length of the pedicels, ca. 1 mm wide, 1–3 mm long, acute, persistent. Flowers purplish, large, 2.5–3.5 cm deep. Lateral sepals 4; outer 2 large, 1–1.5 cm long, ca. 1 cm wide, 1–3 mm long, obliquely ovate, inequilateral, apex acute, glabrous, purplish; inner 2 small, 2–4 mm long, 1–1.5 mm wide, oblong, apex acuminate glabrous, purplish or pale green. Lower sepal 2–2.5 cm deep, 1.5–2 mm wide, 2.5–3 cm long, saccate, purplish red, abruptly narrowed into an incurved spur; spur short, ca. 1 cm long, shallowly bifid. Dorsal petal 8–12 mm long, 10–15 mm wide, orbiculate, base truncate, apex rounded, glabrous, purple, midrib thickened. Lateral united petals 2.5–3 cm long, 2-lobed; basal lobes ca. 1 cm long, 5 mm wide, subtriangular, apex obtuse, glabrous, purplish; distal lobes 2.5–3 cm long, 8–12 mm wide, triangular, apex acute glabrous, purplish or buff; auricle inflexed. Stamens 5, anthers obtuse. Capsule linear, 3–4 cm long, five carpels, many seeds per locule. Seeds elliptic-oblong, tuberculate.

Phenology. Flowering occurs from September to October, fruiting from September to November.

Distribution and ecology. This species is only known to be found in Dêqên County, Yunnan, China (Fig. 3); under evergreen broadleaf forests and along the river; alt. 1780–2500 m.

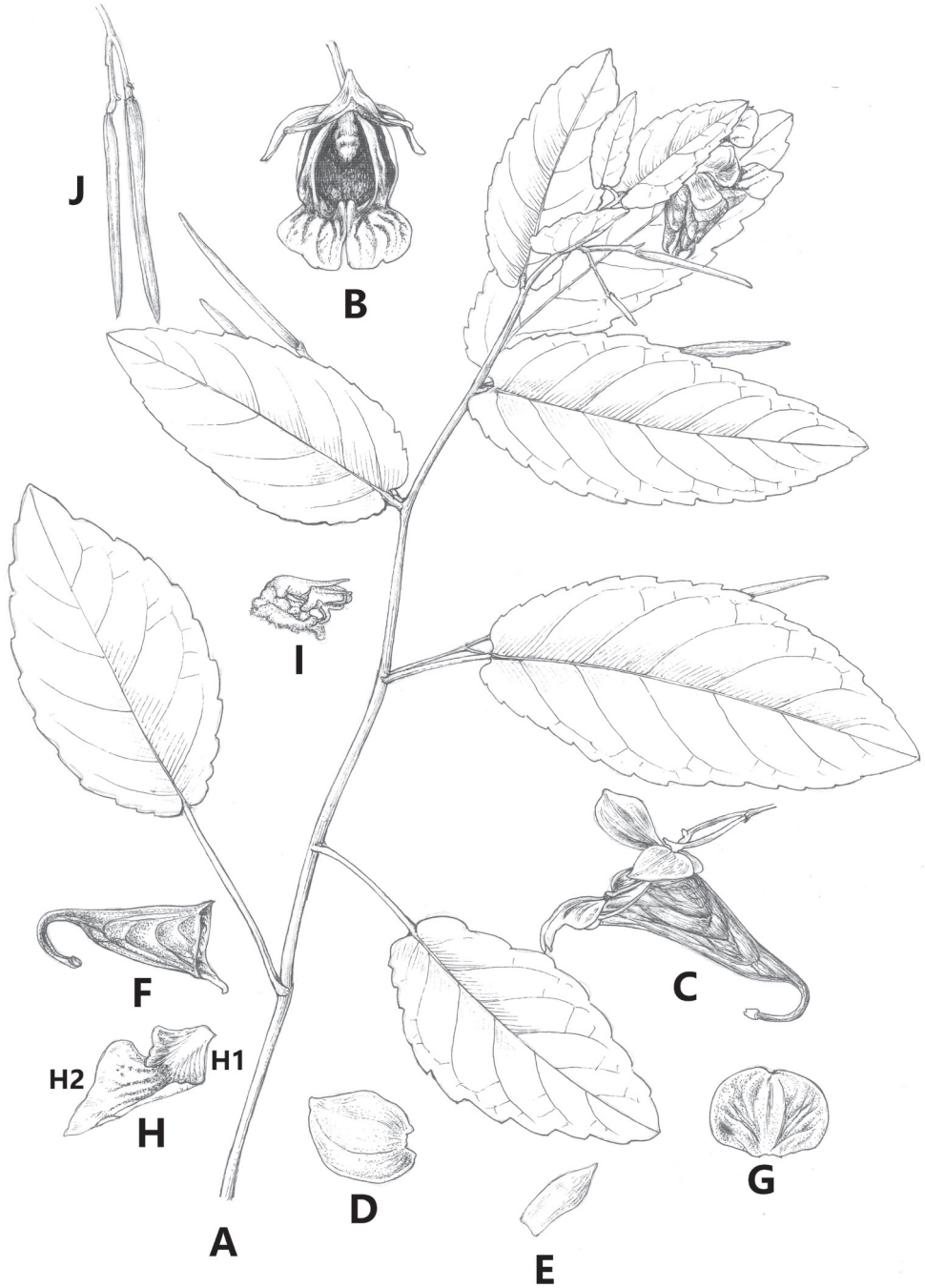


Figure 1. *Impatiens yunlingensis* S.X. Yu, Chang Y. Xia & J.H. Yu, sp. nov. **A** branch with leaves, flowers and capsules **B** flower, front view **C** flower, lateral view **D** outer lateral sepal **E** inner lateral sepal **F** lower sepal **G** dorsal petal **H** lateral united petals (H1) basal lobe (H2) distal lobe **I** filaments and anthers **J** capsules (Drawing by Wen-Hong Lin).



Figure 2. A–F *Impatiens yunlingensis* A habitat B plant C branch with flower D flower, front view E flower, lateral view F flower anatomy (a) dorsal petal (b) lateral united petals (c) outer lateral sepal (d) inner lateral sepal (e) lower sepal (f) filaments and anthers G *Impatiens delavayi* branch with flowers H *Impatiens delavayi* flower.

Conservation status. *Impatiens yunlingensis* is only known from the type locality with two middle-sized populations in an area that has been severely disturbed by over-grazing. Based on lack of additional local studies, we consider its status as Data Deficient [DD] (IUCN 2017). However, since the Hengduan Mountains are characterized by the high diversity of narrow-ranged species, including endemic, threatened, rare, and nationally protected species (Qin et al. 2017; Sun et al. 2017; Xu et al. 2019), all of which have been considered as a conservation priority for its global biodiversity hotspot and high species richness (Myers et al. 2000; Brooks et al. 2006; Xu et al. 2019). The conservation status of this apparently rare and narrow-ranged species is of high concern.

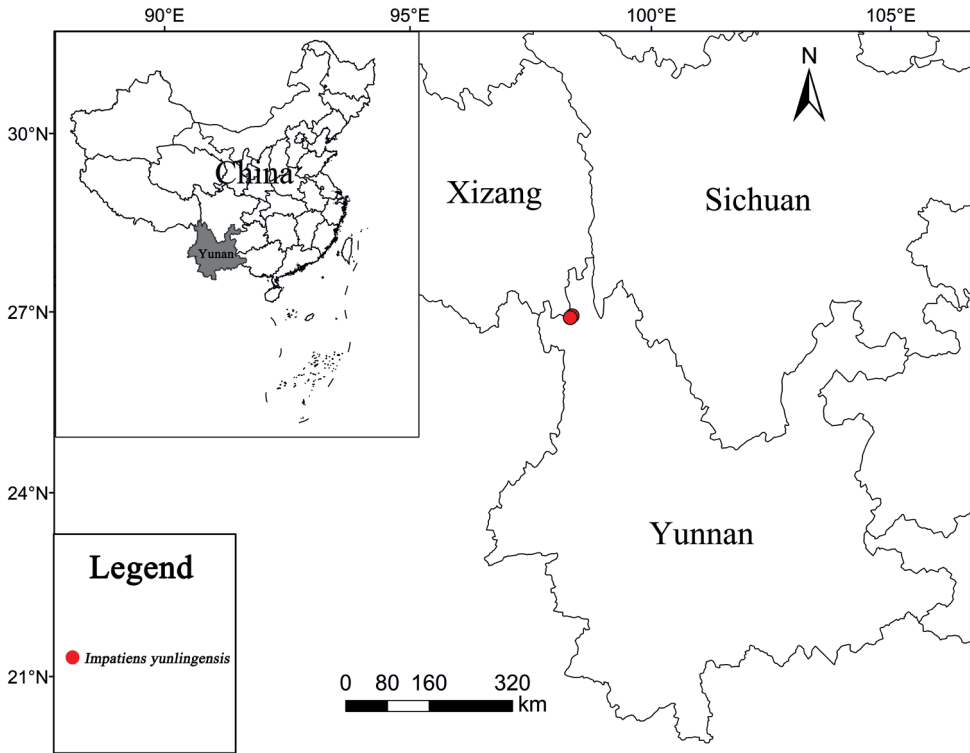


Figure 3. Geographical distribution of *Impatiens yunlingensis*.

Etymology. The specific epithet ‘*yunlingensis*’ refers to the locality of the type specimen, Yunling Township, Dêqên County, Yunnan, China.

Additional specimen examined. Paratype. CHINA. Yunnan: Dêqên County, Yunling Township, Shualao Village; hillside and understory, alt. 2500 m, 28°09'N, 98°47'E, 07 Oct. 2018, Shengxiang Yu, Changying Xia, Xuexue Wu and Xiaping Liu 10002 (PE).

Seed description and palynology. Seeds of *I. yunlingensis* are elliptic-oblong, with a size of 2.6×1.9 mm, L (long) / W (wide) = 1.37 (Fig. 4 A–C). The surface is equipped with coarse tubercular ornamentation mostly covered by grain-shaped appendages. While the seeds of *I. delavayi* are also elliptic-oblong, with a size of 3.5×2.3 mm, L (long) / W (wide) = 1.52 (Fig. 4 D–F), the surface contains coarse tubercular ornamentation glabrous and no grain shaped appendages on the top. Pollen grains of both *I. yunlingensis* and *I. delavayi* are tetracolpate, elliptic in polar view, exine with irregular reticulate ornamentation, and granules in lumina. *Impatiens yunlingensis* pollen size ($E_1 \times E_2$; length of long equatorial axis \times length of short equatorial axis) is 28.05×16.67 μm (Fig. 4 G–I), while it is 27.78×17.50 μm ($E_1 \times E_2$) for *I. delavayi* (Fig. 4 J–L) (Suppl. material 1: Table S2).

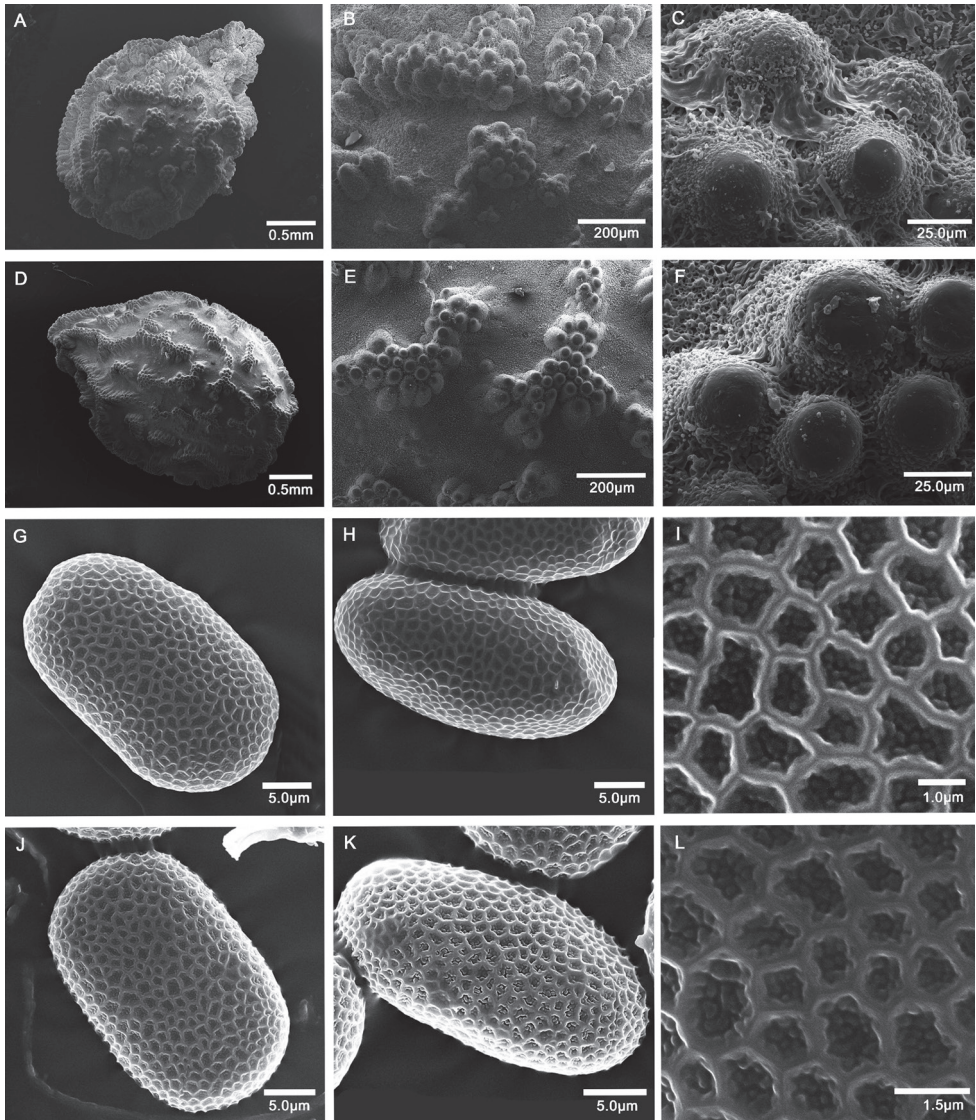


Figure 4. Scanning electron microscope images of seeds and pollen grains **A–C** seeds of *Impatiens yunlingensis* **D–F** seeds of *I. delavayi* **G–I** pollen grains of *I. yunlingensis* **J–L** pollen grains of *I. delavayi*.

Results

Nuclear data phylogenetic analyses

Although phylogenetic analysis was done using all 152 species, we only show a few clades here, along with the position of the root (Figs 5 and 6) (see Suppl. material 1: Figs S1 and S2 for the tree with all the species). Fig. 5 shows that the three individuals of *I. yunlingensis* cluster together in the phylogenetic tree of ITS with strong support (PP = 1.00), and the

tree shows that *I. yunlingensis* is the sister species of *I. delavayi*, although with relatively poor support (PP < 0.95). *Impatiens nubigena* W.W. Smith has the closest relationship to *I. yunlingensis* and *I. delavayi* (PP = 1.00), followed by *I. poculifer* Hook. f. (PP = 1.00), and *I. chiulungensis* Y.L. Chen (PP = 0.98).

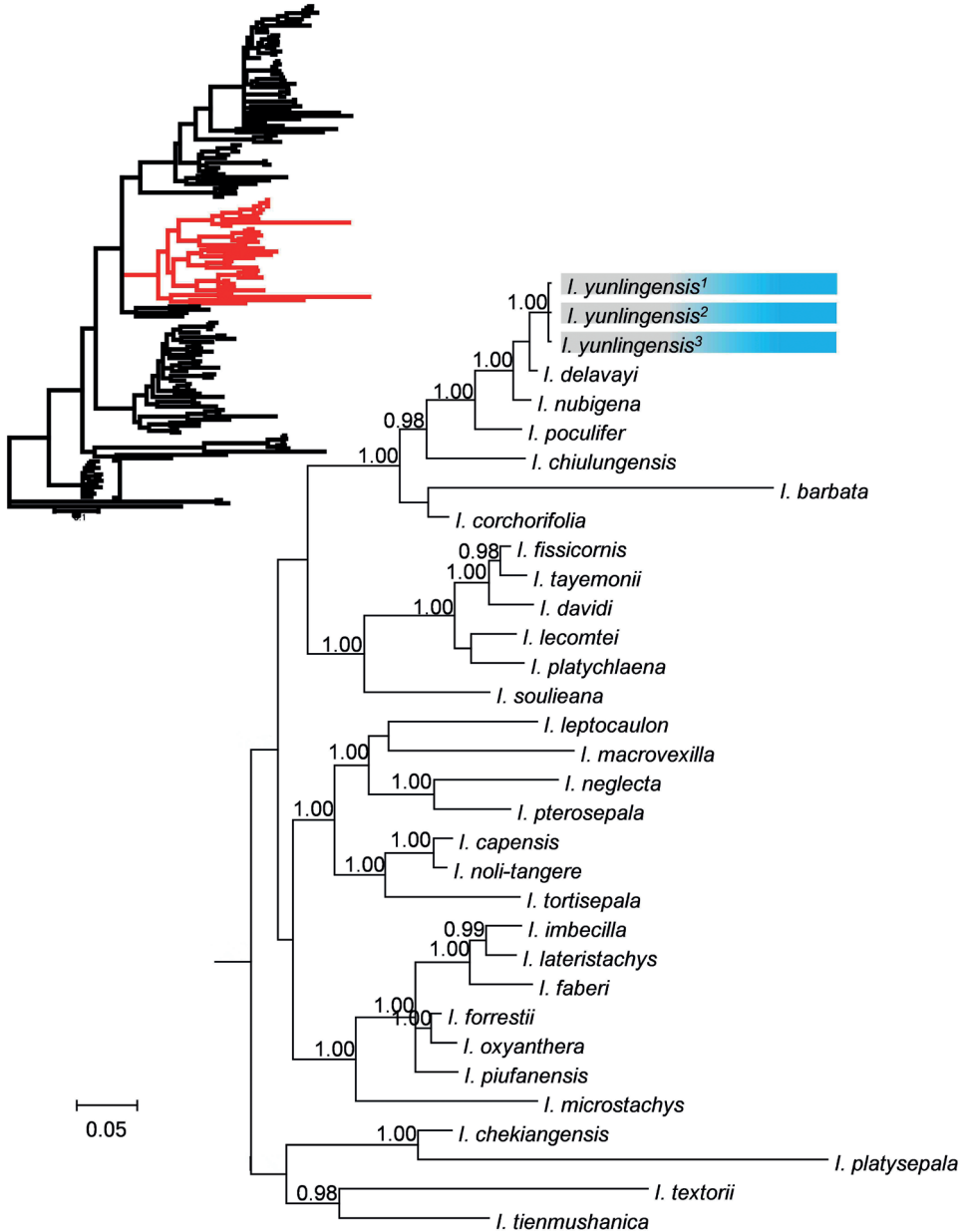


Figure 5. Partial Bayesian consensus phylogram based on ITS sequences. Numbers above branches are Bayesian posterior probabilities (only PP values > 0.95 shown).

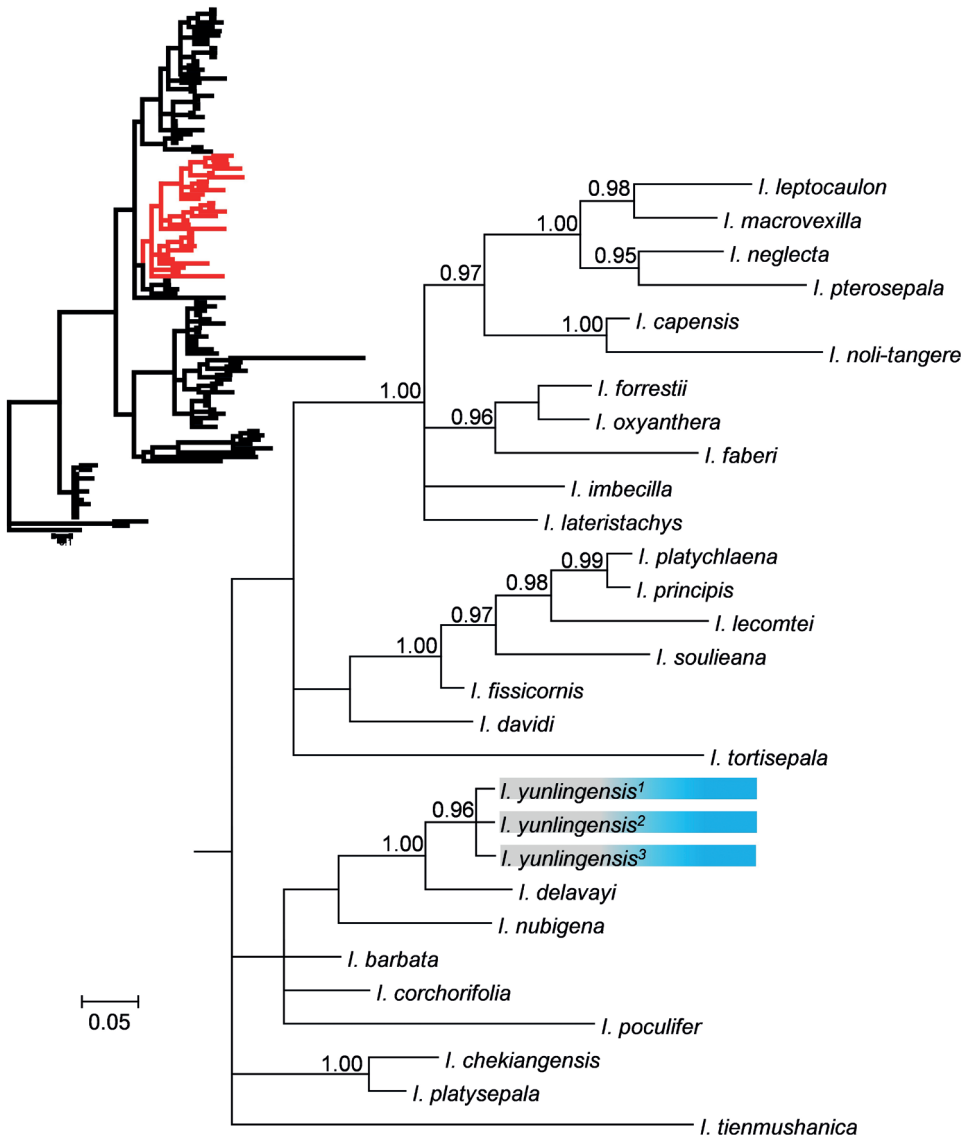


Figure 6. Partial Bayesian consensus phylogram based on *atpB-rbcL* sequences. Numbers above branches are Bayesian posterior probabilities (only PP values > 0.95 shown).

Plastid data phylogenetic analysis

The three individuals of *I. yunlingensis* clustered together with strong support (PP = 0.96) in the phylogenetic tree of *atpB-rbcL* also (Fig. 6), with *I. delavayi* once again as the sister species, and with strong support (PP = 1.00). As in the ITS tree (Fig. 5), *I. nubigena* has the closest relationship to *I. yunlingensis* and *I. delavayi*, but with poor support, and the clade of these three species is in a polytomy with *I. barbata* Comber, *I. corchorifolia* Franch., and *I. poculifer*.

While the ITS tree (Fig. 5) has a higher resolution and more numbers of internal nodes with high support, both tree topologies resemble each other and are also similar to those obtained in previous studies (Yuan et al. 2004; Janssens et al. 2006; Yu et al. 2016; Ruchisansakun et al. 2021).

Based on the position of *I. yunlingensis* in both trees, we conclude that it is a new species to science that belongs to the subgenus *Impatiens* (Yu et al. 2016). This evidence is corroborated by the morphological features of *I. yunlingensis* as well, which are in accordance with those of subg. *Impatiens*, e.g., 2-flowered inflorescences and linear fruits (Yu et al. 2016).

Discussion

Both phylogenetic trees (ITS and *atpB-rbcL*; Figs 5 and 6, respectively) indicate that *I. yunlingensis* is a distinct member of the genus, and furthermore, support its sister taxon relationship with *I. delavayi*, thus corroborating the evidence provided by the morphological and micro-morphological observations. There are two populations of *I. yunlingensis* that have been recorded and observed, and we find that the morphological characters of the species present consistency between the two populations, especially with respect to the morphology and number of lateral sepals (4 lateral sepals including the outer 2 and inner 2). *Impatiens yunlingensis* is similar to *I. delavayi* in having coarsely crenate leaf margins, bracts in the upper part, ca. $\frac{4}{5}$ length of the pedicels, saccate lower sepal with shallowly bifid spur, linear capsules, and elliptic-oblong, tuberculate seeds, but differs from *I. delavayi*, with lateral sepals 4 (vs. 2), lateral united petal basal lobes subtriangular (vs. dolabriliform), and seeds surface contain tubercular ornamentation mostly covered by grain shaped appendages (vs. glabrous and without grain shaped appendage on the top). This feature of lateral sepals 4 is crucial for distinguishing *I. yunlingensis* from *I. delavayi* and other related species, and supports its standing as a separate, and new species. It is worth noting that the morphological characters of *I. delavayi* are consistent in its distribution range. We examined all the specimens of *I. delavayi* preserved in PE and found that there were only two lateral outer sepals, with no lateral inner sepals, not even rudimentary ones. Furthermore, to our knowledge, there is no report of variation in the lateral sepal number of *I. delavayi*. Therefore, we believe that the number of lateral sepals is a reliable trait for this purpose.

As pointed out by previous studies, the characteristic of 4 sepals is seen in many species of section *Semeiocardium* (Ruchisansakun et al. 2015) and in *I. oblongata* (sect. *Impatiens*) (Ruchisansakun et al. 2018). Indeed, only a few species of subgenus *Impatiens* exhibit this character, such as *I. barbata*, *I. chiulungensis*, and *I. chochorifolia*. However, other morphological features of these species clearly distinguish them from *I. yunlingensis*. For example, *I. barbata* is characterized by yellow-haired flowers and the plant is puberulent, and the latter two species can be readily differentiated from *I. yunlingensis* by the apex of the basal lobe, and the distal lobe of lateral united petal narrowing into a single long and hair-like appendage, respectively.

Our phylogenetic analyses generated a result consistent with previous studies (Yuan et al. 2004; Janssens et al. 2006; Yu et al. 2016; Ruchisansakun et al. 2021), in-

dicating that the *I. yunlingensis* belongs to subg. *Impatiens*. The ITS-based phylogenetic tree has a higher resolution and contains more nodes with high support, but it does not provide sufficient support for the relationship between *I. yunlingensis* and its close relatives, while the *atpB-rbcL* tree does. It is also worth noting that while the position of the clade itself is different between the two trees, at least two of the three previously mentioned species with the character of lateral sepals 4 (*I. barbata*, *I. chiulungensis*, and *I. chochorifolia*) are nested in the same large clade as *I. yunlingensis* in both phylogenetic trees. In summary, *I. yunlingensis*, with its morphological, micro-morphological, and phylogenetic distinctiveness, adds another external node to the growing *Impatiens* phylogeny and should help in elucidating the evolutionary significance of the genus, particularly with respect to its propensity for diversification.

Additional specimen examined. *Impatiens delavayi* Franch—CHINA. Sichuan: Kangwu Temple, near Muli Bridge, Muli County, Sichuan Province, 21 Feb 2012, S.X. Yu, Y.T. Hou, X.X. Zhang & Y.M. Zhao 4664 (PE). Xizang: Zayü County, Xizang, alt. 3700 m, 27 Sep 1982, *Qinghai-Tibet expedition* 10807 (PE); Dzer-nar, Tsa-wa-rung, Xizang, alt. 3000 m, Sep 1935, C.W. Wang 66212 (PE). Yunnan: East slope of Haba Snow Mountain, Zhongdian County, Yunnan Province, alt. 3500–3800 m, 11 Aug 1981, *Hengduan Mountains Research Team, Institute of Botany, the Chinese Academy of Sciences* 2938 (PE); Yulong Mountains, Lijiang County, Yunnan Province, alt. 3200 m, 6 Aug. 1959, *anonymous* 22522 (PE); Zhongdian County, Yunnan Province, 27°27'33"N, 99°55'2"E, alt. 3050 m, 26 July 2006, D.E. Boufford, S.L. Kelley, R.H. Ree, H. Sun, B. Xü, J.P. Yue, D.C. Zhang & W.D. Zhu 35372 (PE); Wei-se County, Yunnan Province, alt. 2600 m, 15 Sep 1934, *anonymous* 57925 (PE); Huan-fu-ping, A-tun-tze, Dêqên County, Yunnan Province, alt. 3500 m, Aug 1935, C.W. Wang 69058 (PE).

Acknowledgements

The authors wish to thank the keepers of the herbaria of BM, E, K, KUN and PE for permission to inspect the specimens, Wen-Hong Lin for the line drawing, and Xue-Xue Wu and Xia-Xing Liu for their help in collecting specimens. This work was supported by the Special Funds for Young Scholars of Taxonomy of the Chinese Academy of Sciences (ZSBr-004), National Natural Foundation of China (31770235, 31170177), and Main direction Program of knowledge Innovation of Chinese Academy of Sciences (grant no. kSCX2-eW-Z-1).

References

- Bi HY, Hou YT, Zhou XR, Yu SX (2009) *Impatiens chashanensis* (Balsaminaceae) sp. nov. from Sichuan, China. *Nordic Journal of Botany* 27(5): 372–375. <https://doi.org/10.1111/j.1756-1051.2009.00474.x>

- Brooks TM, Mittermeier RA, Da Fonseca GAB, Gerlach J, Hoffmann M, Lamoreux JF, Mittermeier CG, Pilgrim JD, Rodrigues ASL (2006) Global Biodiversity Conservation Priorities. *Science* 313(5783): 58–61. <https://doi.org/10.1126/science.1127609>
- Cai XZ, Hu GW, Cong YY (2015) *Impatiens xanthinoides* (Balsaminaceae), a new species from Yunnan, China. *Phytotaxa* 227(3): 261–267. <https://doi.org/10.11646/phytotaxa.227.3.5>
- Chen YL (2001) Balsaminaceae. In: Chen YL (Ed.) *Flora Reipublicae Popularis Sinica*, 47(2), Science Press, Beijing, 1–243.
- Chen YL, Akiyama S, Ohba H (2007) Balsaminaceae. In: Wu ZY, Raven PH (Eds) *Flora of China*, vol. 12. Science Press, Beijing & Missouri Botanical Garden Press, St. Louis, 43–113.
- Ding B, Gadagkar SR, Wang JC, Guo MH, Yu SX (2016) *Impatiens wawuensis* (Balsaminaceae): A new species from Sichuan, China. *Phytotaxa* 273(4): 293–298. <https://doi.org/10.11646/phytotaxa.273.4.5>
- Ding B, Wang JC, Deng HP, Wang CY (2017) *Impatiens baishaensis* (Balsaminaceae): A new species from Sichuan, China. *Phytotaxa* 319(2): 191–196. <https://doi.org/10.11646/phytotaxa.319.2.8>
- Doyle JJ, Doyle JL (1987) A rapid DNA isolation procedure for small quantities of fresh leaf material. *Phytochemistry* 19: 11–15. [https://doi.org/10.1016/0031-9422\(80\)85004-7](https://doi.org/10.1016/0031-9422(80)85004-7)
- Fischer E (2004) Balsaminaceae. In: Kubitzki K (Ed.) *The Families and Genera of Vascular Plants*, Vol. 6, Berlin, Springer, 20–25.
- Grey-Wilson C (1980) Introduction to the genus *Impatiens*. In: Balkema AA (Ed.) *Impatiens of Africa*, Rotterdam, 1–57.
- Hall TA (1999) BioEdit: A user-friendly biological sequence alignment editor and analysis program for Windows 95/98/NT. *Nucleic Acids Symposium Series* 41: 95–98. <https://doi.org/10.1021/bk-1999-0734.ch008>
- Hooker JD (1908) Les espèces du genre “*Impatiens*” dans l’herbier du Muséum de Paris. *Nouvelles archives du Muséum d’histoire naturelle de Paris* 10(5): 234–272.
- IUCN (2017) Guidelines for Using the IUCN Red List Categories and Criteria. Version 13. <http://cmsdocs.s3.amazonaws.com/RedListGuidelines.pdf>
- Janssens SB, Geuten K, Yuan YM, Song Y, Küpfer P, Smets E (2006) Phylogenetics of *Impatiens* and *Hydrocera* (Balsaminaceae) using chloroplast *atpB-rbcL* spacer sequences. *Systematic Botany* 31(1): 171–180. <https://doi.org/10.1600/036364406775971796>
- Liu CJ, Lin Q, He JX (2004) Methods and terminology of study on seed morphology from China. *Acta Botanica Boreali-Occidental Sinica* 24(1): 178–188. <https://doi.org/10.1088/1009-0630/6/5/011>
- Lu YQ (1991) Pollen morphology of *Impatiens* L. (Balsaminaceae) and its taxonomic implications. *Acta Phytotaxonomica Sinica* 29(4): 352–357. <https://doi.org/10.14232/abs.2020.2.207-219>
- Lu YQ, Chen YL (1991) Seed morphology of *Impatiens* L. (Balsaminaceae) and its taxonomic significance. *Acta Phytotaxonomica Sinica* 29(3): 252–257. <https://doi.org/10.3767/000651905X622699>
- Luo Q, Wang TJ, Zhao LH (2015) *Impatiens shimianensis* sp. nov. (Balsaminaceae) from Sichuan, China. *Nordic Journal of Botany* 33(2): 204–208. <https://doi.org/10.1111/njb.00573>

- Myers N, Mittermeier RA, Mittermeier CG, Da Fonseca GA, Kent J (2000) Biodiversity hotspots for conservation priorities. *Nature* 403(6772): 853–858. <https://doi.org/10.1038/35002501>
- Posada D, Crandall KA (1998) Modeltest: Testing the model of DNA substitution. *Bioinformatics* 14(9): 817–818. <https://doi.org/10.1093/bioinformatics/14.9.817>
- Qin HN, Zhao LN, Yu SX, Liu HY, Liu B, Xia NH, Hua P (2017) Evaluating the endangerment status of China's angiosperms through the red list assessment. *Biodiversity Science* 25(7): 745–757. <https://doi.org/10.17520/biods.2017156>
- Ronquist F, Huelsenbeck JP (2003) MrBayes 3: Bayesian phylogenetic inference under mixed models. *Bioinformatics* 19(12): 1572–1574. <https://doi.org/10.1093/bioinformatics/btg180>
- Ruchisansakun S, van der Niet T, Janssens SB, Triboun P, Techaprasan J, Jenjittikul T, Suksathan P (2015) Phylogenetic analyses of molecular data and reconstruction of morphological character evolution in Asian *Impatiens* Section *Semeiocardium* (Balsaminaceae). *Systematic Botany* 40(4): 1063–1074. <https://doi.org/10.1600/036364415X690102>
- Ruchisansakun S, Suksathan P, van der Niet T, Smets EF, Saw-Lwin, Janssens SB (2018) Balsaminaceae of Myanmar. *Blumea Journal of Plant Taxonomy and Plant Geography* 63(3): 199–267. <https://doi.org/10.3767/blumea.2018.63.03.01>
- Ruchisansakun S, Mertens A, Janssens SB, Smets EF, van der Niet T (2021) Evolution of pollination syndromes and corolla symmetry in Balsaminaceae reconstructed using phylogenetic comparative analyses. *Annals of Botany* 127(2): 267–280. <https://doi.org/10.1093/aob/mcaa184>
- Song Y, Yuan YM, Küpfer P (2003) Chromosomal evolution in Balsaminaceae, with cytological observations on 45 species from Southeast Asia. *Caryologia* 56(4): 463–481. <https://doi.org/10.1080/00087114.2003.10589359>
- Song Y, Yuan YM, Küpfer P (2005) Seedcoat micromorphology of *Impatiens* (Balsaminaceae) from China. *Botanical Journal of the Linnean Society* 149(2): 195–208. <https://doi.org/10.1111/j.1095-8339.2005.00436.x>
- Sun H, Zhang JW, Tao D, Boufford DE (2017) Origins and evolution of plant diversity in the Hengduan Mountains, China. *Plant Diversity* 39(4): 161–166. <https://doi.org/10.1016/j.pld.2017.09.004>
- Taberlet P, Gielly L, Pautou G, Bouvet J (1991) Universal primers for amplification of three non-coding regions of chloroplast DNA. *Plant Molecular Biology* 17(5): 1105–1109. <https://doi.org/10.1007/BF00037152>
- Tan YH, Liu YN, Jiang H, Zhu XX, Zhang W, Yu SX (2015) *Impatiens pandurata* (Balsaminaceae), a new species from Yunnan, China. *Botanical Studies* 56(1): 29. <https://doi.org/10.1186/s40529-015-0108-4>
- Thiers B (2022) Index Herbariorum: A global directory of public herbaria and associated staff. New York Botanical Garden's Virtual Herbarium. <http://sycamore.nybg.org/science/ih> [accessed 03.04.2022]
- Thompson JD, Gibson TJ, Plewniak F, Jeanmougin F, Higgins DG (1997) The CLUSTAL_X windows interface: Flexible strategies for multiple sequence alignment aided by quality analysis tools. *Nucleic Acids Research* 25(24): 4876–4882. <https://doi.org/10.1093/nar/25.24.4876>

- Wang KF, Wang XZ (1983) An introduction to palynology. Peking University Press, Beijing, 1–205.
- White TJ, Bruns T, Lee S, Taylor J (1990) Amplification and direct sequencing of fungal ribosomal RNA genes for phylogenetics. In: Innis MA, Gelfand DH, Sninsky JJ, White TJ (Eds) PCR Protocols: A Guide to Methods and Applications, Academic Press, New York, 315–322. <https://doi.org/10.1016/B978-0-12-372180-8.50042-1>
- Xia CY, Gadagkar RS, Zhao XL, Do TV, Zhu XY, Qin Y, Deng HP, Yu SX (2019) *Impatiens maculifera* sp. nov. (Balsaminaceae) Yunnan, China. Nordic Journal of Botany 37(8): e02422. <https://doi.org/10.1111/njb.02422>
- Xu Y, Huang JH, Lu XH, Zang RG (2019) Priorities and conservation gaps across three biodiversity dimensions of rare and endangered plant species in China. Biological Conservation 229: 30–37. <https://doi.org/10.1016/j.biocon.2018.11.010>
- Yu SX (2012) Balsaminaceae of China. Peking University Press, Beijing.
- Yu SX, Lidén M, Han BC, Zhang XX (2013) *Impatiens lixianensis*, a new species of Balsaminaceae from Sichuan, China. Phytotaxa 115(1): 25–30. <https://doi.org/10.11646/phytotaxa.115.1.3>
- Yu SX, Janssens SB, Zhu XY, Lidén M, Gao TG, Wang W (2016) Phylogeny of *Impatiens* (Balsaminaceae): Integrating molecular and morphological evidence into a new classification. Cladistics 32(2): 179–197. <https://doi.org/10.1111/cla.12119>
- Yuan YM, Song Y, Geuten K, Rahelivololona E, Wohlhauser S, Fischer E, Smets E, Küpfer P (2004) Phylogeny and biogeography of Balsaminaceae inferred from ITS sequence data. Taxon 53(2): 391–403. <https://doi.org/10.2307/4135617>

Supplementary material I

Appendix S1

Authors: Jiang-Hong Yu, Ming-Tai An, Fei Qin, Chang-Ying Xia, Ying Qin, Sudhindra R. Gadagkar, Sheng-Xiang Yu

Data type: Morphological, phylogenetic, GenBank accession numbers, images.

Explanation note: **Table S1**. Species and GenBank accession numbers for the marker sequences used in this study **Table S2**. Morphological characteristics of *Impatiens yunlingensis* and *I. delavayi* **Figures S1, S2**. Bayesian posterior probabilities figure.

Copyright notice: This dataset is made available under the Open Database License (<http://opendatacommons.org/licenses/odbl/1.0/>). The Open Database License (ODbL) is a license agreement intended to allow users to freely share, modify, and use this Dataset while maintaining this same freedom for others, provided that the original source and author(s) are credited.

Link: <https://doi.org/10.3897/phytokeys.212.89347.suppl1>

Primula surculosa (Primulaceae), a new species from Yunnan, China

Yuan Xu^{1,2}, De-Ming He³, Lin-Zhong Yang³, Gang Hao⁴

1 Key Laboratory of Plant Resources Conservation and Sustainable Utilization, South China Botanical Garden, Chinese Academy of Sciences, Guangzhou 510650, China **2** Center of Conservation Biology, Core Botanical Gardens, Chinese Academy of Sciences, Guangzhou 510650, China **3** Administration of Wenshan National Natural Reserve, Wenshan Zhuang and Miao Autonomous Prefecture 663000, China **4** College of Life Sciences, South China Agricultural University, Guangzhou 510642, Guangdong, China

Corresponding author: Gang Hao (haogang@scau.edu.cn)

Academic editor: Avelinah Julius | Received 2 August 2022 | Accepted 12 October 2022 | Published 28 October 2022

Citation: Xu Y, He D-M, Yang L-Z, Hao G (2022) *Primula surculosa* (Primulaceae), a new species from Yunnan, China. *PhytoKeys* 212: 29–35. <https://doi.org/10.3897/phytokeys.212.91133>

Abstract

A new species, *Primula surculosa*, is described and illustrated. In gross morphology, it is clearly allied to section *Petiolares* and is most similar to *P. taliensis* from the group *Taliensis*, but is distinctive in its indumentum in the throat of the corolla tube, and the markedly stoloniferous habit.

Keywords

morphological characteristics, new species, *Primula taliensis*, taxonomy, Yunnan

Introduction

The genus *Primula* L. (Primulaceae) is one of the rapid speciation groups in angiosperms, which comprises about 500 species that are almost exclusively confined to temperate and arctic zones of the Northern Hemisphere. Its modern center of diversity falls in the Hengduan-Himalayan region, harboring more than 300 species (Hu 1990; Hu and Kelso 1996). Its ancestral or original center, however, is speculated to be in the montane region of SW China (southern Yunnan, Guizhou and Guangxi) and adjacent northern Vietnam, Myanmar and Thailand, since many presumably primitive taxa of *Primula*, *Lysimachia* and *Androsace* (Primulaceae) occur there (Hu 1994; Hao et al. 2004).

Primula sect. *Petiolares* Pax has approximately 60 species worldwide, and is abundantly distributed in the Hengduan-Himalaya Mts., with only a few members extending into central China, N Myanmar, N Vietnam and Kashmir (Hu 1990; Hu and Kelso 1996). One of the most important diagnostic characters of this section is its globose capsule with a persistent calyx that does not open by valves but by crumbling at the membrane apex (Smith and Fletcher 1944; Hu 1990). This section was further divided into seven groups based on the presence or absence of the basal bud scales and farina, the shape of the leaf margin, and the type of hair (Smith and Fletcher 1944).

In the spring of 2020, while the authors were investigating flora of *Primula* in south-eastern Yunnan, a population of *Primula* was discovered in Wenshan city. In the flowering time, particularly from the appearances of leaves and flowers, it looked a bit like *Primula taliensis*, which occurs in western Yunnan and northern Myanmar. In the following fruiting time, the plants notably developed several leafy stolons. Detailed examination proved that it eventually represents an unreported taxon of *P.* sect. *Petiolares*, and is described below.

Materials and methods

Firstly, we examined the relevant taxonomic literature (e.g., Smith and Fletcher 1944; Hu 1990; Hu and Kelso 1996) to infer the similar species for the new species and the main diagnostic characters (habit, the indumentum of leaves and corolla, the shape of leaves, calyx lobe and corolla lobe, and the length of petiole) which should be compared. Then, the observations and measurements of morphological characters of the new taxon were conducted in the field and at the herbarium. Indumentum and other tiny morphological features were observed under a stereomicroscope. Flowers were dissected and photographed. Morphological comparison with similar species was performed based on living plants (for *P. taliensis* collected from Jingdong and Dali of Yunnan Province), specimens from IBSC, KUN and PE, and the images of specimens from the JSTOR Global Plants (<http://plants.jstor.org/>). The conservation status of the new species was assessed following the guidelines for using the IUCN Red List categories and criteria (IUCN Standards and Petitions Subcommittee 2022).

Taxonomic treatment

Primula surculosa Y.Xu & G.Hao, sp. nov.

urn:lsid:ipni.org:names:77307377-1

Figs 1, 2

Type. CHINA, Yunnan: Wenshan City, Bozhu Town, Bozhu Mt. 23°22'N, 104°12'E, alt. 2910 m, 27 Feb. 2022 (fl.), Deming He Xu211011 (holotype: IBSC!).

Diagnosis. *Primula surculosa* is morphologically most similar to *P. taliensis*, but is distinctive in its indumentum in the throat of the corolla tube, and the markedly stoloniferous habit.

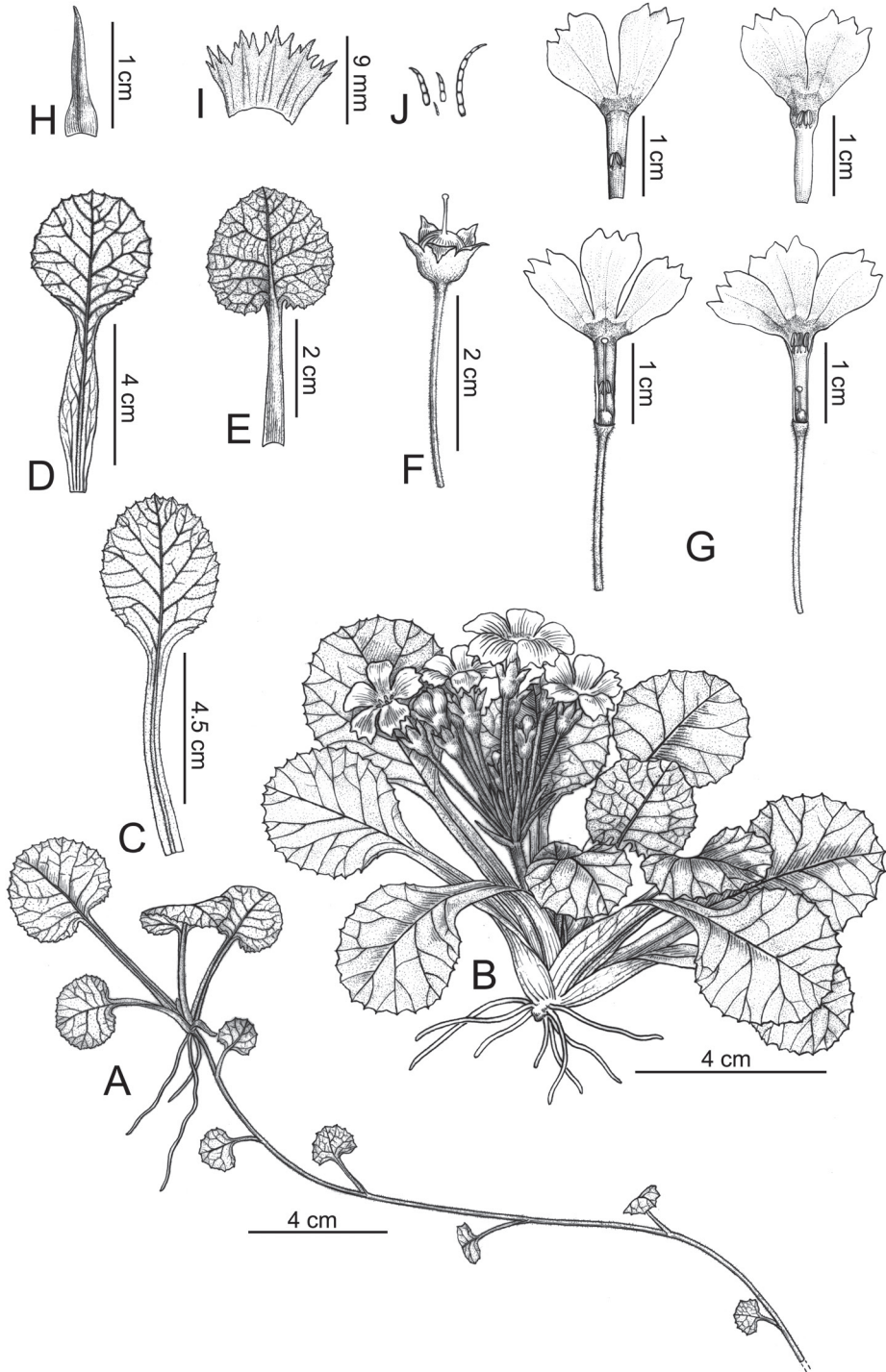


Figure 1. *Primula surculosa* sp. nov. **A** stolon **B** habit **C** leaf on abaxial surface (fruiting time) **D** outer leaf on abaxial surface (anthesis) **E** inner leaf on adaxial surface (anthesis) **F** capsule with persistent calyx **G** long and short-styled flowers **H** bract **I** calyx (dissected) **J** multicellular hairs. Drawn by Yun-Xiao Liu.

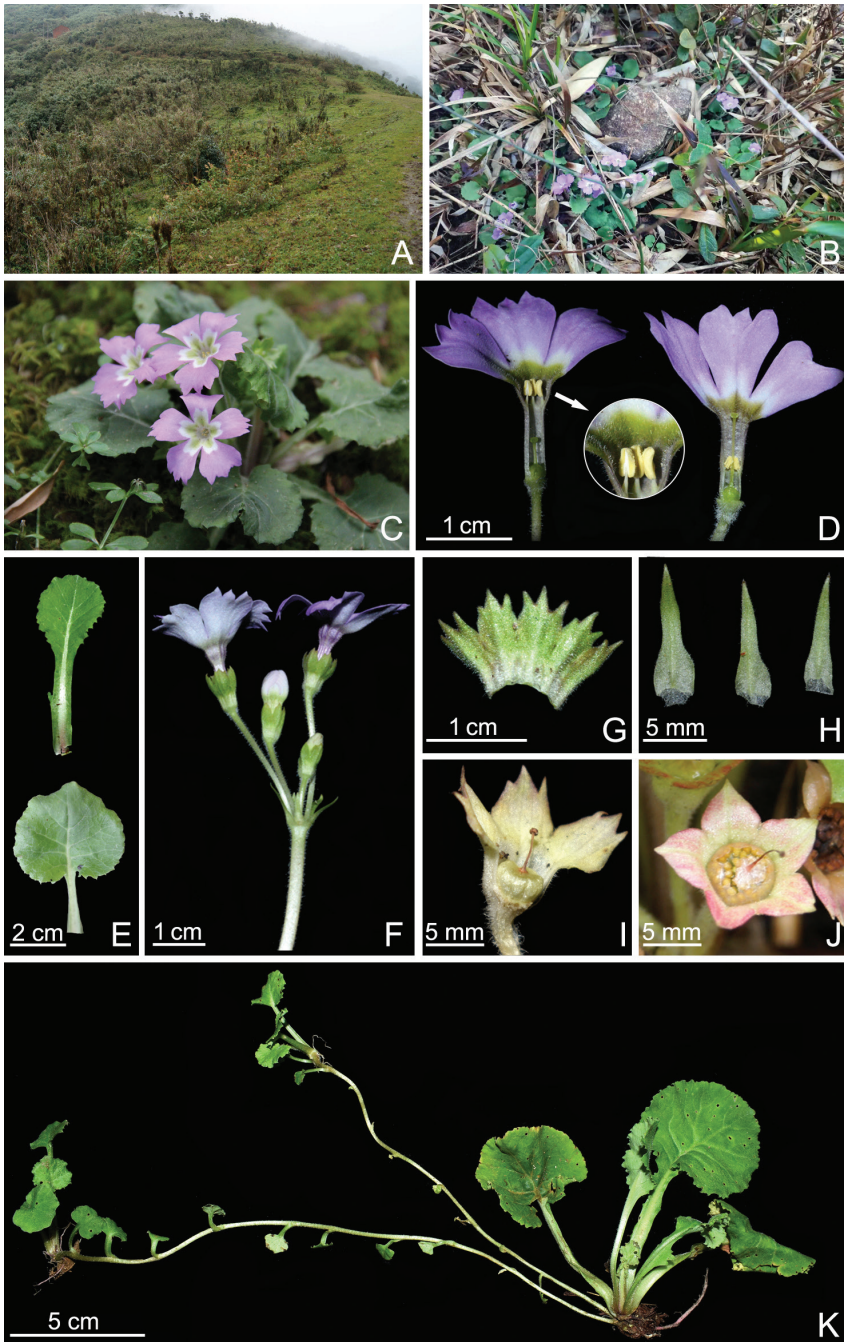


Figure 2. Living plant of *Primula surculosa* sp. nov. **A, B** habitat **C** habit (blooming) **D** long and short-styled flowers, also showing pilose corolla tube (the circular image) **E** outer and inner leaves on adaxial surfaces, showing indumentum, venation, and margin shapes **F** inflorescence **G** calyx (dissected) **H** bracts **I** capsule with persistent calyx **J** capsule (crumbling) **K** habit (stoloniferous after anthesis) Photographed by De-Ming He.

Description. A perennial herb, efarinose, stoloniferous, lacking basal bud scales at anthesis. *Leaves* dimorphic, forming a rosette of 9.0–2.0 cm in diameter, with short appressed pubescent on both surfaces. *Outer leaves* spatulate to obovate-spatulate, 2.5–5.0 × 2.5–3.5 cm, tapering to base forming a broadly winged petiole, margin crenate to dentate, apex rounded. *Inner leaves* long petiolate; blade broadly ovate to suborbicular in outline, 4.0–7.0 cm in diameter, base rounded or cordate, margin coarsely dentate; petiole 3.0–6.0 cm long, up to 12 cm at fruiting time. *Stolons* arising from the basal of the leaf rosette after anthesis, terminated in a leaf rosette, with alternate and reduced ovate leaves (5–18 × 8–20 mm) on lower part, growing upwards to 5–8 cm, afterwards elongating up to 20–25 cm long, procumbent along the surface of the ground and rooting at the nodes. *Scapes* 1.5–3.0 cm, reaching 6.0 cm at fruiting, copiously pilose; umbel solitary, 2–8 flowered; bracts lanceolate, 3–6 mm. *Pedicel* 2–3 cm. *Flowers* heterostylous. *Calyx* campanulate, 6–8 mm, parted to 1/3; lobes ovate to broadly lanceolate, margin 3-toothed at apex and occasionally entire in fruiting. *Corolla* purplish rose to purple-blue; tube 8–12 mm, with a tuft of white hairs projecting the yellowish green annulus in throat; limb 1.2–1.6 cm wide; lobes broadly obovate, 3-toothed. *Pin flowers*: stamens 5–6 mm above base of corolla tube; style nearly as long as tube. *Thrum flowers* with positions reciprocal. *Capsule* subglobose, included in calyx, disintegrating at maturity.

Distribution and habitat. The new species is presently known only from the type locality in Yunnan, Wenshan City, and is clustered in small groups in deep moss under secondary evergreen broad-leaved forests.

Phenology. Flowering from February to April, fruiting from April to June.

Etymology. Latin *surculus*, sucker, and suffix *-osa*, abundant, alluding to remarkable root-suckers (stolons), with long slender internodes and reduced leaves arising after anthesis.

Conservation status. Based on our field investigations in Wenshan City and adjacent regions (e.g., Pingbian, Maguan, Malipo and Mengzi) during the last three years, only one population with ca. 800 individuals of the new species has been found in an area of 10 km². Moreover, according to the result of our investigation in the villages near the type locality, the local folks often collect this new species as a medicinal plant. Therefore, the conservation status of the new species is assessed as vulnerable (VU D1+2) according to the guidelines for using the IUCN Red List categories and criteria (IUCN Standards and Petitions Subcommittee 2022).

Additional specimens examined (paratypes). The same locality as holotype, 9 May 2021, Deming He Xu210577 (IBSC!); 26 April 2022, Deming He Xu211017 (IBSC!); 2 July 2022, Deming He Xu221030 (IBSC!).

Relationship with related species. Group *Taliensis* is a small group of two species (*P. taliensis* and *P. comata*) in sect. *Petiolares*, characterized by plants without basal bud scales at anthesis, scape equaling or exceeding the leaves at flowering time, plant glandular hairy, and efarinose (Smith and Fletcher 1944). This group is mainly distributed in western Yunnan and adjacent northern Myanmar (Smith and Fletcher 1944). The present new species is assigned to this group, being distinctive in the markedly stoloniferous habit, and some other morphological features, which are summarized in Table 1.

Table 1. Main morphological differences between *Primula surculosa* and two similar species (Hu 1990; Hu and Kelso 1996).

Features	<i>P. surculosa</i>	<i>P. taliensis</i>	<i>P. comata</i>
Stolon	present	absent	absent
Leaves			
Indumentum	short appressed pubescent	short appressed pubescent	long fulvous hairs
Inner blade shape	ovate to suborbicular	ovate-rounded to reniform	elliptic
Petiole of inner leaves at fruiting	2–3 times as long as blade	1–2 times as long as blade	slightly longer than blade
Calyx lobe apex	3-teethed, occasionally entire in fruiting	subacuminate to acute, occasionally denticulate	obtuse to rounded
Corolla lobe apex	3-teethed	3-teethed	entire
Throat of the corolla tube	pilose	glabrous	pilose

The stolon, an unusual mechanism of vegetative propagation, is an outstanding feature of the new species. However, this feature appears to have multiple origins in this genus, since it also occasionally occurs in some species of other sections which are presumably not intimately connected, e.g., *P. heucherifolia* (sect. *Cortusoides* Balf. f.), *P. ranunculoides* (sect. *Ranunculoides* Chen et C.M.Hu), *P. caldaria* (sect. *Aleuritia* Duby), and *P. pseudodenticulata* (sect. *Denticulata* Watt) (Hu 1990; Hu and Kelso 1996; Shao et al. 2012). So the stolon may have no phylogenetic significance in the genus *Primula*.

Acknowledgements

The study was financially supported by the National Natural Science Foundation of China (grants no. 32070220 and 32070230), Guangdong Basic and Applied Basic Research Foundation (grant no. 2020A1515011578), Guangdong Forestry Bureau (Investigation, Monitoring, Conservation and Application Demonstration of Rare and Endemic Wild Plants and Medicinal Plants in Guangdong) and the Science and China Scholarship Council. We thank Yun-Xiao Liu for the line drawings of types.

References

- Hao G, Yuan YM, Hu CM, Ge XJ, Zhao NX (2004) Molecular Phylogeny of *Lysimachia* (Myrsinaceae s.l.) based on chloroplast *trnL-F* and nuclear ribosomal ITS sequences. *Molecular Phylogenetics and Evolution* 31(1): 323–339. [https://doi.org/10.1016/S1055-7903\(03\)00286-0](https://doi.org/10.1016/S1055-7903(03)00286-0)
- Hu CM (1990) *Primula*. In: Chen FH, Hu CM (Eds) *Flora Reipublicae Popularis Sinicae* Vol. 59. Science Press, Beijing, 1–245.
- Hu CM (1994) On the geographical distribution of the Primulaceae. *Redai Yaredai Zhiwu Xuebao* 2: 1–14.

- Hu CM, Kelso S (1996) Primulaceae. In: Wu ZY, Raven PH (Eds) Flora of China. Vol. 15. Beijing, Science Press, and St Louis, Missouri Botanical Garden Press, 99–185.
- IUCN Standards and Petitions Subcommittee (2022) Guidelines for using the IUCN Red List categories and criteria. Version 8.1.: Prepared by the Standards and Petitions Subcommittee in July 2022.
- Shao JW, Wu YF, Kan XZ, Liang TJ, Zhang XP (2012) Reappraisal of *Primula ranunculoides* (Primulaceae), an endangered species endemic to China, based on morphological, molecular genetic and reproductive characters. Botanical Journal of the Linnean Society 169(2): 338–349. <https://doi.org/10.1111/j.1095-8339.2012.01228.x>
- Smith WW, Fletcher HR (1944) The genus *Primula*: Section *Petiolares*. Transactions of the Royal Society of Edinburgh 61(2): 271–314. <https://doi.org/10.1017/S0080456800004750>

Danxiaorchis mangdangshanensis (Orchidaceae, Epidendroideae), a new species from central Fujian Province based on morphological and genomic data

Miao Zhang¹, Xiao-Hui Zhang^{1,2}, Chang-Li Ge^{1,2}, Bing-Hua Chen^{1,2}

1 College of Life Sciences, Fujian Normal University, Fuzhou 350117, China **2** The Public Service Platform for Industrialization Development Technology of Marine Biological Medicine and Products of the State Oceanic Administration, Fujian Key Laboratory of Special Marine Bioresource Sustainable Utilization, Southern Institute of Oceanography, College of Life Sciences, Fujian Normal University, Fuzhou 350117, China

Corresponding author: Bing-Hua Chen (bhchen@fjnu.edu.cn)

Academic editor: Timothée LePéchon | Received 12 August 2022 | Accepted 30 September 2022 | Published 28 October 2022

Citation: Zhang M, Zhang X-H, Ge C-L, Chen B-H (2022) *Danxiaorchis mangdangshanensis* (Orchidaceae, Epidendroideae), a new species from central Fujian Province based on morphological and genomic data. *PhytoKeys* 212: 37–55. <https://doi.org/10.3897/phytokeys.212.91534>

Abstract

Danxiaorchis mangdangshanensis, a new mycoheterotrophic species from Fujian Province, China, is described and illustrated. The new species is morphologically similar to *D. singchiana*, but its callus of labellum is a less distinctive Y-shape with three auricles on the apex, four pollinia that are narrowly elliptic in shape and equal in size, and it lacks fine roots. The plastome of *D. mangdangshanensis* is highly degraded. Phylogenetic analyses distinguished *D. mangdangshanensis* from its congeners, *D. singchiana* and *D. yangii*, with strong support based on nrITS + *matK* and plastomes, respectively.

Keywords

Chloroplast genome, Epidendroideae, morphology, phylogeny, taxonomy

Introduction

The Orchidaceae, one of the largest families of angiosperms, were classified into five subfamilies based on their morphological and molecular characteristics, including Apostasioideae, Cypripedioideae, Vanilloideae, Orchidoideae, and Epidendroideae,

with Epidendroideae being the largest (Chase et al. 2015). Identifying orchid species may be challenging, particularly during the vegetative stage when many orchid species plants exhibit very similar morphological characteristics. Moreover, many orchid species can crossbreed successfully across a wide range, giving rise to many intermediate types and natural variants. Therefore, phylogenetic analysis was more and more often employed to investigate the interrelationships among Orchidaceae species (Zhai et al. 2013; Lee et al. 2020; Li et al. 2020).

More than a few Epidendroideae species lack green leaves, resulting in reduced photosynthetic capacities and reliance on mycoheterotrophy for nourishment, i.e., indirectly exploiting other plants through mycorrhizal fungi (Brundrett 2009). Mycoheterotrophic plants, which are classified into two types, photosynthetic mycoheterotrophs and full mycoheterotrophs, are excellent examples of genomic modification due to relaxed selective constraints on photosynthetic function (Barrett et al. 2019). They possess distinct anatomical, physiological, and genomic features. One of these is a reduction in plastid genome size through loss or pseudogenization of photosynthesis-related genes. Early studies (Wolfe et al. 1992a; Wickett et al. 2008) suggested that the gene order of plastomes was conserved and that a large number of conserved genes were present; however, recent studies have revealed highly reduced (Delannoy et al. 2011; Wicke et al. 2013) and highly rearranged (Logacheva et al. 2014) plastomes. These findings indicate that mycoheterotrophic plants may have more diverse plastomes than previously thought.

Danxiaochis (Calypsoinae, Epidendreae), a recently identified fully mycoheterotrophic orchid genus, was characterized by a distinct Y-shaped callus in its labellum. Only two species of *Danxiaochis* have been documented, *D. singhiana* and *D. yangii* (Zhai et al. 2013; Yang et al. 2017). The plastid genome size of *D. singhiana* was found to have been dramatically reduced to 87,910 dp (Li et al. 2020), however there is no plastome data available for its only congener, *D. yangii*.

In this paper, we describe a new orchid species found in Mangdang Mountain, Nanping City, in Fujian, China. The plant has a distinct morphology from the other known *Danxiaochis* species. On the basis of morphological characteristics and molecular phylogenetic study, we propose a new species of *Danxiaochis* and describe it below.

Materials and methods

Morphological description

The morphological description of the new species was based on the study of specimens collected in a variety of spots in 2022. A stereoscopic zoom microscope (Carl Zeiss, Axio zoom. v.16, Germany), equipped with an attached digital camera (AxioCam), and a digital caliper were used to record the sizes of the morphological characters. Field observations provided habitats and phenology for the new species.

DNA extraction and sequencing

In this study, total DNA was extracted from freeze-dried gynostemium and the ovary of the new species using a DNeasy Plant Mini Kit (Qiagen, Valencia, CA, USA). The phylogenetic position of the new species was determined by nrITS and plastid *matK* sequences. The nrITS (18S-ITS1-5.8S-ITS2-26S) was assembled using GetOrganelle v1.7.5, with -R of 7 and k-mer set of “35, 85, 115”, the embplant_nr library was selected as the reference genome database, then annotated and visualized using Geneious v2021.2.2. The plastid *matK* was extracted from the genome sequence via Geneious v.2021.2.2.

Genome sequencing, assembly, annotation and analysis

Purified total DNA of the new species was fragmented, genome skimming was performed using next-generation sequencing technologies on the Illumina Novaseq 6000 platform with 150 bp paired-end reads and 480 bp insert size by Berry Genomics Co. Ltd. (Beijing, China), and 15.88 GB of reads was obtained.

The paired-end reads were filtered and assembled into complete plastome using a GetOrganelle v1.7.5.0 (Jin et al. 2020a) with appropriate parameters, with K-mer set “21,45,65,85,105”, the word size is 0.6. Following previous studies, our workflow includes five key steps as well: 1. Mapping reads to seed and assembling seed-mapped reads for parameter estimation; 2. Recruiting more target-associated reads through extending iterations; 3. Conducting de novo assembly; 4. Roughly filtering fortarget-like contigs; 5. Identifying target contigs and exporting all configurations (Camacho et al. 2009; Bankevich et al. 2012; Langmead and Salzberg 2012; Jin et al. 2020). Graphs of the final assembly were visualized by Bandage (Wick et al. 2015) to assess their completeness. Gene annotation was performed using CPGAVAS2 (Shi et al. 2019) and PGA (Qu et al. 2019). The different annotations of protein coding sequences were confirmed using BLASTx. The tRNAs were checked with tRNAscan-SE v2.0.3. Final chloroplast genome maps were created using OGDRAW.

Phylogenetic analysis

The phylogenetic relationship was constructed using Maximum likelihood (ML) and Bayesian Inference (BI) analyses with the combined ITS and *matK* sequences. In total, 39 samples of *Calypso*, *Changnienia*, *Chysis*, *Corallorhiza*, *Cremastra*, *Dactylosteinia*, *Danxiaorchis*, *Ephippianthus*, *Govenia*, *Tipularia*, *Yuania* and *Yunorchis* were included in our analysis. A species of *Chysis* was used as outgroup. Each individual locus was aligned using MAFFT 7.310 (Katoh and Standley 2013) with default settings. A concatenated supermatrix of the ITS sequences and *matK* was generated using PhyloSuite v1.1.15 (Zhang et al. 2019) for the phylogenetic analysis. All missing data were treated as gaps. The best nucleotide substitution model according to the Bayesian

Information Criterion (BIC) was K3Pu+F+R2, which was selected by ModelFinder (Kalyaanamoorthy et al. 2017) implemented in IQTREE v.1.6.8. Maximum likelihood phylogenies were inferred using IQ-TREE (Nguyen et al. 2015) under the model automatically selected by IQ-TREE ('Auto' option in IQ-TREE) for 2000 ultrafast (Minh et al. 2013) bootstraps. Bayesian Inference phylogenies were inferred using MrBayes 3.2.6 (Ronquist et al. 2012) under the GTR+F+G4 model (2 parallel runs, 2000000 generations). Phylograms were visualized in iTOLv.5 (iTOL: Interactive Tree Of Life (embl.de)).

To construct a phylogenetic tree based on plastome sequences, a total of 20 plastome sequences of *Calypso*, *Corallorhiza*, *Cremastra*, *Danxiaorchis*, *Cattleya*, *Anathallis*, *Masdevallia*, *Neofinetia* and *Calanthe* were included. Among them, *Calypso*, *Corallorhiza*, *Cremastra* and *Danxiaorchis* belong to Calypsoinae; *Cattleya* belongs to *Laeliinae*; and *Anathallis* and *Masdevallia* belong to *Pleurothallidinae*. *Neofinetia falcata* and *Calanthe triplicata* were used as outgroups. Each individual locus was aligned using MAFFT 7.310 (Katoh and Standley 2013) with default settings. The best nucleotide substitution model according to the Bayesian Information Criterion (BIC) was TVM+F+R4, which was selected by ModelFinder (Kalyaanamoorthy et al. 2017) implemented in IQTREE v.1.6.8. Maximum likelihood phylogenies were inferred using IQ-TREE (Nguyen et al. 2015) under the model automatically selected by IQ-TREE ('Auto' option in IQ-TREE) for 2000 ultrafast (Minh et al. 2013) bootstraps. Bayesian Inference phylogenies were inferred using MrBayes 3.2.6 (Ronquist et al. 2012) under the GTR+F+I+G4 model (2 parallel runs, 2000000 generations), in which the initial 25% of sampled data were discarded as burn-in. Phylograms were visualized in iTOLv.5 (iTOL: Interactive Tree Of Life (embl.de)).

Results

Comparative analysis of the plastomes

The plastome of *Danxiaorchis mangdangshanensis* was compared to those of the other 18 species in the subtribe Epidendreae. The plastome size of these species varied greatly from 85,273 bp in *D. mandangshanensis* to 157,423 bp in *Masdevallia coccinea* (a photosynthetic orchid) (Table 1), with the new species being the smallest. The length of the IR region of *D. mandangshanensis* was the shortest across all compared species, while the length of the LSC region was slightly longer than that of *D. singchiana*, but shorter than the remaining species studied. The SSC region of *D. mangdangshanensis* was intermediate in length compared to those of the other orchid species. The plastome size of mycoheterotrophic species showed high correlation with the size of both the SSC and IR.

Table 1. Statistics on the basic features of the plastid genomes of *Danxiaorchis mangdangshanensis* and related taxa.

Species	Accession No.	Voucher	Number of Genes			Length (bp)				GC Content (%)			
			PCGs	tRNA	rRNA	Total	LSC	SSC	IR	Total	LSC	SSC	IR
<i>Danxiaorchis mangdangshanensis</i>	OP122564	Huang & Chen	32	20	4	85,273	42,605	18,766	11,951	34.41	30.84	37.95	37.99
<i>Danxiaorchis singchiana</i>	MN990438	Jin	29	22	4	87,910	42,494	17,890	13,763	34.55	31.12	39.01	36.97
<i>Calypso bulbosa</i> var. <i>occidentalis</i>	MG874037	CFB	71	30	4	149,313	84,543	14,846	24,962	37.13	34.54	29.36	43.52
<i>Corallorhiza bentleyi</i>	MG874035	Freudenstein 2550	52	31	4	124,482	64,420	10,722	24,670	36.60	32.62	25.81	42.94
<i>Corallorhiza bulbosa</i>	KM390013	–	68	30	4	148,643	83,422	15,343	24,939	37.14	34.31	29.16	43.37
<i>Corallorhiza macrantha</i>	KM390017	Salazar A	66	30	4	151,031	84,262	12,545	27,112	37.21	34.42	29.38	43.35
<i>Corallorhiza mertensiana</i>	KM390018	Freudenstein 1999	54	30	4	147,941	81,109	13,774	26,529	36.78	33.92	28.10	43.41
<i>Corallorhiza odontorhiza</i>	KM390021	–	67	30	4	147,317	82,259	13,508	25,775	36.99	34.24	28.28	43.66
<i>Corallorhiza striata</i>	MG874034	CFB	47	29	4	141,202	75,701	13,319	26,091	36.34	33.12	27.33	43.27
<i>Corallorhiza trifida</i>	MG874036	Freudenstein 2763a	67	30	4	149,376	83,685	15,285	25,203	37.21	34.55	28.99	43.75
<i>Corallorhiza wisteriana</i>	KM390020	Freudenstein 2462	67	30	4	146,437	82,350	11,743	26,172	37.05	34.27	28.11	43.43
<i>Cremastra appendiculata</i>	MG925366	–	73	30	4	155,320	87,098	15,478	26,372	37.19	34.55	30.41	43.54
<i>Cattleya crispate</i>	KP168671	–	71	30	4	148,343	86,254	13,261	24,614	37.26	34.88	29.35	43.36
<i>Cattleya liliputana</i>	KP202881	–	71	30	4	147,092	85,804	13,900	23,694	37.35	34.88	30.19	43.45
<i>Anathallis obovata</i>	MH979332	UPCB:M.C. Santos	81	30	4	155,515	83,694	20,047	25,542	37.05	34.65	30.05	43.10
<i>Masdevallia coccinea</i>	KP205432	–	79	30	4	157,423	84,957	18,448	27,009	36.81	34.42	29.44	43.10
<i>Masdevallia picturata</i>	KJ566305	–	80	29	4	156,045	85,145	20,742	25,079	36.88	34.44	29.74	43.22
<i>Neofinetia falcate</i>	KT726909	PDBK	67	30	4	156,045	84,948	18,029	26,534	36.64	34.44	29.74	43.22
<i>Calanthe triplicata</i>	KF753635	–	80	30	4	132,271	87,263	18,476	26,510	36.74	34.40	29.73	43.03

Phylogenetic analysis

Phylogenetic relationships were first reconstructed by Maximum likelihood (ML) and Bayesian Inference (BI) analyses using combined ITS and *matK* sequences, as well as the plastome data. The nrITS and *matK* tree (Fig. 1) clearly indicated the distinctiveness of *Danxiaorchis mangdangshanensis* from its two congeners, *D. singchiana* and *D. yangii*, with strong support (PP = 1, BS = 100), and the new species is closer to *D. singchiana*. *Danxiaorchis* is sister to *Cremastra*, which is consistent with previous studies (Freudenstein et al 2017; Li et al. 2019; 2020). In addition, the phylogenetic analysis based on entire plastomes also separates the new species from *D. singchiana* with strong support (PP = 1, BS = 100) (Fig. 2).

Taxonomic treatment

Danxiaorchis mangdangshanensis Q. S. Huang, Miao Zhang, B. Hua Chen & Wang Wu, sp. nov.

urn:lsid:ipni.org:names:77307479-1

Figs 3–5

Diagnosis. *Danxiaorchis mangdangshanensis* can be easily distinguished from *D. singchiana* by having no fine roots, fewer flowers in the raceme, the side lobes of the labellum are ivory-white rather than yellow, and it has only 3 colored strips rather than 4–5 pairs. Additionally, its callus is a less distinctive Y-shape and has three auricles, with a purple-red spot on each auricle at the front, and the callus has a remarkable striped appendage adaxially. Furthermore, there are narrow wings on the side of column, and the four pollinia are narrowly elliptic in shape and equal in size.

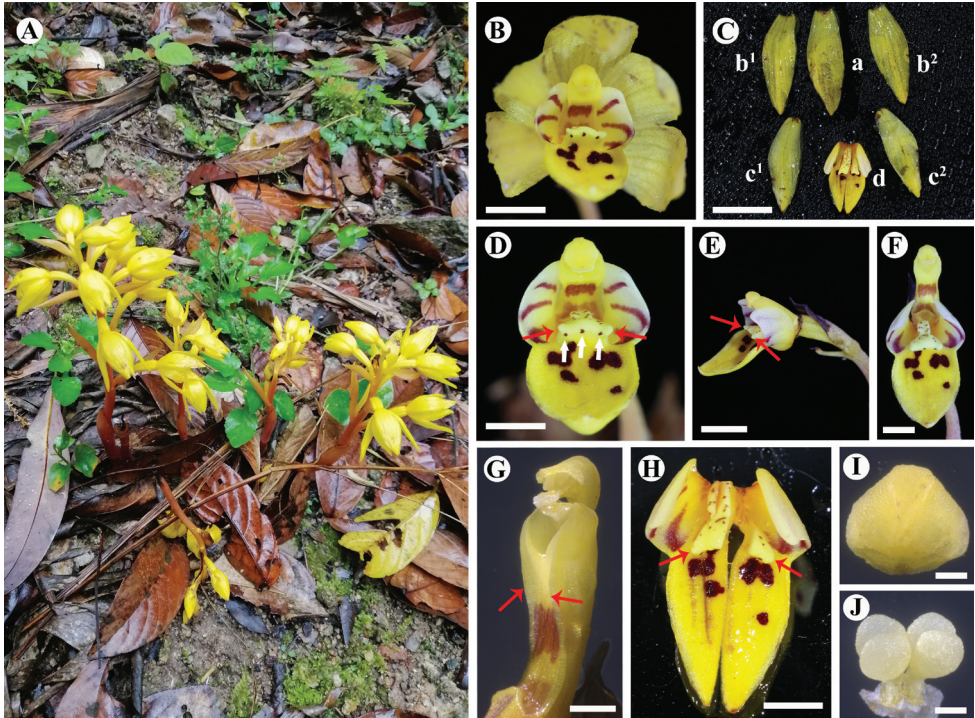


Figure 3. *Danxiaorchis mangdangshanensis* Q. S. Huang, Miao Zhang, B. Hua Chen & Wang Wu, sp. nov. **A** flowering and habitat (photographed by Wang Wu) **B** front view of a flower **C-a** dorsal sepal **C-b** lateral sepals **C-c** petals **C-d** labellum **D** gynostemium and labellum, front view, showing three purple-red spots (white arrows) on the Y-shaped callus (red arrows) **E** gynostemium and labellum, side view, showing three auricles (red arrows) **F** labellum, showing remarkable striped appendage **G** gynostemium, showing narrow wings on the both sides (red arrows) **H** cross section of labellum, showing indistinct Y-shaped callus (red arrows) **I** anther cap **J** pollinarium, front view, showing pollinia 4 in 2 pairs. Scale bars: 5 mm (**B**); 1 cm (**C**); 4 mm (**D**); 5 mm (**E**); 4 mm (**F**); 1 mm (**G**); 4 mm (**H**); 500 μ m (**I**, **J**).

Type. CHINA. Fujian (福建) Province, Nanping (南平) City, Yanping (延平) District, Mangdangshan Mountain, Mangdangshan National Nature Reserve, forest margins, 26°41'N, 118°2'E, elevation 375 m, 5 May 2022, Q.S. Huang & B. Hua Chen *CBH 04593* (Holotype, FNU, barcode FNU0041324; Isotype, FNU, barcode FNU0041325).

Description. Plant erect, 10.6–22.2 cm tall, holomycotrophic. Rhizome tuberous, fleshy, cylindrical, 2.5–5.3 cm long, 7.0–11.2 mm thick, with short branches, 4.5–5.6 mm long, without roots. Scape terete, pale red-brown, 4.2–5.8 mm thick, 3-sheathed; sheaths cylindrical, clasping stem, membranous, 16.2–43.4 × 4.5–8.7 mm. Inflorescence racemose, 2.9–9.6 cm long, 4- to 10-flowered; floral bracts oblong-lanceolate, 10.5–29.8 × 3.0–11.1 mm, apex acuminate, pale yellow; pedicel and ovary bright yellow, 13.8–22.9 mm long, glabrous; sepals yellow, obovate elliptic, dorsal sepals 13.5–17.2 × 4.8–6.5 mm, obtuse; lateral sepals 16.3–18.6 × 5.9–6.7 mm, obtuse; petals yellow, narrowly elliptic, 15.5–19.7 × 6.0–6.5 mm, acute; labellum 3-lobed, with 3 pairs of purple-red stripes on side lobes and purple-red spots on middle lobe; side lobes erect, ivory-white, slightly clasping the column, subsquare, 4.5–5.6 × 5.3–6.2 mm; mid-lobe oblong, 7.8–10.2 × 6.1–7.8 mm, apex acute to obtuse; labellum with two sacs at the base and a fleshy callus centrally, indistinctive Y-shaped (in the transition to “T-shape”), with 3 auricles on the apex, each of which has 1 purple-red spot at the front; callus extending from the base of disc to the base of mid-lobe, triangular at the base of mid-lobe, fleshy, ca. 3.1 mm wide, 0.25 mm long, narrows into a raised band when extended, ca. 1.5 mm wide, 0.4 mm long, with sparse purple-red spots; column cream colored, straight, semi-cylindrical, narrow wings on the side, 4.9–6.3 mm long, 2.9 mm wide, footless; stigma concave, triangular, terminal; anther cap ellipsoid, ca. 1.3 mm in diameter; pollinia four, in two pairs, narrowly elliptic, granular-farinaceous, composed of friable massulae, each

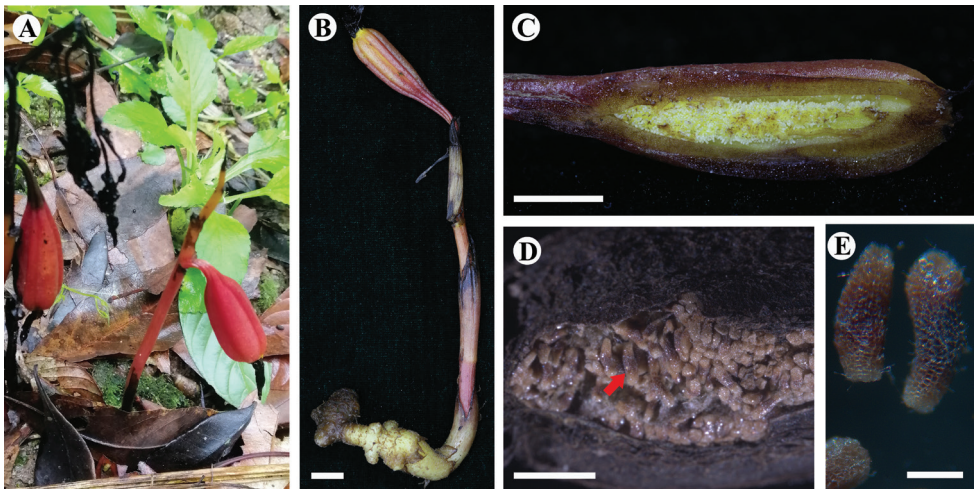


Figure 4. *Danxiaorchis mangdangshanensis* Q. S. Huang, Miao Zhang, B. Hua Chen & Wang Wu, sp. nov. **A** fruit-bearing plant (photographed by Wang Wu) **B** infructescence and rhizome **C** longitudinal section of immature capsule **D** mature capsule, showing mature seeds (red arrow) **E** mature seeds. Scale bars: 1 cm (**B, C**); 1 mm (**D, E**).

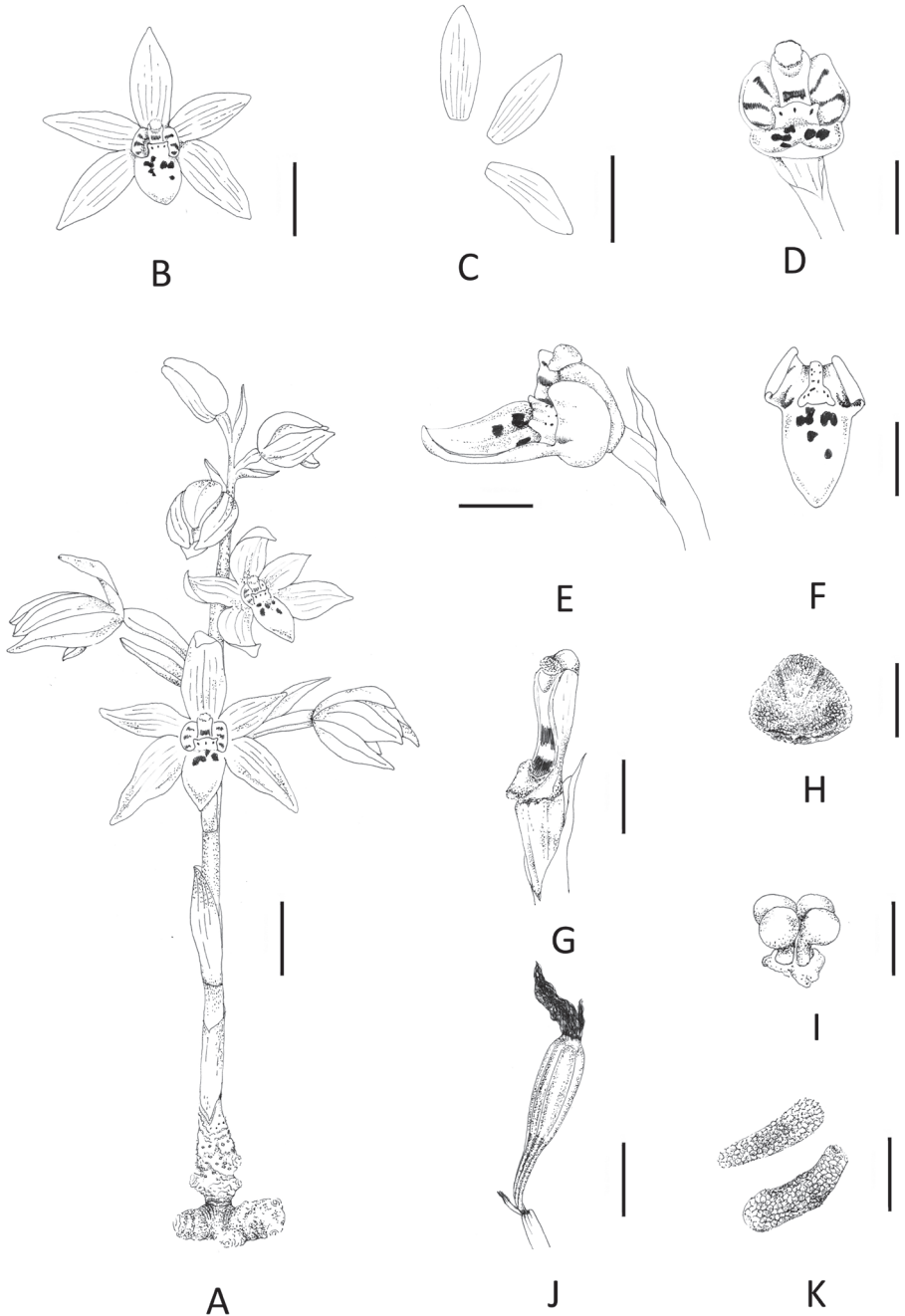


Figure 5. *Danxiaorchis mangdangshanensis* Q. S. Huang, Miao Zhang, B. Hua Chen & Wang Wu, sp. nov. **A** flowering plant **B** flower, front view **C** dissection of a flower, showing dorsal sepal, petal, lateral sepal **D** gynostemium and labellum, front view **E** gynostemium and labellum, side view **F** labellum **G** gynostemium **H** anther cap **I** pollinarium **J** immature capsule **K** mature seeds. Scale bars: 1.0 cm (**A, B, C, J**); 0.5 cm (**D–F**); 0.2 cm (**G**); 1.0 mm (**H, I, K**).

pair containing two pollinia equal in size with a thick caudicle attached to a common subsquare viscidium, ca. 0.5 mm in diameter. Capsule purple red, fusiform, 3 evident banded ridges, 37.3–46.8 mm long, 8.9–10.1 mm thick. Seeds light dark brown, cylindrical, 1.3×0.3 mm, fleshy, honeycombed stripes on the seed coat surface.

Distribution and habitat. *Danxiaorchis mangdangshanensis* is only found in Mangdangshan National Nature Reserve, Fujian, China (Fig. 6), where it grows at the margin of mid-subtropical evergreen broad-leaved forest, beside a canal near a *Musa balbisiana* forest. Many other plants grow in the surrounding habitat, whose tree layer includes *Castanopsis fargesii* Franch. (Fagaceae), *C. fissa* (Champion ex Benth) Rehder et E. H. Wilson (Fagaceae), and *Vernicia montana* Lour. (Euphorbiaceae); the shrub layer includes *Ficus erecta* Thunb. (Moraceae), *Fhirta* Vahl (Moraceae), *Maesa japonica* (Thunb.) Moritzi. ex Zoll. (Primulaceae), *Callicarpa kochiana* Makino (Lamiaceae), and *Aucuba chinensis* Benth. (Garryaceae); the vegetation layer includes *Angiopteris fokiensis* Hieron. (Marattiaceae), *Viola diffusa* Ging. (Violaceae), *Mazus fukiensis* Tsoong (Mazaceae), *Gynostemma pentaphyllum* (Thunb.) Makino (Cucurbitaceae), *Iris japonica* Thunb. (Iridaceae), *Musa balbisiana* Colla (Musaceae), and *Miscanthus floridulus* (Lab.) Warb. ex Schum et Laut. (Poaceae); the interlayer plants include *Fissistigma oldhamii* (Hemsl.) Merr. (Annonaceae), and *Stauntonia obovatifoliola* Hayata subsp. *urophylla* (Hand.-Mazz.) H.N.Qin (Lardizabalaceae).

Phenology. Flowering was observed from mid-April to early May, and fruiting from mid-May to mid-June.

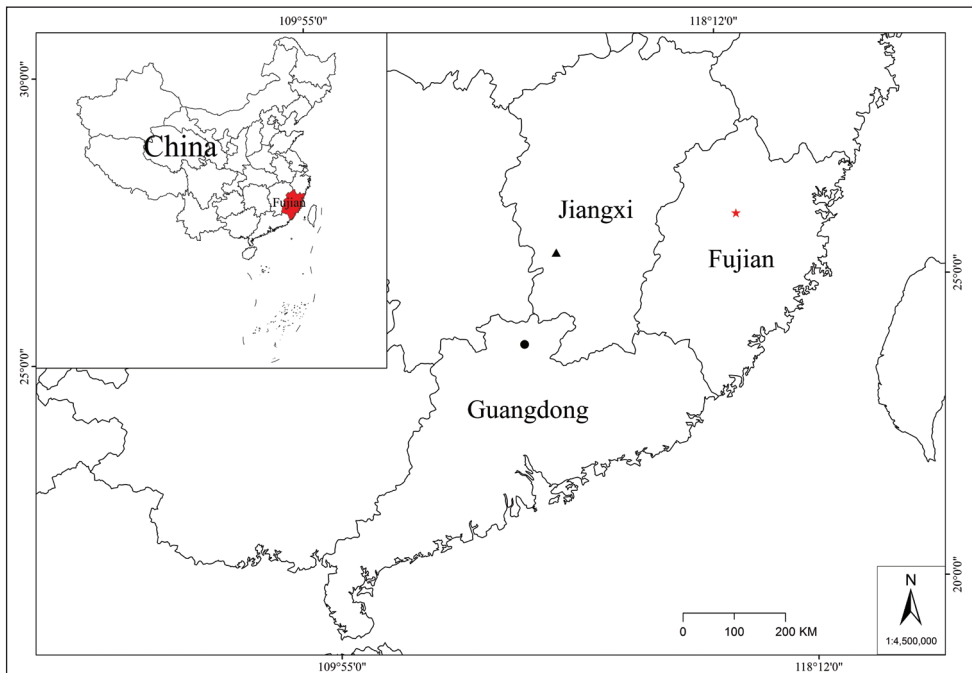


Figure 6. Distribution of *Danxiaorchis mangdangshanensis*, *D. singchiana*, *D. yangii* in China. Legend: (red star) *D. mangdangshanensis*, (black circle) *D. singchiana*, (black triangle) *D. yangii*.

Etymology. The *Mang dang shan dang xia lang* (茫荡山丹霞兰). The epithet *mangdangshanensis* (茫荡山) refers to Mangdangshan Mountain, Mangdangshan National Nature Reserve, Fujian Province where this new species was found.

Conservation status. During our fieldwork in 2022, three populations of about 14 plants of the new species were found in Mangdangshan National Nature Reserve, Fujian Province, China. And hence, we suggest its placement in the Data Deficient category of IUCN (2022). According to the Updated List of National Key Protected Wild Plants (Decree No. 15) by the country's State Forestry and Grassland Administration and the Ministry of Agriculture and Rural Affairs, *Danxiaorchis* are classified in the national secondary protection list. The new recorded genus should also be included on the national secondary protection list during the upcoming revision process.

Characteristics of the *Danxiaochis mangdangshanensis* plastome

The highly reduced plastid genome of *Danxiaochis mangdangshanensis* still has a quadripartite structure and is 85,273 bp with a large single-copy (LSC) region of 42,605 bp separated from a small single-copy (SSC) region of 18,766 bp by two inverted repeat regions (IRs), each of 11,951 bp (Fig. 7). A total of 56 unique genes were identified in the plastome and it contains 32 protein-coding genes, 20 tRNAs, and four rRNAs. A total of seven genes were duplicated in the IR regions, including *rpl22*, *rps19*, *trnH-GUG*, *rpl2*, *rpl23*, *trnI-CAU*, *ycf2* (Table 2). The total GC content of the plastome

Table 2. Gene contents in the plastid genome of *Danxiaorchis mangdangshanensis*.

Category, group of Genes	Gene names
Photosynthesis:	
Subunits of photosystem I	<i>psaC</i> , <i>psaI</i>
Subunits of photosystem II	–
Subunits of NADH dehydrogenase	–
Subunits of cytochrome b/f complex	<i>petG</i> , <i>petL</i> , <i>petN</i>
Subunits of ATP synthase	–
Large subunit of rubisco	–
Subunits photochlorophyllide reductase	–
Self-replication:	
Proteins of large ribosomal subunit	<i>rpl14</i> , <i>rpl16*</i> , <i>rpl2*(2)</i> , <i>rpl20</i> , <i>rpl22(2)</i> , <i>rpl23(2)</i> , <i>rpl32</i> , <i>rpl33</i> , <i>rpl36</i>
Proteins of small ribosomal subunit	<i>rps11</i> , <i>rps12**</i> , <i>rps14</i> , <i>rps16*</i> , <i>rps18</i> , <i>rps19(2)</i> , <i>rps2</i> , <i>rps3</i> , <i>rps4</i> , <i>rps7</i> , <i>rps8</i>
Subunits of RNA polymerase	–
Ribosomal RNAs	<i>rrn16S</i> , <i>rrn23S</i> , <i>rrn4.5S</i> , <i>rrn5S</i>
Transfer RNAs	<i>trnC-GCA</i> , <i>trnD-GUC</i> , <i>trnE-UUC</i> , <i>trnF-GAA</i> , <i>trnG-GCC</i> , <i>trnH-GUG (2)</i> , <i>trnI-CAU (2)</i> , <i>trnL-UAA*</i> , <i>trnL-UAG</i> , <i>trnM-CAU</i> , <i>trnN-GUU</i> , <i>trnP-UGG</i> , <i>trnQ-UUG</i> , <i>trnR-ACG</i> , <i>trnS-GGA</i> , <i>trnT-UGU</i> , <i>trnV-GAC</i> , <i>trnW-CCA</i> , <i>trnY-GUA</i> , <i>trnY-M-CAU</i>
Other genes:	
Maturase	<i>matK</i>
Protease	<i>clpP**</i>
Envelope membrane protein	–
Acetyl-CoA carboxylase	<i>accD</i>
c-type cytochrome synthesis gene	–
Translation initiation factor	<i>infA</i>
Genes of unknown function:	
Conserved hypothetical chloroplast ORF	<i>ycf1</i> , <i>ycf15</i> , <i>ycf2(2)</i>

Notes: *gene with one introns; **gene with two introns; #Pseudo gene; Gene (2): Number of copies of multi-copy genes.

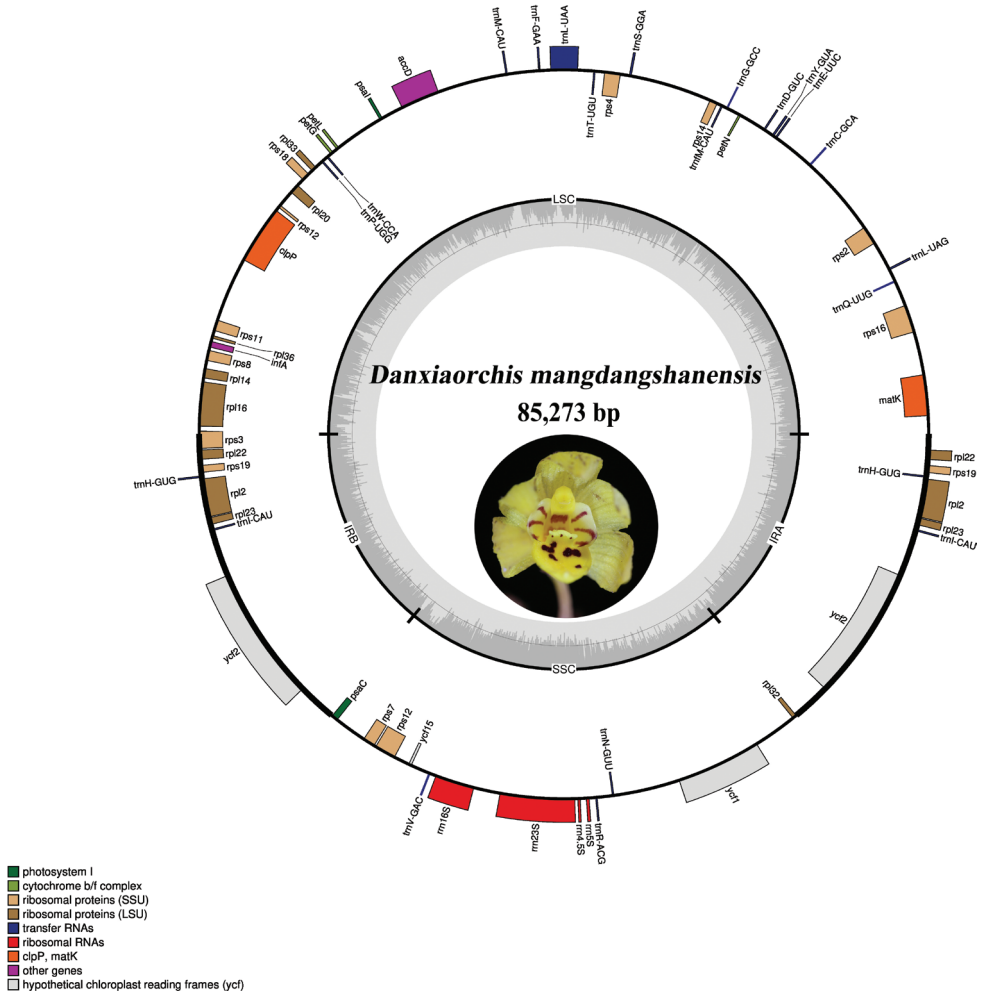


Figure 7. Circular gene map of the plastid genome of *Danxiaorchis mangdangshanensis*. Genes inside the circle are transcribed clockwise, while those drawn outside are transcribed counterclockwise. Genes are color-coded according to their functional groups. The circle inside the GC content graph marks the 50% threshold.

is 34.40%. Two inversions were detected in the plastome of *D. mangdangshanensis* (Suppl. material 1: Fig. S1), which are also reported for *D. singchiana* (Li et al. 2020). The annotated plastome was deposited in GenBank (accession number OP122564).

Discussion

The characteristic Y-shaped callus on its labellum clearly indicates the new species *Danxiaorchis mangdangshanensis* belongs to the genus *Danxiaorchis*, and this conclusion was strongly supported by phylogenetic analyses based on combined datasets of ITS and

matK, as well as the whole plastome. On the basis of a comprehensive morphological comparison, the new species can be distinguished from its two congeners, *D. singchiana* and *D. yangii* (Table 3). It was noticeable that the callus of *D. mangdangshanensis* had a less distinctive Y-shape, with three auricles on the apex, and a purple-red spot on each auricle at the front. Adaxially, the callus features a unique striped appendage. The Y-shaped callus of *D. yangii* was remarkably large and had an obovoid appendage at its base adaxially (Yang et al. 2017). Among the mycoheterotrophic taxa of Epidendroideae, *Danxiaorchis* have four sectile pollinia that are granular-farinaceous, with distinct caudicles and viscidium (Zhai et al. 2013; Yang et al. 2017). This configuration is unique in Epidendreae (i.e., *Yuania*; Chen et al. 2009), and its possible taxonomic significance awaits further study.

The plastome of *Danxiaorchis mangdangshanensis* was compared to those of the other 18 species in the subtribe Epidendreae. Although the genome sizes of the investigated species varied greatly, they all possessed typical quadripartite structures. This variance in genome size was mostly caused by variations in the length of the IR and SSC regions. The plastome of *Danxiaorchis* is more “degraded” than those of the other orchid species in the tribe Epidendreae examined, which is mostly due to gene losses associated with mycoheterotrophic habitats. However, the 15 essential genes among orchid plastomes to maintain minimal plastome activity (Kim et al. 2020) were all present in the plastome of *D. mangdangshanensis*, including the three subunits of *rpl* (14, 16, and 36), seven subunits of *rps* (2, 3, 4, 7, 8, 11, and 14), three subunits of *rrn* (5s, 16s, and 23s), *trnC-GCA*, and *clpP* genes. The IR region of *D. mangdangshanensis* was half that of most orchid species studied, and even smaller than its congener, *D. singchiana* (Li et al. 2020). The IR region plays a role in the structural stability of plastomes and its expansion or contraction due to changes in the amount of repeated DNA and/or changes in sequence complexity (Palmer and Thompson 1982).

The loss of the plastid genes within heterotrophic lineages occurred in a general order. The first was the loss of the NADH dehydrogenase-like (*ndh*) complex, which may frequently trigger irreversible evolutionary cascade losses of photosynthetic genes (*atp*, *psalpsb*, *pet*, *rbcL*, *ycf3*, 4) and a plastid-encoded RNA polymerase (*rpo*). Followed by the loss of housekeeping genes involved in basic organellar functions such as intron splicing and translation (*rpl*, *rps*, *rrn*, *trn*, *accD*, *clpP*, *matK*, *ycf1*, 2) (Barrett and Davis 2012; Kim et al. 2020). In *Danxiaorchis mandangshanensis*, the *ndh* genes have completely disappeared, which is common in mycoheterotrophic orchids. This is interesting because they are also lost or become pseudogenized in photosynthetic orchids, such as *Oncidium* (Wu et al. 2010) and *Phalaenopsis* (Chang et al. 2006), raising questions about their significance to photosynthetic chloroplasts. In addition, nearly all photosynthetic genes and the *rpo* gene were lost in *D. mangdangshanensis*, representing whole-organismal loss of photosynthetic functions, which thus is a major transitory event in both physiology and genome evolution of the plant. *Ycf3* and *ycf4*, which are crucial to photosystem polypeptide function, were lost in *D. mangdangshanensis*, although the former was present but has become pseudogene in *D. singchiana* (Li et al. 2020). Furthermore, several housekeeping genes, including *rps15* and some *trn* genes, were lost in *D. mangdang-*

Table 3. Morphological and distribution altitude differences between *Danxiaorchis mangdangshanensis*, *D. singchiana* and *D. yangii*.

Characteristics	<i>D. mangdangshanensis</i>	<i>D. singchiana</i>	<i>D. yangii</i>
Roots	Branches, no fine roots	Fine roots and branches	Fine branches, no fine roots
Flowers in the raceme	4–10	6–18	5–30
Color of side lobes of labellum	Ivory-white	Yellow	Yellow
Number of stripes on the side lobes callus	3	4–5	3
Front view of the callus	Indistinctive Y-shaped, three auricles at the front	Distinctive Y-shaped	Y-shaped, remarkable large
Callus adaxially bearing	3 distinct purple-red spots	None	None
Size of four pollinia	A remarkable striped appendage	An obovoid appendage	A remarkable obovoid appendage
Narrow wings on the side of the stamen column	Equal in size	Different in size	Equal in size
Distribution altitude/m	Yes	No	No
	ca. 370	ca.130	ca. 360

shanensis, which might be due to the increasing dependence on external carbon. It has been hypothesized that perhaps only a few loci, such as tRNA-Glu, tRNA-fMet, are absolutely essential in heterotrophic plants (Barbrook et al. 2006).

Plastid genome evolution in mycoheterotrophic lineages should be of concern in relation to the conservation of these plants, as many of them are rare or endangered (Leake 1994; Merckx and Freudenstein 2010). The mycoheterotrophs represent replicated evolutionary experiments in the loss of photosynthetic function, and its effect on genome evolution. It is evident that photosynthesis-related genes are the first to become pseudogenes or to be deleted in heterotrophic plants (Wolfe et al. 1992b; Wickett et al. 2008; Delannoy et al. 2011; Barrett and Davis 2012; Logacheva et al. 2014; Li et al. 2020). In spite of this, a number of questions remain unanswered regarding the evolution of heterotrophic plastomes, and the current study provides new information on these issues.

Acknowledgements

We are grateful to Ms. D.L. Cai for the illustration, Mr. Wang Wu for the finding and the preceding observation of the new species and Mr. Q.S. Huang for his kind help during our fieldwork. This work was financially supported by the biodiversity investigation programme of Fujian Mangdangshan National Nature Reserve (2022–2025), Special Project of Orchid Survey of National Forestry and Grassland Administration (contract no. 2020-07), the Sub-project VI of National Program on Key Basic Research Project (Grant No. 2015FY110200), the National Special Fund for Chinese medicine resources Research in the Public Interest of China (Grant No.2019-39), the Natural Science Foundation of Fujian Province (2020J05037 to MZ), the Foundation of Fujian Educational Committee (JAT190089 to MZ), and the scientific research innovation program “Xiyuanjiang River Scholarship” of College of Life Sciences, Fujian Normal University (22FSSK018).

References

- Bankevich A, Nurk S, Antipov D, Gurevich AA, Dvorkin M, Kulikov AS, Lesin VM, Nikolenko SI, Pham S, Prjibelski AD (2012) SPAdes: a new genome assembly algorithm and its applications to single-cell sequencing. *Journal of Computational Biology* 19: 455–477. <http://doi.org/10.1089/cmb.2012.0021>
- Barbrook AC, Howe CJ, Purton S (2006) Why are plastid genomes retained in non-photosynthetic organisms? *Trends Plant Science* 11: 101–108. <http://doi.org/10.1016/j.tplants.2005.12.004>
- Barrett CF, Davis JI (2012) The plastid genome of the mycoheterotrophic *Corallorhiza striata* (Orchidaceae) is in the relatively early stages of degradation. *American Journal of Botany* 99(9): 1513–1523. <http://doi.org/10.3732/ajb.1200256>
- Barrett CF, Sinn BT, Kennedy AH (2019) Unprecedented parallel photosynthetic losses in a heterotrophic orchid genus. *Molecular Biology and Evolution* 36 (9): 1884–1901. <http://doi.org/10.1093/molbev/msz111>
- Brundrett M (2009) Mycorrhizal associations and other means of nutrition of vascular plants: understanding the global diversity of host plants by resolving conflicting information and developing reliable means of diagnosis. *Plant and Soil* 320: 37–77. <https://doi.org/10.1007/s11104-008-9877-9>
- Camacho C, Coulouris G, Avagyan V, Ma N, Papadopoulos J, Bealer K, Madden TL (2009) BLAST+: architecture and applications. *BMC Bioinformatics* 10: 421–429. <https://doi.org/10.1186/1471-2105-10-421>
- Chang CC, Lin HC, Lin IP, Chow TY, Chen HH, Chen WH, Cheng CH, Lin CY, Liu SM, Chang CC, Chaw SM (2006). The chloroplast genome of *Phalaenopsis aphrodite* (Orchidaceae): Comparative analysis of evolutionary rate with that of grasses and its phylogenetic implications. *Molecular Biology and Evolution* 23: 279–291. <https://doi.org/10.1093/molbev/msj029>
- Chase MW, Cameron KM, Freudenstein JV, Pridgeon AM, Salazar G, van den Berg C Schuiteman A (2015) An updated classification of Orchidaceae. *Botanical Journal of the Linnean Society* 177(2): 151–174. <https://doi.org/10.1111/boj.12234>
- Chen SC, Liu ZJ, Zhu GH, Lang KY, Ji ZH, Luo YB, Jin XH, Cribb PJ, Wood JJ, Gale SW, Ormerod P, Vermeulen JJ, Wood HP, Clayton D, Bell A (2009) Orchidaceae. In: Wu ZY, Raven PH, Hong D (Eds) *Flora of China*, vol. 25. Science Press, Beijing & Missouri Botanical Garden Press, St. Louis, 210–221.
- Delannoy E, Fujii S, Colas des Francs-Small C, Brundrett M, Small I (2011) Rampant gene loss in the underground orchid *Rhizanthella gardneri* highlights evolutionary constraints on plastid genomes. *Molecular Biology and Evolution* 28: 2077–2086. <https://doi.org/10.1093/molbev/msr028>
- Freudenstein JV, Yukawa T, Luo Y-B (2017) A reanalysis of relationships among Calypsoinae (Orchidaceae: Epidendroideae): floral and vegetative evolution and the placement of *Yoania*. *Systematic Botany* 42(1): 17–25. <http://doi.org/10.1600/036364417x694944>
- IUCN (2022) Guidelines for using the IUCN red list categories and criteria. Version 15. Prepared by the Standards and Petitions Subcommittee. <https://www.iucnredlist.org/resources/redlistguidelines>

- Jin JJ, Yu WB, Yang JB, Song Y, Li DZ (2020) GetOrganelle: a fast and versatile toolkit for accurate de novo assembly of organelle genomes. *Genome Biology* 21: 241–272. <https://doi.org/10.1101/256479>
- Kalyaanamoorthy S, Minh BQ, Wong TKF, Haeseler AV, Jermiin L (2017) ModelFinder: fast model selection for accurate phylogenetic estimates. *Nature Methods* 14: 587–589. <http://doi.org/10.1038/nmeth.4285>
- Katoh K, Standley DM (2013) MAFFT multiple sequence alignment software version 7: improvements in performance and usability. *Molecular Biology and Evolution* 30: 772–780. <https://doi.org/10.1093/molbev/mst010>
- Kim YK, Jo S, Cheon SH, Joo MJ, Hong JR, Kwak M, Kim KJ (2020) Plastome evolution and phylogeny of Orchidaceae, with 24 new sequences. *Frontiers in Plant Science* 11: e22. <http://doi.org/10.3389/fpls.2020.00022>
- Langmead B, Salzberg SL (2012) Fast gapped-read alignment with Bowtie 2. *Nature Methods* 9: 357–359. <https://doi.org/10.1038/nmeth.1923>
- Leake JR (1994) The biology of mycoheterotrophic ('saprophytic') plants. *New Phytologist* 127(2): 171–216. <http://doi.org/10.1111/j.1469-8137.1994.tb04272.x>
- Lee SY, Meng K, Wang H, Zhou R, Liao W, Chen F, Zhang S, Fan Q (2020) Severe plastid genome size reduction in a mycoheterotrophic orchid, *Danxiaorchis singchiana*, reveals heavy gene loss and gene relocations. *Plants* 9: e521. <http://doi.org/10.3390/plants9040521>
- Li YX, Li ZH, Schuiteman A, Chase MW, Li JW, Huang WC, Hidayat A, Wu SS, Jin XH (2019) Phylogenomics of Orchidaceae based on plastid and mitochondrial genomes. *Molecular Phylogenetics and Evolution* 139: e106540. <http://doi.org/10.1016/j.ympev.2019.106540>
- Li ZH, Jiang Y, Ma X, Li JW, Yang JB, Wu JY, Jin XH (2020) Plastid genome evolution in the subtribe Calypsoinae (Epidendroideae, Orchidaceae). *Genome Biology and Evolution* 12(6): 867–870. <https://doi.org/10.1093/gbe/evaa091>
- Logacheva MD, Schelkunov MI, Nuraliev MS, Samigullin TH, Penin AA (2014) The plastid genome of mycoheterotrophic monocot *Petrosavia stellaris* exhibits both gene losses and multiple rearrangements. *Genome Biology and Evolution* 6: 238–246. <http://doi.org/10.1093/gbe/evu001>
- Merckx V, Freudenstein JV (2010) Evolution of mycoheterotrophy in plants: a phylogenetic perspective. *New Phytologist* 185: 605–609. <http://doi.org/10.1111/j.1469-8137.2009.03155.x>
- Minh BQ, Nguyen MAT, von Haeseler A (2013) Ultrafast approximation for phylogenetic bootstrap. *Molecular Biology and Evolution* 30: 1188–1195. <https://doi.org/10.1093/molbev/mst024>
- Nguyen LT, Schmidt HA, von Haeseler A, Minh BQ (2015) IQ-TREE: a fast and effective stochastic algorithm for estimating maximum-likelihood phylogenies. *Molecular Biology and Evolution* 32: 268–274. <https://doi.org/10.1093/molbev/msu300>
- Palmer JD, Thompson WF (1982) Chloroplast DNA rearrangements are more frequent when a large inverted repeat sequence is lost. *Cell* 29: 537–550. [http://doi.org/10.1016/0092-8674\(82\)90170-2](http://doi.org/10.1016/0092-8674(82)90170-2)
- Qu XJ, Moore MJ, Li DZ, Yi TS (2019) PGA: a software package for rapid, accurate, and flexible batch annotation of plastomes. *Plant Methods* 15(1): 1–12. <http://doi.org/10.1186/s13007-019-0435-7>

- Ronquist F, Teslenko M, van der Mark P, Ayres DL, Darling A, Höhna S, Larget B, Liu L, Suchard MA, Huelsenbeck JP (2012) MrBayes 3.2: efficient Bayesian phylogenetic inference and model choice across a large model space. *Systematic Biology* 61: 539–542. <http://doi.org/10.1093/sysbio/sys029>
- Shi L, Chen H, Jiang M, Wang L, Wu X, Huang L, Liu C (2019) CPGAVAS2, an integrated plastome sequence annotator and analyzer. *Nucleic Acids Research* 47(W1): W65–W73. <https://doi.org/10.1093/nar/gkz345>
- Wick RR, Schultz MB, Zobel J, Holt KE (2015). Bandage: interactive visualization of *de novo* genome assemblies. *Bioinformatics* 31: 3350–3352. <https://doi.org/10.1093/bioinformatics/btv383>
- Wickert NJ, Zhang Y, Hansen SK, Roper JM, Kuehl JV, Plock SA, Wolf PG, dePamphilis CW, Boore JL, Goffinet B (2008) Functional gene losses occur with minimal size reduction in the plastid genome of the parasitic liverwort *Aneura mirabilis*. *Molecular Biology and Evolution* 25: 393–401. <https://doi.org/10.1093/molbev/msm267>
- Wicke S, Muller KF, dePamphilis CW, Quandt D, Wickert NJ, Zhang Y, Renner SS, Schneeweiss GM (2013) Mechanisms of functional and physical genome reduction in photosynthetic and nonphotosynthetic parasitic plants of the broomrape family. *Plant Cell* 25: 3711–3725. <https://doi.org/10.1105/tpc.113.113373>
- Wolfe KH, Katz-Downie DS, Morden CW, Palmer JD (1992a) Evolution of the plastid ribosomal RNA operon in a nongreen parasitic plant: Accelerated sequence evolution, altered promoter structure, and tRNA pseudogenes. *Plant Molecular Biology* 18: 1037–1048. <http://doi.org/10.1007/BF00047707>
- Wolfe KH, Morden CW, Palmer JD (1992b) Function and evolution of a minimal plastid genome from a nonphotosynthetic parasitic plant. *Proceedings of the National Academy of Sciences of the United States of America* 89: 10648–10652. <http://doi.org/10.1073/pnas.89.22.10648>
- Wu FH, Chan MT, Liao DC, Hsu CT, Lee YW, Daniell H, Duvall MR, Lin CS (2010) Complete chloroplast genome of *Oncidium* Gower Ramsey and evaluation of molecular markers for identification and breeding in Oncidiinae. *BMC Plant Biology* 10: e68. <https://doi.org/10.1186/1471-2229-10-68>
- Yang B, Xiao S, Jiang Y, Luo H, Xiong D, Zhai J, Li B (2017) *Danxiaorchis yangii* sp. nov. (Orchidaceae: Epidendroideae), the second species of *Danxiaorchis*. *Phytotaxa* 306(4): 287–295. <https://doi.org/10.11646/phytotaxa.306.4.5>
- Zhai JW, Zhang GQ, Chen LJ, Xiao XJ, Liu KW, Tsai WC, Hsiao YY, Tian HZ, Zhu JQ, Wang MN, Wang FG, Xing FW, Liu ZJ (2013) A new orchid genus, *Danxiaorchis*, and phylogenetic analysis of the tribe Calypsoeae. *PLoS ONE* 8(4): e60371. <http://doi.org/10.1371/journal.pone.0060371>
- Zhang D, Gao FL, Jakovlić I, Zou H, Zhang J, Li WX, Wang GT (2019) PhyloSuite: an integrated and scalable desktop platform for streamlined molecular sequence data management and evolutionary phylogenetics studies. *Molecular Ecology Resources* 20: 348–355. <https://doi.org/10.1111/1755-0998.13096>

Supplementary material I

Appendix S1

Authors: Miao Zhang, Xiao-Hui Zhang, Chang-Li Ge, Bing-Hua Chen

Data type: Docx file.

Explanation note: **Figure S1.** The two inversions in the plastome of *Danxiaorchis mangdangshanensis*. **Table S1.** GenBank information for the taxa used in the present study (matK and nrITS). **Table S2.** GenBank information for the taxa used in the present study (plastid genome).

Copyright notice: This dataset is made available under the Open Database License (<http://opendatacommons.org/licenses/odbl/1.0/>). The Open Database License (ODbL) is a license agreement intended to allow users to freely share, modify, and use this Dataset while maintaining this same freedom for others, provided that the original source and author(s) are credited.

Link: <https://doi.org/10.3897/phytokeys.212.91534.suppl1>

Phedimus daeamensis (Crassulaceae), a new species from Mt. Daeam in Korea

Tae-Young Choi^{1*}, Dong Chan Son^{2*}, Takashi Shiga³, Soo-Rang Lee¹

1 Department of Biology Education, College of Education, Chosun University, Gwangju 61452, Republic of Korea **2** Division of Forest Biodiversity and Herbarium, Korea National Arboretum, Pocheon 11186, Republic of Korea **3** Faculty of Education, Niigata University, Niigata, Japan

Corresponding author: Soo-Rang Lee (ra1130@hotmail.com, ra1130@chosun.ac.kr)

Academic editor: Yassen Mutafchiev | Received 22 February 2022 | Accepted 28 September 2022 | Published 3 November 2022

Citation: Choi T-Y, Son DC, Shiga T, Lee S-R (2022) *Phedimus daeamensis* (Crassulaceae), a new species from Mt. Daeam in Korea. *PhytoKeys* 212: 57–71. <https://doi.org/10.3897/phytokeys.212.82604>

Abstract

Phedimus individuals from Mt. Daeam, once referred to as *Phedimus sikokianus*, exhibit certain morphological characters that are unique within the genus. *Phedimus* is one of the most notorious groups for taxonomic problems due to the high morphological variation found in leaf shape, stem numbers, phyllotaxis and seed structure. Taxa in *Phedimus* also easily hybridize, further leading to taxonomic confusion. To carefully confirm the identity of the putative new species from Mt. Daeam, we examined morphological characters from ~100 herbarium sheets of six closely related *Phedimus* species. A molecular phylogenetic approach was also employed to delimit the species boundary and infer the phylogenetic relationships among the seven *Phedimus* species, including the species from Mt. Daeam. Both morphological and molecular phylogenetic results indicated that the species found on Mt. Daeam is a new species that is more closely related to *P. middendorffianus* and *P. takeshimensis* than to the remaining four *Phedimus* species. Here, we provided a full description of the new species *P. daeamensis* as well as an updated key for the seven *Phedimus* species examined.

Keywords

Molecular diagnosis, new species, *Phedimus*, phylogeny

* Those authors contributed equally to this work.

Introduction

Until 't Hart (1995) resurrected the genus *Phedimus* Rafinesque (Rafinesque 1817) by separating it from *Sedum*, the taxonomic group had been buried for approximately over a century. Since its resurrection, ca. 20 species have been added to *Phedimus* (Fu et al. 2001; 't Hart and Bleij 2003). Most taxa in the genus are distributed throughout Eurasia; their primary habitats are rocky slopes and grasslands (Fu et al. 2001). It is now widely accepted that the two genera, *Phedimus* and *Sedum*, are primarily distinguished by their leaf and testa shapes, which is further supported by several molecular studies (Ohba et al. 2000; Mayuzumi and Ohba 2004; Gontcharova et al. 2006; Gontcharova and Gontcharov 2009). *Phedimus*, a perennial herb, is divided into two subgenera (*Phedimus* and *Aizoon*) that differ in petal colors, sterile stems, and testa structures. In East Asia, approximately 15 taxa are recognized based on the aforementioned morphological traits, with more emphasis on the number of stems and phyllotaxis (Borisova 1939; Fu et al. 2001; Ohba 2001). However, in many cases, the delimitation of taxa is challenging because of the extensive morphological variations (Mayuzumi and Ohba 2004; Moon and Jang 2020) within the genus. Furthermore, the wide use of *Phedimus* as a core source of horticultural cultivars complicates the taxonomic issues (Stephenson and Harris 1991; Han et al. 2020). Given the taxonomic challenges, reporting a new species only by morphological features (e.g., Chao 2020) may need an additional molecular examination.

There are eight *Phedimus* species including two endemic species and one with two infraspecific taxa in Korea [*Phedimus aizoon* (L.) 't Hart var. *aizoon*, *P. aizoon* (L.) 't Hart var. *latifolius* (Maxim.) H. Ohba, *P. kamtschaticus* (Fisch. & C.A. Mey.) 't Hart, *P. latiovalifolius* (Y.N. Lee) D.C. Son & H.J. Kim, *P. middendorffianus* (Maxim.) 't Hart, *P. selskianus* (Regel & Maack) 't Hart, *P. takesimensis* (Nakai) 't Hart, *P. zokuriensis* (Nakai) 't Hart] (Park 2007; Korea National Arboretum 2021). According to Lee et al. (2003), all Korean species belong to the subgenus *Aizoon*. However, some species show considerable intraspecific morphological variation leading to taxonomic confusion, particularly where identity and species boundaries are concerned (Ryu et al. 2011; Moon and Jang 2020). *Phedimus kamtschaticus* (Fisch.) 't Hart is a compelling example of the marked infraspecific morphological variation (e.g., wide variety of leaf shapes) (Park 2007; Moon and Jang 2020). In fact, during a 2019 study of specimens at the herbarium of the Korea National Arboretum (KH), multiple sheets collected on Mt. Daeam and Gangwon province differed substantially from the rest of the collection. Specimens with unique morphotypes were identified as *P. kamtschaticus* or *P. middendorffianus* (Maxim.) 't Hart. (Oh 1985; Oh et al. 2015). Of those, the Mt. Daeam specimens were identified as *P. sikokianus* (Chung and Kim 1989); however, the distribution of this species is restricted to high mountain areas in Japan, suggesting that the Mt. Daeam specimens were likely misidentified. Accordingly, a close investigation of the *Phedimus* plants collected on Mt. Daeam was carried out.

Mt. Daeam, is a high-altitude mountain (> 1300 m) in Korea, which owing to its diverse geographical and environmental characteristics is an area of substantial biodiversity (Ministry of Environment 2007). The primary soil components of Mt. Daeam are granite and gneiss followed by sand (~11%), silt, and clay (~10%; Ministry of Environment 2007). Notably, Korea's only reported peatland (Min et al. 2000; Kim et al. 2005), Yongneup, which consists of five swamps, is located in high altitudes (1000–1200 m) of the mountain. The climate is typically temperate with cold and humid conditions (average annual temperature = ~10 °C and average annual relative humidity = 71%; Ministry of Environment 2007), thus serving as a refuge for several northern plants (Min et al. 2000; Kim et al. 2005). Over 300 taxa, including 20 Korean endemics, have been recorded on Mt. Daeam, and ca. 70 are protected by Korean law (Ministry of Environment 2007). The unique environmental properties of Mt. Daeam may have contributed to high species richness as discoveries of new plant taxa are ongoing (Lee et al. 2013; Gil et al. 2019).

In the present study, we report a new plant species, *P. daeamensis* T.Y. Choi & D.C. Son of the genus *Phedimus* subgenus *Aizoon*. We described the morphological characters and habitat features of the new species with a detailed botanical illustration in gray-scale hand drawing. To delimit the species boundary from the six closest related taxa, we performed morphological observations as well as a molecular phylogenetic study. A key to the Korean species of *Phedimus* (subgenus *Aizoon*) including the new species was established based on the examined morphological characters.

Materials and methods

Morphological examination

We collected four living samples of *P. daeamensis* and prepared a voucher specimen. Referring to the relevant protologues, floras, and monographs (Fu et al. 2001; Ohba 2001; Lee et al. 2003; Park 2007), we determined six target congeneric taxa for examination. All samples used for the study were collected legally. To compare the morphological characteristics of the new species with the six most closely related congeners, we borrowed ca. 100 herbarium specimens deposited in the KH and the Makino Herbarium (Suppl. material 1: Table S1). Using an Olympus dissecting stereo microscope (SZX16), morphological observations were made on all parts of the plants with a particular focus on the shape of leaves and leaf parts as well as the features of the reproductive organs. Microscopic floral parts such as the carpels and stamens were dissected when required. Five characters associated with the leaf (the phyllotaxis, length and width of the leaves, shape of the petioles, and the blades), and several associated with the flower (including size and shape of the calyx lobes, number and shape of the petals, and numbers of stamen and carpel; Table 1 and Suppl. material 1: Table S2; Fig. 1) were assessed.

Molecular diagnosis

To delimit the new species from the six most closely related taxa we examined their phylogeny. Sixteen samples of the seven taxa (three *P. daeamensis* and remaining of the six closely relatives) were collected from 14 localities across South Korea and Japan (see Suppl. material 1: Table S3). Three samples of the new species were included to determine the species' monophyly. We first examined the three regions of cpDNA (*atpF-atpH* IGS, *trnL-trnF* IGS, and *psbA-trnH* IGS) and the nrITS region discovered by Mayuzumi and Ohba (2004) in test samples from all seven taxa. After the DNA polymorphism test, we excluded the *atpF-atpH* and *trnL-trnF* IGS regions because of the lack of polymorphism among the seven taxa. Genomic DNAs of the 16 samples were extracted from either fresh or dried leaf samples using DNeasy plant mini kit (Qiagen, Hilden, Germany) following the manufacturer's protocol. The PCR amplifications were carried out using GeneAmp PCR system 9700 with a total reaction volume of 50 μ L containing 50 ng of template DNA. The amplification conditions are provided in Suppl. material 1: Table S4. After a series of purification steps performed by MacroGen (Seoul, Korea), the PCR products were sequenced on an ABI Prism 3730XL genetic analyzer (Applied Biosystems, Waltham, USA) using ABI Prism BigDye terminator v 3.1 cycle sequencing kit (Applied Biosystems, Waltham, USA) at the MacroGen facility (MacroGen, Seoul, Korea).

We also included seven accessions of three *Phedimus* taxa (*P. latiovalifolius*, *P. aizoon* var. *floribundus*, *P. takesimensis*) downloaded from GenBank to test the species boundaries across all *Phedimus* taxa co-occurring in Korea and Japan (Suppl. material 1: Table S5). We assigned two *Rhodiola* species (*Rhodiola brevipetiolata* and *R. alsia*) to the out-group based on previous phylogenetic research (Mayuzumi and Ohba 2004). All sequences were edited and aligned using Geneious Aligner in Geneious Prime ver. 2020.0.5, whereas other parameters were set as defaults. We then manually adjusted the aligned sequences. All DNA sequences obtained from the study were deposited in GenBank (accession numbers in Suppl. material 1: Table S3). We inferred phylogeny for the nrITS and cpDNA regions independently. Data concatenation was not considered because previous studies on *Phedimus* phylogeny showed substantial incongruence between nrITS and cpDNA trees (Seo et al. 2020). The phylogenetic trees were instead inferred from maximum likelihood (ML) and Bayesian interference (BI) methods. ML analyses were performed using RAxML plugin v4.0 implemented in Geneious Prime with the GTR CAT approximation (Lartillot and Philippe 2004). Node supports were evaluated with 1000 bootstrap replicates (Felsenstein 1985). BI analyses were performed in MrBayes 3.2.6 (Ronquist and Huelsenbeck 2003) using four chains (three heated and one cold) for 5 million generations while sampling every 1000th generation. The first 25% of the samples were discarded as a burn-in, and the remaining trees were used to produce a 50% majority-rule consensus tree.

Results

Morphological examination

We used the plant habit, leaf shapes, and margins to distinguish the newly described *Phedimus* species (Fu et al. 2001; Ohba 2001; Lee et al. 2003; Park 2007). *Phedimus aizoon*, *P. kamtschaticus*, and *P. takesimensis* were easily distinguished from the five remaining species by height (> 20 cm) and leaf margin (entirely toothed; Table 1). *Phedimus daeamensis* was morphologically most similar to *P. middendorffianus* and *P. sikokianus* in terms of the following characters: fibrous roots, not robust, and stems shorter than 20 cm, somewhat prostrate (Table 1). However, *P. daeamensis* was distinguished from *P. middendorffianus* by its leaf shape (*P. daeamensis* leaf shape-obovate, 1–2.3 cm long; leaf margins with 4–5 teeth from apex to mid; sepals (calyx lobes) lanceolate) and from *P. sikokianus* by its leaf phyllotaxis and seed shape (Fig. 1 and Table 1).

Table 1. Summary of diagnostic characters observed in *Phedimus daeamensis* and the two morphologically closest taxa. The full diagnostic morphological characters of all seven *Phedimus* taxa investigated in the study are presented as supplementary information (Suppl. material 1: Table S2).

	<i>P. middendorffianus</i>	<i>P. sikokianus</i>	<i>P. daeamensis</i>
Leaves	alternate	opposite	alternate
• blade shape	linear-spatulate	widely oblanceolate to obovate	obovate
• blade size	1.2–4 cm long, 0.2–0.5 cm wide	0.8–2.3 cm long, 0.6–1.3 cm wide	1–2.3 cm long, 0.5–1.2 cm wide
• margins	margin apically serrate 2–3, apex obtuse	margin apically to mid crenate 2–4, apex rounded	margin apically to mid serrate 4–5, apex obtuse
Calyx lobes	5, linear, 2–3 mm long, apex obtuse	5, lanceolate, 2–3 mm long, apex obtuse	5, lanceolate, 3–4 mm long, apex obtuse
Seeds	obovoid	ellipsoid, ca. 0.8–1 mm long	obovoid, ca. 0.7–1 mm long

Taxonomic treatment

***Phedimus daeamensis* T.Y. Choi & D.C. Son, sp. nov.**

urn:lsid:ipni.org:names:77307628-1

Fig. 1

Type. REPUBLIC OF KOREA. Gangwon-do, Inje-gun, Buk-myeon, Wolhak-ri, Mt. Dae-am. Elevation 1,000 m. 20 August 2014. K.H. Lee & S.K. So 0001 (holotype KH; isotypes 2 sheet, KH).

Perennial herbs. Rhizome woody, elongated. Roots not tuberous; rootstock not robust. Stems numerous, more basally branched, tufted, creeping, ascending, 12–21 cm long, glabrous. Leaves alternate, sessile, coarsely arranged; leaf blade obovate, 1–2.3 cm long, 0.5–1.2 cm wide, flat, base narrowly cuneate, margin apically to mid serrate 4–5×, entire at base, apex obtuse; lower leaves almost all entire. Inflorescence

corymbiform-cymose, many-flowered; bracts leaf-like. Flowers bisexual, mostly 5-merous, shortly pedicelled. Calyx tube 2.1–3.2 mm long; lobes spurless, lanceolate, 1–1.2 mm long, apex obtuse. Petals free, yellow, lanceolate to oblong, 5–6.5 mm long, abaxially keeled, apex acuminate, spreading at anthesis. Stamens 10, in 2 series, erect, shorter than petals, those opposite to petals adnate to them to 1/4 of length from the base; anthers red, ellipsoid, ca. 1 mm long; filaments yellow. Pistils 4.5–5 mm long; ovaries ca. 2.5 mm long, connate at the base; styles slender, 2–3 mm long. Carpels 5, erect, equaling or slightly shorter than the petals, adaxially gibbous, shortly connate at the base. Follicles greenish, stellately and horizontally spreading, ca. 4 mm long, with a very short beak. Seeds 0.8–0.9 mm long, brown, obovoid, scalariform, ribbed, striate.

Flowers in May to June, fruiting in July to August.

Distribution and habitat. Republic of Korea (Prov. Gangwon). Stony cliffs and rock crevices, at ca. 1000 m.

Etymology. The specific epithet, “*daeamensis*”, is based on the name of the location, Mt. Daeam, where *Phedimus daeamensis* was discovered.

Korean name. Dae-am-gi-rin-cho.

Molecular diagnosis. In total, 32 sequences of two DNA regions (ITS and *psbA-trnH* IGS) were newly obtained from the 16 accessions of *P. daeamensis* and the six most closely related taxa (Suppl. material 1: Table S3). We also used 15 sequences from eight accessions obtained from GenBank (*P. aizoon* var. *floribundus*, *P. latiovalifolius*, *P. takesimensis*) for the phylogenetic analysis. The lengths of the ITS and *psbA-trnH* IGS alignment were 588 and 272 base pairs, respectively (Table 2). After an alignment of 24 accessions, we found 173 variable sites and 144 of these were parsimony informative (Table 2 and Suppl. material 1: Table S6). Overall, the GC ratio was 50.5% and 22.5% for ITS and *psbA-trnH* IGS, respectively (Table 2). K2P genetic distances among in-group individuals ranged from 0 to 0.043 (mean 0.023) for ITS and 0 to 0.048 (mean 0.018) for *psbA-trnH* IGS (Table 2). We also found a 6 bp inversion in the *psbA-trnH* IGS of all *P. daeamensis* accessions and one accession of *P. takesimensis* (Suppl. material 1: Table S6). We excluded this inversion from further phylogenetic analysis.

Overall, the inferred phylogenies from the two regions differ, particularly in the basal nodes (Figs 2, 3). There was a congruence between the ML and BI trees inferred from the ITS and *psbA-trnH* IGS data sets (Figs 2, 3, Suppl. materials 2, 3: Figs S1, S2; posterior probabilities are indicated in ML trees). In the *psbA-trnH* IGS trees, *P. daeamensis* was separated but formed an unresolved polytomy (Fig. 3 and Suppl. material 3: Fig. S2). *Phedimus sikokianus* formed a monophyletic group, whereas all other species showed more complicated and mixed clustering patterns (Fig. 3 and Suppl. material 3: Fig. S2). In the ITS trees, two major clades were recognized, but only clade 1 was statistically robust (Fig. 2 and Suppl. material 2: Fig. S1). The three samples of the putative new species, *P. daeamensis*, formed a well-supported monophyletic clade (bootstrap value; BS = 95%; posterior probability; PP = 0.99) that was separated from the other species. *Phedimus daeamensis* again formed a clade together with *P. middendorffianus* (one sample) and *P. takesimensis* (three samples), but the statistical support was very weak (Fig. 2 and Suppl. material 2: Fig. S1). All accessions of *P. sikokianus* formed a well-supported clade

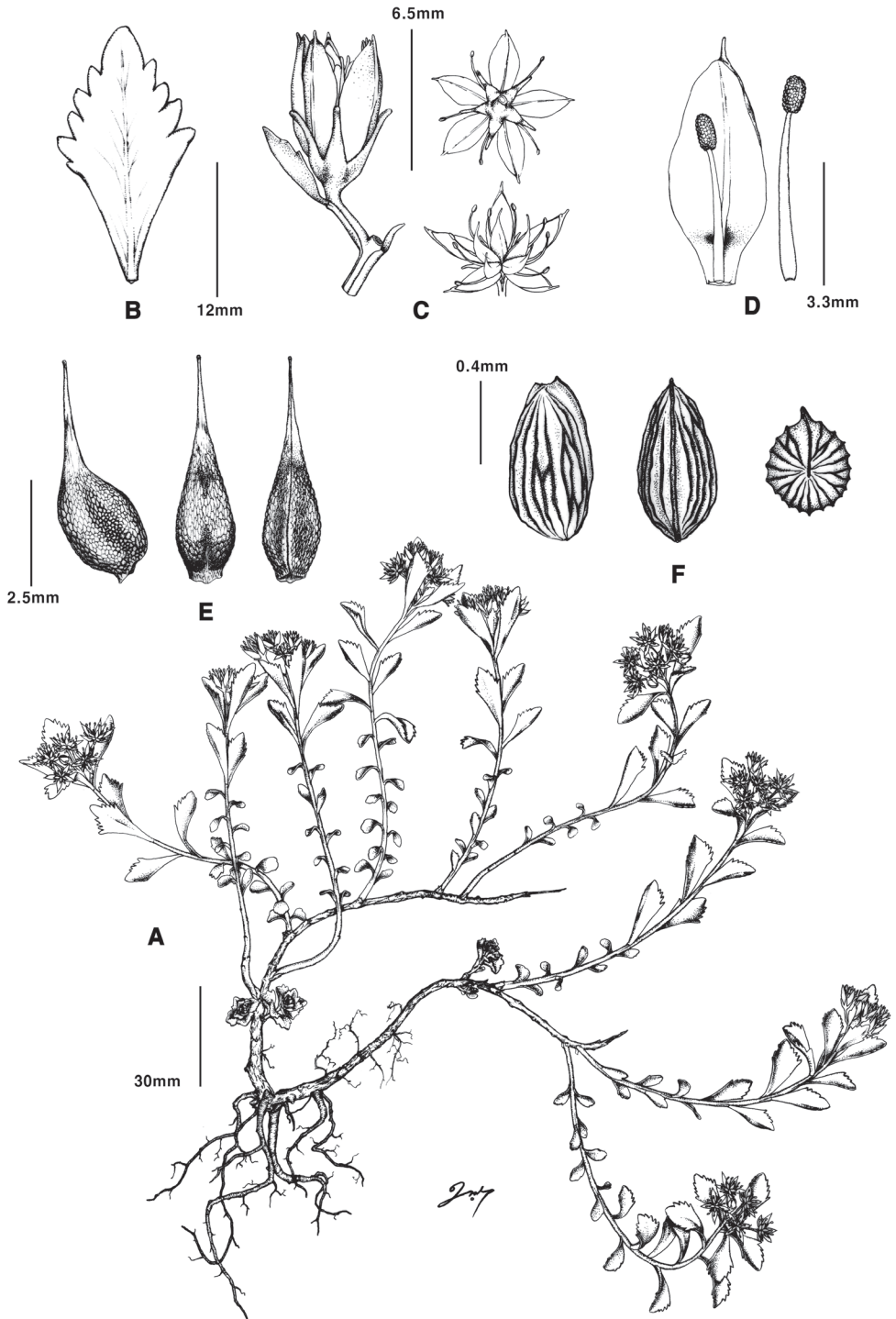


Figure 1. *Phedimus daeamensis* **A** habit **B** leaf **C** flower **D** petal and stamen **E** carpel **F** seed. (Illustrated by Kyungsoo Eo).

(BS = 95.9%; PP = 0.99) with samples of *P. kamtschaticus* and *P. aizoon*, both of which were not monophyletic (Fig. 2, Suppl. material 2: Fig. S1). *Phedimus latiovalifolius* was nested within a clade containing samples of *P. kamtschaticum* and *P. aizoon* (Fig. 2).

Table 2. Results of the cpDNA data sets used in this study. The out-group taxa were included in the analyses, except for the K2P distance.

	ITS	<i>psbA-trnH</i> IGS
Sequence length (bp)	572–579	234–266
Aligned length (bp)	588	272
Mean G+C ratio (%)	50.5	22.5
No. of variable characters	144	29
No. of parsimony informative characters (%)	120 (85.7)	24 (82.8)
K2P distance (mean)*	0–0.043 (0.023)	0–0.048 (0.018)

* Out-group taxa excluded.

Key to *Phedimus daeamensis* and related species

- 1 Stems 1–3, erect; leaves lanceolate, apex acuminate..... *Phedimus aizoon*
- Stems many, ascending to prostrate; leaves spatulate, obovate, oblanceolate or elliptic-oblanceolate, apex obtuse to rounded **2**
- 2 Roots thick, robust; stems 20–50 cm long, ascending **3**
- Roots fibrous; stems less than 20 cm long, prostrate **4**
- 3 Leaves oblanceolate or spatulate, margins serrate in upper half.....
..... *Phedimus takesimensis*
- Leaves spatulate, obovate or elliptic, margins entire or with few acute to obtuse teeth *Phedimus kamtschaticus*
- 4 Leaves broadly ovate, margins irregularly dentate ... *Phedimus latiovalifolius*
- Leaves obovate to linear, margins serrate or crenate **5**
- 5 Leaves obovate, somewhat concave **6**
- Leaves linear-spatulate or elliptic-oblanceolate, flat **7**
- 6 Leaves opposite, margins crenate, seeds ellipsoid *Phedimus sikokianus*
- Leaves alternate, margins serrate, seeds obovoid *Phedimus daeamensis*
- 7 Stems prostrate; leaves 1.2–2.5 cm × 3–5 mm, with 2 or 3 teeth.....
..... *Phedimus middendorffianus*
- Stems decumbent; leaves 2.5–3.5 cm × 1.1–1.6 cm, with many teeth.....
..... *Phedimus zokuriensis*

Discussion

Phedimus has been a rather unexplored taxonomic group until the resurrection of the genus by Hart (1995). Since then, the genus has attracted substantial attention because of its frequent use in horticultural practices (Han et al. 2020). However, *Phedimus* is difficult to categorize taxonomically because of complex morphological variations,

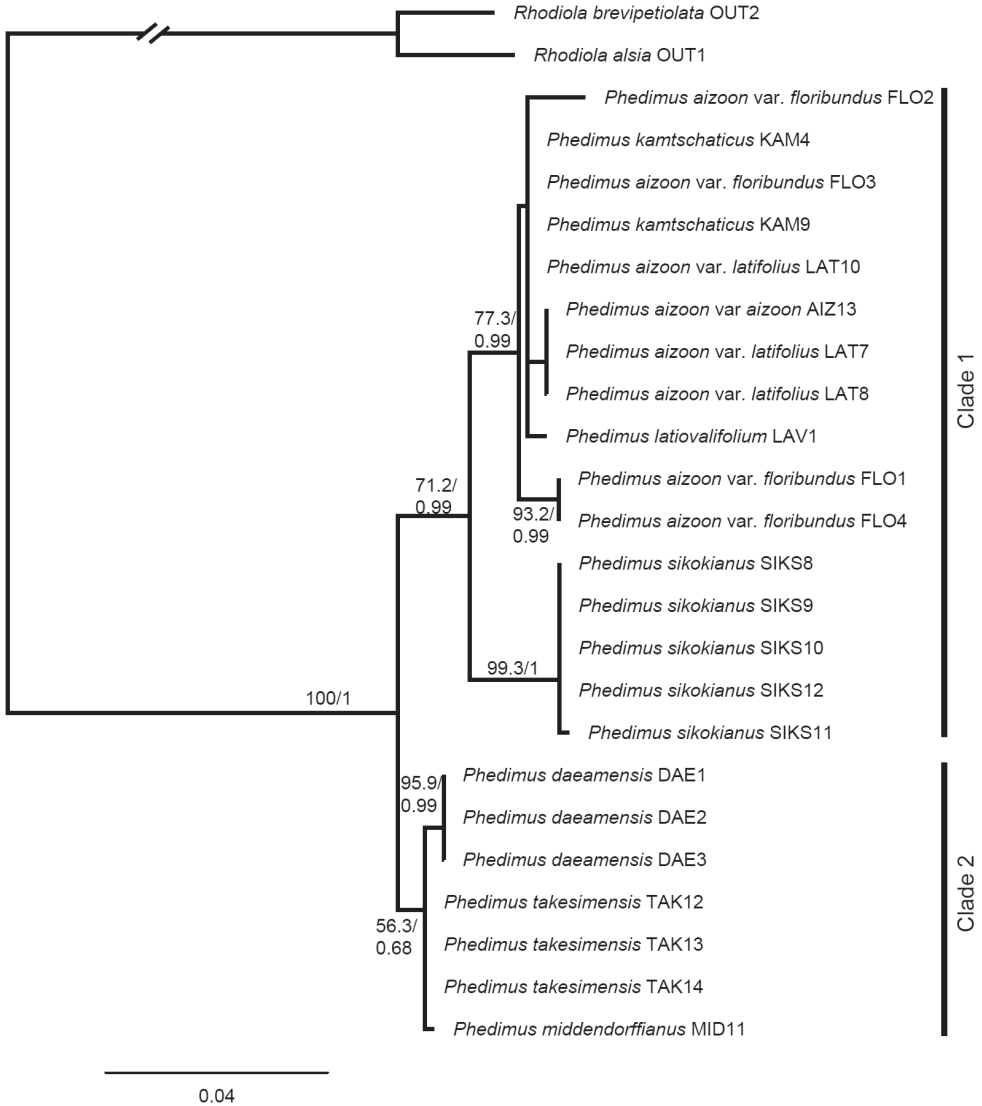


Figure 2. Maximum likelihood tree for individuals of *Phedimus daeamensis* and related taxa based on nrITS. Numbers above branches indicate bootstrap values (> 50%) and posterior probabilities (> 0.5).

potential hybridization, and introgression among congeneric taxa (Yoo and Park 2016; Han et al. 2020). The possibility of polyploidy (including aneuploidy in *Phedimus*) was also suggested by several empirical studies (Baldwin 1943; Uhl and Moran 1972; Amano 1990; Amano and Ohba 1992; Chung et al. 2020). Accordingly, taxon delimitation in the genus *Phedimus* based solely on morphological characters can easily be misleading and inconclusive, particularly in the early developmental stages when there are no well-developed reproductive organs present. With the recent advancement of molecular tools, molecular markers have helped overcome many of the limitations

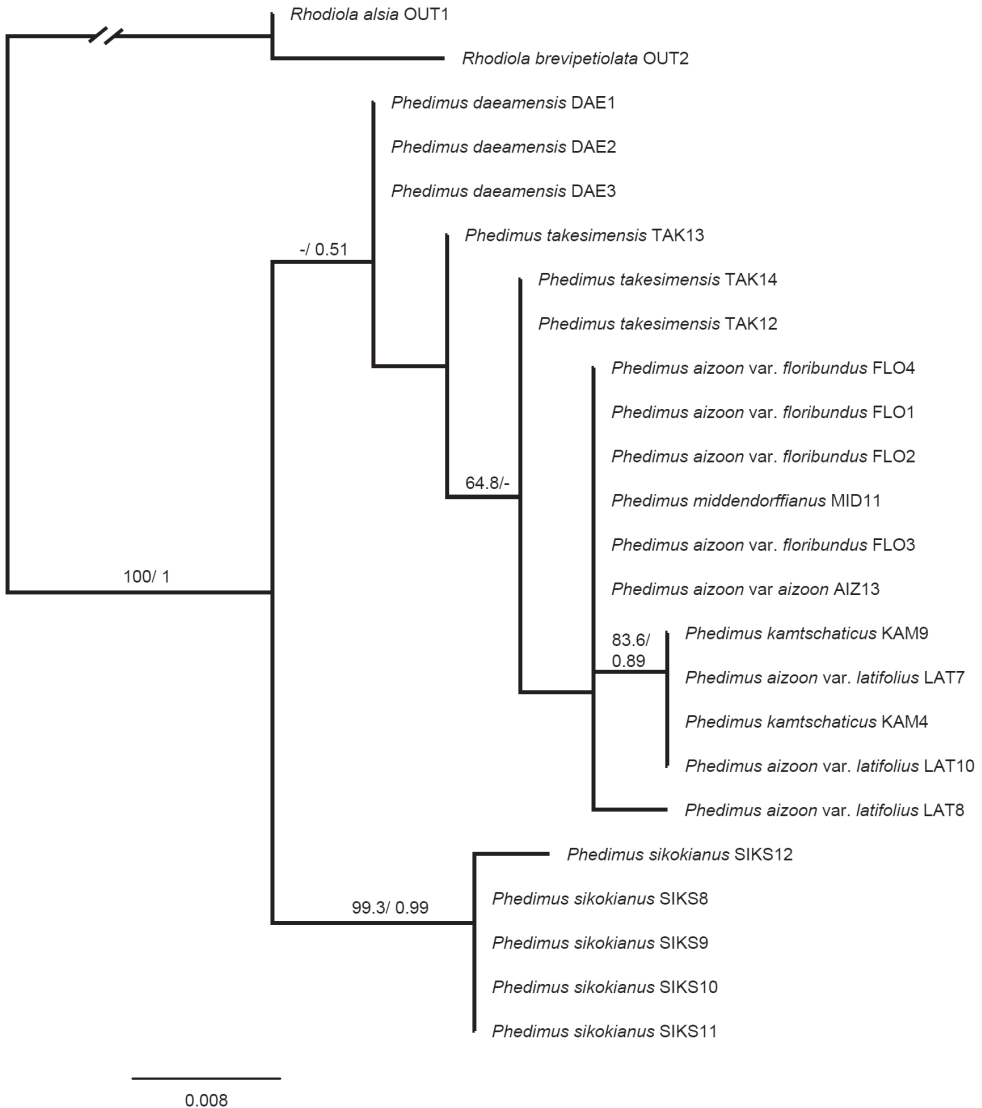


Figure 3. Maximum likelihood tree for individuals of *Phedimus daeamensis* and related taxa based on *psbA-trnH* IGS. Numbers above branches indicate bootstrap values (> 50%) and posterior probabilities (> 0.5).

associated with species delimitation (Pelser et al. 2017; Perkins 2019). Coupled with morphological examinations, our molecular analysis found that *P. daeamensis* is well-separated from the *P. kamtschaticus* complex and *P. sikokianus*, although the taxa were nearly indistinguishable by morphological characters in the early developmental stages.

Overall, our study characterized the morphological distinctiveness of the newly described species (*P. daeamensis*) from the six closest related congeners. However, most characters of examination were vegetative and thus showed significant

intraspecific variation across varying environments. *Phedimus kamtschaticus* and *P. aizoon* showed substantial morphological variation. Although *P. kamtschaticus*, the most commonly occurring *Phedimus* species in Korea (Korea National Arboretum 2016), can easily be distinguished from the newly described species (*P. daeamensis*) when the plants are fully mature, the identification may not be as straightforward in the early stage of the development. Our results highlighted a key morphological feature differentiating *P. daeamensis* from *P. kamtschaticus*; however, extreme care must be taken with juvenile plants. *Phedimus daeamensis* was initially recognized as *P. sikokianus* by Chung and Kim (1989) because of its morphological affinities. According to our results, the putative new species differs from *P. sikokianus* by the type of phyllotaxis and the seed shape, but intraspecific variations in those characters should be considered. The leaf shape of *P. middendorffianus* was prominently linear, which differs substantially from the remaining congeners; however, a very limited number of specimens were examined in our study (Suppl. material 1: Table S1). The morphological analyses we performed provided several key characters distinguishing *P. daeamensis* from the remaining six *Phedimus* taxa, however, some taxa, e.g., *P. middendorffianus* and *P. sikokianus*, only had a limited number of sheets. Therefore, we further employed a molecular phylogenetic approach to support the morphological results.

Notably, phylogenetic trees reconstructed based on the ITS and *psbA-trnH* IGS regions were consistent with the morphological results. In both ML trees from nrITS and cpDNA, the three morphotypes sharing the same morphological characters as the newly reported *P. daeamensis* came out as a monophyletic group or as an unresolved polytomy. *Phedimus daeamensis* was always placed separate from both *P. kamtschaticus* and *P. sikokianus*, but the phylogenetic relationship of the species with its closest related taxa was inconclusive because of low clade support and inconsistency between nrITS and cpDNA trees. In the ITS trees, *P. daeamensis* fell into the same clade as *P. takesimensis* and *P. middendorffianus* (Fig. 2), whereas in the *psbA-trnH* IGS trees, *P. daeamensis* was “sister” to all other species except for *P. sikokianus* (Fig. 3). Although the phylogenetic relationship among *P. daeamensis*, *P. takesimensis*, and *P. middendorffianus* was rather ambiguous, the taxa were relatively easy to distinguish based on morphological characters. *Phedimus takesimensis* was much larger (20–50 cm tall) and characterized by thick roots, whereas *P. middendorffianus* has linear leaves. Considering all the evidence and consistent with our hypothesis, *P. daeamensis* is a species in its own right and well-separated from the remaining six species.

Acknowledgements

This work was supported by the National Research Foundation of Korea (NRF) grant funded by the Korea government(MSIT) (No. NRF-2021R1A6A3A01086610). We thank Dr. Jungsim Lee and Kang Hyup Lee for providing valuable specimens and materials. We also thank Kyungsoo Eo for providing Fig. 1.

References

- Amano M (1990) Biosystematic study of *Sedum* L. subgenus *Aizoon* (Crassulaceae). Cytological and morphological variations of *Sedum aizoon* L. var. *floribundum* Nakai. Botanical Magazine Tokyo 103: 67–85. <https://doi.org/10.1007/BF02488412>
- Amano M, Ohba H (1992) Biosystematic study of *Sedum* L. subgenus *Aizoon* (Crassulaceae) II. Chromosome Numbers of Japanese *Sedum aizoon* var. *aizoon*. Botanical Magazine Tokyo 105: 431–441. <https://doi.org/10.1007/BF02497658>
- Baldwin JT (1943) Polyploidy in *Sedum pulchellum*-I. Cytogeography. Bulletin of the Torrey Botanical Club 70(1): 26–33. <https://doi.org/10.2307/2481678>
- Borisova AG (1939) Crassulaceae. Flora USSR. Botanical Institute of the Academy of Sciences of the USSR, Moskwa and Leningrad, 8–133.
- Chao Z (2020) *Phedimus yangshanicus* (Crassulaceae), a new species from limestone hills in Guangdong, China. Phytotaxa 429: 148–156. <https://doi.org/10.11646/phytotaxa.429.2.5>
- Chung YH, Kim JH (1989) A taxonomic study of *Sedum* section *Aizoon* in Korea. Korean Journal of Plant Taxonomy 19(4): 189–227. <https://doi.org/10.11110/kjpt.1989.19.4.189>
- Chung GY, Choi MJ, Nam B, Choi HJ (2020) Chromosome numbers of 36 vascular plants in South Korea. Journal of Asia-Pacific Biodiversity 13(3): 504–510. <https://doi.org/10.1016/j.japb.2020.06.009>
- Felsenstein J (1985) Confidence limits on phylogenies: An approach using the bootstrap. Evolution; International Journal of Organic Evolution 39(4): 783–791. <https://doi.org/10.1111/j.1558-5646.1985.tb00420.x>
- Fu K, Ohba H, Gilbert MG (2001) Crassulaceae. In: Wu ZY, Raven PH (Eds) Flora of China vol. 8. Science Press and Missouri Botanical Garden, Beijing and St. Louis, 202–268.
- Gil H-Y, Lee K-H, Ha Y-H, Jang C-S, Kim D-K (2019) *Sparganium glomeratum* (Typhaceae): A new record from South Korea. Korean Journal of Plant Taxonomy 49(4): 374–379. <https://doi.org/10.11110/kjpt.2019.49.4.374>
- Gontcharova SB, Gontcharov AA (2009) Molecular phylogeny and systematics of flowering plants of the family Crassulaceae DC. Molecular Biology 43(5): 794–803. <https://doi.org/10.1134/S0026893309050112>
- Gontcharova SB, Artyukova EV, Gontcharov AA (2006) Phylogenetic relationships among members of the subfamily Sedoideae (Crassulaceae) inferred from the ITS region sequences of nuclear rDNA. Russian Journal of Genetics 42(6): 654–661. <https://doi.org/10.1134/S102279540606010X>
- Han SK, Kim TH, Kim JS (2020) A molecular phylogenetic study of the genus *Phedimus* for tracing the origin of “Tottori Fujita” cultivars. Plants 9(2): e254. <https://doi.org/10.3390/plants9020254>
- Kim B-W, Lee J-S, Oh Y-J (2005) A study on the flora in the Mt. Daeam high moor. Journal of Environmental Science (Korea) 11: 1–8.
- Korea National Arboretum (2021) Checklist of Vascular Plants in Korea (Native Plants). Korea National Arboretum, 1–1006.

- Korea National Arboretum (2016) Distribution Maps of Vascular Plants in Korea. Korea National Arboretum, 1–809.
- Lartillot N, Philippe H (2004) A Bayesian mixture model for across-site heterogeneities in the amino-acid replacement process. *Molecular Biology and Evolution* 21(6): 1095–1109. <https://doi.org/10.1093/molbev/msh112>
- Lee K, Yoo Y-G, Park K-R (2003) Morphological relationships of Korean species of *Sedum* L. subgenus *Aizoon* (Crassulaceae). *Korean Journal of Plant Taxonomy* 33(1): 1–15. <https://doi.org/10.11110/kjpt.2003.33.1.001>
- Lee BY, Kwak M, Han JE, Jung E-H, Nam G-H (2013) Ganghwal is a new species, *Angelica reflexa*. *Journal of Species Research* 2(2): 245–248. <https://doi.org/10.12651/JSR.2013.2.2.245>
- Mayuzumi S, Ohba H (2004) The phylogenetic position of eastern Asian Sedoideae (Crassulaceae) inferred from chloroplast and nuclear DNA sequences. *Systematic Botany* 29(3): 587–598. <https://doi.org/10.1600/0363644041744329>
- Min WK, Chang C-S, Jeon JI, Kim H, Choi DY (2000) Flora of Mt. Dae-am-san. *Bulletin of Seoul National University Arboretum* 20: 38–82.
- Ministry of Environment (2007) 2007 Detailed Investigation of Wetland Protection Area - Yongneup of Mt. Daeam and Jangdo Wetland of Shinan Province, 1–488.
- Moon A-R, Jang C (2020) Taxonomic study of genus *Sedum* and *Phedimus* (Crassulaceae) in Korea based on external morphology. *Korean Journal of Plant Resources* 33: 116–129.
- Oh S-Y (1985) The phytogeographical studies of Crassulaceae in Korea. *Research Review of Kyungpook National University* 39: 123–159.
- Oh H, Kim Y, Kim E, Kim D, Kim S, Eum J (2015) Conservation management methods and flora in the Hanbuk Jeongmaeka. *Proceedings of the Korean Society of Environment and Ecology Conference* 25: 7–8.
- Ohba H, Bartholomew BM, Turland NJ, Kunjun F (2000) New combinations in *Phedimus* (Crassulaceae). *Novon* 10: 400–402. <https://doi.org/10.2307/3392995>
- Ohba H (2001) Crassulaceae. In: Iwatsuki K, Boufford DE, Ohba H (Eds) *Flora of Japan*. Kodansha, Tokyo, 10–31.
- Park KR (2007) *Sedum*. In: *Flora of Korea Editorial Committee (Eds) The Genera of Vascular Plants of Korea*. Academy Press, Seoul, 515–517.
- Pelser PB, Nickrent DL, Gemmill CEC, Barcelona JF (2017) Genetic diversity and structure in the Philippine *Rafflesia lagascae* complex (Rafflesiaceae) inform its taxonomic delimitation and conservation. *Systematic Botany* 42(3): 543–553. <https://doi.org/10.1600/036364417X696186>
- Perkins AJ (2019) Molecular phylogenetics and species delimitation in annual species of *Hydrocotyle* (Araliaceae) from South Western Australia. *Molecular Phylogenetics and Evolution* 134: 129–141. <https://doi.org/10.1016/j.ympev.2019.02.011>
- Rafinesque CS (1817) Descriptions of four new genera of Dicotyle Sicilian Plants. *American Monthly Magazine and Critical Review* 1: 437–439.
- Ronquist F, Huelsenbeck JP (2003) MrBayes 3: Bayesian phylogenetic inference under mixed models. *Bioinformatics* 19: 1572–1574. <https://doi.org/10.1093/bioinformatics/btg180>

- Ryu H-S, Jeong J-H, Kim S-T, Paik W-K (2011) Morphological analyses of natural populations of *Sedum kamschaticum* (Crassulaceae) and the investigation of their vegetations. Korean Journal of Plant Resources 24(4): 370–378. <https://doi.org/10.7732/kjpr.2011.24.4.370>
- Seo S-H, Kim S-H, Kim S-C (2020) Chloroplast DNA insights into the phylogenetic position and anagenetic speciation of *Phedimus takesimensis* (Crassulaceae) on Ulleung and Dokdo Islands, Korea. PLoS ONE 15(9): e0239734. <https://doi.org/10.1371/journal.pone.0239734>
- Stephenson R, Harris JGS (1991) How *Sedum takesimense* was introduced into cultivation. Sedum Society Newsletter 19: 4.
- ‘t Hart H, Bleij B (2003) *Phedimu*. In: Eggl U (Ed.) Illustrated Handbook of Succulent Plants: Crassulaceae. Springer, Berlin, 204–210.
- ‘t Hart H (1995) Intrafamilial and generic classification of the Crassulaceae. In: ‘t Hart H, Eggl U (Eds) Evolution and systematics of the Crassulaceae. Backhuys, Leiden, 159–172.
- Uhl CH, Moran R (1972) Chromosomes of Crassulaceae from Japan and South Korea. Cytologia 37(1): 59–81. <https://doi.org/10.1508/cytologia.37.59>
- Yoo Y-G, Park K-R (2016) A test of the hybrid origin of Korean endemic *Sedum latiovalifolium* (Crassulaceae). Korean Journal of Plant Taxonomy 46(4): 378–391. <https://doi.org/10.11110/kjpt.2016.46.4.378>

Supplementary material I

Tables S1–S6

Authors: Tae-Young Choi, Dong Chan Son, Takashi Shiga, Soo-Rang Lee

Data type: occurrence, morphology (docx./xlsx. files in zip. archive)

Explanation note: **Table S1.** List of examined specimens for morphological study.

Table S2. Diagnostic characters observed in *Phedimus daeamensis* and the six closest related taxa. **Table S3.** Voucher information and GenBank accession numbers for the 16 accessions of *P. daeamensis* and closely related taxa examined in this study.

Table S4. PCR/sequencing primers and PCR cycling conditions for the DNA regions examined in this study. **Table S5.** Voucher information and GenBank accession numbers for 10 *Phedimus* accessions downloaded from GenBank. **Table S6.** Variable sites obtained from the ITS and *psbA-trnH* IGS regions.

Copyright notice: This dataset is made available under the Open Database License (<http://opendatacommons.org/licenses/odbl/1.0/>). The Open Database License (ODbL) is a license agreement intended to allow users to freely share, modify, and use this Dataset while maintaining this same freedom for others, provided that the original source and author(s) are credited.

Link: <https://doi.org/10.3897/phytokeys.212.82604.suppl1>

Supplementary material 2

Figure S1

Authors: Tae-Young Choi, Dong Chan Son, Takashi Shiga, Soo-Rang Lee

Data type: Image (Adobe PDF file)

Explanation note: **Figure S1.** Bayesian inference tree for individuals of *P. daeamensis* and related taxa based on ITS. Numbers above branches are posterior probabilities.

Copyright notice: This dataset is made available under the Open Database License (<http://opendatacommons.org/licenses/odbl/1.0/>). The Open Database License (ODbL) is a license agreement intended to allow users to freely share, modify, and use this Dataset while maintaining this same freedom for others, provided that the original source and author(s) are credited.

Link: <https://doi.org/10.3897/phytokeys.212.82604.suppl2>

Supplementary material 3

Figure S2

Authors: Tae-Young Choi, Dong Chan Son, Takashi Shiga, Soo-Rang Lee

Data type: Image (Adobe PDF file)

Explanation note: **Figure S2.** Bayesian inference tree for individuals of *P. daeamensis* and related taxa based on *psbA-trnH* IGS. Numbers above branches are posterior probabilities.

Copyright notice: This dataset is made available under the Open Database License (<http://opendatacommons.org/licenses/odbl/1.0/>). The Open Database License (ODbL) is a license agreement intended to allow users to freely share, modify, and use this Dataset while maintaining this same freedom for others, provided that the original source and author(s) are credited.

Link: <https://doi.org/10.3897/phytokeys.212.82604.suppl3>

Further clarification on *Androsace mollis* Hand.-Mazz. (Primulaceae), with a description of a new species of *Androsace*

Yuan Xu^{1,2}, Hai-Fei Yan^{1,2}, Gang Hao³

1 Key Laboratory of Plant Resources Conservation and Sustainable Utilization, South China Botanical Garden, Chinese Academy of Sciences, Guangzhou 510650, China **2** Center of Conservation Biology, Core Botanical Gardens, Chinese Academy of Sciences, Guangzhou 510650, China **3** College of Life Sciences, South China Agricultural University, Guangzhou 510642, China

Corresponding author: Gang Hao (haogang@scau.edu.cn)

Academic editor: Avelinah Julius | Received 25 August 2022 | Accepted 14 October 2022 | Published 3 November 2022

Citation: Xu Y, Yan H-F, Hao G (2022) Further clarification on *Androsace mollis* Hand.-Mazz. (Primulaceae), with a description of a new species of *Androsace*. *PhytoKeys* 212: 73–83. <https://doi.org/10.3897/phytokeys.212.94037>

Abstract

The syntypes (*H.R.E. Handel-Mazzetti 8896* and *H.R.E. Handel-Mazzetti 9280*) of *Androsace mollis* Hand.-Mazz. are identified as two separate taxa based on critical examinations of herbarium specimens and field investigation. While *H.R.E. Handel-Mazzetti 8896* has been designated as the lectotype of *A. mollis*, we describe the other taxon, represented by *H.R.E. Handel-Mazzetti 9280*, as *A. chimingiana* Y.Xu & G.Hao **sp. nov.** The new species is morphologically similar to *A. hookeriana* Klatt and *A. laxa* C.M.Hu & Y.C.Yang but can be easily differentiated by its white corolla and obovate bracts.

Keywords

Androsace chimingiana, new taxon, Primulaceae, taxonomy, Yunnan

Introduction

Androsace L. is a large genus of Primulaceae, which contains ca. 150 species (Smith and Lowe 1997). This genus is widely distributed in the temperate and arctic zones of the Northern Hemisphere, with the modern center of diversity in Pan-Himalaya, which harbors more than 50% of the species (Hu and Yang 1986; Hu and Kelso 1996; Xu et al. 2016; Chen 2019).

When we revised the Chinese species of *Androsace*, the name *A. mollis* Hand.-Mazz. caught our attention. This name was described by Handel-Mazzetti (1924) based on two collections: *H.R.E. Handel-Mazzetti 8896* (Fig. 1) and *H.R.E. Handel-Mazzetti 9280* (Fig. 2) from Yunnan Province, China. However, in his later treatment of the *Androsace* species from China, he identified the herbarium specimens of *A. sublanata* Hand.-Mazz. (*J.M. Delavay 69* and *1038*) as his *A. mollis* (Handel-Mazzetti 1927; Xu et al. 2018). Then we checked the original description and the type specimens of *A. mollis*. According to the protologue, the leaves of *A. mollis* are scarcely dimorphous. But, the leaf morphology of the plants in *H.R.E. Handel-Mazzetti 8896* is homomorphic, while in *H.R.E. Handel-Mazzetti 9280* it is obviously dimorphous (Fig. 2): where the outer leaves are obovate while the inner leaves are spatulate and 1.5 to 2 times longer than the outer leaves. With our additional specimen examination and the field investigation in northwest Yunnan and southeast Xizang, it is confirmed that these two collections, cited in the protologue of *A. mollis*, represent two separate taxa. They can easily be differentiated by the morphology of leaf (homomorphic vs. obviously dimorphous) and bract (linear vs. obovate), the length of pedicel (same as the bract vs. 1.5 to 2 times of the bract), the depth of calyx splitting (less than 1/2 vs. 1/2 to 3/4) and the color of corolla (pink vs. white). Since Handel-Mazzetti (1936) designated *H.R.E. Handel-Mazzetti 8896* (Fig. 1) as the lectotype of *A. mollis* (corolla pink) under Art. 7.11 of the CIN (Turland et al. 2018), we describe the other taxon (corolla white) as a new species herein.

Materials and methods

For morphological comparisons, both fresh and pressed specimens of the new species and its relatives were observed and measured. The main diagnostic characters (such as the indumentum of the plant, the shape of the leaf, calyx, calyx lobe and corolla lobe, the length of the shoot, scape and pedicel, and the color of the corolla) were measured and/or compared in the lab. Indumentum and other tiny morphological features were observed under a stereomicroscope. The herbarium specimens in Herbaria E, IBSC, K, KUN, LIV, P, SYS, SZ, US and WU were examined, with special attention on the specimens identified as *A. mollis* or cited by Handel-Mazzetti (1924, 1927). Field observations were conducted in 2012, 2013, 2015 and 2021 and focused on the variations of the morphology of leaf and bract, the depth of calyx splitting and the color of corolla. The field investigation covers all known distribution areas of the new species and *A. mollis*, including Dali Bai Autonomous Prefecture, Lijiang City, Diqing Tibetan Autonomous Prefecture and Nujiang Lisu Autonomous Prefecture of Yunnan, Zayu County of Xizang and MuLi County of Sichuan. The conservation status of *A. mollis* and the new species were assessed following the guidelines for using the IUCN Red List categories and criteria (IUCN Standards and Petitions Subcommittee 2022).

Taxonomy treatment

1. *Androsace mollis* Hand.-Mazz.

Fig. 1

Androsace mollis Hand.-Mazz. in Anzeiger der Akademie der Wissenschaften in Wien, Sitzung der Mathematisch-Naturwissenschaftliche Klasse 61: 136, 1924, p.p. *quoad specim.* Handel-Mazzetti 8896; Handel-Mazzetti in Notes from the Royal Botanic Garden, Edinburgh 15: 291, 1927, p.p. *quoad specim.* F. K. Ward 6963, G. Forrest 7370, 14263, 14917, 19307, J. F. Rock 8733; C.M. Hu and Y.C. Yang in Acta Phytotaxonomica Sinica 24(3): 226, 1986, p.p. *quoad specim.* G. Forrest 14263, H. R. E. Handel-Mazzetti 8896, J. F. Rock 21964, T. T. Yu 3703; Y.C. Yang and R.F. Huang in Flora Reipublicae Popularis Sinicae vol. 59(1): 183, 1989, p.p. *excl. syn.* *Androsace sarmentosa* var. *yunnanensis* R. Knuth, *excl. specim.* G. Forrest 1810; C.M. Hu and S. Kelso in Flora of China vol. 15: 99, 1996, p.p. *excl. syn.* *Androsace sarmentosa* var. *yunnanensis* R. Knuth, *excl. speciminibus Sichuanensibus*; R.Z. Fang in Flora Yunnanica vol. 15: 392, 2003, p.p. *quoad specim.* *Deqinense*, *Fugongense*, *Gongshanense*.

Type. CHINA. Yunnan Province: Deqin County, in regione temperate jugi Si-la inter fluvios Landsang-djiang (Mekong) et Lu-djiang (Salween), 28°N, 3600–4000 m a.s.l., 16 June 1916, H. R. E. Handel-Mazzetti 8896 (lectotype WU! barcode WU0059690; isolectotype E! barcode E00024874; K! barcode K000750338).

Description. A perennial herb, laxly cespitose. **Shoots** densely villous and green when young, becoming glabrescent and dark reddish-brown, internodes 0.3–1.5 cm, with old petiole or leaf rosettes on nodes. **Leaf rosettes** 4–11 mm in diam. **Leaves** sessile, obovate-ligulate, uncostate, 3–7 mm × 1–2 mm, ciliate, densely covered with white multicellular hairs along the midrib on abaxial surface, and glabrescent on abaxial surface, apex obtuse to subacute. **Scapes** solitary, 0.5–3.5 cm long, sparsely white villous, carrying a terminal umbel with 1–6 flowers; bracts linear to linear-spatulate, uncostate, 2–4 mm × 0.5–1.5 mm, ciliate, densely covered with white multicellular hairs on distal 1/2 of abaxial surface, and sparsely villous on adaxial surface, base sacate, apex rounded; pedicels 2–4 mm long and can extend to 1 cm in fruiting, sparsely villous, dark reddish-brown. **Calyx** campanulate, 2–3 mm long, sparsely pubescent, parted less than 1/2 of its length; lobes ovate to ovate-oblong, ciliate, apex obtuse and reddish. **Corolla** pink with a yellow eye, limb 5–7 mm across, lobes obovate, apex entire or emarginate. **Stamens** ca. 1 mm, near corolla tube apex. **Style** ca. 2 mm. **Capsules** globose, glabrous, tawny, ca. 3 mm in diam, splitting to the base in valves. **Blooming** from June to August and fruiting from August to October.

Conservation status. Based on our field investigation and specimen examination, *A. mollis* is widely distributed in northwest Yunnan, southeast Xizang and north Myanmar. Thus, the conservation status of *A. mollis* is assessed as Least Concern (LC) according to the guidelines for using the IUCN Red List categories and criteria (IUCN Standards and Petitions Subcommittee 2022).



Figure 1. Lectotype sheet of *Androsace mollis* (H.R.E. Handel-Mazzetti 8896, WU barcode WU0059690, <https://wu.jacq.org/WU0059690>).

Specimens examined. China. Yunnan: *G. Forrest* 7370 (E, K), 14263 (K), 14917 (K), 19307 (K); Deqin County *J.F. Rock* 8733 (E, K, SYS barcode SYS00112510, US barcode 03124157), 23239 (K, KUN barcode 0211554, SYS barcode SYS00112511, US barcode 03124155), *K.M. Feng* 5151 (KUN barcode 0211526, 0211527), 6580 (KUN barcode 0211529), 6644 (KUN barcode 0211530, 0211531), *T.T. Yu*, 22293 (KUN barcode 0211521, 0211522); Gongshan Derung and Nu Autonomous County *J.F. Rock* 21964 (K, SYS barcode SYS00112512, US barcode 03124156), *T.T. Yu* 19769 (KUN barcode 0211520), 22357 (KUN barcode 0211523, 0211524), 22783 (KUN barcode 0211525); Weixi Lisu Autonomous County *B. Xu Tsui*-2038 (KUN). **Xizang:** Zayu County *Y. Xu Xu* 130135 (IBSC), *Y. Xu*, *S. Chen*, *J. Li Xu* 210933 (IBSC), *Y. Xu*, *T.J. Liu & G.H. Huang* 150223 (IBSC), *J.F. Rock* 22522 (K). **Upper Myanmar.** *F. K. Ward* 6963 (K).

Additional notes. Although Handel-Mazzetti (1927) cited the specimens of *A. sublanata* (*J.M. Delavay* 69 and 1038) under his *A. mollis*, these two species are in fact quite different. The habit of *A. mollis* is laxly caespitose with obvious shoots while the leaf rosette of *A. sublanata* is solitary or 2–4 in small clumps without shoots. Moreover, *A. sublanata* is a somewhat larger species, with scapes 9–30 cm in length while the scapes of *A. mollis* are only 0.5–3.5 cm (Xu et al. 2018).

Hu and Kelso (1996) recorded that *A. mollis* is also distributed in western Sichuan. Then, Fang (2003) further indicated that *A. mollis* is distributed in MuLi County of Sichuan Province. We checked the Muli specimen (*Qinghai-Xizang Exped.* 14477 KUN barcode 0211555) determined by Fang. It is *A. minor* (Hand.-Mazz.) C.M.Hu & Y.C.Yang instead of *A. mollis*. Based on our field investigation and herbarium specimen examination, the distribution areas of *A. mollis* only include northwestern Yunnan and southeastern Xizang of China and Northern Myanmar.

2. *Androsace chimingiana* Y.Xu & G.Hao, sp. nov.

urn:lsid:ipni.org:names:77307629-1

Figs 2–4

Androsace mollis auct. non. Hand.-Mazz., Handel-Mazzetti in Anzeiger der Akademie der Wissenschaften in Wien, Sitzung der Mathematisch-Naturwissenschaftliche Klasse 61: 136, 1924, p.p. *quoad specim. Handel-Mazzetti* 9280.

Type. CHINA. Yunnan Province: Dali City, Cangshan, 25°40'N, 100°05'E, alt. 3830 m, 25 Jun. 2013 (fl.), *H.F. Yan*, *Y. Xu & S. Yuan* Y2013045 (holotype IBSC!, isotype IBSC!).

Diagnosis. *Androsace chimingiana* is similar to *A. hookeriana* Klatt and *A. laxa* C.M.Hu & Y.C.Yang, but differs in its white corolla with a yellow eye, obovate bracts, and campanulate calyx which is parted to 1/2–3/4 of its length.



Figure 2. Paratype sheet of *Androsace chimingiana* (H.R.E. Handel-Mazzetti 9280, WU barcode WU0059689, <https://wu.jacq.org/WU0059689>).

Description. A perennial herb, laxly caespitose. **Shoots** densely villous and green when young, becoming glabrescent and dark reddish-brown, internodes 0.5–3 cm, with old petiole or leaf single or rosettes on nodes. **Leaves** dimorphic; outer leaves sessile, obovate, unicostate, 3–8 mm × 1.5–2.5 mm, ciliate, densely covered with white multicellular hairs on abaxial surface, and sparsely villous on adaxial surface; inner leaves spatulate, unicostate, 8–14 mm × 2–5 mm, petiole indistinct to 1/2 as long as leaf blade, leaf blade elliptic to obovate, sparsely covered with white multicellular hairs on abaxial surface, and glabrescent on adaxial surface, margin spreading villous, more densely so at apex, apex obtuse to subrounded. **Scapes** 2.5–5.5 cm long, densely spreading white villous, carrying a terminal umbel with 4–8 flowers; bracts obovate, unicostate, 3–6 mm × 1–3 mm, ciliate, densely covered with white multicellular hairs on abaxial surface, and sparsely villous on adaxial surface; pedicels 5–8 mm long, sparsely villous, dark reddish-brown. **Calyx** campanulate, 2–3 mm long, sparsely pubescent, parted to 1/2–3/4 of its length; lobes narrowly ovate, ciliate, apex obtuse, margin reddish. **Corolla** white with a yellow eye, limb ca. 5 mm across, lobes obovate, apex subrounded or emarginate. **Stamens** 0.8–1 mm, near corolla tube apex. **Style** ca. 2 mm. **Capsules** ellipsoidal, glabrous, tawny, ca. 3 mm long, splitting to the base in valves.

Phenology. *Androsace chimingiana* was observed blooming from May to July and fruiting from July to August.

Etymology. The species name honors the Chinese botanist Prof. Chi-Ming Hu, who has made outstanding contributions to the taxonomy of Primulaceae.

Distribution and habitat. Based on the collection records over the past 138 years (since 1884, *J.M. Delavay 1037*, P) as well as our recent field investigation, the new species is narrowly distributed in Cangshan Mountain (Dali City and Yangbi Yi Autonomous County) and the north part of Gaoligong Mountains (Gongshan Derung and Nu Autonomous County) in Nujiang River and Dulong River divide. However, *A. mollis* has a broader distribution range. It is distributed in the north part of Biluo Snow Mountain (*H.R.E. Handel-Mazzetti 8896* E, K, WU; *J.F. Rock 8733* E, K, SYS, US; *K.M. Feng 6580, 6644* KUN; *T.T. Yu 22293* KUN) and west of Meri Snow Mountain (*J.F. Rock 23239* K, KUN, SYS, US) in Lancang River and Nujiang River divide and from the north part of Gaoligong Mountains in Nujiang River and Dulong River divide (*J.F. Rock 21964* K, SYS, US) to the southeast Xizang (*J.F. Rock 22522* K) and Upper Burma (*F.K. Ward 6963* K). Both the new species and *A. mollis* are distributed in the north part of Gaoligong Mountains. But no sympatric populations have been observed. The distribution area of *A. mollis* is more northerly than the new species. The habitats of these two species are also different. The new species grows under fir forest or *Rhododendron* thickets at 3000–4000 m a.s.l., while *A. mollis* grows on alpine meadow at 3800–4400 m a.s.l.

Conservation status. The new species is narrowly distributed in Cangshan Mountain and the north part of Gaoligong Mountains with a limited number of populations. But each population includes numerous mature individuals and the habitat is usually intact. Therefore, the conservation status of the new species is assessed as Least Concern (LC) according to the guidelines for using the IUCN Red List categories and criteria (IUCN Standards and Petitions Subcommittee 2022).

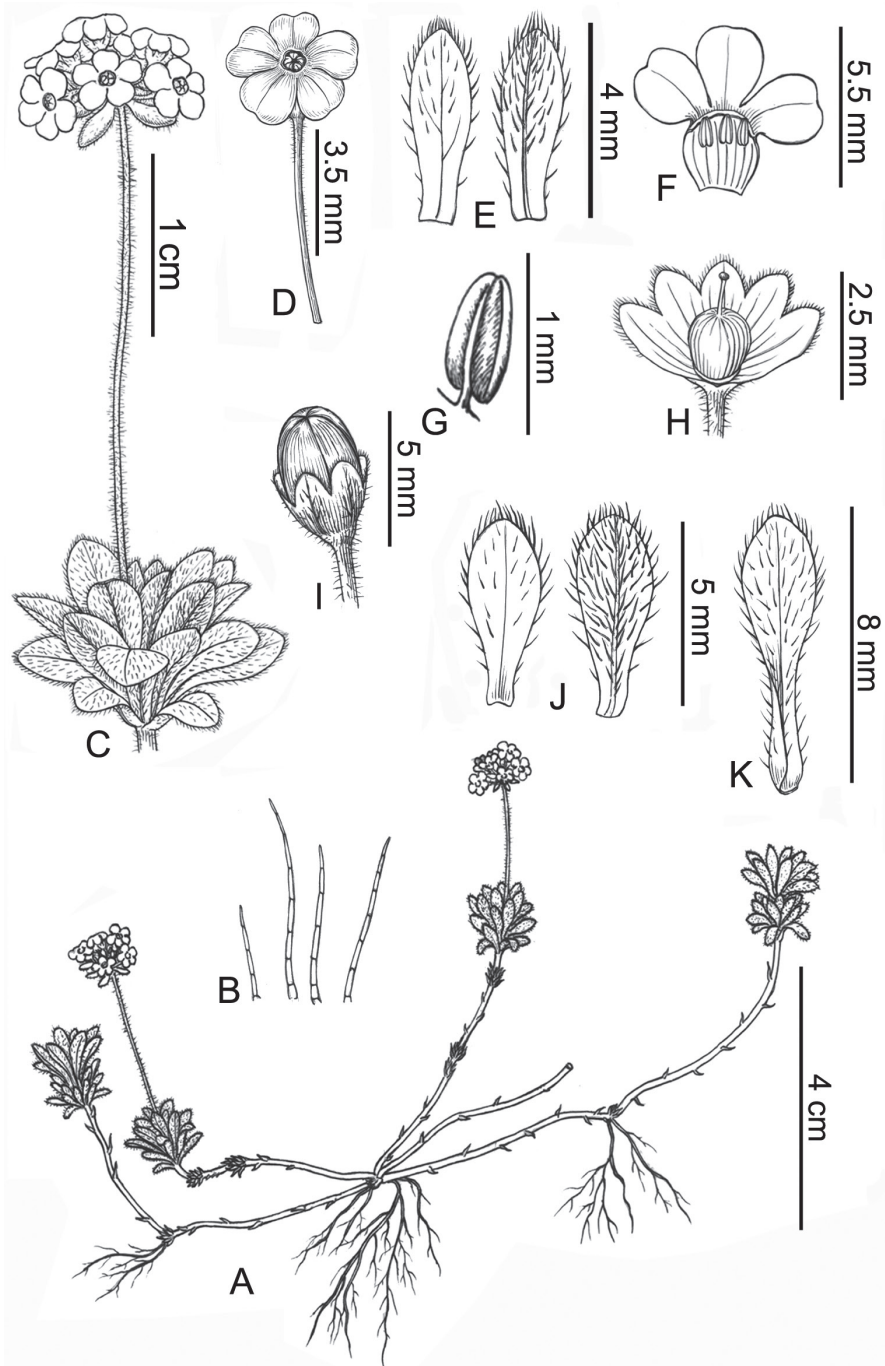


Figure 3. *Androsace chimingiana* sp. nov. **A** habit **B** multicellular hairs **C** leaf rosette on node and inflorescence **D** flower **E** bract on adaxial and abaxial surface **F** corolla (dissected) **G** anther **H** capsule with persistent calyx **I** capsule (split in valves) **J** outer leaf on adaxial and abaxial surface **K** inner leaf on abaxial surface. Drawn by Yun-Xiao Liu.

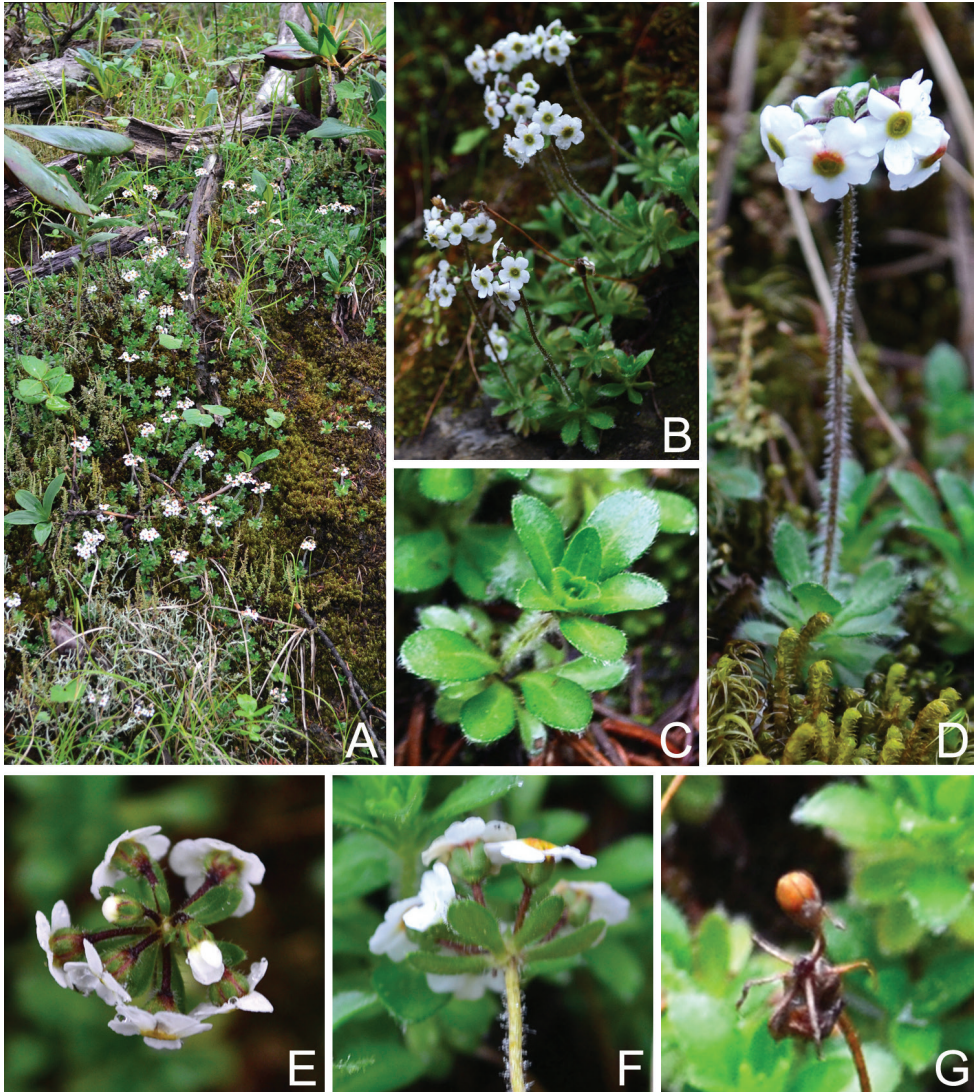


Figure 4. Living plant of *Androsace chimingiana* sp. nov. **A** habitat **B** habit **C** leaves **D** inflorescence **E** inflorescence showing calyx **F** inflorescence showing bract **G** capsule. Photographed by Yuan Xu.

Additional specimens examined (paratypes). **China. Yunnan:** Dali City, Cangshan, *Alpine Garden Society Expedition to China* 956 (LIV, K), *G. Forrest* 7108 (E), 11678 (E), 1810 (E, K), *H.C. Wang* 1236 (KUN barcode 0211513), *H.T. Tsai* 53970 (E, KUN barcode 0211538, 0211539, 0211540, SZ barcode 00061069), *J.M. Delavay* 1037 (E, P barcode P04907037, P01060625), 2800 (P barcode P05191797, P04623719, P04623720), *s.n.* (P barcode P01060637, P05191798), *K.L. Chu* 228 (SZ barcode 00061070), *McLaren's Collectors* 95B (P barcode P04553735), *R.C. Ching* 25039 (KUN barcode 0211547, 0211548), *Sino-Amer. Bot. Exped.* 1049 (E,

KUN barcode 0211553, US barcode 03124154), *Zhongdian Exped. 63-3925* (KUN barcode 0211549, 0211550, 0211551); Gongshan Derung and Nu Autonomous County, Salwin-Kiukiang Divide, *H.R.E. Handel-Mazzetti 9280* (WU barcode WU0059689), *T.T. Yu 19385* (E, KUN barcode 0211515); Yangbi Yi Autonomous County, Diancangshan, *Sino-Amer. Bot. Exped. 539* (KUN barcode 0211552, US barcode 03124151).

Similar species and remarks. The plants included in the paratype sheet (*H.R.E. Handel-Mazzetti 9280*, Fig. 2) of the new species are very small in size. Thus, the new species looks like *A. mollis*, but also can be easily distinguished by its obviously dimorphic leaves. The later collections from the type location and Cangshan also indicate that the leaves of new species are dimorphic and larger than *A. mollis*. Based on the result of our morphological observation, the new species is allied to *A. hookeriana* and *A. laxa*. All of them are laxly caespitose and both the morphology and the size of their inner leaves are similar. Handel-Mazzetti even identified the new species as *A. hookeriana* (e.g., signed on the sheet of *G. Forrest 7108* and *1810 E*). But *A. hookeriana* is unique by its trimorphic leaves among these three species. The new species can also be easily distinguished from the other two species by its white flowers, obovate bracts, and campanulate calyx parted more than 1/2 of its length. The main morphological differences between the new species and its allies are listed in Table 1. In addition, the geographical isolation among these three species is significant. The new species is distributed in northwestern Yunnan, while *A. hookeriana* is distributed in the central Himalayas and *A. laxa* is distributed in Qinling-Daba Mountains.

Table 1. Main morphological differences among *Androsace chimingiana* and its allies.

Features	<i>A. chimingiana</i>	<i>A. laxa</i>	<i>A. hookeriana</i>	<i>A. mollis</i>
Leaves	Dimorphic	dimorphic	trimorphic	homomorphic, obovate-ligulate
Outer leaves	Obovate	spatulate to oblanceolate	lanceolate	n/a
Inner leaves	spatulate, petiole indistinct	elliptic to suborbicular, petiole narrowly winged	ovate-elliptic to suborbicular, petiole wingless	n/a
Bract	Obovate	lanceolate	linear	linear
Calyx	parted to 1/2 – 3/4	parted to 1/2	parted less than 1/2	parted to less than 1/2
Corolla	White	pink	pink	Pink
Capsule	ellipsoidal	ellipsoidal	nearly spheroidal	nearly spheroidal

Acknowledgements

We thank the curators of E, IBSC, K, KUN, LIV, P, SYS, SZ, US and WU for allowing us to examine specimens or use images of specimens, and Ms. Yun-Xiao Liu for the line drawings of the new species. This study was financially supported by the National Natural Science Foundation of China (grants no. 32070230 and 32070220), the Science and Technology Program of Guangzhou, China (grant no. 202002030332), and the China Scholarship Council.

References

- Chen YS (2019) A Preliminary Catalogue of Vascular Plants in the Pan-Himalaya. In: Hong DY (Ed.) Flora of Pan-Himalaya. Science Press, Beijing, 1–371.
- Fang RZ (2003) Primulaceae. In: Fang RZ (Ed.) Flora Yunnanica. Vol. 15. Science Press, Beijing, 326–514.
- Handel-Mazzetti H (1924) Plantae novae Sinenses, diagnosibus brevibus descriptae a Dre. Henr. Handel-Mazzetti (28. Fortsetzung). Anzeiger der Akademie der Wissenschaften in Wien. Sitzung der Mathematisch-Naturwissenschaftliche Klasse 61: 131–138.
- Handel-Mazzetti H (1927) A revision of the Chinese species of *Androsace*, with remarks on other Asiatic species. Notes from the Royal Botanic Garden Edinburgh 15: 259–298.
- Handel-Mazzetti H (1936) Symbolae Sinicae. Vol. 7(4). Julius Springer, Wien, 731–1186.
- Hu CM, Kelso S (1996) Primulaceae. In: Wu ZY, Raven PH, Hong DY (Eds) Flora of China. Vol. 15. Science Press, Beijing, and Missouri Botanical Garden Press, St. Louis, 39–189.
- Hu CM, Yang YC (1986) A revision of the genus *Androsace* L. in China. Zhiwu Fenlei Xuebao 24: 215–232.
- IUCN Standards and Petitions Subcommittee (2022) Guidelines for using the IUCN Red List categories and criteria. Version 8.1. Prepared by the Standards and Petitions Subcommittee in July 2022.
- Smith G, Lowe D (1997) The genus *Androsace*. Alpine Garden Society, 1–208.
- Turland NJ, Wiersema JH, Barrie FR, Greuter W, Hawksworth DL, Herendeen PS, Knapp S, Kusber WH, Li DZ, Marhold K, May TW, McNeill J, Monro AM, Prado J, Price MJ, Smith GF [Eds] (2018) International Code of Nomenclature for algae, fungi, and plants (Shenzhen Code) adopted by the Nineteenth International Botanical Congress Shenzhen, China, July 2017. Regnum Vegetabile 159. Koeltz Botanical Books, Glashütten. <https://doi.org/10.12705/Code.2018>
- Xu Y, Hu CM, Hao G (2016) Pollen morphology of *Androsace* (Primulaceae) and its systematic implications. Journal of Systematics and Evolution 54(1): 48–64. <https://doi.org/10.1111/jse.12149>
- Xu Y, Hao G, Hu CM (2018) On the identity of *Androsace sarmentosa* var. *yunnanensis* (Primulaceae) from Yunnan, China. Nordic Journal of Botany 36(9): e01886. <https://doi.org/10.1111/njb.01886>

Paraphlomis hsiwenii (Lamiaceae), a new species from the limestone area of Guangxi, China

Ya-Ping Chen¹, Jin-Fei Xiao¹, Chun-Lei Xiang¹, Xiong Li²

1 CAS Key Laboratory for Plant Diversity and Biogeography of East Asia, Kunming Institute of Botany, Chinese Academy of Sciences, Kunming, 650201, China **2** Guangxi Forestry Inventory and Planning Institute, Nanning, 530011, China

Corresponding authors: Xiong Li (469745664@qq.com), Chun-Lei Xiang (xiangchunlei@mail.kib.ac.cn)

Academic editor: Eberhard Fischer | Received 2 August 2022 | Accepted 13 October 2022 | Published 3 November 2022

Citation: Chen Y-P, Xiao J-F, Xiang C-L, Li X (2022) *Paraphlomis hsiwenii* (Lamiaceae), a new species from the limestone area of Guangxi, China. *PhytoKeys* 212: 85–96. <https://doi.org/10.3897/phytokeys.212.91174>

Abstract

The indumentum of nutlets is shown to be of phylogenetic importance in previous molecular phylogenetic studies of *Paraphlomis*, a genus of Lamiaceae with approximately 30 species distributed mainly in southern China and Southeast Asia. Nearly half the species of *Paraphlomis* are known from limestone areas. In this study, we described and illustrated a new species, *P. hsiwenii*, from the karst mountain forests in Guangxi Zhuang Autonomous Region, China. Our molecular phylogenetic analyses revealed that *P. hsiwenii* is recovered in a clade consisting of species with hairy nutlets. The new species is morphologically most similar to *P. pagantha* from the same clade, but they differ in the morphology of lamina bases, length of pedicels and calyces, as well as the morphology of upper corolla lips.

Keywords

Ajugoides, karst, *Matsumurella*, nutlet, Paraphlomideae

Introduction

In a recently updated phylogenetic and taxonomic study of Lamioideae, the tribe Paraphlomideae was established to accommodate three genera, *Ajugoides* Makino, *Matsumurella* Makino, and *Paraphlomis* (Prain) Prain (Bendiksby et al. 2011). *Ajugoides* is a monotypic genus endemic to Japan and *Matsumurella* comprises five species distributed in East Asia (Harley et al. 2004; Bendiksby et al. 2011). As the largest genus of Paraphlomideae, *Paraphlomis* consists of ca. 30 species occurring mainly in

China (especially in the south of the Yangtze River) and Southeast Asia (Wu and Li 1977; Li and Hedge 1994; Harley et al. 2004; Chen et al. 2021).

Morphologically, *Paraphlomis* can be distinguished by its herbaceous habit with stoloniferous stems and simple hairs, two to many-flowered verticillasters, actinomorphic and tubular to obconical calyces, 2-lipped (1/3) corollas, and apically truncate ovaries (Wu and Li 1977; Li and Hedge 1994; Harley et al. 2004; Chen et al. 2021). Two sections and five series were recognized in a previous infrageneric classification of *Paraphlomis* from China, divided based on the shape of calyx (tubular or obconical) and calyx teeth (e.g., conspicuous or inconspicuous, broadly triangular or subulate) (Li 1965; Wu and Li 1977). However, the most recent molecular phylogenetic study of *Paraphlomis* indicated that nutlet morphology (e.g., glabrous or hairy, obviously inflated or not) rather than the above-mentioned calyx characters is of phylogenetic value for the subdivision of the genus.

Species of *Paraphlomis* are mostly accustomed to shady and moist places in tropical and subtropical evergreen and mixed forests, and nearly half of the species are karst-adapted (Wu and Li 1977; Li and Hedge 1994; Zhang et al. 2020; Chen et al. 2022a). During our recent field investigations in the limestone area of Diding Natural Reserve in Guangxi Zhuang Autonomous Region, China, we found a putative new species of *Paraphlomis* which is characterized by hairy nutlets. We further confirmed its specific status as a new species and placement within the genus based on molecular phylogenetic and morphological evidence, and named it *P. hsiwenii* Y.P.Chen & XiongLi.

Materials and methods

Molecular phylogenetic analyses

We sampled a total of 34 accessions representing 19 species and four varieties/subspecies of *Paraphlomis* and two species of *Matsumurella* as the ingroups, and included two taxa, *Phlomis fruticosa* L. and *Phlomoides dentosa* var. *glabrescens* (Danguy) C.L. Xiang & H. Peng from tribe Phlomideae as the outgroups. Only two accessions of the new species and one accession of *Paraphlomis pagantha* Doan were newly sampled and sequenced here, while sequences of the remaining accessions were all retrieved from our previous studies (Chen et al. 2021, 2022a, b).

Total genomic DNA was extracted from silica-gel-dried leaf material using the modified CTAB method (Doyle and Doyle 1987). We selected five DNA markers for the phylogenetic reconstruction following previous studies (Chen et al. 2021, 2022a, b), i.e. the nuclear ribosomal internal and external transcribed spacers (ITS and ETS) and three plastid DNA regions (*rpl32-trnL*, *rps16*, and *trnL-trnF*). Primers used for the polymerase chain reaction (PCR) amplification and sequencing of the five regions, as well as the PCR mixtures and procedures, were the same as those described in Chen et al. (2021). Voucher information and GenBank accession numbers for all sequences are listed in Appendix 1.

Previous phylogenetic studies of *Paraphlomis* revealed significant topological incongruences between the nuclear and plastid trees (Chen et al. 2021, 2022a, b), therefore, we performed partitioned maximum likelihood (ML) and partitioned Bayesian infer-

ence (BI) analyses for the combined nuclear data set and combined plastid data set separately. Both the ML and BI analyses were conducted on the Cyberinfrastructure for Phylogenetic Research Science (CIPRES) Gateway (<http://www.phylo.org/>; Miller et al. 2010), using RAxML-HPC2 (Stamatakis 2014) and MrBayes (Ronquist et al. 2012), respectively. Detailed settings for the two analyses followed those described in Chen et al. (2019). TreeGraph 2 (Stover and Müller 2010) was employed to visualize and annotate the resulting trees.

Taxonomic studies

Type specimens and protologues for all species of *Paraphlomis* were collated. Specimens of the genus from 21 public herbaria (BM, CDBI, E, GNNU, GXMI, HAST, HIB, IBK, IBSC, JIU, JJF, K, KUN, KYO, MW, NAS, PE, SM, SZ, TI, and WUK; abbreviations follow Thiers 2022) were also checked for the morphological comparison of *P. hsiwenii* with other species of *Paraphlomis*. Living plants of some species of the genus were observed and collected during our field investigation, and these specimens were further used for the morphological comparison of the new species. Other taxonomic and floristic literature related to *Paraphlomis* was reviewed, and the terminology used by Li and Hedge (1994) was adopted here for the morphological description of the new species.

Results and discussion

A total of 15 sequences (i.e., the five DNA regions of the two accessions of *P. hsiwenii* and one accession of *P. pagantha*) were newly generated in the present study. The aligned length of the combined nuclear data set and combined plastid data set was 1251 bp (808 bp for ITS, 443 bp for ETS) and 2479 bp (850 bp for *rpl32-trnL*, 812 bp for *rps16*, 817 bp for *trnL-trnF*), respectively. The topologies of the BI and ML trees were largely consistent with each other, but the BI trees are slightly better resolved. Thus, only the Bayesian 50% majority-rule consensus trees of the two combined data sets are presented, the posterior probabilities (PP) and Bootstrap support (BS) values being superimposed on the nodes (Figs 1, 2).

Both the nuclear and plastid data sets recovered species of *Matsumurella* within the *Paraphlomis* clade (Fig. 1: PP = 1.00/BS = 100%; Fig. 2: PP = 1.00/BS = 98%), indicating that neither of the two genera is monophyletic. As for relationships within the *Paraphlomis*-*Matsumurella* clade, some deep nodes in the nuclear tree (Fig. 1) and most shallow nodes in the plastid tree (Fig. 2) are poorly resolved, and topological conflicts between the two trees can be immediately recognized, especially at the placements of *P. javanica* var. *pteropoda* D. Fang & K.J. Yan, *P. albiflora* (Hemsl.) Hand.-Mazz., and *P. nana* Y.P. Chen, C. Xiong & C.L. Xiang. The backbone topologies of *Paraphlomis* recovered in the present study are largely consistent with those of previous studies (Chen et al. 2021, 2022a, b), and the intergeneric relationships within Paraphlomideae and phylogenetic relationships within *Paraphlomis* have been discussed in Chen et al. (2021). Therefore, our following discussion will focus on the placement of the new species.

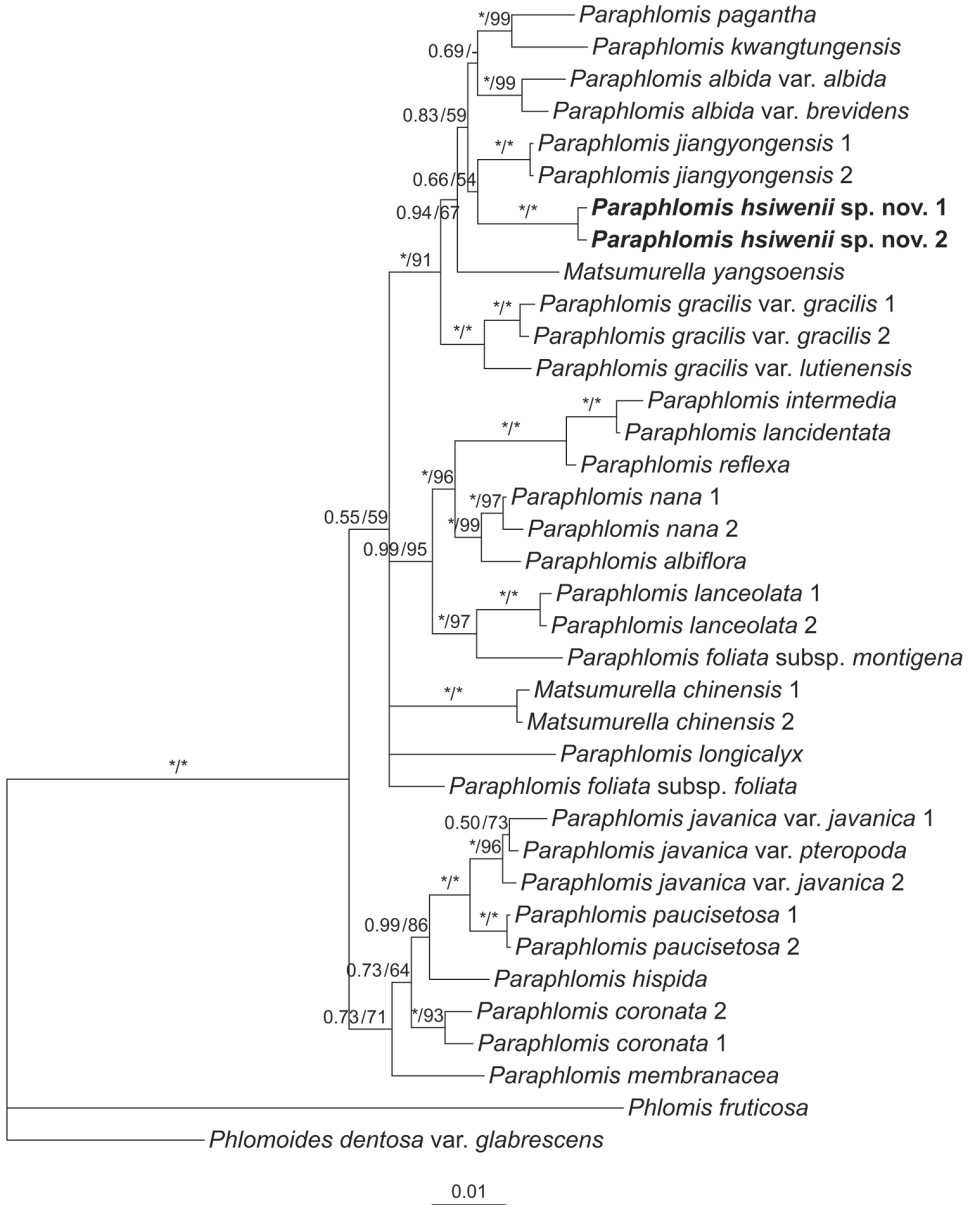


Figure 1. Bayesian 50% majority-rule consensus tree of *Paraphlomis* based on combined nuclear (ITS and ETS) data set. Support values ≥ 0.50 PP or 50% BS are displayed above the branches (an “*” indicates a support value = 1.00 PP or 100% BS and a “-” indicates a support value < 50% BS). Multiple accessions of the same species are numbered according to Appendix 1.

The two accessions of *P. hsiwenii* group together and form a strongly supported clade (Fig. 1: PP = 1.00/BS = 100%; Fig. 2: PP = 1.00/BS = 100%). In the plastid tree, relationships between *P. hsiwenii* and other species of *Paraphlomis* are not resolved (Fig. 2). In the nuclear tree, the new species is sister to *P. jiangyongensis* X.L. Yu & A.

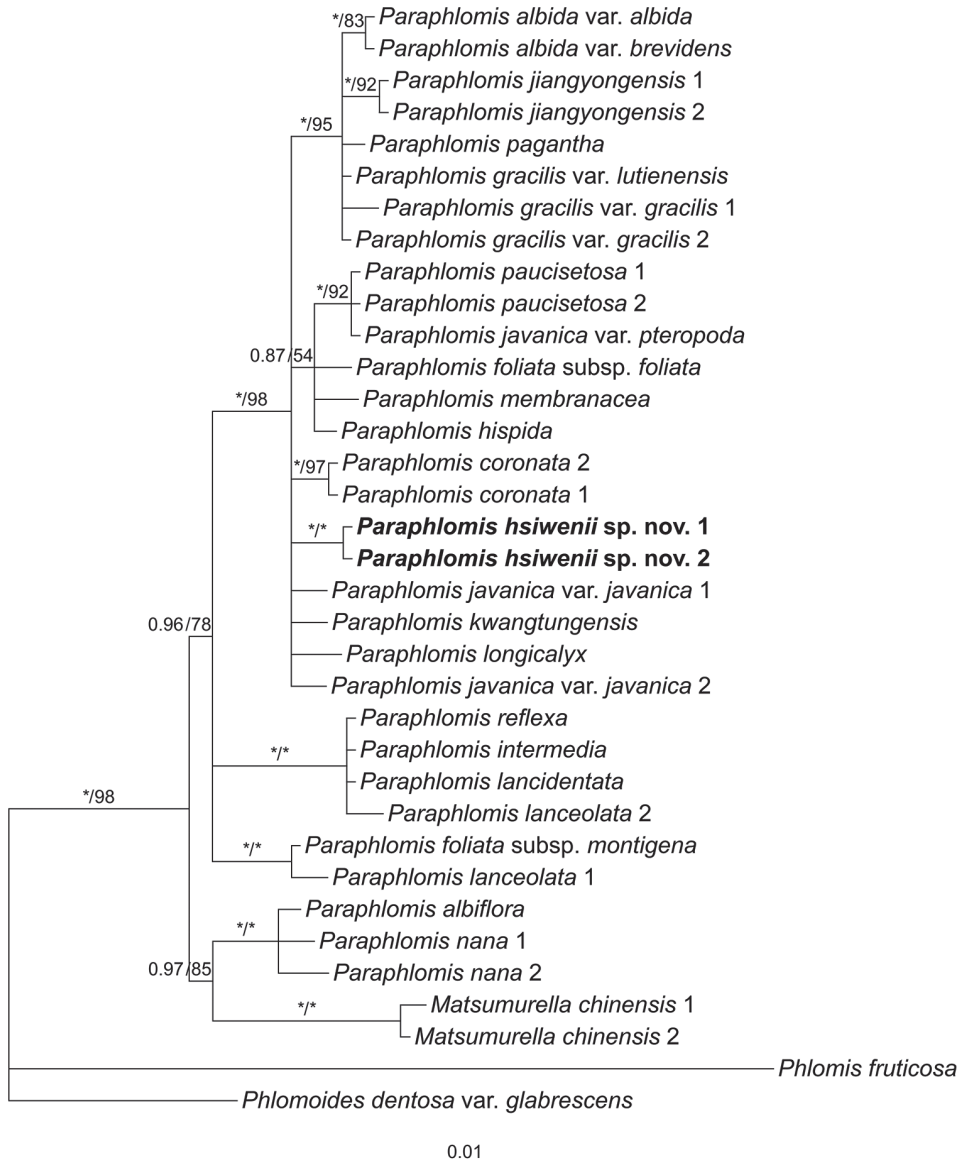


Figure 2. Bayesian 50% majority-rule consensus tree of *Paraphlomis* based on combined plastid (*rpl32-trnL*, *rps16*, and *trnL-trnF*) data set. Support values ≥ 0.50 PP or 50% BS are displayed above the branches (an “*” indicates a support value = 1.00 PP or 100% BS). Multiple accessions of the same species are numbered according to Appendix 1.

Liu but with weak support values (Fig. 1: PP = 0.66/BS = 54%). The two species are further placed within a robustly supported clade (Fig. 1: PP = 1.00/BS = 91%) together with *P. albida* Hand.-Mazz., *P. gracilis* (Hemsl.) Kudô, *P. kwangtungensis* C.Y. Wu & H.W. Li, *P. pagantha*, and *Matsumurella yangsoensis* (Y.Z. Sun) Bendiksby. This clade is corresponding to “Clade III” in Chen et al. (2021) and all its members have hairy

Table 1. Morphological comparisons between *Paraphlomis hsiwenii* and *P. pagantha*.

Characters	<i>P. hsiwenii</i>	<i>P. pagantha</i>
Lamina	Papery, ovate, base not decurrent, glabrous above	Papery to membranous, ovate to oblong, base decurrent, sparsely strigose above
Pedicel	2–3 mm long	Approximately 1 mm long
Calyx	Approximately 6 mm long, teeth ca. 2 mm long	Approximately 4 mm long, teeth ca. 1 mm long
Corolla	Tube purplish-red at upper part; upper lip greenish-yellow, ca. 8 × 6 mm, apex emarginate; lower lip ca. 8 × 10 mm, lateral lobes greenish-yellow	Tube with purplish-red spots at upper part; upper lip yellow to white, ca. 7 × 3 mm, apex entire; lower lip ca. 6 × 6 mm, lateral lobes yellow to white

nutlets/ovaries. The densely hispid and glandular nutlets of *P. hsiwenii* and its recovery within Clade III further support that nutlet morphology might be of phylogenetic significance for the infrageneric classification of *Paraphlomis* (Chen et al. 2021).

Morphologically, *P. hsiwenii* is most similar to *P. pagantha*, when comparing it with other species with hairy nutlets. For example, most species of Clade III are characterized by densely hispid or strigose stems and laminae, whereas both *P. hsiwenii* and *P. pagantha* have densely hispidulous stems and subglabrous to glabrous laminae (Fig. 3). They also share ovate laminae with serrate margins and triangular calyx teeth (Figs 3, 4). The two species differ mainly in the morphology of lamina bases, which are not decurrent in *P. hsiwenii* (Fig. 3) but obviously decurrent in *P. pagantha*. Another difference is that the length of pedicels and calyces is much longer in the new species (Fig. 4). Moreover, the upper corolla lips are ca. 6 mm wide with emarginate apices in *P. hsiwenii* (Fig. 4), but much narrower (ca. 3 mm wide) with entire apices in *P. pagantha*. Other morphological differences between the two species can be found in Table 1. Geographically, the new species is now only discovered from the limestone area in Diding Natural Reserve at the Sino-Vietnamese border, whereas *P. pagantha* usually grows in the evergreen forests in northern Vietnam and Hainan Province, China (Fig. 5). Notably, *P. pagantha* was treated as a synonym of *P. lancidentata* Y.Z. Sun by Suddee and Paton (2006). However, the nutlets of *P. lancidentata* are glabrous and the two species are recovered within different clades in the phylogenetic trees (Figs 1, 2).

Taxonomic treatment

Paraphlomis hsiwenii Y.P.Chen & XiongLi, sp. nov.

urn:lsid:ipni.org:names:77307630-1

Figs 3, 4

Type. CHINA, Guangxi, Jingxi City, Nanpo Town, Longting, Diding Natural Reserve, among shrubs in forests of limestone area, 23°3'29.55"N, 105°57'13.82"E, alt. 1181 m, 25 Jun 2022, J.F. Xiao & X.L. Ma XJF095 (holotype: KUN!; isotypes: K!, KUN!, MO!, PE!).

Diagnosis. *Paraphlomis hsiwenii* is morphologically most similar to *P. pagantha*, but differs in having laminae glabrous above (vs. sparsely strigose above), bases of laminae not decurrent (vs. decurrent), calyces ca. 6 mm long (vs. ca. 4 mm long) with teeth ca. 2 mm long (vs. ca. 1 mm long), and upper corolla lips emarginate at apex (vs. entire at apex).

Perennial herbs 50–120 cm tall, stoloniferous. Stems erect, simple or branched, obtusely 4-angled, densely retrorse hispidulous and glandular. Leaves opposite; lamina ovate, papery, 3–11 × 2.5–5 cm, apex acute to acuminate, margin serrate, base cuneate to broadly cuneate, adaxially green, glabrous, abaxially light green, purplish-green, or purple, densely glandular, lateral veins 3–5-paired; petioles 0.5–2 cm long, densely retrorse hispidulous and glandular. Verticillasters 2–14-flowered; bracteoles subulate, ca. 0.5 mm long, early deciduous; pedicels 2–3 mm long, densely retrorse hispidulous and glandular. Calyx green to yellowish-green, campanulate, ca. 6 mm long, densely hispidulous and glandular outside; teeth 5, subequal, triangular, reflexed, ca. 2 mm long, sparsely hispidulous inside, apex acute. Corolla ca. 1.4 cm long; tube ca. 6 mm long, ca. 1.5 mm wide, purplish-red at upper part; 2-lipped, upper lip oblong, yellowish-green, erect, concave, ca. 8 mm long, ca. 6 mm wide, sparsely pubescent outside, apex emarginate, lower lip ca. 8 mm long, ca. 1 cm wide, sparsely pubescent outside, 3-lobed, medium lob largest, white, dotted with purplish-red spots, subcircular, concave, apex emarginate, ca. 6 mm long, ca. 6 mm wide, lateral lobes ovate, yellowish-green, dotted with purplish-red spots, reflexed, ca. 4 mm long, ca. 2 mm wide. Stamens 4, straight, included, filaments hispid at base, anther cells 2, divergent. Style included, glabrous, apex subequally 2-lobed, lobes

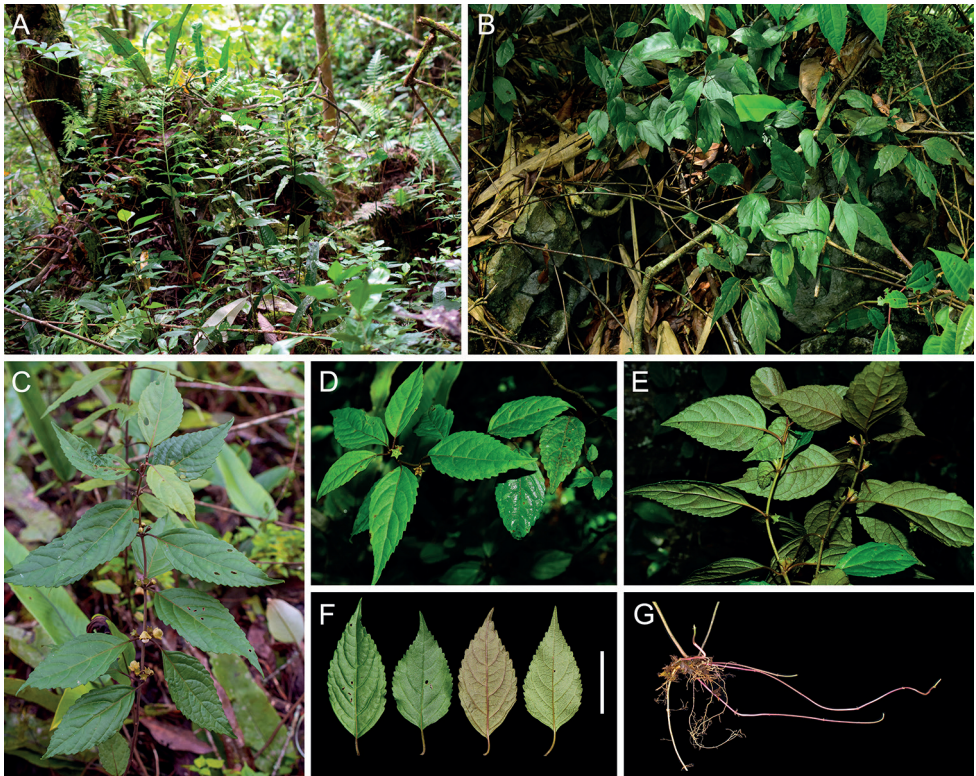


Figure 3. Morphology of *Paraphlomis hsiwenii* from the type locality **A, B** habitat **C–E** habit **F** leaves **G** stolons. Scale bar: 5 cm (**A, C** photographed by Xiao-Lei Ma **B, D, E** photographed by Xiong Li **F** photographed by Ya-Ping Chen **G** photographed by Jin-Fei Xiao).

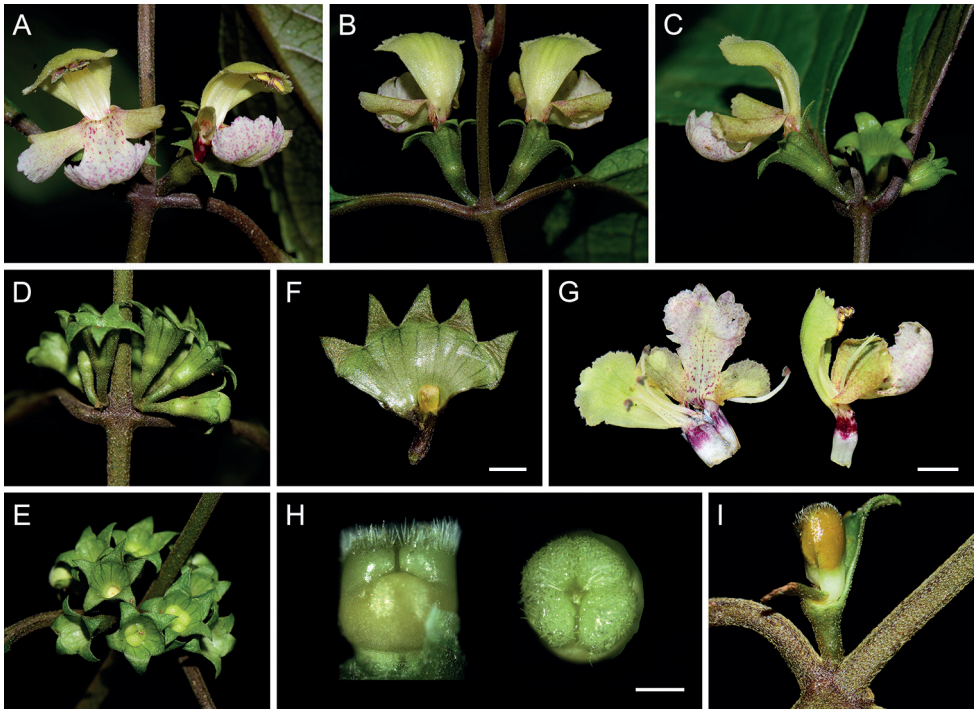


Figure 4. Floral traits of *Paraphlomis hsiwenii*. **A** frontal view of flowers **B** dorsal view of flowers **C** lateral view of flowers **D** lateral view of calyces **E** frontal view of calyces **F** dissected calyx **G** dissected corolla and lateral view of corolla **H** lateral and frontal view of ovary **I** lateral view of nutlet. Scale bars: 2 mm (**F**); 4 mm (**G**); 500 μ m (**H**) (**A–C, G, H** photographed by Jin-Fei Xiao **D–F** photographed by Ya-Ping Chen **I** photographed by Xiong Li).

subulate. Ovary truncate at apex, densely hispid and glandular. Nutlets yellowish-brown, triquetrous-oblong, ca. 3.5 mm long, apex hispid and glandular.

Phenology. Flowering from June to July, fruiting from July to August.

Distribution and habitat. *Paraphlomis hsiwenii* is currently known from Diding Natural Reserve in Guangxi, China (Fig. 5). It occurs in shady places in evergreen broad-leaved forests or among shrubs in limestone mountains at an altitude of ca. 1200 m.

Etymology. The new species is named after the Chinese taxonomist Hsi-Wen Li, who passed away in 2021 and had contributed tremendously to the taxonomy of Lamiaceae from China.

Chinese name (assigned here). xī wén jiǎ cǎo sū (锡文假糙苏).

Additional specimens examined. CHINA. Guangxi: Jingxi City, Nanpo Town, Longdingtun, Diding Natural Reserve, alt. 1231 m, 19 Aug 2020, W.H. Wu et al. DD426 (KUN).

Specimens of *P. pagantha* examined. CHINA. Hainan: Danzhou City, Shaposhan (Mt. Shamaoling), 29 Aug 1927, W.T. Tsang 672-16171 (IBSC0718446, IBSC0585106, PE00834801); Ledong County, Chang'e Village, Mt. Chang'eling, 16 Jun 1936, S.K. Lau 27154 (IBK00059945, IBSC0585103, KUN0274797,

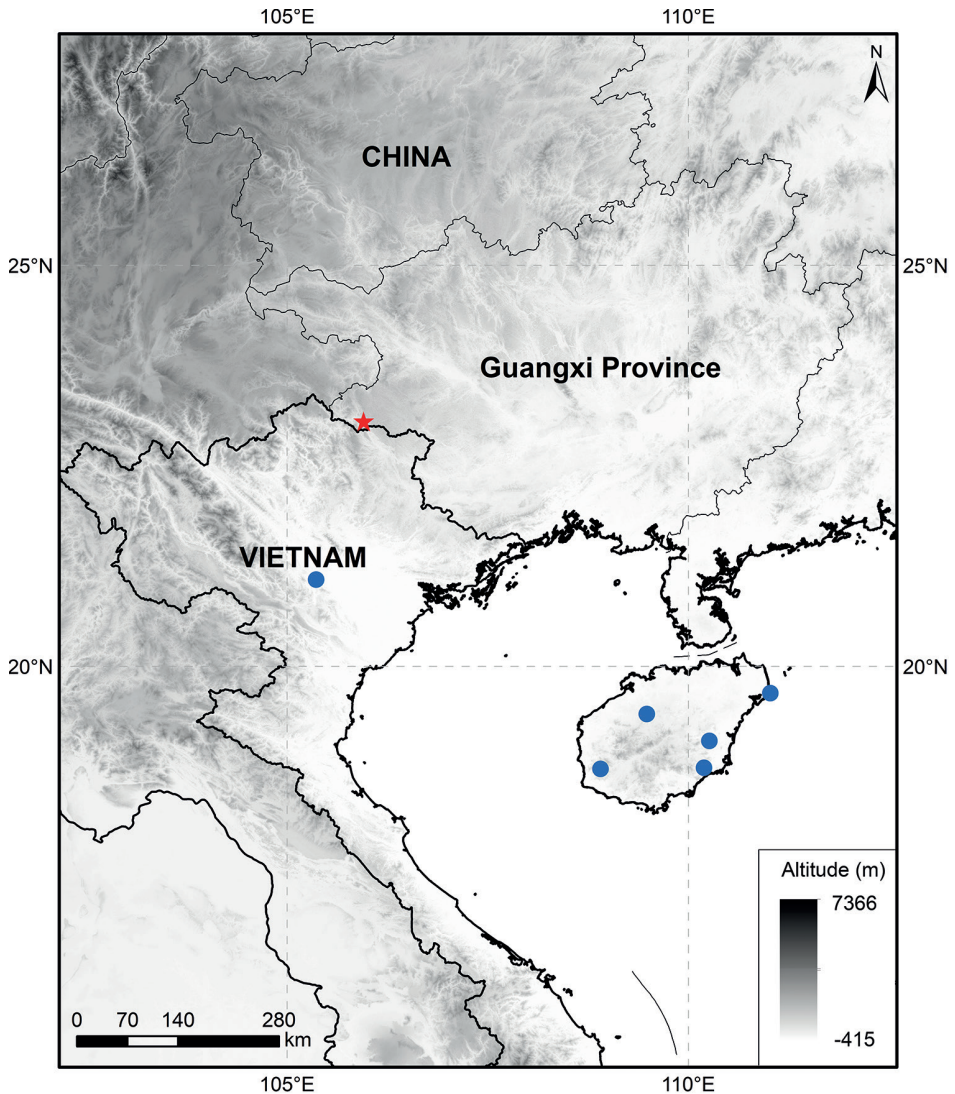


Figure 5. Distribution of *Paraphlomis hsiwenii* (star) and *P. pagantha* (circle).

NAS00224460, PE00834800); Ledong County, Mt. Jianfengling, alt. 750 m, 16 Jun 1959, Z.F. Wei 122572 (IBSC0585104); Qionghai City, Huishan Natural Reserve, 21 Apr 2021, L.X. Yuan et al. s.n. (KUN); Wanning City, Xinglong Town, Langmingtian Village, Wutiaosang, 17 Jul 1935, F.C. How 73217 (IBK00059942, IBSC0585105, PE00834802); Wanning City, Xinglong Town, Mt. Niuguling, 16 Apr 1935, F.C. How 71953 (BM, IBK00059943, IBSC0585102); Wanning City, mountain behind Nanlin Nongchang, 5 May 1984, Z.X. Li et al. 1661 (IBSC0585107); Wenchang City, Tongguling Natural Reserve, 4 Aug 2021, L.X. Yuan et al. s.n. (KUN). VIETNAM. Tonkin (Hanoi): Mont. Bavi, Aug 1887, B. Balansa 2914 (Type: K000928198); Ba Vi, Son Tay, alt. 800 m, 14 Jun 1962, Ban 6893 (IBSC0616357).

Acknowledgements

We would like to thank the staff of the following herbaria for their kind help in research facilities: BM, CDBI, E, GXMI, HIB, IBK, IBSC, K, KUN, KYO, MW, NAS, PE, SZ, TI. Thanks are also given to Mr. Xiao-Lei Ma for his help in field collection, and to the reviewers for their valuable suggestions that improved our manuscript. This work was supported by the National Natural Science Foundation of China (Grant No. 31800168) and the Yunnan Fundamental Research Projects (Grant Nos. 202101AU070067 & 202101AT070159) to YPC. Thanks are also given to Mr. Xiao-Lei Ma for his help in field collection, and to the reviewers for their valuable suggestions that improved our manuscript.

References

- Bendiksby M, Thorbek L, Scheen AC, Charlotte L, Olof R (2011) An updated phylogeny and classification of Lamiaceae subfamily Lamioideae. *Taxon* 60(2): 471–484. <https://doi.org/10.1002/tax.602015>
- Chen YP, Wilson TC, Zhou YD, Wang ZH, Liu ED, Peng H, Xiang CL (2019) *Isodon hsiwenii* (Lamiaceae: Nepetoideae), a new species from Yunnan, China. *Systematic Botany* 44(4): 913–922. <https://doi.org/10.1600/036364419X15710776741486>
- Chen YP, Liu A, Yu XL, Xiang CL (2021) A preliminary phylogenetic study of *Paraphlomis* (Lamiaceae) based on molecular and morphological evidence. *Plant Diversity* 43(3): 206–215. <https://doi.org/10.1016/j.pld.2021.03.002>
- Chen YP, Sun ZP, Xiao JF, Yan KJ, Xiang CL (2022a) *Paraphlomis longicalyx* (Lamiaceae), a new species from the limestone area of Guangxi and Guizhou Provinces, southern China. *Systematic Botany* 47(1): 251–258. <https://doi.org/10.1600/036364422X16442668423572>
- Chen YP, Xiong C, Zhou HL, Chen F, Xiang CL (2022b) *Paraphlomis nana* (Lamiaceae), a new species from Chongqing, China. *Turkish Journal of Botany* 46(2): 176–182. <https://doi.org/10.55730/1300-008X.2680>
- Doyle JJ, Doyle JD (1987) A rapid DNA isolation procedure for small quantities of fresh leaf tissue. *Phytochemical Bulletin* 19: 11–15.
- Harley RM, Atkins S, Budantsev AL, Cantino PD, Conn BJ, Grayer R, Harley MM, de Kok R, Krestovskaja T, Morales R, Paton AJ, Ryding O, Upton T (2004) Labiatae. In: Kubitzki K, Kadereit JW (Eds) *The families and genera of vascular plants*, vol. 7. Springer, Berlin and Heidelberg, 167–275. https://doi.org/10.1007/978-3-642-18617-2_11
- Li HW (1965) Revisio generis *Paraphlomis* Labiatarum Sinensium. *Acta Phytotaxonomica Sinica* 10: 57–74.
- Li HW, Hedge IC (1994) Lamiaceae. In: Wu CY, Raven PH (Eds) *Flora of China*, vol. 17. Science Press, Beijing and Missouri Botanical Garden Press, St. Louis, 269–291.
- Miller MA, Pfeiffer W, Schwartz T (2010) Creating the CIPRES Science Gateway for inference of large phylogenetic trees. *Proceedings of the Gateway Computing Environments Workshop (GCE)*. New Orleans, LA, 1–8. <https://doi.org/10.1109/GCE.2010.5676129>

- Ronquist F, Teslenko M, van der Mark P, Ayres DL, Darling A, Höhna S, Larget B, Liu L, Suchard MA, Huelsenbeck JP (2012) MrBayes 3.2: Efficient Bayesian phylogenetic inference and model choice across a large model space. *Systematic Biology* 61(3): 539–542. <https://doi.org/10.1093/sysbio/sys029>
- Stamatakis A (2014) RAxML version 8: A tool for phylogenetic analysis and post-analysis of large phylogenies. *Bioinformatics* 30(9): 1312–1313. <https://doi.org/10.1093/bioinformatics/btu033>
- Stover B, Müller K (2010) TreeGraph 2: Combining and visualizing evidence from different phylogenetic analyses. *BMC Bioinformatics* 11(1): 1–9. <https://doi.org/10.1186/1471-2105-11-7>
- Suddee S, Paton A (2006) Validation of Lamiaceae names. *Kew Bulletin* 61: 619–621.
- Thiers B (2022) Index Herbariorum: a global directory of public herbaria and associated staff. New York Botanical Garden’s Virtual Herbarium. <http://sweetgum.nybg.org/science/ih/> [Accessed Jul 2022]
- Wu CY, Li HW (1977) *Paraphlomis* Prain. In: Wu CY, Li HW (Eds) *Flora Reipublicae Popularis Sinicae*, vol. 65(2). Science Press, Beijing, 545–572.
- Zhang RB, Deng T, Dou QL, Wei RX, He L, Ma CB, Zhao S, Hu S (2020) *Paraphlomis kuankuoshuiensis* (Lamiaceae), a new species from the limestone areas of northern Guizhou, China. *PhytoKeys* 139: 13–20. <https://doi.org/10.3897/phytokeys.139.47055>

Appendix I

Table A1. Sequence information for all samples used in present study. A “/” indicates a missing sequence. Herbarium abbreviations are listed after the vouchers. The accession numbers marked in bold represent sequences newly generated.

Taxon	Voucher	Country	ITS	ETS	<i>rpl32-trnL</i>	<i>rps16</i>	<i>trnL-trnF</i>
<i>Matsumurella chinensis</i> (Benth.) Bendiksby 1	Y. Yang OYY00316 (KUN)	Pingxiang, Jiangxi, China	MW602147	MW602117	MW602021	MW602053	MW602084
<i>Matsumurella chinensis</i> (Benth.) Bendiksby 2	Y. Yang OYY00131 (KUN)	Guilin, Guangxi, China	MW602148	MW602118	MW602022	MW602054	MW602085
<i>Matsumurella yangoensis</i> (Y.Z. Sun) Bendiksby	L. Wu & W.B. Xu 10965 (IBK)	Yangshuo, Guangxi, China	MW602142	MW602112	/	/	/
<i>Paraphlomis albida</i> Hand.-Mazz. var. <i>albida</i>	A. Liu et al. LK0841 (CSFI)	Ningyuan, Hunan, China	MW602124	MW602091	MW601996	MW602028	MW602060
<i>Paraphlomis albida</i> var. <i>brevidens</i> Hand.-Mazz.	Y.P. Chen EM312 (KUN)	Hezhou, Guangxi, China	MW602130	MW602098	MW602003	MW602035	MW602067
<i>Paraphlomis albiflora</i> (Hemsl.) Hand.-Mazz.	C.M. Tan et al. 1806393 (JJF)	Jiujiang, Jiangxi, China	/	MW602101	MW602006	MW602038	MW602069
<i>Paraphlomis coronata</i> (Vaniot) Y.P. Chen & C.L. Xiang 1	E.D. Liu et al. 3043 (KUN)	Emeishan, Sichuan, China	MW602137	MW602107	MW602012	MW602044	MW602075
<i>Paraphlomis coronata</i> (Vaniot) Y.P. Chen & C.L. Xiang 2	C.L. Xiang 358 (KUN)	Jiangkou, Guizhou, China	MW602123	MW602090	MW601995	MW602027	MW602059
<i>Paraphlomis foliata</i> (Dunn) C.Y. Wu & H.W. Li subsp. <i>foliata</i>	S.P. Chen s.n. (KUN)	Jiangle, Fujian, China	/	MW602097	MW602002	MW602034	MW602066
<i>Paraphlomis foliata</i> subsp. <i>montigena</i> X.H. Guo & S.B. Zhou	Y.C. Dai s.n. (KUN)	Hangzhou, Zhejiang, China	OM836064	OM884453	OM884456	OM884459	OM884462
<i>Paraphlomis gracilis</i> (Hemsl.) Kudô var. <i>gracilis</i> 1	A. Liu LK0931 (CSFI)	Changsha, Hunan, China	MW602134	MW602104	MW602009	MW602041	MW602072

Taxon	Voucher	Country	ITS	ETS	<i>rpl32-trnL</i>	<i>rps16</i>	<i>trnL-trnF</i>
<i>Paraphlomis gracilis</i> (Hemsl.) Kudô var. <i>gracilis</i> 2	C.L. Xiang XCL1315 (KUN)	Chongqing, China	MW602141	MW602111	MW602016	MW602048	MW602079
<i>Paraphlomis gracilis</i> var. <i>lutiensis</i> (Y.Z. Sun) C.Y. Wu	C.L. Xiang XCL881 (KUN)	Shibing, Guizhou, China	MW602131	MW602099	MW602004	MW602036	MW602068
<i>Paraphlomis hispida</i> C.Y. Wu	X. Li LX200702 (GXF)	Napo, Guangxi, China	MW602132	MW602102	MW602007	MW602039	MW602070
<i>Paraphlomis hsiwenii</i> Y.P.Chen & XiongLi 1	W.H. Wu et al. DD426 (KUN)	Jingxi, Guangxi, China	OP605346	OP609841	OP609848	OP609855	OP609862
<i>Paraphlomis hsiwenii</i> Y.P.Chen & XiongLi 2	W.H. Wu et al. DD426 (KUN)	Jingxi, Guangxi, China	OP605347	OP609842	OP609849	OP609856	OP609863
<i>Paraphlomis intermedia</i> C.Y. Wu & H.W. Li	X. Zhong et al. ZX16823 (CSH)	Suichang, Zhejiang, China	MW602135	MW602105	MW602010	MW602042	MW602073
<i>Paraphlomis javanica</i> (Blume) Prain var. <i>javanica</i> 1	Y.P. Chen s.n. (KUN)	Kunming, Yunnan, China	MW602121	MW602088	MW601993	MW602025	MW602057
<i>Paraphlomis javanica</i> (Blume) Prain var. <i>javanica</i> 2	L.B. Jia et al. JLB0029 (KUN)	Maguan, Yunnan, China	MW602143	MW602113	MW602017	MW602049	MW602080
<i>Paraphlomis javanica</i> var. <i>pteropoda</i> D. Fang & K.J. Yan	X. Li 2020090501 (GXF)	Jingxi, Guangxi, China	MW602140	MW602110	MW602015	MW602047	MW602078
<i>Paraphlomis jiangyongensis</i> X.L. Yu & A. Liu 1	A. Liu et al. LK1104 (CSFI)	Jiangyong, Hunan, China	MW602128	MW602095	MW602000	MW602032	MW602064
<i>Paraphlomis jiangyongensis</i> X.L. Yu & A. Liu 2	A. Liu et al. LK1104 (CSFI)	Jiangyong, Hunan, China	MW602129	MW602096	MW602001	MW602033	MW602065
<i>Paraphlomis kuangtungensis</i> C.Y. Wu & H.W. Li	Y.P. Chen & Y. Zhao EM1391 (KUN)	Huaiji, Guangdong, China	MW602126	MW602093	MW601998	MW602030	MW602062
<i>Paraphlomis lanceolata</i> Hand- Mazz. 1	C.Z. Huang s.n. (KUN)	Guidong, Hunan, China	MW602145	MW602115	MW602019	MW602051	MW602082
<i>Paraphlomis lanceolata</i> Hand- Mazz. 2	A. Liu et al. LK0825 (CSFI)	Ningyuan, Hunan, China	MW602146	MW602116	MW602020	MW602052	MW602083
<i>Paraphlomis lancidentata</i> Y.Z. Sun	X. Zhong et al. ZX16824 (CSH)	Suichang, Zhejiang, China	MW602136	MW602106	MW602011	MW602043	MW602074
<i>Paraphlomis longicalyx</i> Y.P. Chen & C.L. Xiang	Y.P. Chen et al. EM583 (KUN)	Huanjiang, Guangxi, China	OK104771	OK104774	OK104778	OK104780	OK104783
<i>Paraphlomis membranacea</i> C.Y. Wu & H.W. Li	M.S. Nuraliev 1057 (MW)	Thanh Son, Phu Tho, Vietnam	/	MW602100	MW602005	MW602037	/
<i>Paraphlomis nana</i> Y.P. Chen, C. Xiong & C.L. Xiang 1	C. Xiong XC21097 (KUN)	Chengkou, Chongqing, China	OM836062	OM884451	OM884454	OM884457	OM884460
<i>Paraphlomis nana</i> Y.P. Chen, C. Xiong & C.L. Xiang 2	C. Xiong & H.L. Zhou XC21126 (KUN)	Wushan, Chongqing, China	OM836063	OM884452	OM884455	OM884458	OM884461
<i>Paraphlomis pagantha</i> Dunn	L.X. Yuan et al. s.n. (KUN)	Qionghai, Hainan, China	OP605345	OP609840	OP609847	OP609854	OP609861
<i>Paraphlomis paucisetosa</i> C.Y. Wu 1	X.X. Zhu s.n. (KUN)	Malipo, Yunnan, China	MW602125	MW602092	MW601997	MW602029	MW602061
<i>Paraphlomis paucisetosa</i> C.Y. Wu 2	X. Li LX200704 (GXF)	Napo, Guangxi, China	MW602133	MW602103	MW602008	MW602040	MW602071
<i>Paraphlomis reflexa</i> C.Y. Wu & H.W. Li	Z.Z. Yang et al. s.n. (HIB)	Tongshan, Hubei, China	MW602122	MW602089	MW601994	MW602026	MW602058
<i>Phlomis fruticosa</i> L.	Y. Tong s.n. (KUN)	Shanghai, China (cultivated)	MW602119	MW602086	MW601991	MW602023	MW602055
<i>Phlomidoides dentosa</i> var. <i>glabrescens</i> (Dangyui) C.L. Xiang & H. Peng	Y.P. Chen EM360 (KUN)	Beijing, China (cultivated)	MW602120	MW602087	MW601992	MW602024	MW602056

A new species of *Encelia* (Compositae, Heliantheae, Enceliinae) from the southern Baja California Peninsula

Jose Luis Leon-De La Luz¹, Isaac H. Lichter-Marck^{2,3}

1 Programa de Protección Ambiental y Cambio Global, Centro de Investigaciones Biológicas de Noreste, Apdo. Postal 128, La Paz, Baja California Sur, 23000 Mexico **2** Department of Integrative Biology & Jepson Herbarium, University of California Berkeley, Berkeley, California, USA **3** Department of Ecology and Evolutionary Biology, University of California Los Angeles, Los Angeles, California, USA

Corresponding author: Isaac H. Lichter-Marck (ilichtermark@berkeley.edu)

Academic editor: Peter de Lange | Received 2 August 2022 | Accepted 18 October 2022 | Published 4 November 2022

Citation: Leon-De La Luz JL, Lichter-Marck IH (2022) A new species of *Encelia* (Compositae, Heliantheae, Enceliinae) from the southern Baja California Peninsula. *PhytoKeys* 212: 97–109. <https://doi.org/10.3897/phytokeys.212.91190>

Abstract

Here, we describe and illustrate *Encelia balandra* **sp. nov.**, a new species of Compositae from the Baja California Peninsula. It is rare and known only from the rocky hills around Puerto Balandra and Pichilingüe, inside the bay of La Paz, in the State of Baja California Sur, Mexico. We determine that this new species has affinities with *Encelia*, based on its suffruticose woody habit, neuter ray florets and compressed disc cypselae with a cleft apex. The taxonomic placement within *Encelia* is supported by nuclear ribosomal sequence data from two regions, ITS and ETS. We also present detailed photographs, a conservation assessment and a dichotomous key to the *Encelia* of the southern Baja California Peninsula. Finally, we discuss the uniqueness of *Encelia balandra* amongst peninsular *Encelia* and its potential significance for understanding the enigmatic biogeography of this ecologically important genus.

Resumen

Se ilustra y describe a una nueva especie de Asteraceae, *Encelia balandra*. Se conoce solo de las laderas rocosas de los cerros próximos a puerto Balandra y Pichilingue, dentro de la bahía de La Paz, en Baja California Sur, México. Encontramos que esta nueva especie tiene ciertas semejanzas con otras de *Encelia* por su hábito semi-arbustivo, las flores radiales neutras y cipselas comprimidas con ápice hendido. Confirmamos tal condición con datos de secuencia para las regiones ITS y ETS del genoma. También presentamos fotografías detalladas, un evaluación de conservación, y un clave dichotomus para los *Encelia* de Baja California sur. Se discute la semejanza con las especies peninsulares más cercanas de *Encelia*, se presenta una clave dicotómica para los taxones australes de la península de Baja California, y finalmente se muestran imágenes detalladas de esta nueva especie.

Keywords

Asteraceae, Cape region, DNA barcoding, narrow endemism, synanthology, taxonomy

Palabras clave

Asteraceae, Código de barras ADN, Micro-endemismo, Región de Los Cabos, Sinanterología, Taxonomía

Introduction

Encelia Adans is a genus of New World sunflowers nested within tribe Heliantheae, *sensu* Panero and Funk (2002), based on the presence of paleae, agamous ray florets and obcompressed cypselae with flattened margins. The genus includes shrubs, suffrutescent perennials and few herbaceous perennials that are a dominant and ecologically important element in arid environments in the southwest U.S. and northwest Mexico, as well as western South America. The genus was most recently treated by Clark (1998) who cited 17 species and seven subspecies within two subclades, the *Californica* and *Frutescens* groups. These subgeneric groups were supported with molecular phylogenetic data by Fehlberg and Ranker (2007), who included all 20 minimum-rank taxa of *Encelia* in their study of subtribe Enceliinae Panero, encompassing the additional genera, *Enceliopsis* (A. Gray) A. Nelson, *Flourensia* DC. and *Geraea* Torr. & A. Gray. Recently, a phylogeny, based on next generation sequencing (RADseq) data by Singhal et al. (2021), has resolved species level relationships within *Encelia* and provided support for the *Californica* and *Frutescens* groups with the exceptions of two narrow endemics in the Baja California Peninsula, *E. densifolia* C. Clark & Kyhos and *E. ravenii* Wiggins, which form a previously undetected early-diverging clade.

The Baja California Peninsula harbours the majority of species diversity in *Encelia*, with nine taxa that fully, or partially, overlap in geographical distribution. The two major subclades proposed by Clark (1998), the *Californica* and *Frutescens* groups, contain five and four taxa on the Peninsula, respectively. According to Rebman et al. (2016) and distribution maps in Clark (2000), three taxa of *Encelia* are found in the Cape region of Baja California Sur: *E. farinosa* A. Gray ex Torrey var. *radians* Brandegees ex S.F. Blake (362: 1913), *E. farinosa* A. Gray ex Torrey var. *phenicodonta* (S.F. Blake) I.M. Johnston (1198: 1924) and *E. palmeri* Vasey & Rose (535: 1889). *E. farinosa* var. *radians* is found in the lowlands of the eastern Cape region, while *E. farinosa* var. *phenicodonta* and *E. palmeri* reach their southernmost extent in the Cape region, but are more common in desert habitats in the northern peninsula. An additional taxon, *E. conspersa* Benth. (26: 1844) is an endemic of Magdalena Bay, close to the Cape region.

The Balandra/Pichilingue area is an important recreation destination for residents and visitors of the City of La Paz, in the State of Baja California Sur (BCS), Mexico. A relatively small area of 2,512 hectares were decreed in 2012 as a combined marine and terrestrial area, or Zona de Protección de Flora y Fauna (ZPFF) by the Comisión Nacional de Areas Naturales Protegidas (CONANP) of Mexico. The area encompasses a coastal wetland, composed mainly of intertidal habitats, sand dunes, mangroves and xeric shrubland on the slopes of low mountains and hills. In September 2014, the first author was asked to make a floristic checklist of the ca. 1,000 hectares of terrestrial

surface in the Balandra/Pichilingue area as part of an integrated management plan for the protected area. One plant observed during this survey was an uncommon suffrutescens, low perennial herb, in vegetative stage, with characteristics of the Heliantheae alliance of the sunflower family (Compositae). Based on limited sampling of mostly vegetative material, we were able to discern basic characters, such as solitary, terminal capitula on long, scape-like peduncles and receptacular bracts, which led the plant to be determined as *Heliopsis* Pers. in the checklist, following the taxonomic key in Wiggins (1980).

Heavy rainfall in the early winter of 2019–2020 brought favourable conditions to the Balandra/ Pichilingue area, allowing us to collect suitable material, photograph the plant in flower and fruit and determine the genus of the plant with confidence using dichotomous keys (Shreve and Wiggins 1964; Wiggins 1980) and, later, to sequence DNA from two regions of the nuclear ribosomal cistron, the Internal Transcribed Spacer (ITS) and External Transcribed Spacer (ETS). This approach allowed us to present both morphological and molecular phylogenetic evidence that this new plant is a previously undescribed member of the genus *Encelia*, which we describe and illustrate here.

Materials and methods

Study site

Biogeographically, the Balandra or Pichilingue Hills constitute a disjunct fragment of the Sonoran Desert Province (*sensu* Shreve and Wiggins 1964) that falls within the Central Gulf Coast sub-province (Rebman et al. 2016). This region forms a long strip of lowlands along the east coast of most of the Baja California Peninsula, under the environmental influence of the Gulf of California. The Balandra/Pichilingue Hills form the southern point of the great Bay of La Paz. Geologically, the rocks are part of the complex Comondú Formation (Aranda-Gómez and Pérez-Venzor 1988), whose orogenesis occurred during the early Miocene age, these volcanic mountains representing the backbone of the Baja California Peninsula (see Fig. 1 for the location of the study area, including the distributional range of *Encelia* spp. in BCS).

Field collection

The exceptional rainy season of winter 2019–2020 made it possible to locate additional individuals of the focal plant in the Balandra Hills. Three populations were located, separated by approximately 800 m, at el Tecolote Beach, the hills of Rancho San Lorenzo and Balandra Beach. Reviewing the collections of undetermined Compositae at HCIB Herbarium (abbreviations following Thiers 2020) revealed two additional exemplars of this same plant previously collected within the Balandra Protected Area in 1994 and 1995. To our knowledge, specimens of this new taxon have not yet been accessioned at other herbaria.

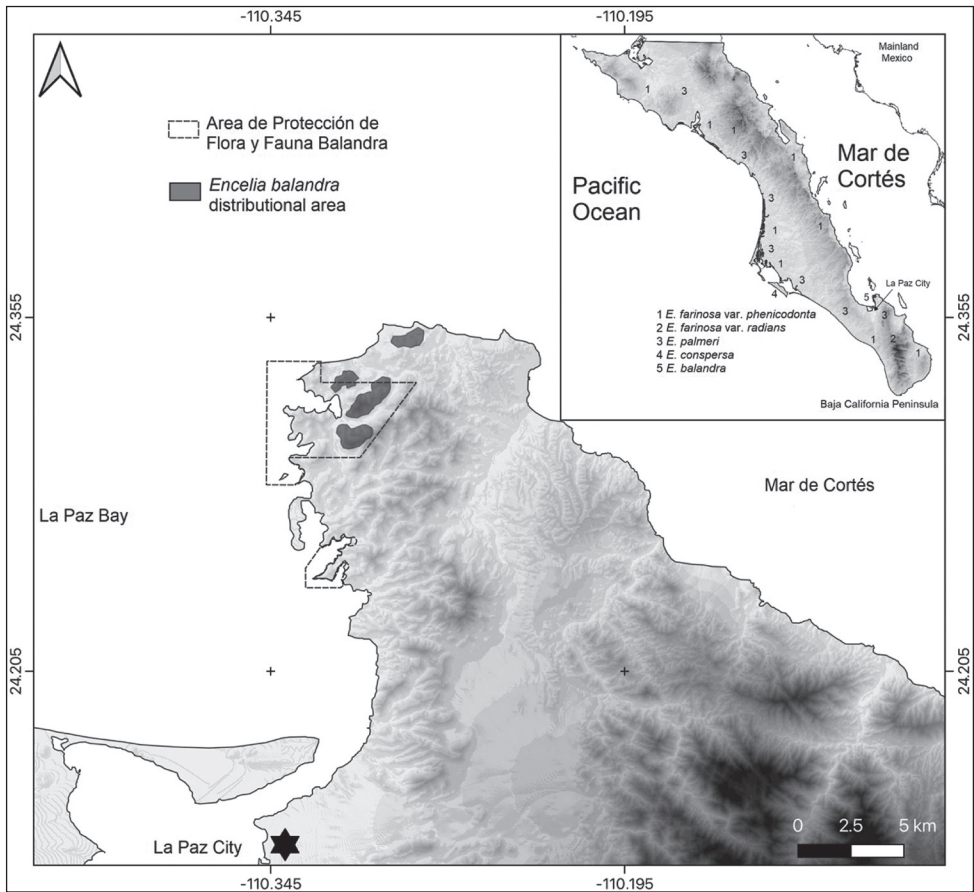


Figure 1. Range map of *Encelia balandra*. Geographical location of the study site in Baja California Sur (BCS), Mexico illustrating the Balandra/Pichilingüe Protected Area with a dashed polygon. The dark-grey area marks the zone where 17 plants were located and collected. The light-grey tone shows mountainous terrain. Numbers (1–5) show the distribution of the southern *Encelia* taxa in Baja California Sur, Mexico.

Morphological study

A careful examination of morphological characters was carried out based on the samples of the vegetative and reproductive material. Morphology was compared with images of all currently recognised minimum rank taxa of *Encelia* of the Baja California Peninsula and western Mexico in several taxonomic treatments (Blake 1913; Shreve and Wiggins 1964; Wiggins 1980; Clark 1998), as well online image databases (Clark 2000; NaturaLista 2020; BajaFlora 2021). Measurements of vegetative and reproductive structures were made in the field, as well as on rehydrated herbarium material. Photographs were taken using a Stereo Stemi DV4 Spot microscope (Zeiss, Jena, Germany), a Coolpix B500 digital camera (Nikon, Minato City, Tokyo, Japan), and a Tough TG-5 digital camera (Olympus, Shinjuku City, Japan).

DNA extraction, amplification and sequencing

Total genomic DNA was obtained from 3–5 silica-dried leaves using a DNeasy plant mini-kit (Qiagen, inc., Valencia, California) following the protocol recommended by Qiagen. To counteract the PCR prohibitive effects of co-precipitated polysaccharides present in some Asteraceae, genomic DNA was diluted to 1:50 parts with nuclease free water. Amplification and sequencing of the Internal Transcribed Spacer (ITS) region was achieved using primers ITS4 and ITS5 (White et al. 1990). The External Transcribed Spacer (ETS) was amplified and sequenced using primers 18S-ETS (Markos and Baldwin 2001) and ETS-HEL-1 (Baldwin and Markos 1998). Both ITS and ETS were amplified with Accupower PCR premix (Bioneer, Daejeon, South Korea) and 17 µl of 1:50 diluted DNA. PCR conditions using the MJ PCT-100 thermalcycler (Marshall scientific, Hampton, NH) replicating the protocol developed by Fehlberg and Ranker (2007) for *Encelia* as follows: 97 °C for 1 min; 40 cycles of 97 °C for 10 sec, 48 °C for 30 sec, 72 °C for 20 sec with an additional 4 sec per cycle; and 72 °C for 7 min. Post-PCR products were cleaned using magnetic SPRA beads and forward and reverse reads of all loci obtained using Sanger sequencing at the Barker Hall sequencing facility at UC Berkeley. Sequences were assembled and edited in sequencer v. 4.2 (Gene codes corp, Ann Arbor, Michigan). After a query of publicly available sequence data using nucleotide BLAST confirmed a close match to previously sequenced members of *Encelia*, we aligned sequences visually with the ITS and ETS alignments of Fehlberg and Ranker (2007) for tribe Enceliinae in the software programme Aliview (Larsson 2014). A Maximum Likelihood (ML) phylogenetic tree based on a concatenated matrix of ITS and ETS loci was inferred using RAxML (Stamatakis 2014) on the CIPRES computing portal using 1000 boot strap replicates and a GTRCAT molecular substitution model and visualised in the programme FigTree.

Results

Encelia balandra León De La Luz & Lichter-Marck, sp. nov.

urn:lsid:ipni.org:names:77307631-1

Figs 2, 3

Remark. Capitulum anatomy, particularly solitary heads erect in fruiting, places this new species with members of the frutescens clade, such as *E. frutescens* and *E. virginensis*. Molecular analysis also places the species in alliance with the Frutescens clade. The combination of glabrous, epappose cypselae, strigose hairs, a suffruticose habit and solitary heads are unique to this species.

Description. Deciduous perennial herb, suffrutescens, up to 40 cm high, with dense foliage when present. **Leaves** entire, fleshy, alternate, (2–)3 cm long × 1.5(–2) cm wide, ovate-lanceolate in outline, margins crenate, often with 4 conspicuous, symmetric lobes, basal pair larger than distal, petiole short 2–3 mm long, venation supra-basal

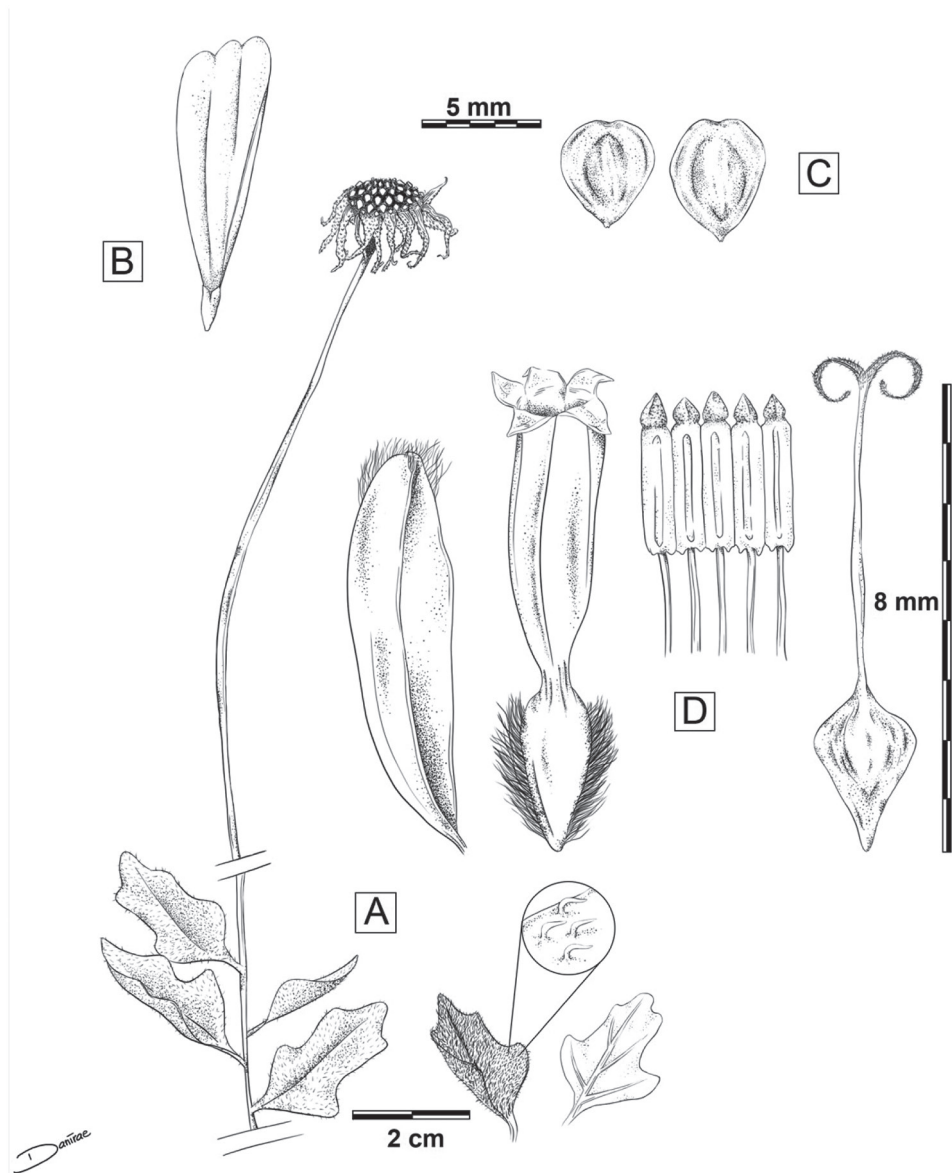


Figure 2. Line drawings of *Encelia balandra* sp. nov. **A** mature branch with basal leaves and terminal peduncle **B** strigulose indumentum on leaves, also present in peduncles and phyllaries; also, leaf venation pattern **C** ray floret, neuter **D** cypsela, note a broad shallow apical cleft and glabrous faces, epappose **E** palea **F** disc floret showing silky villous margins of immature achene **G** anther cylinder, opened out **H** immature achene/cypsela and style. Art by Danira León C, based on material from JLLL 12900.

and imperfect with 1 or 2 pairs of veins, apex acute, indumentum strigulose, eglandular, multicellular trichomes 1 mm, adpressed, with a semi-bulbose base. Solitary **Inflorescence**, capitula terminal, peduncles naked, 14–20 cm long in bloom, up to 25 cm in fruit. **Capitula** 2.5–3 cm diameter, heterogamous, radiate; **involucre** 1.5–2 cm

diameter, phyllaries tri-seriate, 6–9 bracts per series, bracts herbaceous lanceolate to ovate-lanceolate, inner slightly larger than outer, inner 7–8 mm long \times 2 mm wide, outer 6–7 mm long \times 2 mm wide, occasionally villous at the apex, barely connate at base, scariosus to touch, persistent after fruiting; **receptacle** chaffy, slightly convex, 13–15 mm diameter, 4–6 mm high, some paleaes empty < 1 mm long, silky villous; **paleaes** subtending disc florets, scariosus, concave, subulate, acrescent in age, up to 5 mm long \times 3 mm wide, barely villous at ends. **Ray florets** neuter, 12–15, uniseriate, ray limb yellow, \pm spathulate to oblong-elliptic in outline, 10(–12) mm long \times 6 mm wide, apex 2-toothed, tube 2 mm long. **Disc florets** perfect, but either hermaphroditic or functionally male, 40–50+, corolla actinomorphic with narrow cylindrical tube 6 mm long, throat cylindrical-funnelform 1 mm long \times 1 mm wide; corolla lobes 5, acute, dark in colour, reflexed, tiny oil dots sparse in the inner side; style 5–6 mm long, stigma branches coiled, linear subulate \pm 1.5 mm long, surpassing corolla lobes, short pubescent and papillate outside; stamens 5, 4 mm long, surpassing corolla lobes, but not stigma branches, with stiff rhombic-shaped terminal appendage at level of corolla lobes, thinly glandular, sub-auricular at base, filaments distinct, \pm 2 mm long. **Cypselae** monomorphic (but some larger than others), 4–5 mm long \times 4(–3) mm wide, laterally compressed, obovoid in outline, with a broad shallow apical cleft, margins densely silky villous (immature), at maturity margins with a thin chartaceous edge < 1 mm, faces glabrous, black, smooth in texture, epappose.

Type. MEXICO: Baja California Sur: municipio de La Paz, zona de Protección de Flora y Fauna Balandra, colina adyacente al estacionamiento del Balneario Balandra. 24.324894°N, -110.326251°W, ca. 60 m de elevación, laderas rocosas, 19 de Enero 2020, J.L. León-de la Luz 13007 (holotype: HCIB 31869, isotypes to be distributed UC, MEXU, SD).

Paratypes – MEXICO. Baja California Sur: Municipio de La Paz, cerca El Tecolote 6 km al N de Puerto Pichilingue. 24.2000°N, -110.23300°W, ca. 7 m de elevación, 2 de Septiembre 1994, M. Domínguez León 762, HCIB 4740. Municipio de La Paz, Cerro Balandra, 2 km al N de Puerto Pichilingue. 24.323500°N, -110.326700°W, 18 m de elevación, 20 de Enero 1995, M. Domínguez León 959, HCIB 4739. Municipio de La Paz, ladera rocosa cerca de El Pulgero. 24.346067°N, -110.270051°W, 8 m de elevación, 20 de Enero 1995, J.L. León de la Luz 7517, HCIB 5127. Bahía de La Paz, Sierra Riolítica, Cerro Manglar El Merito. 24.301191°N, -110.324712°W, 28 m de elevación, 22 de Noviembre 2013, J.L. León de la Luz 11891, HCIB 624. Bahía de La Paz, Zona de Protección de Flora y Fauna Balandra, Cerro adjunto al Tecolote. 24.3406634°N, -110.304868°W, 15 m de elevación, 10 de Octubre 2019, J.L. León de la Luz 12900, HCIB 31868. Municipio de La Paz, Playa El Tecolote, cerrito al extremo Este de la playa. 24.341095°N, -110.304525°W, 16 m de elevación, 1 de Octubre 2022, J. L. León de la Luz 13125.

Etymology. Balandra Beach is an emblematic place near La Paz, the capitol city of Baja California Sur, which is considered by many to be one of the most scenic beaches in all of Mexico.

Distribution and ecology. This species is known only from the hills of the Balandra/Pichilingue area, where a total of 20 documented individuals occur over an area

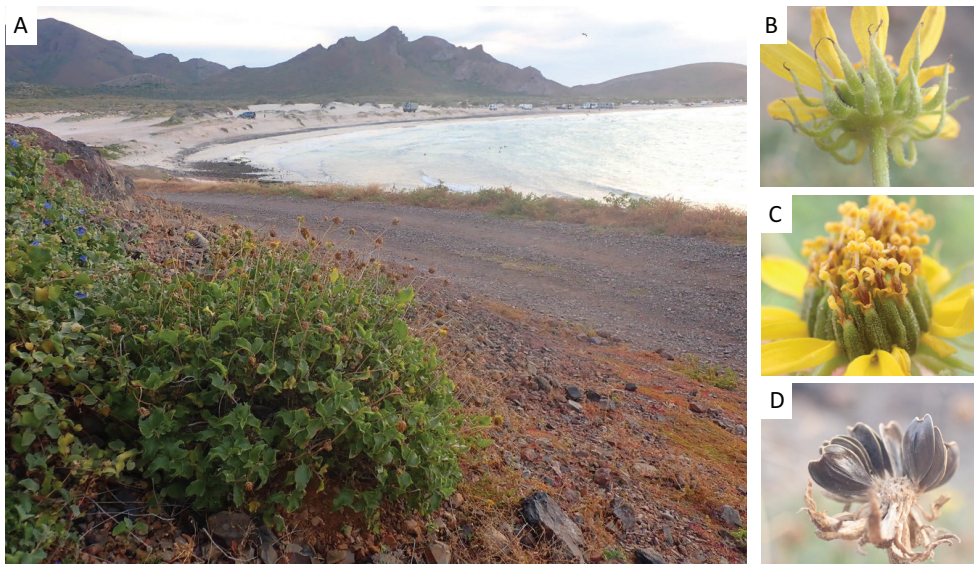


Figure 3. Photographs of *Encelia balandra* illustrating habitat and morphological characters of the capitula and cypselae **A** habitat on the rocky hills north of Playa Balandra **B** abaxial view of capitulum showing phyllaries **C** adaxial view of capitulum showing ray limbs and paleae enfolding disc florets **D** cypselae. Photos by ILM.

of no more than 500 hectares. *E. balandra* grows on coarse gravelly soils to bare rocky outcrops on the slopes of the hills. Some plants were documented on gravelly soil in the immediate vicinity of the seashore. Some insect visitors observed actively pollinating the plants were bees (Apidae), hoverflies (Syrphidae) and wasps (Hymenoptera).

Conservation status. *E. balandra* is a new species described from an area that is an important touristic destination. The area currently faces pressure due the growing influx of local and international visitors, which spend time either at the beaches or hiking in the hills. Thus far, 20 individuals of *E. balandra* have been found. Taxonomic resolution of this new species lays the foundation for more targeted surveys to illuminate its population status, environmental restrictions and threats from anthropogenic pressures. Until more information about its status is collected, *E. balandra* should be categorised as data deficient (DD) under the IUCN current guidelines for Categories and Criteria (IUCN Standards and Petitions Committee 2022). However, we expect that, once surveyed, this rare plant would qualify as having a very restricted distribution with high plausibility of being threatened with extinction (VU). More information and material should be gathered and the environmental authority of Mexico (SEMARNAT) should consider managing visitation within the immediate area as a precautionary measure.

Phenology. *E. balandra* is herbaceous with a woody taproot. Leaves appear to grow opportunistically in response to late summer, autumn or early winter rainfall. The peduncle and its capitulum, or head, reach anthesis some 20–30 days after a heavy rainfall, when foliar growth ceases. Some inflorescences and fruits could be present

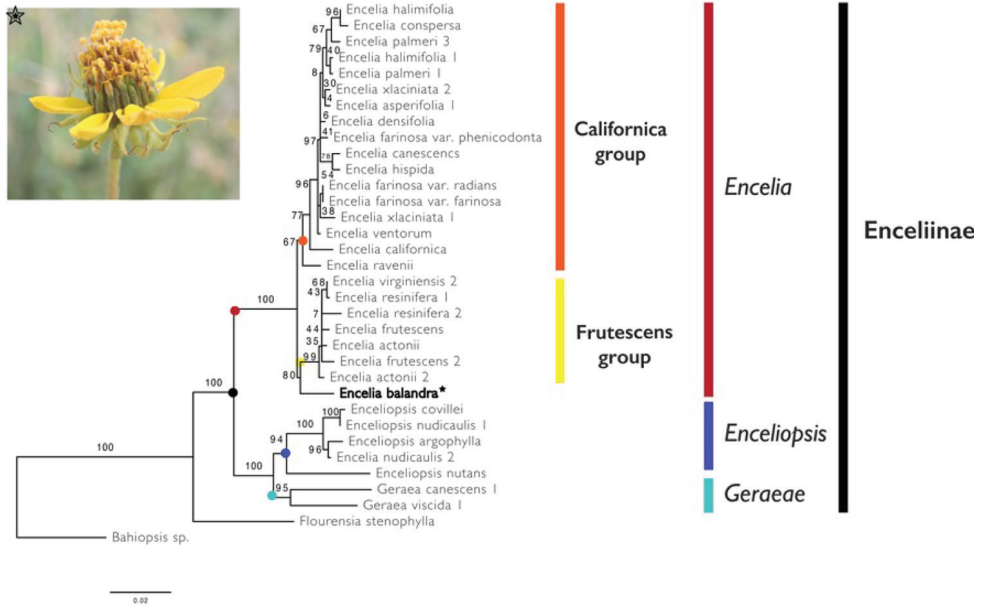


Figure 4. Phylogenetic position of *Encelia balandra*. Maximum Likelihood phylogeny of subtribe Enceliinae, based on a combined data matrix of Internal Transcribed Spacer (ITS) and External Transcribed Spacer (ETS) regions derived from the molecular phylogenetic study of Fehlberg and Ranker (2007), with the addition of *Encelia balandra* (bold and inset photograph). Bootstrap values along branches indicate statistical support for relationships and were generated using 1000 bootstrap replicates in RAXML using a GTRCAT molecular substitution model (Stamatakis 2014).

in the early autumn after summer rainstorms, but vigorous flowering also occurs if enough early winter rain is present.

Evolutionary affinities. To understand phylogenetic affinities of *E. balandra*, we used the Internal Transcribed Spacer (ITS) and External Transcribed Spacer (ETS) of nuclear ribosomal DNA. Both spacers are commonly employed in fine-scale studies of angiosperm relationships and this region has been used for understanding relationships amongst closely-related species within Enceliinae (Fehlberg and Ranker 2007). We extracted DNA and amplified both regions from leaf material sampled from the type specimen. When compared with publicly available DNA sequence data using the BLAST algorithm, our sequences for ITS and ETS were matched to members of *Encelia* with high percentage identity (ITS: 98.3% match with *Encelia frutescens* A. Gray MF963851.1; ETS: 98.34% match with *Encelia farinosa* var. *farinosa* A. Gray DQ383844). The ML phylogeny output from RaxML placed our study species within the genus *Encelia* with high support, confirming conclusions drawn from morphological evidence as shown in Fig. 4. Within *Encelia*, *E. balandra* occupies an early diverging branch of the frutescens clade with moderate bootstrap support.

GenBank accession numbers. ITS MZ892906, ETS MZ576216.

Discussion

With the addition of this new species, *Encelia* includes 16 species and five varieties (Clark 1998) notable for their eco-phenotypic variation across divergent desert microhabitats (Singhal et al. 2021). *E. balandra* represents the first species of *Encelia* endemic to the Cape region of Baja California Sur, an important biodiversity hotspot with heightened plant endemism (Rebman et al. 2016). As an endemic to a relatively frost-free yet arid climate, *E. balandra* may prove to be an important subject for eco-physiological studies. *Encelia* are interfertile and hybrids form with relative ease (Clark 1998), though species boundaries are maintained by strong post-dispersal selection influenced by environmental factors (Kyhos et al. 1981; DiVittorio et al. 2020). The possibility that *E. balandra* may be of hybrid origin is also, therefore, an important hypothesis for future studies to test.

The limited DNA sequence data included in the current study resolves *E. balandra* as a sister lineage to the *Frutescens* clade with moderate statistical support (bs = 80). Morphological affinities between *E. balandra* and the *Frutescens* clade include erect fruiting heads and multicellular strigose trichomes (Clark 1998). Weak affinities to either of the major subclades of *Encelia* suggests that *E. balandra* may fill a Darwinian deficit in our understanding of the biogeographic and evolutionary history of *Encelia*. We recommend its inclusion in broad scale studies of this genus using denser sampling of genomic data and suggest that more intensive botanical surveys in the Cape region are needed for the description and conservation of its unique flora rich in micro-endemics.

Finally, we present a dichotomous key, considering morphological data (Table 1) compiled from taxonomic treatments and floras (Blake 1913; Shreve and Wiggins 1964; Wiggins 1980; Clark 1998). The geographical distribution for three *Encelia* taxa found in the Cape region and that of Magdalena Bay, are illustrated in Fig. 1.

Table 1. Comparison of morphological traits of *Encelia balandra* with other *Encelia* of southern Baja California. (data from: Blake 1913, Shreve and Wiggins 1964, Wiggins 1980 and Clark 1998).

Character/ Taxon	<i>Encelia balandra</i>	<i>Encelia conspersa</i>	<i>Encelia farinosa</i> var. <i>radians</i>	<i>Encelia farinosa</i> var. <i>phenicodonta</i>	<i>Encelia palmeri</i>
Size (cm)	< 60 cm tall	< 120 cm tall	< 170 cm tall	< 170 cm tall	< 120 cm tall
Growth habit	Suffruticose perennial	Suffruticose perennial	Woody shrub	Woody shrub	Suffruticose perennial
Receptacle dimensions (height × diameter [mm])	4–6 × 13–15	4–5 × 10–12	2 × 3–4	2 × 3–4	8–10 × 10–20
Leaf					
Texture	Strigose	Hispid to pubescent, canescent	Glabrate	Silvery tomentose	Hispid canescent
Trichome length (mm)	1	1	-	< 1	< 1
Lamina shape	Ovate lanceolate	Obovate	Lanceolate to ovate	Lanceolate to ovate	Broadly ovate
Lamina size (length × width [cm])	3 × 1.5	3.5 × 2.5	8 × 4	7 × 4	3.5–4 × 3.5

Character/ Taxon	<i>Encelia balandra</i>	<i>Encelia conspersa</i>	<i>Encelia farinosa</i> var. <i>radians</i>	<i>Encelia farinosa</i> var. <i>phenicodonta</i>	<i>Encelia palmeri</i>
Margin	Crenate and lobate	Entire	Dentate and undulate	Entire and undulate	Sparsely dentate
Petiole length (mm)	2–3	4–10	10–40	10–40	3–10
Peduncle length (cm)	20–25	8–12	15–25	15–25	6–8
Capitulum position	Terminal	Terminal and axillary	Terminal	Terminal	Terminal and axillary
Capitula number	Solitary	1(2)	5–10	5–10	2–5
Phyllary shape	Lanceolate to ovate-lanceolate	Linear lanceolate to narrowly ovate	Lanceolate (outer) to ovate-lanceolate (inner)	Lanceolate (outer) to ovate-lanceolate (inner)	Linear to lanceolate
Ray floret number	10–12	12–14	11–18	11–18	14–16(–18)
Ray floret dimensions (length × width [mm])	10 × 6	7–10 × 6	7–11 × 6	7–11 × 6	8–10 × 6
Cypsela					
Shape	Obovoid	Linear-lanceolate	Obovate and emarginate	Obovate and emarginate	Obovate
Dimensions (length × width [mm])	5 × 4	3 × < 1	4.5 × 1	4.5 × 1	4.5 × 1
Texture	Faces glabrous when mature on margin and sides.	Villous marginally, faces pubescent	Margins villous with silky hairs	Margins villous with silky hairs	Villous marginally and sparsely on faces

- 1 Flowering panicle 1–2-branched, each branch monocephalous **2**
- Flowering panicle 2–4-branched, each up to 5–10 capitul..... **3**
- 2 Leaf and peduncle indumentum hispid, with canescent hairs *Encelia conspersa*
- Leaf and peduncle indumentum strigose, with conspicuous trichomes.....
..... *Encelia balandra*
- 3 Leaves typically broadly ovate; ray florets 14–18(–20) *Encelia palmeri*
- Leaves typically lanceolate; ray florets 10–12(–14) **4**
- 4 Disc floret corollas blackish; leaf blades glabrate and green; phyllaries glabrate....
..... *Encelia farinosa* var. *radians*
- Disc floret corollas purplish; leaf blades persistently white farinose; phyllaries puberulent *Encelia farinosa* var. *phenicodonta*

Acknowledgements

We are grateful to Jon Paul Rebman (SD) for the evaluation of this new taxon and for mentorship to ILM. Danira León Coria prepared the illustrations, Alfonso Medel Narváez the maps. Sophia Winitsky and Felipe Zapata provided support to ILM and Nick Marck provided a key technical assist. We also greatly appreciate the participation of HCIB colleague Raymundo Domínguez. The plant material was collected under the Scientific Collection License granted to JLLL by the Directorate General of Wildlife,

No. SGPA / DGVS/ 11324 / 13. ILM's training in Baja California was supported by the Annetta Carter scholarship of the California Botanical Society. We express our gratitude to Peter de Lange and one anonymous reviewer for comments that improved the quality of this manuscript. The authors declare no competing interests. Publication made possible in part by support from the Berkeley Research Impact Initiative (BRII) sponsored by the UC Berkeley Library.

References

- Aranda-Gómez JJ, Pérez-Venzor JA (1988) Estudio geológico de Punta Coyotes, Baja California Sur. *Revista del Instituto de Geología de la Universidad Nacional Autónoma de México* 7(1): 1–21.
- BajaFlora (2021) The Flora of Baja California. <http://www.bajaflora.org> [accessed: 18 January 2021]
- Baldwin BG, Markos S (1998) Phylogenetic utility of the external transcribed spacer (ETS) of 18S–26S rDNA: Congruence of ETS and ITS trees of *Calycadenia* (Compositae). *Molecular Phylogenetics and Evolution* 10(3): 449–463. <https://doi.org/10.1006/mpev.1998.0545>
- Blake SF (1913) Contributions from the Gray Herbarium of Harvard University, No. 41. II. A revision of *Encelia* and some related genera. *Proceedings of the American Academy of Arts and Sciences* 49: 346–396. <https://doi.org/10.5962/p.335973>
- Clark C (1998) Phylogeny and adaptation in the *Encelia* alliance (Asteraceae: Heliantheae). *Aliso: A Journal of Systematic and Evolutionary Botany* 17(2): 89–98. <https://doi.org/10.5642/aliso.19981702.02>
- Clark C (2000) *Encelia* and its relatives. <https://www.cpp.edu/~jclark/encelia/species.html> [accessed: 17 February 2021]
- DiVittorio CT, Singhal S, Roddy AB, Zapata F, Ackerly DD, Baldwin BG, Brodersen CR, Búrquez A, Fine PV, Flores MP, Soltis E (2020) Natural selection maintains species despite frequent hybridization in the desert shrub *Encelia*. *Proceedings of the National Academy of Sciences of the United States of America* 117(52): 33373–33383. <https://doi.org/10.1073/pnas.2001337117>
- Fehlberg SD, Ranker TA (2007) Phylogeny and Biogeography of *Encelia* (Asteraceae) in the Sonoran and Peninsular Deserts Based on Multiple DNA Sequences. *Systematic Botany* 32(3): 692–699. <https://doi.org/10.1600/036364407782250689>
- IUCN Standards and Petitions Committee (2022) Guidelines for Using the IUCN Red List Categories and Criteria. Version 15.1. Prepared by the Standards and Petitions Committee. <https://www.iucnredlist.org/documents/RedListGuidelines.pdf> [accessed: 15 October 2022]
- Kyhos DW, Clark C, Thompson WC (1981) The hybrid nature of *Encelia laciniata* (Compositae: Heliantheae) and control of population composition by post-dispersal selection. *Systematic Botany* 6(4): 399–411. <https://doi.org/10.2307/2418451>
- Larsson A (2014) AliView: A fast and lightweight alignment viewer and editor for large datasets. *Bioinformatics (Oxford, England)* 30(22): 3276–3278. <https://doi.org/10.1093/bioinformatics/btu531>

- Markos S, Baldwin BG (2001) Higher-level relationships and major lineages of *Lessingia* (Compositae, Astereae) based on nuclear rDNA internal and external transcribed spacer (ITS and ETS) sequences. *Systematic Botany* 26(1): 168–183.
- NaturaLista (2020) Comisión Nacional para el Conocimiento y Uso de la Biodiversidad, Cd. de México. www.naturalista.mx [accessed: 15 December 2020]
- Panero J, Funk VA (2002) Toward a phylogenetic subfamilial classification for the Compositae (Asteraceae). *Proceedings of the Biological Society of Washington* 115(4): 909–922.
- Rebman JP, Gibson J, Rich K (2016) Annotated checklist of the vascular plants of Baja California, Mexico. *Proceedings of the San Diego Natural History Museum* 45: 1–352.
- Shreve F, Wiggins IL (1964) *Vegetation and Flora of the Sonoran Desert*, 2 vols. Stanford University Press, Stanford, CA, 1740 pp.
- Singhal S, Roddy AB, DiVittorio C, Sanchez-Amaya A, Henriquez CL, Brodersen CR, Fehlberg S, Zapata F (2021) Diversification, disparification and hybridization in the desert shrubs *Encelia*. *The New Phytologist* 230(3): 1228–1241. <https://doi.org/10.1111/nph.17212>
- Stamatakis A (2014) RAxML version 8: A tool for phylogenetic analysis and post-analysis of large phylogenies. *Bioinformatics (Oxford, England)* 30(9): 1312–1313. <https://doi.org/10.1093/bioinformatics/btu033>
- Thiers B (2020) *Index Herbariorum: a global directory of public herbaria and associated staff*. New York Botanical Garden's Virtual Herbarium, NY. <http://sweetgum.nybg.org/science/ih/> [accessed: 30 March 2021]
- White T, Bruns JT, Lee S, Taylor J (1990) Amplification and direct sequencing of fungal ribosomal RNA genes for phylogenies. In: Innis M, Gelfand D, Sninsky J, White T (Eds) *PCR Protocols: A Guide to Methods and Applications*. Academic Press, San Diego, Ca, 315–322. <https://doi.org/10.1016/B978-0-12-372180-8.50042-1>
- Wiggins IL (1980) *Flora of Baja California*. Stanford University Press, Stanford, CA, 1025 pp.

Morphological, ecological, and molecular phylogenetic approaches reveal species boundaries and evolutionary history of *Goodyera crassifolia* (Orchidaceae, Orchidoideae) and its closely related taxa

Kenji Suetsugu¹, Shun K. Hirota², Narumi Nakato³,
Yoshihisa Suyama², Shunsuke Serizawa⁴

1 Department of Biology, Graduate School of Science, Kobe University, Kobe 657-8501, Sakyo, Japan **2** Field Science Center, Graduate School of Agricultural Science, Tohoku University, 232-3 Yomogida, Naruko-onsen, Osaki, Miyagi, 989-6711, Japan **3** Narahashi 1–363, Higashiyamato, Tokyo 207-0031, Japan **4** Aichi Green Association, Urahata 198-1, Nagamaki, Oharu-sho, Aichi 490-1131, Japan

Corresponding author: Kenji Suetsugu (kenji.suetsugu@gmail.com)

Academic editor: João Farminhão | Received 11 August 2022 | Accepted 23 October 2022 | Published 4 November 2022

Citation: Suetsugu K, Hirota SK, Nakato N, Suyama Y, Serizawa S (2022) Morphological, ecological, and molecular phylogenetic approaches reveal species boundaries and evolutionary history of *Goodyera crassifolia* (Orchidaceae, Orchidoideae) and its closely related taxa. *PhytoKeys* 212: 111–134. <https://doi.org/10.3897/phytokeys.212.91536>

Abstract

Species delimitation within the genus *Goodyera* is challenging among closely related species, because of phenotypic plasticity, ecological variation, and hybridization that confound identification methods based solely on morphology. In this study, we investigated the identity of *Goodyera crassifolia* H.-J.Suh, S.-W. Seo, S.-H.Oh & T.Yukawa, morphologically similar to *Goodyera schlechtendaliana* Rchb.f. This recently described taxon has long been known in Japan as “Oh-miyama-uzura” or “Gakunan” and considered a natural hybrid of *G. schlechtendaliana* and *G. similis* Blume (= *G. velutina* Maxim. ex Regel). Because the natural hybrid between *G. schlechtendaliana* and *G. similis* was described as *G. xtamnaensis* N.S.Lee, K.S.Lee, S.H.Yeau & C.S.Lee before the description of *G. crassifolia*, the latter might be a synonym of *G. xtamnaensis*. Consequently, we investigated species boundaries and evolutionary history of *G. crassifolia* and its closely related taxa based on multifaceted evidence. Consequently, morphological examination enabled us to distinguish *G. crassifolia* from other closely related species owing to the following characteristics: coriaceous leaf texture, laxly flowered inflorescence, long pedicellate ovary, large and weakly opened flowers, and column with lateral appendages. Ecological investigation indicates that *G. crassifolia* ($2n = 60$) is agamosperous, requiring neither pollinators nor autonomous self-pollination for fruit set, whereas *G. schlechtendaliana* ($2n = 30$) is neither autogamous nor agamosperous but is obligately pollinator-

dependent. MIG-seq-based phylogenetic analysis provided no evidence of recent hybridization between *G. crassifolia* and its close congeners. Thus, molecular phylogeny reconstructed from MIG-seq data together with morphological, cytological, and ecological analyses support the separation of *G. crassifolia* as an independent species.

Keywords

chromosome, cryptic species, integrative taxonomy, MIG-seq, phylogeny, reproductive biology, species complex

Introduction

The genus *Goodyera* R.Br. (Orchidaceae, Orchidoideae, Cranichideae) includes ca. 70 species distributed in Africa, Europe, the Western Indian Ocean Islands, Asia, the southwestern Pacific Islands, northeastern Australia, North America, and Mesoamerica (Govaerts et al. 2022). *Goodyera* spp. are terrestrial, lithophytic or epiphytic, and typically grow under shade, on mossy rocks, or along moist tracks of perennial mountain streams (Pridgeon et al. 2003). The characteristic features of the genus include creeping rhizomes; evergreen foliage that often features white or golden venation on the upper surface; and flowers with saccate lips, a single stigmatic lobe, and two sectile pollinia attached to a viscidium (Pridgeon et al. 2003). The flowers present dissimilar sepals and a concave dorsal sepal that forms a hood over the column along with the petals. The lateral sepals are usually connivent, with a lip that is formed from the concave-saccate hypochile and sessile epichile (Guan et al. 2014; Suetsugu and Hayakawa 2019).

The identification of species within *Goodyera* is often a challenge, especially among closely related species, owing to attributes such as phenotypic plasticity, convergent morphological features, and hybridization (Kallunki 1976, 1981; Hu et al. 2016; Suetsugu et al. 2019, 2021a); these eventually hinder tracing the evolutionary history of the genus (Pace 2020). Notably, molecular techniques have recently emerged as invaluable tools for investigating phylogenetic relationships within *Goodyera* (Hu et al. 2016; Suetsugu et al. 2021a). In particular, the internal transcribed spacer (ITS) region of nuclear ribosomal DNA—which exhibits moderate interspecific variation—has served as a primary target for phylogenetic analysis to determine the lower taxonomic levels of plants (Baldwin et al. 1995; Guan et al. 2014). In *Goodyera*, however, the ITS sequences of the morphologically distinct species *G. similis* Blume (= *G. velutina* Maxim. ex Regel) and *G. repens* (L.) R.Br. are identical (Shin et al. 2002). Therefore, phylogenetic resolution may be insufficient for species identification in *Goodyera*. Furthermore, the findings of a more comprehensive phylogenetic study including data from ITS and plastid regions (*trnL-F* and *matK*) could not be correlated with the corresponding species identification using morphological characteristics (Hu et al. 2016). Therefore, a higher resolution genetic marker is needed to elucidate the complex evolutionary history of *Goodyera* species (Suetsugu et al. 2021a, b).

A potential solution to distinguish closely related species would be to implement a high-throughput sequencing technology that enables simultaneous sequencing of numerous loci (Suyama and Matsuki 2015). Indeed, high-throughput sequencing has helped determine the boundaries and evolutionary histories of closely related species (Tamaki et al. 2017; Yoichi et al. 2018; Hirano et al. 2019; Suetsugu et al. 2021a). For example, multiplexed inter-simple sequence repeat (ISSR) genotyping by sequencing (MIG-seq) has recently been identified as a powerful tool for detecting reproductive isolation and hybridization, even between recently diverged species, including closely related *Goodyera* species (Tamaki et al. 2017; Yoichi et al. 2018; Hirano et al. 2019; Suetsugu et al. 2021a).

Ecological data based on breeding systems can further clarify whether morphologically distinct populations should be considered separate, reproductively isolated species (Kallunki 1981; Coyne and Orr 2004; Botes et al. 2020). In the present study, we investigated the identity of *Goodyera crassifolia* H.-J.Suh, S.-W.Seo, S.-H. Oh & T.Yukawa—recently described in Korea and Japan (Oh et al. 2022)—using a multifaceted approach. *Goodyera crassifolia* is morphologically the most similar to *G. schlechtendaliana* Rchb.f. and often grows sympatrically with the latter. *Goodyera crassifolia* has long been recognized as “Oh-miyama-uzura (meaning larger *G. schlechtendaliana*)” or “Gakunan (named after the collection site)” in Japan, differing from *G. schlechtendaliana* by its larger stature, more coriaceous leaves with indistinct reticulation, and more laxly flowered inflorescences (Takahashi 1985; Serizawa 2008; Akiyama 2010). Although the taxon had not been formally described until recently, it was often considered a natural hybrid of *G. schlechtendaliana* and *G. similis* (Takahashi 1985; Akiyama 2010; The Flora-Kanagawa Association 2018). Notably, the natural hybrid between *G. schlechtendaliana* and *G. similis* was described as *G. ×tamnaensis* in Jeju Island, South Korea (Lee et al. 2010, 2012). Suetsugu et al. (2021b) later reported the first occurrence of *G. ×tamnaensis* on the Boso Peninsula, Chiba Prefecture, Japan. Given that *G. ×tamnaensis* was described before *G. crassifolia*, it is possible that *G. crassifolia* is a junior synonym of *G. ×tamnaensis*. However, the report by Oh et al. (2022) did not include a comparison between *G. crassifolia* and *G. ×tamnaensis*.

In this study, we used an integrative taxonomic approach to investigate species boundaries and evolutionary history of *G. crassifolia* and its closely related taxa. Species delimitation that explicitly considers ecological as well as phylogenetic differences represents a crucial step in our understanding of biodiversity (Barrett and Freudenstein 2011). Over the last two decades, integrative taxonomy has helped achieve more robust estimates of biodiversity than those based on one-dimensional representations of variation (such as morphology), especially in the case of taxonomically challenging species (Barrett and Freudenstein 2011; Botes et al. 2020; Barrett et al. 2022). Our multifaceted evidence leads us to conclude that *G. crassifolia* is morphologically, phylogenetically, and ecologically distinct from *G. schlechtendaliana* and *G. ×tamnaensis* and should, therefore, be considered as a separate species.

Materials and methods

Morphological observations

We compared the morphological characters of *G. crassifolia*, *G. schlechtendaliana*, *G. ×tamnaensis*, and *G. similis* from herbarium specimens deposited in AICH, HIBG, HYO, KYO, MAK, SCM, TI, and TNS and from living plants collected throughout Japan during fieldwork between 2011 and 2021. Morphological variations among *G. schlechtendaliana*, *G. ×tamnaensis*, and *G. similis* were further investigated by reviewing the literature. Morphological characters were visually observed under a Leica M165C stereomicroscope and measured using a digital caliper. The dissected floral parts were photographed using an Olympus OM-D E-M1 Mark II digital camera equipped with an Olympus 30 mm macro lens or a Leica MC170 HD digital camera attached to a Leica M165C stereo microscope. Since we revealed that *G. crassifolia* is distributed widely throughout Japan, we also provided a revised description of *G. crassifolia* based on the newly discovered specimens from our field surveys and herbarium investigations. At least one voucher specimen from each new population discovered during our field survey was deposited in KYO and TNS (Suppl. material 1). The herbarium acronyms follow Index Herbariorum (Thiers 2022).

Cytological observations

Root tips were collected from five individuals of *G. crassifolia* (representing five populations) and four individuals of *G. schlechtendaliana* (including a *G. schlechtendaliana* var. *yakushimensis* Suetsugu & H.Hayak. individual; representing three populations). They were used for mitotic chromosome counts, as described in Suetsugu et al. (2019). Root tips were pretreated with 2 mM 8-hydroxyquinoline solution for 4–5 h, fixed in Carnoy's solution for 1–24 h, macerated in 1 N HCl at 60 °C for 1 min, and then squashed in aceto-orcein. The samples were then observed and photographed under a light microscope.

Breeding system

The breeding systems of *G. schlechtendaliana* and *G. crassifolia* were investigated during early-to-late September 2016 in a sympatric population in Kami-shi, Kochi Pref., Japan. Hand-pollination experiments were performed using five treatments: (i) agamosperous treatment—the pollinaria were removed before anthesis using forceps, and the flowers were then bagged (20 flowers from five individuals); (ii) autonomous autogamous treatment—flowers were bagged with a fine-meshed net before anthesis to exclude pollinators (20 flowers from five individuals); (iii) manually autogamous treatment—the pollinaria were removed and used to hand-pollinate the same flower before bagging (20 flowers from five individuals); (iv) manually allogamous treatment—same as treatment (iii) but using the pollinia from a different plant at least 1 m from the

recipient plant (20 flowers from five individuals); and (v) open treatment—flowering individuals were randomly tagged and allowed to develop fruit under natural conditions (40 flowers from 10 individuals). The experimental plants were monitored intermittently over the subsequent 4–6 weeks; fruit set among the treatments was compared via Fisher's exact test. Mature fruits were collected and silica-dried; seed mass was obtained to the nearest 0.0001 g. Thereafter, 200 seeds per capsule were examined to assess the presence of the embryo. After confirming the normality and homogeneity of variance using the Shapiro-Wilk and Bartlett's tests, the effects of pollination treatment on the seed mass and the proportion of seeds with at least one embryo were tested via ANOVA.

MIG-seq-based high-throughput genomic analysis

Eleven *G. crassifolia* individuals representing six populations, ten *G. schlechtendaliana* individuals (including five of *G. schlechtendaliana* var. *yakushimensis*), and fifteen *G. similis* individuals were collected throughout Japan. Three individuals of *G. ×tamnaensis*, a natural hybrid between *G. schlechtendaliana* and *G. similis* (Lee et al. 2010, 2012; Suetsugu et al. 2021b), were included in the comparative study (Suppl. material 1). Genomic DNA was extracted from silica-dried leaves using the CTAB method. An MIG-seq library for the 39 *Goodyera* samples was prepared according to the protocol outlined in Suyama et al. (2022). The library was sequenced using an Illumina MiSeq Sequencer (Illumina, San Diego, CA, USA) with a MiSeq Reagent Kit v3 (150 cycle, Illumina). The raw MIG-seq data of the 15 *G. similis* samples, 10 *G. schlechtendaliana* samples (including five *G. schlechtendaliana* var. *yakushimensis* samples), and three *G. ×tamnaensis* samples had previously been deposited at the DDBJ Sequence Read Archive (DRA, accession number DRA011506) for Suetsugu et al. (2021b). The raw MIG-seq data of the 11 *G. crassifolia* samples were deposited at the DDBJ Sequence Read Archive (DRA, accession number DRA014540).

After removing the primer sequences and low-quality sequencing reads (Suetsugu et al. 2021b), 3 594 716 reads ($92\,172 \pm 3937$ reads per sample) were obtained from 4 058 158 raw reads ($104\,055 \pm 4344$ per sample). Stacks 2.60 pipeline was used for *de novo* single nucleotide polymorphism (SNP) discovery (Rochette et al. 2019), with the following parameters: minimum depth of coverage required to create a stack (m) = 3, maximum distance allowed between stacks (M) = 2, and number of mismatches allowed between sample loci while building the catalog (n) = 2. For the maximum likelihood and SplitsTree phylogenetic analyses, SNPs retained by four or more samples were used; for the population structure analysis, SNPs retained by 16 or more samples were used. SNPs with high heterozygosity ($H_o \geq 0.6$) were removed. SNP sites with fewer than three minor alleles were filtered out. Finally, 4790 SNPs from 2795 loci were retained for phylogenetic analysis. For STRUCTURE analysis, to avoid linked SNPs, we used only the first SNP from each locus, retaining 874 SNPs.

Our SNP-based maximum likelihood phylogeny was inferred using RAxML 8.2.10 (Stamatakis 2014), using a GTR substitution model with Lewis' ascertainment bias

correction and 1000 iterations of parallelized tree search bootstrapping. To examine interspecific hybridization, a Neighbor-Net network was constructed using SplitsTree4 4.14 (Huson and Bryant 2006) using the uncorrelated P distance matrix. Population structure was examined using STRUCTURE 2.3.4 (Pritchard et al. 2000). We performed 20 independent runs, with a burn-in of 100 000 steps and an additional 100 000 steps using an admixture model, and estimated the log-likelihoods for each cluster ($K = 1-10$). Optimal K values were determined using the Delta K method (Evanno et al. 2005) in Structure Harvester (Earl and vonHoldt 2012). The results were visualized using CLUMPAK (Cluster Markov Package Across K) (Kopelman et al. 2015).

Results and discussion

Morphological distinctness of *Goodyera crassifolia*

The most remarkable characteristic of *G. crassifolia* is its column with lateral appendages (Figs 1–5). The lateral column appendages are consistently absent in the closely related taxa. Since the lateral appendages are themselves column-like, they are likely to be enlarged staminodes (Oh et al. 2022). Notably, the lateral appendages of the column differ significantly in size among populations, and in terms of their position on the inflorescence, being often conspicuous in the basal flowers and inconspicuous (or rarely absent) in the apical flowers. We observed an association between the column and lip or rostellum shape; the lip and the rostellum appeared to be three-lobed when the lateral appendages are conspicuous (Figs 2E, F, 3E, F, 4G, H, 5E, G). Given that the floral organ formation is explained mainly by the combined expression of ABCE-class MADS-box transcription factors (Causier et al. 2010; Hsu et al. 2015, 2021; Suetsugu et al. 2022), the spatial expression of the factors underlying this distinctive morphology deserves further investigation. In particular, the enlarged staminodes indicate that *G. crassifolia* exhibits some radial symmetry, unlike most orchid flowers, which are typically zygomorphic.

Detailed morphological examination revealed that *G. crassifolia* can be distinguished from *G. schlechtendaliana* by not only column shape (column with vs. without lateral appendages) but also plant height (20–37 cm vs. ca. 15 cm), leaf texture (coriaceous vs. papyraceous), leaf coloration (glossy green, with narrow pale-white reticulation, to green with no decorations vs. green with obvious and broad white reticulation), inflorescence architecture (lax, internodes 17–24 mm long at inflorescence base vs. dense internodes 6–10 mm long at inflorescence base), pedicellate ovary length (11–20 mm, longer than floral bract vs. 7–9 mm, as long as the floral bract), flower opening (opening weakly vs. widely), flower size (sepal and petal length > 10 mm vs. < 10 mm), shape of lateral sepal (recurved at two-thirds of its entire length from the base vs. strongly recurved at half its entire length from the base), hypochile shape (weakly vs. strongly concave-saccate), and seed shape (often polyembryonic vs. always monoembryonic) (Lee et al. 2010, 2012; Bhattacharjee and Chowdhery 2012; Suetsugu and Hayakawa 2019; Suetsugu et al. 2021b; Oh et al. 2022).



Figure 1. *Goodyera crassifolia* in its natural habitat **A** flowering individual **B** flowers **C** fruiting individual **D** leaves. Scale bars: 30 mm.

It should be noted that *G. crassifolia* has previously been confused with *G. ×tamnaensis* in Japan (Takahashi 1985; Akiyama 2010; The Flora-Kanagawa Association 2018). In fact, *G. crassifolia* is superficially similar to *G. ×tamnaensis* in terms of its weakly opening flowers but differs in plant height (20–37 cm for *G. crassifolia* vs.

10–15 cm for *G. ×tamnaensis*), leaf texture (coriaceous vs. papyraceous), leaf coloration (glossy green with narrow, pale-white reticulation to green with no decoration on upper surface vs. velutinous dark green with a white central vein and reticulate venation), ovary and pedicel length (11–20 mm vs. 7–10 mm long), flower size (petal and sepal length > 10 mm vs. < 10 mm), column shape (column with vs. without lateral appendages), and rostellum shape (acuminate apex, occasionally bi- or trilobed vs. flattened and cuneate apex, never divided) (Lee et al. 2010, 2012; Bhattacharjee and Chowdhery 2012; Suetsugu and Hayakawa 2019; Suetsugu et al. 2021b).

Further detailed comparison of morphological characters among *G. crassifolia*, *G. schlechtendaliana* and *G. ×tamnaensis* is given in Table 1. Additional descriptions and illustrations of *G. crassifolia*, *G. schlechtendaliana*, *G. ×tamnaensis*, and *G. similis* are available in Lee et al. (2010, 2012), Suetsugu and Hayakawa (2019), Suetsugu et al. (2021b), and Oh et al. (2022).

Reproductive barriers between *Goodyera crassifolia* and *G. schlechtendaliana*

Polyploidization is commonly accepted as a vital mechanism of sympatric speciation in plants (Köhler et al. 2010). Owing to chromosome number imbalance during meiosis, backcross between either parent would mostly result in nonviable progenies; those rare survivors with unbalanced chromosome numbers will be primarily sterile (Ramsey and Schemske 1998). The triploid-block is a significant reproductive barrier leading to polyploid speciation (Köhler et al. 2010).

Table 1. Morphological comparison among *Goodyera crassifolia*, *G. schlechtendaliana*, *G. ×tamnaensis* and *G. velutina*.

Characters	<i>G. crassifolia</i>	<i>G. schlechtendaliana</i>	<i>G. ×tamnaensis</i>	<i>G. velutina</i>
inflorescence length	20–37 cm	ca. 15 cm	10–15 cm	6–10 cm
leaf texture	coriaceous	papyraceous	papyraceous	papyraceous
leaf color	glossy green	glossy green	velutinous dark green	velutinous dark green
leaf shape	ovate to lanceolate-ovate	elliptic-ovate	lanceolate-ovate	ovate
leaf central vein	faint	faint	prominent	prominent
leaf lateral vein	faint	prominent	intermediate	hidden
leaf reticulate venation	faint	prominent	faint	visually unrecognizable
ovary and pedicel length	11–20 mm	7–9 mm	7–10 mm	7–10 mm
hair shape and length on peduncle and ovary	0.3–0.5 mm, clavate	0.3–0.4 mm, clavate	0.3–0.4 mm, clavate	0.1 mm, subulate
color of bract, ovary and inflorescence	pale green	pale green	reddish-brown	reddish-brown
flower opening	weekly open	widely open	weekly open	weekly open
flower color	white	white	light reddish pink	light reddish pink
color of lip and lateral petal apex	usually dark brown or rarely brown	usually brown or rarely dark green	light reddish pink	light reddish pink
shape of lip apex	recurved	strongly recurved	recurved	slightly recurved
lateral column appendages	present or rarely absent	absent	absent	absent
rostellum shape	narrowly triangular, 1/2 as long as column, apex acuminate, occasionally bi- or trilobed	narrowly triangular, 1/2 as long as column, apex acuminate, never divided	narrowly triangular, 1/2 as long as column, apex cuneate, never divided	oblong to rectangular, 2/5 as long as column, apex cuneate, never divided



Figure 2. *Goodyera crassifolia* from Kami City, Kochi Prefecture (*Hisanori Takeuchi G161-1*, KYO) **A** dorsal sepal (abaxial view) **B** lateral sepals (left: abaxial view, right: adaxial view) **C** lateral petals (left: abaxial view, right: adaxial view) **D** lip and column (dorsal view) **E** lip (left: adaxial view, right: lateral view) **F** column (left: obliquely dorsal view, right: ventral view) **G** column (left: ventral view, right: lateral view) **H** lateral appendages removed from column (left: dorsal view, right: ventral view) **I** lateral appendages removed from column (both: dorsal view) **J** pollinarium (left: dorsal view, right: ventral view) **K** anther cap (left: dorsal view, right: ventral view). Arrows indicate the conspicuous lateral appendages. Photographs except **G** and **I** are derived from the same flower. **G** and **I** are used to show morphological variation of column within the same individual. Scale bars: 3 mm.

Investigation of chromosome numbers provided evidence of polyploidy in *G. crassifolia*: all of the *G. schlechtendaliana* individuals (including *G. schlechtendaliana* var. *yakushimensis*) showed a chromosome number of $2n = 30$;



Figure 3. *Goodyera crassifolia* from Higashimuro County, Wakayama Prefecture (*Yasuo Takada s.n.*, KYO) **F, G** column The conspicuous lateral appendages are indicated by arrows **H** column removing lateral appendages **I, J** lateral appendages removed from column **K** pollinarium **L** anther cap and pollinarium **A** dorsal sepal (abaxial view) **B** lateral sepals (left: abaxial view, right: adaxial view) **C** lateral petals (left: abaxial view, right: adaxial view) **D** lip and column (dorsal view) **E** lip (left: adaxial view, right: lateral view) **F** column (left: dorsal view, right: ventral view) **G** column (obliquely lateral view) **H** column removing lateral appendages (ventral view) **I** lateral appendages removed from column (left: dorsal view, right: ventral view) **J** lateral appendages removed from column (ventral view) **K** pollinarium (ventral view) **L** anther cap and pollinarium (left: dorsal view, right: ventral view). Arrows indicate the conspicuous lateral appendages. Photographs except **G, H, J, K** are derived from the same flower **G, H, J** show the variation of column morphology within the same individual, while **K** is used because pollinaria were detached from anther cap of a flower that was mainly used. Scale bars: 3 mm.

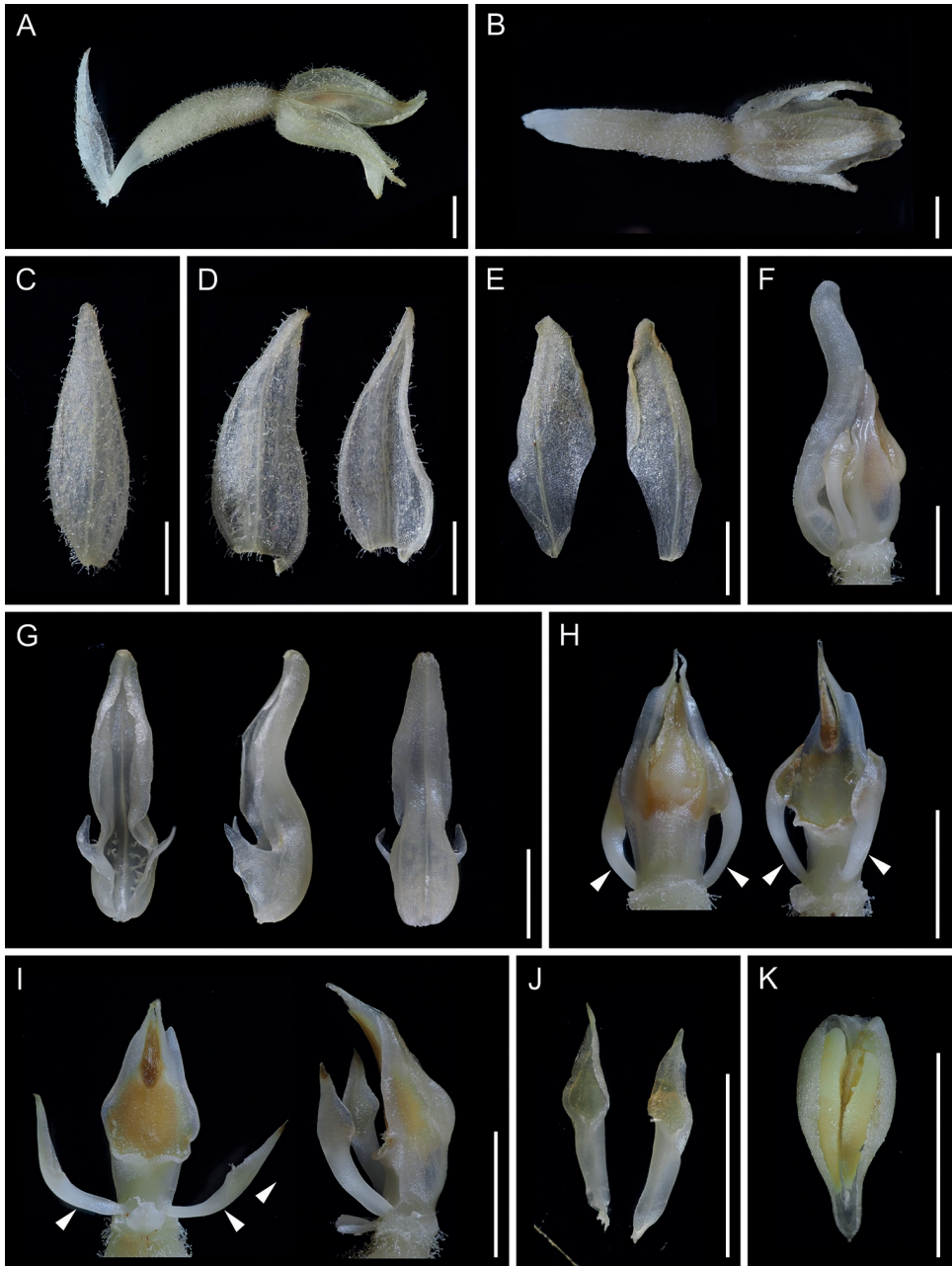


Figure 4. *Goodyera crassifolia* (Koji Tanaka KS209, KYO; photographed after immersion in 50 percent ethanol) **A** flower (lateral view) **B** flower (dorsal view) **C** dorsal sepal (abaxial view) **D** lateral sepals (left: abaxial view, right: adaxial view) **E** lateral petals (left: abaxial view, right: adaxial view) **F** lip and column (lateral view) **G** lip (left: adaxial view, middle: lateral view, right: abaxial view) **H** column (left: dorsal view, right: obliquely ventral view) **I** column with partially detached lateral appendages (left: ventral view, right: lateral view) **J** lateral appendages removed from column (ventral view) **K** anther cap and pollinarium (ventral view). Arrows indicate the conspicuous lateral appendages. All photographs are derived from the same flower. Scale bars: 3 mm.



Figure 5. *Goodyera crassifolia* (Hisanori Takeuchi & Kenji Suetsugu KS208, KYO) **A** dorsal sepal (adaxial view) **B** lateral sepal (adaxial view) **C** lateral petal (adaxial view) **D** lip and column (dorsal view) **E** lip (left: adaxial view, right: lateral view) **F** longitudinal section of lip (adaxial view) **G** column and anther (left: top view, right: lateral view) **H** column (left: dorsal view, middle: lateral view, right: ventral view) **I** pollinarium (left: dorsal view, right: ventral view) **J** anther cap (dorsal view). Arrows indicate the conspicuous lateral appendages. All photographs are derived from the same flower. Scale bars: 3 mm.

whereas all *G. crassifolia* individuals (Fig. 6) showed $2n = 60$. In line with the results obtained in this study, Oh et al. (2022) reported $2n = 60$ for a Korean *G. crassifolia* individual. Intriguingly, Sera (1990) reported $2n = 60$ in five “*G. schlechtendaliana*” plants from four localities, while reporting $2n = 30$ for most *G. schlechtendaliana*

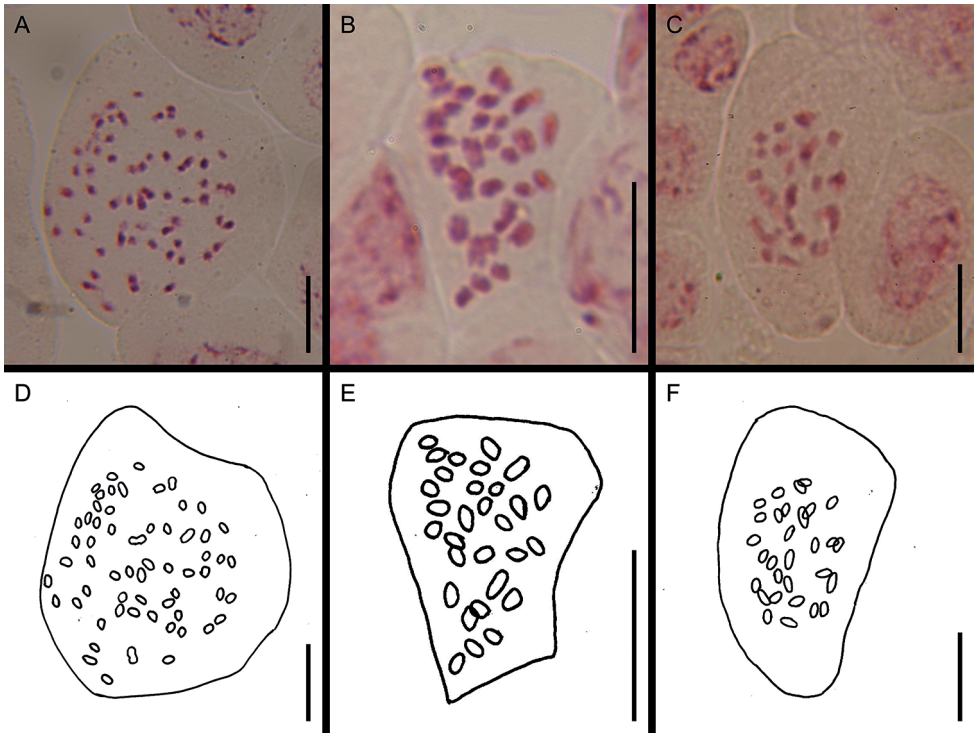


Figure 6. Somatic chromosomes (**A–C**) and their explanatory drawings (**D–F**) of *Goodyera crassifolia* and its closely related taxa **A, D** *G. crassifolia* **B, E** *G. schlechtendaliana* **C, F** *G. schlechtendaliana* var. *yakushimensis*. Scale bars: 10 μ m.

individuals (60 plants from 22 localities collected throughout Japan). However, Sera (1990) noted that the $2n = 60$ “*G. schlechtendaliana*” plants possess coriaceous leaves with faint reticulate variegation. The photographs listed in Sera (1990) indicate that they also have laxly flowered inflorescences and a longer pedicellate ovary, which are characteristic features of *G. crassifolia*. Although three of the voucher specimens from Sera (1990) have unfortunately been lost, possibly during the relocation of the herbarium HIBG (T. Sera, personal communication), we could identify the two remaining voucher specimens as *G. crassifolia*. It is likely that all of the $2n = 60$ plants of Sera (1990) could be *G. crassifolia*. Given that $2n = 30$ is the only chromosome number reported in *G. schlechtendaliana* as determined by other previous studies (Matsuura and Nakahira 1958; Shoji 1963; Tanaka 1965; Sun et al. 1996; Tae et al. 1997), $2n = 30$ is arguably the typical chromosome number of *G. schlechtendaliana*. In addition, $2n = 30$ has been reported in *G. ×tamnaensis* (Lee et al. 2012), although speciation via hybridization without a change in chromosome number is considered rare (Schumer et al. 2014). Thus, as suggested by Oh et al. (2022), the cytological distinctness of *G. crassifolia* may have partially contributed to its reproductive isolation.

Our pollination experiments revealed the contrasting breeding systems of *G. crassifolia* and *G. schlechtendaliana*. The latter, although self-compatible, is neither autogamous nor agamospermous, and shows low fruit set under natural conditions; pollinator limitation was the major cause of low fruit set, which was significantly improved by manual autogamy and allogamy (Table 2, $P < 0.001$). By contrast, the natural populations of *G. crassifolia* consistently exhibited high fruit set (Fig. 1). Given that high fruit set was obtained in agamospermous, bagged, manually geitonogamous, manually allogamous, and open flowers, *G. crassifolia* flowers are not pollinator-limited under natural conditions. Neither seed mass nor the proportion of seeds with embryo varied significantly with pollination treatment (Table 2). Given that the rostellum functionally prevents autonomous autogamy, agamospermy is arguably the main cause of high fruit set in *G. crassifolia*. Therefore, agamospermy provides reproductive assurance under pollinator limitation in *G. crassifolia*.

Notably, the viscidium of *G. crassifolia* exhibits almost no adhesion, hindering its attachment onto its potential pollinators. No pollinia removal or deposition was observed during the field study. Because (i) *G. crassifolia* has weakly opened flowers with less-adhesive pollinia and (ii) its stigma is sometimes covered with column appendages (Figs 2G, 3F), there are arguably few opportunities for outcrossing. Thus, agamospermy is probably its dominant, if not exclusive, reproductive strategy. The reduced selection pressure on outcrossing may have led to the aforementioned variations in the lip, column appendages, and rostellum morphology, even within a single inflorescence. The polyembryony detected in *G. crassifolia* is further indicative of agamospermy, given that adventitious embryony, the most common form of apomixis, is characterized by a high number of polyembryonic seeds (Catling 1982; Campacci et al. 2017; Naumova 2018).

During our field study, we confirmed the phenological isolation between *G. crassifolia* and *G. schlechtendaliana* as previously reported by Takahashi (1985) and Oh et al. (2022). In many regions where both are sympatric (e.g., Hongdo, Korea: Oh et al. 2022; southern and central Japan: Takahashi (1985) and field observations in this study), *G. schlechtendaliana* starts to flower ca. 3–4 weeks earlier than *G. crassifolia*.

Table 2. Effects of pollination treatment on fruit set, seed mass and proportion of seeds with embryo in *Goodyera crassifolia* and *G. schlechtendaliana*.

Species		Agamospermy	Autonomous autogamy	Manual autogamy	Manual allogamy	Open
<i>G. crassifolia</i>	Fruit set (%)	85.0 ^a	95.0 ^a	90.0 ^a	85.0 ^a	87.5 ^a
	Seed mass (mg)	8.1 ± 2.5 ^a	8.1 ± 2.3 ^a	7.9 ± 2.0 ^a	7.9 ± 2.3 ^a	8.1 ± 1.8 ^a
	Seeds with embryo	165.7 ± 9.9 ^a	163.4 ± 9.2 ^a	164.2 ± 9.0 ^a	164.1 ± 9.5 ^a	162.6 ± 8.0 ^a
<i>G. schlechtendaliana</i>	Fruit set (%)	0 ^a	0 ^a	90.0 ^b	90.0 ^b	32.5 ^c
	Seed mass (mg)	–	–	2.8 ± 1.5 ^a	3.4 ± 1.5 ^a	3.1 ± 1.5 ^a
	Seeds with embryo	–	–	185.8 ± 7.5 ^a	187.1 ± 8.0 ^a	187.2 ± 5.7 ^a

Different superscript letters indicate significant differences ($P < 0.05$) between treatment groups. Both seed mass and seeds with embryo are expressed by mean ± SD.

Despite the slight overlap in their flowering periods, the temporal isolation could significantly reduce interspecific cross-pollination. In addition, the predominantly agamosperous breeding system of *G. crassifolia* helps maintain its reproductive isolation from *G. schlechtendaliana*. A similar reproductive isolation mechanism was proposed to explain the maintenance of integrity between sexually reproducing taxa and agamosperous taxa within the same genus (Catling and Brown 1983).

Phylogenetic distinctness of *Goodyera crassifolia*

MIG-seq-based maximum likelihood phylogenetic tree generated in this study revealed that *G. crassifolia* forms a separate clade from *G. similis* and *G. schlechtendaliana* (100% bootstrap value; Fig. 7). *Goodyera schlechtendaliana* was paraphyletic, while the monophyly of *G. schlechtendaliana* var. *yakushimensis* was supported (100% bootstrap value). Neighbor-Net phylogenetic analysis indicated that *G. crassifolia*, *G. schlechtendaliana*, and *G. similis* represent three distinct genetic clusters (Fig. 8). In the Neighbor-Net analysis, we show that the genetic diversity of *G. schlechtendaliana* as a whole, including *G. schlechtendaliana* var. *yakushimensis*, is comparable to that of *G. similis*. Therefore, *G. schlechtendaliana* var. *yakushimensis* is more likely to be an intraspecific variant of *G. schlechtendaliana* rather than an independent species. The interpretation is also based on the results of STRUCTURE analysis mentioned below, as well as on the relatively small morphological differences between var. *schlechtendaliana* and var. *yakushimensis* indicated by Suetsugu and Hayakawa (2019).

The STRUCTURE analysis at $K = 2$ (the largest delta K for our data) classified *G. crassifolia* and *G. schlechtendaliana* (including var. *yakushimensis*) into the same cluster, while at $K = 3$ (the second-largest delta K), *G. crassifolia*, *G. schlechtendaliana* (including var. *yakushimensis*), and *G. similis* formed three groups (Fig. 9). These findings, together with its multiple morphological differences from those observed in *G. schlechtendaliana* and *G. similis*, support the status of *G. crassifolia* as an independent species. Furthermore, genetic variation, which was high in the outcrossing *G. schlechtendaliana*, was low in the predominantly agamosperous *G. crassifolia*, both between and within populations. Similar patterns have been observed in other orchids, including *Nigritella* Rich., which includes both outcrossing and agamosperous species (Hedrén et al. 2018).

Molecular data obtained in this study provide further evidence that *G. crassifolia* has a different evolutionary origin from *G. ×tamnaensis*. Both phylogenetic and population structure analyses showed that *G. ×tamnaensis* has genetic components of both *G. schlechtendaliana* and *G. similis* (Figs 7–9). By contrast, although *G. crassifolia* was suspected as a natural hybrid of *G. schlechtendaliana* and *G. similis* (Takahashi 1985; Akiyama 2010), neither the phylogenetic analysis nor the population structure analyses support genetic admixture between *G. crassifolia* and any of its close congeners (Figs 7–9).

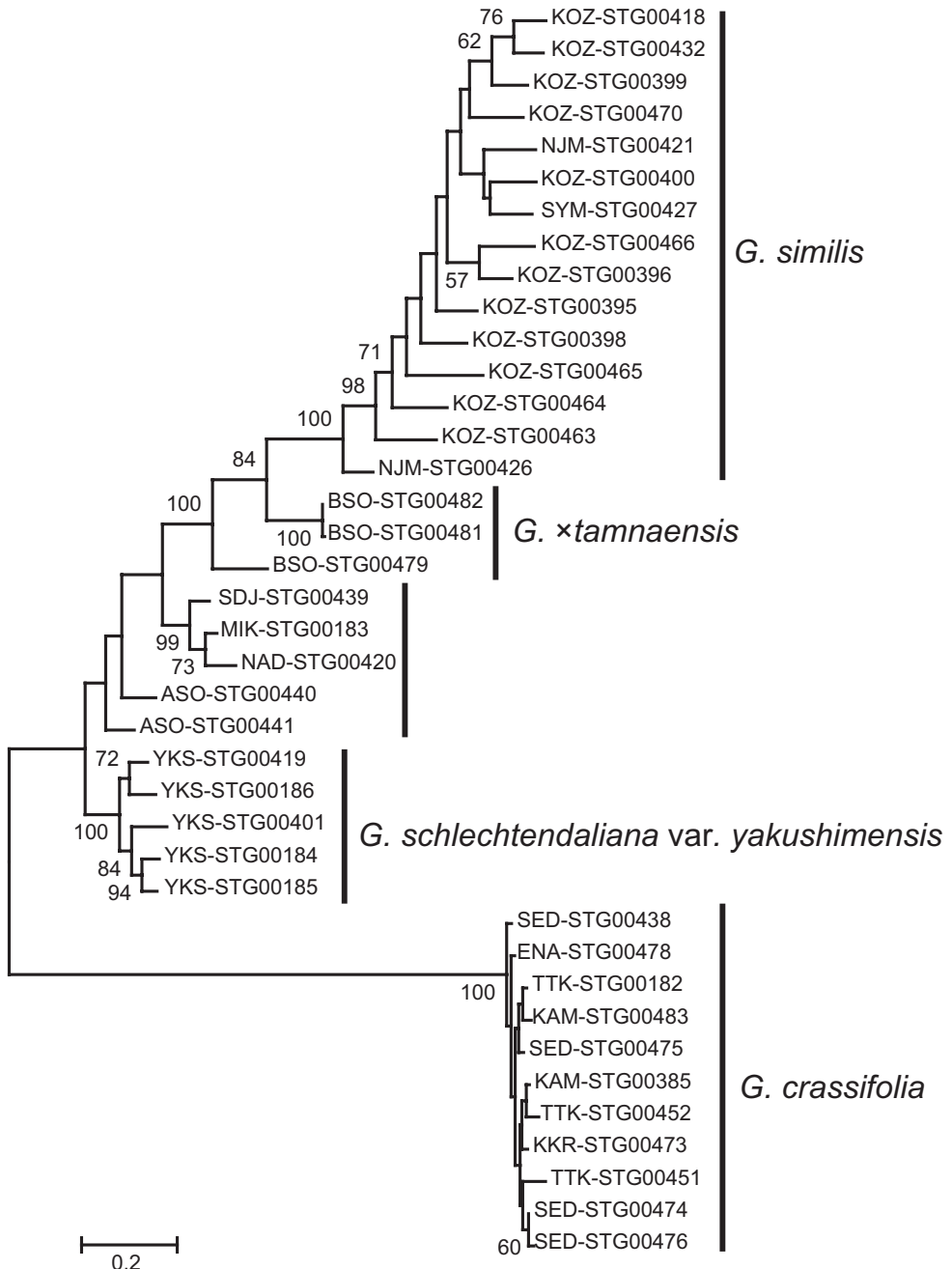


Figure 7. Phylogenetic tree of *Goodyera crassifolia* and its closely related taxa reconstructed using MIG-seq data. Bootstrap values within species, and those less than 50%, are not shown. Branch length represents the average number of substitutions per site.

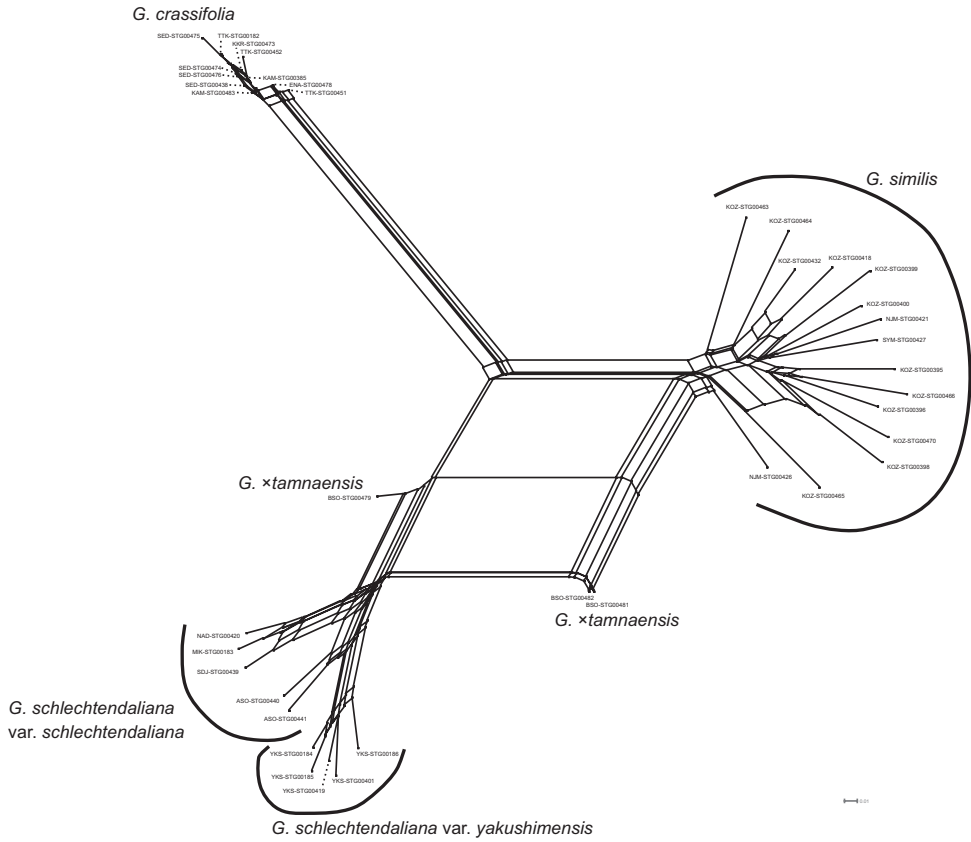


Figure 8. Neighbor-Net network for *Goodyera crassifolia* and its closely related taxa, based on uncorrected P distances calculated from 4790 SNPs.

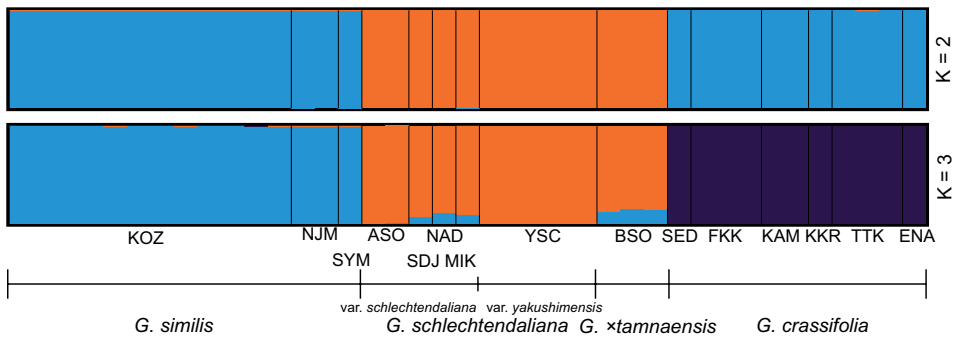


Figure 9. Population structure of *Goodyera crassifolia* and its closely related taxa, inferred with STRUC-TURE 2.3.4. Using $K = 2$ and $K = 3$ generated the largest and second-largest delta K , indicating that they were the most and second most optimal, respectively. Species and populations are separated by broad and narrow vertical black lines, respectively.

Conclusion

The results obtained in this study confirm that *G. crassifolia* is distinct from *G. ×tammaensis*, refuting the hybrid origin hypothesis. Our rejection of the hybrid origin hypothesis is consistent with the karyological study of Sera (1990) concluding that the $2n = 60$ plants (= *G. crassifolia*) are autopolyploids of the typical *G. schlechtendaliana*, given their similar resting-stage and mitotic-prophase chromosome morphology. Different chromosome number, agamosperous breeding, and early flowering possibly contributed to the pre-mating isolation of *G. crassifolia* from its morphologically most similar species, the sympatric *G. schlechtendaliana*. Overall, the molecular phylogeny reconstructed from MIG-seq data together with morphological, cytological, and ecological analyses, support the separation of *G. crassifolia* as an independent species.

Updated taxonomic treatment

Goodyera crassifolia H.-J.Suh, S.-W.Seo, S.-H.Oh & T.Yukawa

Type. KOREA. Jeollanam-do, Sinan-gun, Heuksando Island, 26 September 2016, S.-H. Oh et al. 7155 (holotype: KB, isotypes: BH, TNS!, TUT).

Terrestrial herb, 20–37 cm tall. Rhizome pale green to brownish green, rooting at nodes. Roots fleshy, yellowish-brown, with minute root hairs. Stems erect, terete, 20–37 cm long, 3.4–7.5 mm in diam., pale green, glabrous. Leaves 5–15, widely spaced or somewhat clustered toward apex along the stem, 4.0–9.2 cm long; lamina ovate to lanceolate-ovate, 3.3–7.5 × 1.3–3.1 cm, length: width ratio 1.6–2.8, coriaceous, rounded at base, acute at apex, dorsally green with pale white reticulation or without any color decoration; petiole-like. Inflorescence a lax secund raceme, 6–14-flowered, with 2–4 sterile bracts; rachis 6.9–17.1 cm, internodes 17–24 mm long at inflorescence base; floral bracts lanceolate, 8–16 mm, pubescent, acuminate to acute at apex, pale green, shorter than the pedicellate ovary. Ovary and pedicel cylindrical-fusiform, 11–20 mm, pale green, pubescent; hair on ovary and pedicel 0.3–0.5 mm, clavate. Flowers resupinate, weekly open. Sepals free, sub-similar, white tinged with pale yellow, pubescent on the outer surface, 1-veined; dorsal sepal narrowly elliptic-lanceolate, cymbiform, 10.1–12.8 × 3.3–4.4 mm, subacute at apex, forming a hood with petals; lateral sepals obliquely ovate-lanceolate, 9.7–12.5 × 3.2–4.8 mm, recurved at 2/3 of its entire length from the base, acute at apex, weekly spreading. Petals obliquely rhombic-oblong to oblong-oblongate, 10.0–12.0 × 3.5–4.6 mm, hood recurved at apex, white tinged with pink or pale yellow, glabrous, 1-veined. Lip ovate-lanceolate, 9.5–11.5 × 2.7–4.0 mm; hypochile weekly concave-saccate, occasionally three-lobed, papillose inside; epichile ligulate, subacute at apex with 2 keels along the midrib. Column with lateral appendages; 5.8–7.3 mm long; stigma orbicular, slightly protruding; rostellar arms slender, occasionally three-lobed, sharp at apex; lateral appendage, rarely absent, usually 2 (–4), subulate or clavate, somewhat column-like, up to 6.0 mm long; anther ovate, 3.4–4.0 mm long; pollinia clavate, ca 4.0 mm; viscidium elliptic, ca. 2.0 mm

long. Fruits cylindrical-fusiform, 13–22 mm long. Seeds fusiform, 0.8–1.1 mm long; embryo 1–3, ellipsoid, ca. 0.2 mm long.

Specimens examined. JAPAN. **Kyushu District**—Miyazaki Pref.: Nishiusuki-gun, Gokase-cho, Kuraoka, 25 September 2013, *T. Minamitani s.n.* (AICH). Fukuoka Pref.: Kitakyushu-shi, Kokuraminami-ku, 11 September 2016, *K. Tanaka KS209* (KYO); Kitakyushu-shi, Kokuraminami-ku, 23 September 2018, *K. Tanaka STG00473* (KYO, herbarium sheet and spirit collection labelled as the same specimen); Tagawa-gun, Soeda-cho, Fukakura, 1 October 2016, *K. Tanaka STG00438* (KYO, spirit collection); Tagawa-gun, Soeda-cho, Fukakura, 24 September 2018, *Koji Tanaka STG00474* (KYO, herbarium sheet and spirit collection labelled as the same specimen); Kaho-cho, Mt. Kosyo, 4 May 1980, *T. Sera HIBG12487* (HIBG). **Shikoku District**—Ehime Pref.: Siyo-shi, Nomura-cho, Komatsu, 9 May 1981, *H. Yoshioka HIBG4684* (HIBG). Kochi Pref.: Agawa-gun, along Nano River, 21 July 1888, *s.n.* (TI); Takaoka-gun, Niyodo-mura, 13 September 1962, *G. Murata s.n.* (KYO); Bandamori, September 1889, *T. Makino s.n.* (MAK); Aki-gun, Kitagawa-mura, date unknown 1886, *S. Watanabe s.n.* (MAK); Kami-shi, Kahoku-cho, 17 September 2015, *H. Takeuchi & K. Suetsugu KS208* (KYO, spirit collection); Kami-shi, Kahoku-cho, 14 September 2016, *K. Suetsugu STG00385* (KYO, spirit collection); Kami-shi, Kahoku-cho, 28 September 2021, *H. Takeuchi G161-1* (KYO, herbarium sheet and spirit collection labeled as the same specimen); Muroto-shi, Sakihama-cho, 15 September 1974, *S. Takafuji s.n.* (KYO); Hata-gun, Hashigami-mura, 25 September 1914, *H. Yamaguchi s.n.* (TNS); Nyodogawa-cho, along Nakano River, 29 September 2020, *S. Hyodo KS767* (KYO, spirit collection). **Chugoku District**—Yamaguchi Pref.: Abu-gun, Akiragi-mura, 24 September 1919, *S. Nikai s.n.* (TNS). Hiroshima Pref.: Otake-shi, Kuritani-cho, Kokuribayashi, 9 September 2021, *K. Takeuchi et al. HIBG25924* (HIBG); Otake-shi, Kuritani-cho, Kokuribayashi, 9 September 2021 *K. Takeuchi et al. HIBG25925* (HIBG); Otake-shi, Kuritani-cho, Kokuribayashi, 9 September 2021, *K. Takeuchi et al. HIBG25926* (HIBG). Hyogo Pref.: Miki-shi, Fukui, 11 September 2021, *K. Umeki s.n.* (HYO). **Kinki District**—Nara Pref.: Totsukawa-mura, 26 September 2009, *K. Suetsugu KS207* (TNS); Yoshino-gun, Totsukawa-mura, 2 March 2017, *K. Suetsugu STG00182* (KYO); Yoshino-gun, Totsukawa-mura, 18 July 2018, *K. Suetsugu STG00451* (KYO). Wakayama Pref.: Nishimuro-gun, Kawazoe-mura, 23 September 1927, *N. Nakashima s.n.* (TI); Shingu-shi, Dorohaccho, 7 November 1950, *G. Nakai 5020* (KYO); Mt. Koya, 24–25 September 1955, *G. Murata s.n.* (KYO); Higashimuro-gun, Nachikatsuura-cho, September 1904, *K. Minakata s.n.* (MAK); Higashimuro-gun, Kogagawa-cho, 10 October 2021, *Y. Takada s.n.* (MAK); Arida-gun, Aridagawa-cho, Kusumoto, 29 September 2013, *A. Naitou 1592* (AICH). Mie Pref.: Kihoh-cho, Ainotani, 27 April 2009, *K. Suetsugu & T. Tonda KS206* (KYO); along Choshi River, 25 September 1955, *K. Iwatsuki s.n.* (KYO); Inabe-shi, Hokusei-cho, Betsumyo, 4 October 2013, *Y. Deguchi s.n.* (AICH). **Chubu District**—Gifu Pref.: Ena-shi, 16 September 2018, *K. Iwahori STG00478* (KYO, herbarium sheet and spirit collection labelled as the same specimen). Aichi Pref.: locality unknown, September 1897, collector unknown (KYO); Toyohashi-shi,

Iwasaki-cho, Nagao, 28 September 2020, *Y. Kitada* KS871 (KYO, spirit collection); Atsumi-gun, Atsumi-cho, Takaki, 24 September 2001, *M. Kobayashi* 73668 (AICH); Higashikamo-gun, Asahi-cho, Yawata, 22 August 1992, *S. Serizawa* 62497 (AICH); Toyota-shi, Sasabara-cho, 28 August 1991, *S. Serizawa* 60088 (AICH); Toyota-shi, Tamomi-cho, Fujibora, 10 September 2007, *S. Serizawa* 82210 (AICH); Nukata-gun, Kota-cho, Fukozu, 22 September 1995, *R. Kaneko* 1275 (AICH); Hazu-gun, Kira-cho, Madarame, 11 March 1991, *H. Okada* 28 (AICH); Seto-shi, Kawahira-cho, 12 September 1999, *T. Tsukamoto* 2833 (AICH); Seto-shi, Sono-cho, 6 September 1999, *T. Tsukamoto* 2828 (AICH); Seto-shi, Sono-cho, 25 September 2000, *T. Tsukamoto* 2924 (AICH); Seto-shi, Anada-cho, 20 September 1992, *O. Hibino* 856 (AICH); Seto-shi, Umagajo-cho, 26 September 1992, *T. Tsukamoto* 397 (AICH); Seto-shi, Higashiyamaji-cho, 10 September 1998, *T. Tsukamoto* 2701 (AICH); Seto-shi, Hirokute-cho, 21 September 1999, *S. Serizawa* 76414 (AICH); Seto-shi, Uenoyama-cho, 20 September 2000, *T. Tsukamoto* 2921 (AICH); Owariasahi-shi, Hirako-cho, 23 September 2013, *M. Muramathu* 27088 (AICH); Komaki-shi, Oyama, 29 April 1997, *M. Kobayashi* 60932 (AICH); Kasugai-shi, Hazama-cho, 18 September 2005, *K. Yamada* 1256 (AICH); Nagoya-shi, Moriyama-ku, Togoku, 13 September 2008, *S. Serizawa* 83258 (AICH); Nagoya-shi, Moriyama-ku, Kikko, 19 July 2017, *S. Serizawa* 92748 (AICH). Shizuoka Pref.: Kosai-shi, Tame, 23 September 1995, *U. Naitou* 5558 (AICH). **Kanto District**—Kanagawa Pref.: Sagamihara-shi, Midori-ku, 23 October 2010, *M. Nagai s.n.* (SCM). Tokyo Metropolis: Hachijo Island, 9 October 1974, *T. Nakaike* 50067 (TNS).

Note. Although Oh et al. (2022) noted that *G. crassifolia* is restricted to two offshore islands of the Korean peninsula and to a few locations in Japan, we have recognized many other new localities in Japan. Notably, all the *G. crassifolia* herbarium specimens (except the SCM specimen treated as *G. xtamnaensis*) have been annotated as *G. schlechtendaliana*. Therefore, *G. crassifolia* may have been misidentified as *G. schlechtendaliana* in the other areas. Extensive surveys during the flowering season are needed to elucidate the distribution of *G. crassifolia*.

Acknowledgements

We thank Koji Tanaka, Hisanori Takeuchi, Yoshiaki Kitada, Takashi Honda, Shoji Hyodo and Katsumi Iwahori for their help with the sampling. We also thank Takuto Shitara, Masayuki Ishibashi and Yoshiaki Kitada for their skillful technical assistance with photography. We are equally thankful to the curators of AICH, HIBG, HYO, KYO, MAK, SCM, TI, and TNS for access to herbaria or collection databases. We are grateful to Takako Shizuka, Kohei Yamana and Kazuma Takizawa for technical assistance. We thank Hirokazu Tsukaya and Tetsuya Sera for their valuable discussions. We would like to thank Editage (www.editage.com) for English language editing. This study was financially supported by the Environment Research and Technology Development Fund (#4-2001, KS and YS) from the Ministry of Environment, Japan.

References

- Akiyama K (2010) A putative hybrid between *Goodyera schlechtendaliana* and *G. velutina*. *Flora Kanagawa* 71: 862–863. [In Japanese]
- Baldwin BG, Sanderson MJ, Porter JM, Wojciechowski MF, Campbell CS, Donoghue MJ (1995) The ITS region of nuclear ribosomal DNA: A valuable source of evidence on angiosperm phylogeny. *Annals of the Missouri Botanical Garden* 82(2): 247–277. <https://doi.org/10.2307/2399880>
- Barrett CF, Freudenstein JV (2011) An integrative approach to delimiting species in a rare but widespread mycoheterotrophic orchid. *Molecular Ecology* 20(13): 2771–2786. <https://doi.org/10.1111/j.1365-294X.2011.05124.x>
- Barrett CF, Santee MV, Fama NM, Freudenstein JV, Simon SJ, Sinn BT (2022) Lineage and role in integrative taxonomy of a heterotrophic orchid complex. *Molecular Ecology* 31(18): 4762–4781. <https://doi.org/10.1111/mec.16617>
- Bhattacharjee A, Chowdhery HJ (2012) Notes on two species of *Goodyera* (Orchidaceae). *Kew Bulletin* 67(3): 503–510. <https://doi.org/10.1007/s12225-012-9388-y>
- Botes C, van der Niet T, Cowling RM, Johnson SD (2020) Is biodiversity underestimated by classical herbarium-based taxonomy? A multi-disciplinary case study in *Satyrium* (Orchidaceae). *Botanical Journal of the Linnean Society* 194(3): 342–357. <https://doi.org/10.1093/botlinnean/boaa041>
- Campacci TVS, Castanho CT, Oliveira RLF, Suzuki RM, Catharino ELM, Koehler S (2017) Effects of pollen origin on apomixis in *Zygopetalum mackayi* orchids. *Flora* 226: 96–103. <https://doi.org/10.1016/j.flora.2016.11.013>
- Catling PM (1982) Breeding systems of northeastern North American *Spiranthes* (Orchidaceae). *Canadian Journal of Botany* 60(12): 3017–3039. <https://doi.org/10.1139/b82-358>
- Catling PM, Brown JR (1983) Morphometrics and ecological isolation in sympatric *Spiranthes* (Orchidaceae) in southwestern Ontario. *Canadian Journal of Botany* 61(10): 2747–2759. <https://doi.org/10.1139/b83-302>
- Causier B, Schwarz-Sommer Z, Davies B (2010) Floral organ identity: 20 years of ABCs. *Seminars in Cell & Developmental Biology* 21(1): 73–79. <https://doi.org/10.1016/j.semcdb.2009.10.005>
- Coyne JA, Orr HA (2004) *Speciation*. Sinauer Associates, Sunderland, MA, 545 pp.
- Earl DA, vonHoldt BM (2012) STRUCTURE HARVESTER: A website and program for visualizing STRUCTURE output and implementing the Evanno method. *Conservation Genetics Resources* 4(2): 359–361. <https://doi.org/10.1007/s12686-011-9548-7>
- Evanno G, Regnaut S, Goudet J (2005) Detecting the number of clusters of individuals using the software STRUCTURE: A simulation study. *Molecular Ecology* 14(8): 2611–2620. <https://doi.org/10.1111/j.1365-294X.2005.02553.x>
- Govaerts R, Bernet P, Kratochvil K, Gerlach G, Carr G, Alrich P, Pridgeon A, Pfahl J, Campacci M, Holland Baptista D, Tigges H, Shaw J, Cribb P, George A, Kreuz K, Wood J (2022) World Checklist of Orchidaceae. <http://wmsp.science.kew.org/> [October 3, 2022]
- Guan QX, Chen GZ, Li MH, Chen SP (2014) *Goodyera malipoensis* (Cranichideae, Orchidaceae), a new species from China: Evidence from morphological and molecular analyses. *Phytotaxa* 186(1): 51–60. <https://doi.org/10.11646/phytotaxa.186.1.4>

- Hedrén M, Lorenz R, Teppner H, Dolinar B, Giotta C, Griebel N, Hansson S, Heidtke U, Klein E, Perazza G, Ståhlberg D, Surina B (2018) Evolution and systematics of polyploid *Nigritella* (Orchidaceae). *Nordic Journal of Botany* 36(3): njb-01539. <https://doi.org/10.1111/njb.01539>
- Hirano T, Saito T, Tsunamoto Y, Koseki J, Prozorova L, Do VT, Matsuoka K, Nakai K, Suyama Y, Chiba S (2019) Role of ancient lakes in genetic and phenotypic diversification of freshwater snails. *Molecular Ecology* 28(23): 5032–5051. <https://doi.org/10.1111/mec.15272>
- Hsu H-F, Hsu W-H, Lee Y-I, Mao W-T, Yang J-Y, Li J-Y, Yang C-H (2015) Model for perianth formation in orchids. *Nature Plants* 1(5): 15046. <https://doi.org/10.1038/nplants.2015.46>
- Hsu H-F, Chen W-H, Shen Y-H, Hsu W-H, Mao W-T, Yang C-H (2021) Multifunctional evolution of B and AGL6 MADS box genes in orchids. *Nature Communications* 12(1): 902. <https://doi.org/10.1038/s41467-021-21229-w>
- Hu C, Tian H, Li H, Hu A, Xing F, Bhattacharjee A, Hsu T, Kumar P, Chung S (2016) Phylogenetic analysis of a ‘jewel orchid’ genus *Goodyera* (Orchidaceae) based on DNA sequence data from nuclear and plastid regions. *PLoS ONE* 11(2): e0150366. <https://doi.org/10.1371/journal.pone.0150366>
- Huson DH, Bryant D (2006) Application of phylogenetic networks in evolutionary studies. *Molecular Biology and Evolution* 23(2): 254–267. <https://doi.org/10.1093/molbev/msj030>
- Kallunki JA (1976) Population studies in *Goodyera* (Orchidaceae) with emphasis on the hybrid origin of *G. tessellata*. *Brittonia* 28(1): 53–75. <https://doi.org/10.2307/2805559>
- Kallunki JA (1981) Reproductive biology of mixed-species populations of *Goodyera* (Orchidaceae) in northern Michigan. *Brittonia* 33(2): 137–155. <https://doi.org/10.2307/2806308>
- Köhler C, Scheid OM, Erilova A (2010) The impact of the triploid block on the origin and evolution of polyploid plants. *Trends in Genetics* 26(3): 142–148. <https://doi.org/10.1016/j.tig.2009.12.006>
- Kopelman NM, Mayzel J, Jakobsson M, Rosenberg NA, Mayrose I (2015) CLUMPAK: A program for identifying clustering modes and packaging population structure inferences across K. *Molecular Ecology Resources* 15(5): 1179–1191. <https://doi.org/10.1111/1755-0998.12387>
- Lee CS, Yea SH, Lee KS, Lee NS (2010) A new taxon of *Goodyera* (Orchidaceae): *G. × tamnaensis*. *Korean Journal of Plant Taxonomy* 40(4): 251–254. <https://doi.org/10.11110/kjpt.2010.40.4.251>
- Lee CS, Kim S-C, Yea SH, Lee NS (2012) Nuclear and cpDNA sequences demonstrate spontaneous hybridization between *Goodyera schlechtendaliana* Rchb. f. and *G. velutina* Maxim. (Orchidaceae) in Jeju Island, Korea. *Systematic Botany* 37(2): 356–364. <https://doi.org/10.1600/036364412X635421>
- Matsuura O, Nakahira R (1958) Chromosome numbers of the family orchidaceae in Japan (1). *The Scientific Reports of Kyoto Prefectural University* 2: 23–30.
- Naumova TN (2018) Apomixis in angiosperms: nucellar and integumentary embryony. CRC press, Boca Raton, 152 pp.
- Oh S-H, Suh H-J, Seo S-W, Chung K-S, Yukawa T (2022) A new species of *Goodyera* (Orchidaceae: Orchidoideae) from Korea and Japan. *Journal of Plant Biology* 65(5): 357–363. <https://doi.org/10.1007/s12374-022-09358-1>

- Pace MC (2020) A recircumscription of *Goodyera* (Orchidaceae), including the description of *Paorchis* gen. nov., and resurrection of *Cionisaccus*, *Eucosia*, and *Salacistis*. *Brittonia* 72(3): 257–267. <https://doi.org/10.1007/s12228-020-09623-y>
- Pridgeon AM, Cribb PJ, Chase MW, Rasmussen FN (2003) *Genera Orchidacearum* 3. Orchidoideae (part 2), Vanillaioideae. Oxford University Press, Oxford, 358 pp.
- Pritchard JK, Stephens M, Donnelly P (2000) Inference of population structure using multilocus genotype data. *Genetics* 155(2): 945–959. <https://doi.org/10.1093/genetics/155.2.945>
- Ramsey J, Schemske DW (1998) Pathways, mechanisms, and rates of polyploid formation in flowering plants. *Annual Review of Ecology and Systematics* 29(1): 467–501. <https://doi.org/10.1146/annurev.ecolsys.29.1.467>
- Rochette NC, Rivera-Colón AG, Catchen JM (2019) Stacks 2: Analytical methods for paired-end sequencing improve RADseq-based population genomics. *Molecular Ecology* 28(21): 4737–4754. <https://doi.org/10.1111/mec.15253>
- Schumer M, Rosenthal GG, Andolfatto P (2014) How common is homoploid hybrid speciation? *Evolution* 68(6): 1553–1560. <https://doi.org/10.1111/evo.12399>
- Sera T (1990) Karyomorphological studies on *Goodyera* and its allied genera in Orchidaceae. *Bulletin of the Hiroshima Botanical Garden* 12: 71–144.
- Serizawa S (2008) A new *Goodyera* species discovered in several swamps in Aichi Prefecture, Honshu, Japan. *Proceedings of the Annual Meeting of the Japanese Society for Plant Systematics* 7: 83. [In Japanese]
- Shin K-S, Shin YK, Kim J-H, Tae K-H (2002) Phylogeny of the genus *Goodyera* (Orchidaceae; Cranichideae) in Korea based on nuclear ribosomal DNA ITS region sequences. *Journal of Plant Biology* 45(3): 182–187. <https://doi.org/10.1007/BF03030312>
- Shoji T (1963) Cytological studies on Orchidaceae, II. Chromosome numbers and karyotypes of six Japanese species. *La Kromosomo* 55: 1823–1828.
- Stamatakis A (2014) RAxML version 8: A tool for phylogenetic analysis and post-analysis of large phylogenies. *Bioinformatics* 30(9): 1312–1313. <https://doi.org/10.1093/bioinformatics/btu033>
- Suetsugu K, Hayakawa H (2019) A new variety of *Goodyera schlechtendaliana* (Orchidaceae) from Yakushima and Okinawa, Japan. *Acta Phytotaxonomica et Geobotanica* 70: 49–55.
- Suetsugu K, Shitara T, Nakato N, Ishida K, Hayakawa H (2019) First record of *Goodyera* × *maximo-velutina* (Orchidaceae) from Kozu Island, Japan. *Taiwania* 64: 347–352.
- Suetsugu K, Hirota SK, Suyama Y (2021a) A new natural hybrid, *Goodyera* × *tanakae* (Orchidaceae) from Japan with a discussion on the taxonomic identities of *G. foliosa*, *G. sonoharae*, *G. velutina*, *G. ×maximo-velutina* and *G. henryi*, based on morphological and molecular data. *Taiwania* 66: 277–286.
- Suetsugu K, Hirota SK, Suyama Y (2021b) First record of *Goodyera* × *tamnaensis* (Orchidaceae) from Boso Peninsula, Chiba Prefecture, Japan, based on morphological and molecular data. *Taiwania* 66: 113–120.
- Suetsugu K, Fukushima K, Makino T, Ikematsu S, Sakamoto T, Kimura S (2022) Transcriptional heterochrony and completely cleistogamous flower development in the mycoheterotrophic orchid *Gastrodia*. *New Phytologist*: nph.18495. <https://doi.org/10.1111/nph.18495>

- Sun B-Y, Park J-H, Kwak M-J, Kim C-H, Kim K-S (1996) Chromosome counts from the flora of Korea with emphasis on Apiaceae. *Journal of Plant Biology* 39: 15–22.
- Suyama Y, Matsuki Y (2015) MIG-seq: An effective PCR-based method for genome-wide single-nucleotide polymorphism genotyping using the next-generation sequencing platform. *Scientific Reports* 5(1): 16963. <https://doi.org/10.1038/srep16963>
- Suyama Y, Hirota SK, Matsuo A, Tsunamoto Y, Mitsuyuki C, Shimura A, Okano K (2022) Complementary combination of multiplex high-throughput DNA sequencing for molecular phylogeny. *Ecological Research* 37(1): 171–181. <https://doi.org/10.1111/1440-1703.12270>
- Tae KH, Lee EH, Ko SC (1997) A systematic study of the genus *Goodyera* in Korea by morphological and cytological characters. *Korean Journal of Plant Taxonomy* 27(1): 89–116. <https://doi.org/10.11110/kjpt.1997.27.1.089>
- Takahashi K (1985) *Interesting Wild Orchid*. The Mainichi Newspapers Co., Ltd., Tokyo, 176 pp. [In Japanese]
- Tamaki I, Yoichi W, Matsuki Y, Suyama Y, Mizuno M (2017) Inconsistency between morphological traits and ancestry of individuals in the hybrid zone between two *Rhododendron japonoheptamerum* varieties revealed by a genotyping-by-sequencing approach. *Tree Genetics & Genomes* 13(1): 1–10. <https://doi.org/10.1007/s11295-016-1084-x>
- Tanaka R (1965) Chromosome numbers of some species of Orchidaceae from Japan and its neighbouring areas. *Shokubutsu Kenkyu Zasshi* 40: 54–77.
- The Flora-Kanagawa Association (2018) *Flora of Kanagawa 2018*. The Flora-Kanagawa Association, Odawara, 335 pp.
- Thiers B (2022) *Index Herbariorum*, New York Botanical Garden. <http://sweetgum.nybg.org/science/ih/> [October 6, 2022]
- Yoichi W, Kawamata I, Matsuki Y, Suyama Y, Uehara K, Ito M (2018) Phylogeographic analysis suggests two origins for the riparian azalea *Rhododendron indicum* (L.) Sweet. *Heredity* 121(6): 594–604. <https://doi.org/10.1038/s41437-018-0064-3>

Supplementary material I

Newly collected materials used for morphological, cytological and MIG-seq analysis

Authors: Kenji Suetsugu, Shun K. Hirota, Narumi Nakato, Yoshihisa Suyama, Shunsuke Serizawa

Data type: excel file.

Copyright notice: This dataset is made available under the Open Database License (<http://opendatacommons.org/licenses/odbl/1.0/>). The Open Database License (ODbL) is a license agreement intended to allow users to freely share, modify, and use this Dataset while maintaining this same freedom for others, provided that the original source and author(s) are credited.

Link: <https://doi.org/10.3897/phytokeys.212.91536.suppl1>

An update on the taxonomy of *Calamagrostis nagarum* (Bor) G.Singh and its allies (Poaceae, Agrostidinae): morphometrics and micro-morphology

Dileshwar Prasad^{1,2}, Ravindra Kumar^{1,2}, Shubham Jaiswal¹,
Rekha Yadav¹, Smita Tiwari¹, Priyanka Agnihotri^{1,2}

1 Plant Diversity, Systematics & Herbarium Division, CSIR–National Botanical Research Institute, Rana Pratap Marg, Lucknow–226001, India **2** Academy of Scientific and Innovative Research (AcSIR), Sector 19, Kamla Nehru Nagar, Ghaziabad–201002, India

Corresponding author: Priyanka Agnihotri (priyagni_2006@yahoo.co.in)

Academic editor: Marcin Nobis | Received 18 June 2022 | Accepted 28 September 2022 | Published 4 November 2022

Citation: Prasad D, Kumar R, Jaiswal S, Yadav R, Tiwari S, Agnihotri P (2022) An update on the taxonomy of *Calamagrostis nagarum* (Bor) G.Singh and its allies (Poaceae, Agrostidinae): morphometrics and micro-morphology. *PhytoKeys* 212: 135–155. <https://doi.org/10.3897/phytokeys.212.89253>

Abstract

Calamagrostis nagarum, previously considered to be a poorly known species, has been reassessed taxonomically. It is a member of *C. labulensis*-*C. scabrescens* complex and may be segregated by morphological characters such as the presence of pilose hairs on adaxial surface of leaf blades, spreading panicle branches, filiform awn and nerve prolongation of lemma. Besides, the micromorphology of adaxial surface of leaf blades, dorsal surface of glume and lemma differentiates *Calamagrostis nagarum* from its allies, *C. labulensis* and *C. scabrescens*. It is known from Nagaland and Uttarakhand, India, and Bhutan. In this study, we have provided an emended description of the species, a discussion of its habitat and distribution, and taxonomic notes along with field photographs and photo plates for its correct identification. In addition, we also lectotypify the names *C. labulensis* and *C. scabrescens*.

Keywords

Cool season grass, *Deyeuxia*, lectotypification, micro-morphology, taxonomy, Western Himalaya

Introduction

The genus *Calamagrostis* Adans. s. str., including *Deyeuxia* Clarion ex P.Beauv., belongs to the subtribe Agrostidinae (Poaceae, Pooideae, Poae) and includes about 130 species globally (Soreng et al. 2022). Several American species previously recognized under *Calamagrostis* have been transferred to the genera *Cinnagrostis* Griseb., *Greeneochloa* P.M. Peterson, Soreng, Romasch. & Barberá, *Laegaardia* P.M. Peterson, Soreng, Romasch. & Barberá, *Paramochloa* P.M. Peterson, Soreng, Romasch. & Barberá, *Peyritschia* E. Fourn, and *Deschampsia* (Saarela et al. 2017; Peterson et al. 2019). *Calamagrostis* s. str. is characterized by plants rhizomatous or not, with or without extravaginal branching; lemma awns straight or slightly bent, readily distinguished from callus hairs, inserted at base to middle or rarely near the apex; rachilla extension penicillate hairy along the length or glabrous, or, if rudimentary, then callus with long hairs; callus hairs $1/10$ – $3/4$ as long as the lemma in length or longer than lemma; lodicules entire and lanceolate, sometimes with an isolated lateral lobe, glabrous; ovary glabrous, distinctly sulcate, hilum $1/6$ – $1/3$ the grain in length (Peterson et al. 2019). It is also similar to the genus *Agrostis* L. and both genera have several notoriously difficult species complexes, as well as hybrids at the global level (Howard et al. 2009; Paszko and Nobis 2010; Paszko and Ma 2011; Paszko 2012b, 2013). In India, *Calamagrostis* s. str. comprises about 22 species which are mainly confined to Himalayan region (Bor 1960; Paszko 2012a; Paszko and Soreng 2013; Kellogg et al. 2020; Prasad et al. 2021) and formed several species complexes such as the *C. emodensis* Griseb. complex, the *C. epigeios* (L.) Roth complex, the *C. lahulensis* G.Singh-*C. scabrescens* Griseb. complex, and the *C. pseudophragmites* (Haller f.) Koeler complex, however, the majority of these have been recently resolved (Paszko and Ma 2011; Paszko 2012a, 2012b, 2013, 2014a, 2014b). *C. lahulensis*-*C. scabrescens* complex is characterized by the presence of rachilla with penicillate hairs which is as long as or more than the length of lemma, callus hairs shorter than half of the length of lemma and awn inserted $2/3^{\text{rd}}$ from base to near the tip on the dorsal side of lemma (Bor 1960; Paszko 2014a 2015, 2016).

Calamagrostis nagarum (Bor) G.Singh was originally described by Bor (1938) under the genus *Deyeuxia* Clarion ex P. Beauv as *D. nagarum* Bor. At the time of its description, it was only known from the type locality Naga Hills, Nagaland, India, but was later also reported in the grass flora of Bhutan (Noltie 2000). Furthermore, it has been documented in the updated checklist of grasses of Uttarakhand, India (Kandwal and Gupta 2009). The diagnosis and keys, provided by Bor (1940, 1960), Shukla (1996) and Noltie (2000), are overlapping with *C. elatior*, *C. lahulensis* and *C. scabrescens*, therefore, do not adequately segregate *C. nagarum* from them. Although the morphological descriptions provided by Bor (1940) and Shukla (1996) exactly correspond to *C. nagarum*, the features of panicles, narrow and up to 07 cm long, provided by Noltie (2000), have created confusion for the species identity. Furthermore, Bor (1940) and Shukla (1996) stated that *C. nagarum* is morphologically similar to *C. lahulensis* G.Singh and *C. scabrescens* Griseb., whereas Noltie (2000) assumed that it is more similar to *C. elatior*, perhaps on the basis of pilose hairs on adaxial side of leaf blades. Since the existing taxonomic literature is unable to distinguish *C. nagarum* from its allied species, we conducted a taxonomic reassessment of *C. nagarum* to clarify its identity.

In the present study, we also lectotypify the names *C. lahulensis* G. Singh and *C. scabrescens* Griseb. since no specimen was selected as type specimen for either name (Art. 9.3 of ICN; Turland et al. 2018). Both species were originally described by Grisebach, a German botanist, who worked in Kew herbarium and studied Hooker's specimens of grasses collected from India and described and/or recorded a total of about 43 taxa within the Agrostideen group including *Calamagrostis pulchella* Griseb. (replaced synonym of *C. lahulensis*) and *C. scabrescens* Griseb.

Materials and methods

This study is based on an examination of herbarium specimens as well as field collections belonging to *Calamagrostis lahulensis*, *C. nagarum* and *C. scabrescens*. Self-collected specimens, deposited at CSIR-National Botanical Research Institute, Lucknow (**LWG**) herbarium were gathered during botanical trips in several localities of Western and Eastern Himalaya. The following Indian Herbaria: Botanical Survey of India, Regional Centre, Dehradun (**BSD**), Central National Herbarium, Botanical Survey of India, Howrah (**CAL**), Indian Council of Forestry Research and Education, Dehradun (**DD**), University of Kashmir, Srinagar (**KASH**) and LWG were also consulted in person (see Appendix 1). The identification of *Calamagrostis* spp. was done through a consultation of international, national and regional floras and taxonomic studies (Hooker 1896; Bor 1938, 1940, 1960; Chowdhary and Wadhwa 1984; Aswal and Mehrotra 1994; Shukla 1996; Gaur 1999; Noltie 2000; Lu and Phillips 2006; Pusalkar and Singh 2012; Paszko et al. 2013; Paszko 2014a; Paszko et al. 2017; Prasad et al. 2021). Besides, specimens that belong to *C. lahulensis*, *C. nagarum* and *C. scabrescens* were identified by their respective protologue (Grisebach 1868; Bor 1938). Morphological measurements were recorded from 26 spikelets of *C. lahulensis*, 23 spikelets of *C. nagarum* and 42 spikelets of *C. scabrescens*, from the specimens housed at LWG, usually on one spikelet from one individual, using a Stereo Zoom Trinocular microscope equipped with a MC 120 HD camera. Photographs of *C. nagarum* were also taken. The recorded quantitative data of morphological characters (Table 1) of *C. lahulensis*, *C. nagarum* and *C. scabrescens* were subjected to univariate variance analysis. For Principal component analysis (PCA), the statistic software XLSTAT BASIC + (<https://www.xlstat.com/en/>) was used. The morphological data recorded from spikelets (except panicle length and ligule length) were included in the PCA analysis. To analyse the morphological boundaries between *C. lahulensis*, *C. scabrescens* and *C. nagarum*, a scatter plot of PCA loadings ≥ 0.70 of the selected morphological characters was conducted. We prepared distribution map of *C. nagarum* by using DIVA-GIS computational program (Hijmans et al. 2001) based on examined specimens and localities documented in Bor (1960) and Noltie (2000).

For the micro-morphological study of *C. lahulensis*, *C. nagarum*, and *C. scabrescens*, we examined leaf blades, glumes, and lemmas from the collections *D. Prasad et al.* 326642, 339372 and 326717 (LWG), respectively. All the materials were fixed in formalin-acetic-alcohol (ratio 1:3:1) solution for 48 hr. The samples were then dehydrated with increasing

Table 1. Morphological characters used in the present study.

Morphological characters	Character abbreviation (unit)
Panicle length	PNL (cm)
Ligule length	LIGL (mm)
Lower glume length	LGL (mm)
Lower glume width	LGW (mm)
Upper glume length	UGL (mm)
Upper glume width	UGW (mm)
Lemma length	LL (mm)
Palea length	PL (mm)
Awn length	AL (mm)
Rachilla hairs length	RHL (mm)
Lemma nerves prolongation length (intermediate nerve and lateral nerve)	LNP (mm)
Lemma base to awn insertion point length	LBTAIP (mm)
Awn insertion point to lemma tip length	AIPTLT (mm)
Ratio: lower glume length to upper glume length	LGL/UGL
Ratio: lower glume width to lower glume length	LGW/LGL
Ratio: lemma length to lower glume length	LL/LGL
Ratio: palea length to lemma length	PL/LL
Ratio: rachilla hair length to lemma length	RHL/LL
Ratio: awn length to lemma length	AI/LL
Ratio: awn insertion points to lemma tip, to lemma base to awn insertion point	AIPTLT/LBTAIP

strengths of ethyl alcohol solutions. Thereafter, the prepared samples were examined using a FEI QUANTA250F scanning electron microscope (SEM) in low vacuum mode (Doğan 1988) at CSIR-National Botanical Research Institute, Lucknow, India.

Specimens of *C. lahulensis* and *C. scabrescens* matching the criteria of original material were examined online at Montpellier University, Montpellier, France (MPU), National Museum of Natural History, Paris, France (P), Natural History Museum, Vienna, Austria (W), Royal Botanic Garden, U.K. Scotland, Edinburgh (E), Royal Botanic Gardens Kew, U.K. England, Kew (K) and The Natural History Museum, London (BM), as well as in person at CAL.

Result and discussion

Morphological variation and morphometrics

Analysis of selected morphological characters of *Calamagrostis nagarum* revealed that most of the characters overlap with *C. lahulensis* and *C. scabrescens* except nerve prolongation of lemma (LNP) and ratio of lower glume width to lower glume length (LGW/LGL) (Fig. 1). The lemma apex in *C. lahulensis* and *C. scabrescens* is erose (like four small unequal lobes), usually without nerve prolongation or rarely with a nerve prolongation, which is 0.08–0.26 (0.38) mm long, whereas in *C. nagarum* the nerve prolongation of lemma is (0.3–)0.4–0.7(–0.9) mm long. We have observed a nerve prolongation of lemma only in six spikelets of *C. lahulensis*, four spikelets of *C. scabrescens* and all spikelets of *C. nagarum*. A strongly geniculate and long awn is common in *C. scabrescens*, but straight and short awns are also observed in some

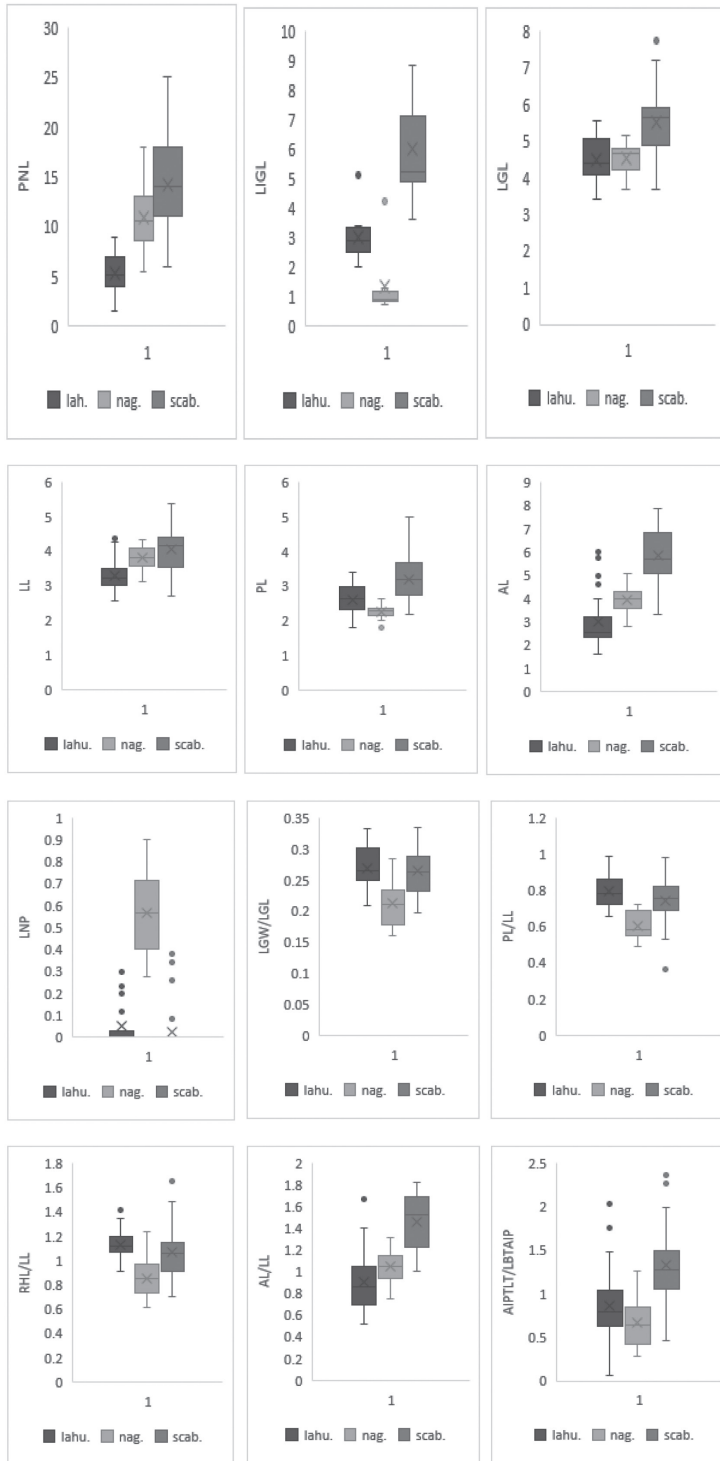


Figure 1. Box plots for selected morphological variables showing mean (cross), mean \pm SD (box), outliers (dot) and range of variation (whiskers) for *C. lahulensis* (lahu.), *C. nagarum* (nag.) and *C. scabrescens* (scab.).

spikelets in which the glume margin is ciliate. The point of awn insertion on the dorsal side of the lemma is highly variable in *C. labulensis*, inserted on lower 2/3rd to the tip of the lemma, and similar variation is also observed in *C. nagarum*. In *C. scabrescens*, however, the awn is inserted on the middle to lower 2/3rd of lemma. The ratio of palea to lemma is constant in a range of (0.65–)0.70–0.85(–0.99) in both *C. labulensis* and *C. scabrescens* while a narrower range of variation, (0.48–)0.55–0.68(–0.75) is observed in *C. nagarum*. The ratio of rachilla hair length to lemma length in *C. labulensis* ranges from (0.90–)1.06–1.19(–1.35) and has a wide range of variation in both *C. nagarum* and *C. scabrescens*.

The first principal component (PC1) had relatively high (positive or negative) loading for lower and upper glume length and width, lemma length, rachilla hairs length, awn length, awn insertion points to lemma tip length and palea length, however, PC2 had relatively high loading for lemma nerve prolongation and ratio of lower glume width to lower glume length (Fig. 2). According to PC1 vs. PC2, *C. nagarum* is separable from *C. labulensis* and *C. scabrescens* on the basis of nerve prolongation of lemma (Fig. 3), whereas *C. labulensis* and *C. scabrescens* overlap.

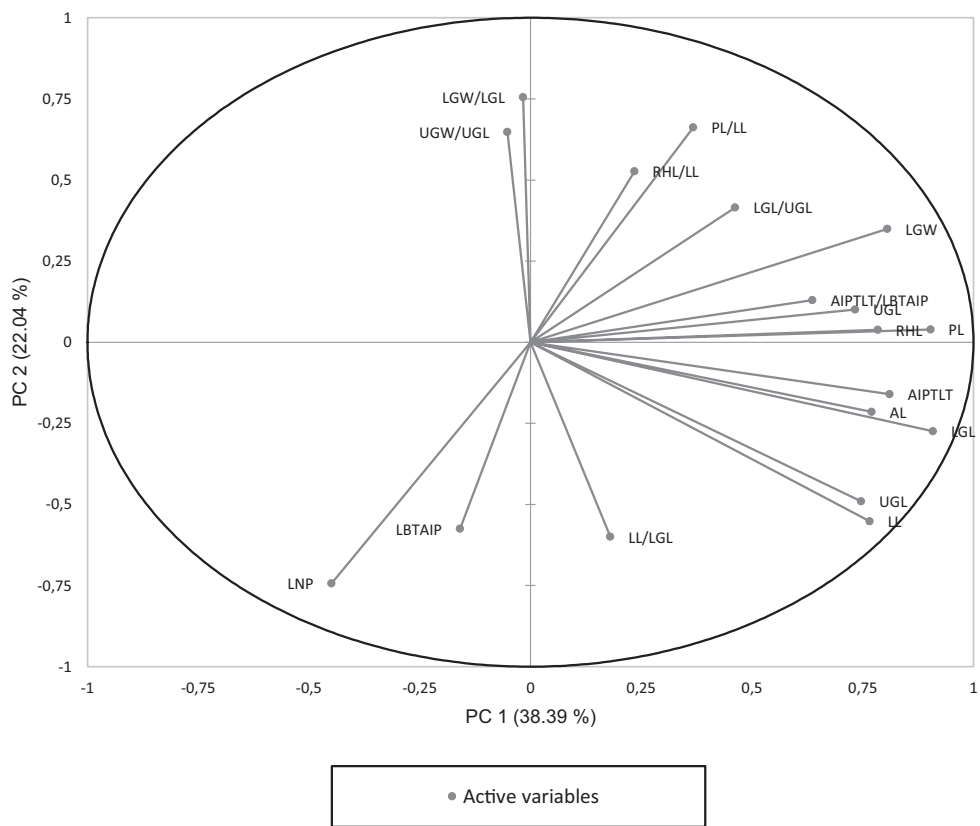


Figure 2. Projection of variables on principal component (PC1 × PC2) scored for *C. labulensis*, *C. nagarum* and *C. scabrescens*.

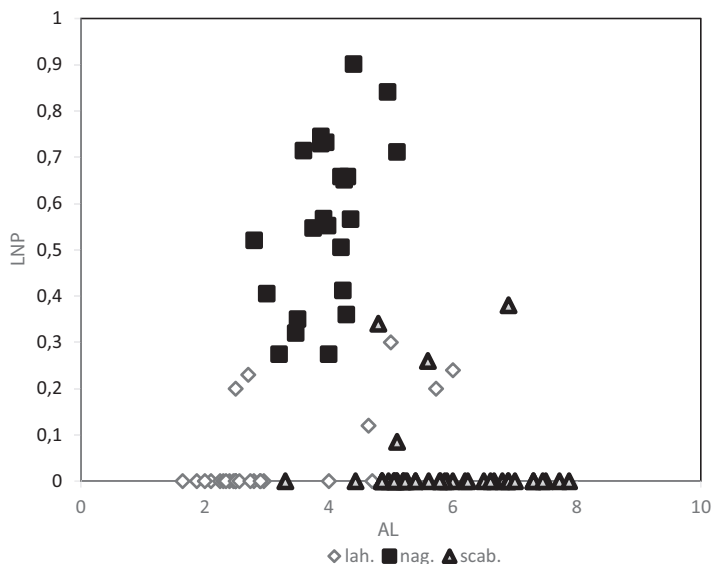


Figure 3. Scatterplot of lemma nerve prolongation length (LNP) against awn length (AL) for *C. labulensis*, *C. nagarum* and *C. scabrescens*.

Micro-morphology of leaf blades, glume, and lemma

On the adaxial surface of leaves, *C. labulensis* has less prominent grooves or sometimes absent (Fig. 5A), while in *C. nagarum* (Fig. 5B) and *C. scabrescens* (Fig. 5C) grooves are prominent with deep furrows. Rigid spicules of adaxial side of leaf blades are of two different types: prickle (short-pointed apex) and hooked (long pointed apex). The former is usually densely or sometimes sparsely present in *C. labulensis* (Fig. 4A), while in *C. nagarum* (Fig. 4B) and *C. scabrescens* (Fig. 4C) both are present. In *C. nagarum*, spicules are arranged in four rows along the grooves (Fig. 4B), while in *C. scabrescens* there are two rows of densely and sparsely arranged spicules on grooves (Fig. 4C). Length of spicules is 49.7–57.2 μm long (Fig. 4A) and 42.5–54.9 μm long (Fig. 4C) in *C. labulensis* and *C. scabrescens*, respectively, but in *C. nagarum* length of spicules is 21.7–45.60 μm long (Fig. 4B). However, the pilose hairs, present on the adaxial surface of leaf blades in *C. nagarum*, shed during the preparation of the sample. The dorsal glume surface is scabrous because of rigid spicules in all three species (Fig. 4D–F). Prickles on dorsal glume surface are sparsely arranged in *C. nagarum* (Fig. 4E), while in *C. labulensis* (Fig. 4D) and *C. scabrescens* (Fig. 4F) prickles are absent, but hooks are densely arranged. *C. labulensis* and *C. scabrescens* have spicules 35.8–47.3 μm long (Fig. 4D) and 47.27–75.01 μm long (Fig. 4F), respectively, that are comparatively longer than *C. nagarum*, in which spicules are usually 19.51–26.43 μm long (Fig. 4E). The dorsal lemma surface shows a high degree of variability among all three species (Fig. 4G–I). The hooks are arranged antrorsely

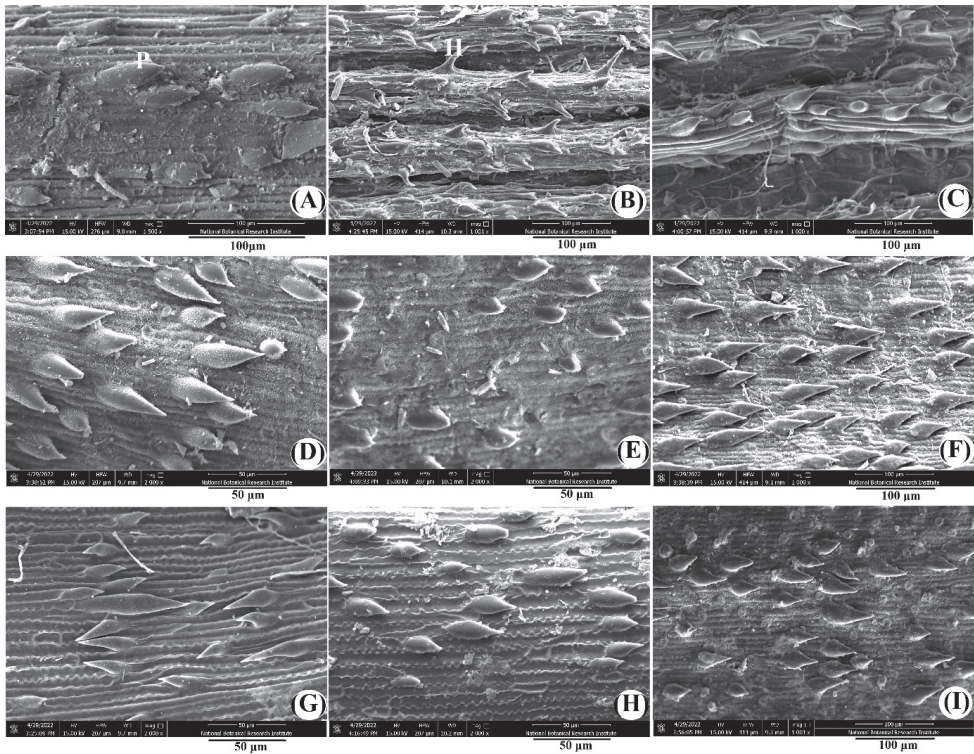


Figure 4. SEM morphology of adaxial side of leaf blades (**A–C**), dorsal surface of glume (**D–F**) and dorsal surface of lemma (**G–I**) in *C. labulensis* (**A, D, G**), *C. nagarum* (**B, E, H**) and *C. scabrescens* (**C, F, I**).

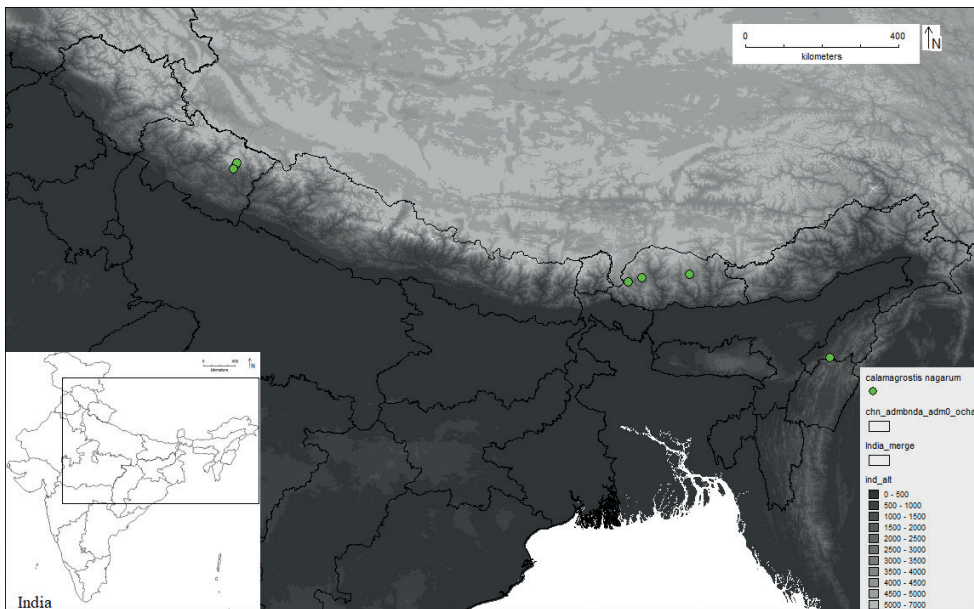


Figure 5. Geographic distribution of *Calamagrostis nagarum*.

and retrorsely in *C. labulensis* and are of two different lengths, short (27.42–37.80 μm long) and long (0.65–0.75 μm long) (Fig. 5G). However, in both *C. nagarum* and *C. scabrescens* prickles are 25.82–63.38 μm long (Fig. 4H) and 25.37–39.51 μm long (Fig. 4I), respectively.

Taxonomic treatment

***Calamagrostis nagarum* (Bor) G.Singh in Taxon 33(1): 94 (1984); Shukla, Grass. N. E. India, 47 (1996)**

Deyeuxia nagarum Bor in Indian Forest Rec., Bot. 1: 69 (1938); Bor, Fl. Assam, 5: 145 (1940); Bor, Grass. Burma, Ceylon, India & Pakistan, 399 (1960). Basionym.

Type. INDIA. Nagaland [earlier in Assam], Naga hills, Japvo range, 9,500 ft [2895 m], September 1937, *NL Bor 2834* (holo. K: K000032378, digital image!).

Amended description. A perennial, rhizomatous, robust grass, 50–100 cm tall. Culms 40–80 cm long, simple, terete, glabrous, 2–3 nodes below the panicle. Node glabrous, compressed. Leaf sheaths split, overlapping, loose, connate toward base, smooth, sometimes scaberulous. Leaf blades 7–20 \times 0.3–0.7 cm, flat, narrowly-linear, adaxial scabrous with distantly pilose and abaxial surface scabrous; apex attenuate; margin scabrid. Ligules 0.75–4.2 mm long, membranous, adaxial surface glabrous, abaxial surface scabrous; apex obtuse, lacerate. Inflorescence a panicle, 5–18 \times 5–8 cm, very lax with spreading branches; lower panicle branches paired or in whorls of 3–5; 1–8 cm long, almost smooth or sometime scabrous, filiform, flexuous. Rachis slender, glabrous or scabrous. Spikelets 5.1–6.7 \times 1.5–2 mm, lanceolate to wedge shaped at maturity, bearing 1-floret, disarticulating above the glume and below the floret, greenish with pink tinged; glumes subequal, persistent; floret hermaphroditic. Pedicel shorter than spikelet, slender, scabrous. Lower glume 3.7–5.2 \times 0.65–1.3 mm, 1-nerved, 1-keeled, lanceolate, greenish with pink tinge near margin, scaberulous to somewhat glabrous; apex acuminate; margin narrowly hyaline, entire; keel scabrous. Upper glume 3.8–5.4 \times 0.87–1.34 mm, 3-nerved, 1-keeled, lanceolate, greenish with pink tinged, scabrous; apex acuminate; margin narrowly hyaline, entire; keel scabrous. Callus evenly bearded, hairs 1.1–1.9 mm long, nearly half of the length of lemma or shorter. Lemma 3.1–4.3 \times 1.0–1.6 mm, 5-nerved, membranous, surface scaberulous with papillate, awned; apex acute with 4-nerve prolongation 0.27–0.9 mm long; margin hyaline. Rachilla 1.2–1.9 mm long, penicillate hairy, usually bare at base; rachilla with hairs 2.5–4.9 mm long. Awn 2.8–5.1 mm long, straight, filiform, slender, scabrous-antorse, exerted from the spikelet, arising from above the middle of lemma back. Palea 1.8–2.7 mm long, 2-nerved, 2-keeled, hyaline-membranous, rounded on back; apex slightly bifid. Lodicules 2, 0.7–0.8 mm long, lanceolate. Stamens 3; anthers 1.5–2.3 mm long, narrowly linear. Mature caryopsis not seen.

Phenology. September to October (flowering and fruiting).

Habitat and distribution. *Calmagrostis nagarum* was discovered in the Japvo range of Naga Hills situated in Nagaland, which is geographically located in the eastern region of Assam, southernmost of Arunachal Pradesh and northern Manipur, India and close to the political boundary of Myanmar. Approximately 3% of the total geographical region of Nagaland is part of the Himalayan region, while the rest of the region is situated in a complex mountain system forming Naga Hills. Previously, it was only known from the type locality in a sub-temperate region at about 2800 m elevation and was considered to be endemic for that geographic range (Bor 1938, 1940, 1960; Shukla 1996). Later, it was recorded from Bhutan, geographically located in Eastern Himalayas, by Noltie (2000), where it was found not only on damp shady cliffs in blue pine and oak forest but also in riverbanks and scrubland, at 2400–2840 m elevation. Recently, it was documented in an updated checklist of grasses of Uttarakhand, Western Himalaya (Kandwal and Gupta 2009), but this geographic range was not included by Kellogg et al. (2020) as part of the species distributional range. During the present study, we collected specimens of *C. nagarum* from Pindari Valley, located in Bageshwar district of Uttarakhand, and confirmed its occurrence in Western Himalaya (Fig. 5). It was found growing in *Danthonia* grassland in association with *Polygonum* sp., *Anagalis* sp., and *Gaultheria* sp., at 3000–3050 m elevation in Phurkia village and, in Dhakuri top at about 2900 m elevation on forest margin as well as on Pindar riverbank in Dwali village at 2500–2800 m elevation. The vertical distribution shows *C. nagarum* is mainly confined to 2500–3100 m elevation, below the tree line, at about 3,300 m elevation, whereas *C. lahulensis* is widely distributed above the treeline at about 3350–4200 m elevation, which overlaps with the elevation range of *C. scabrescens* (Fig. 6).

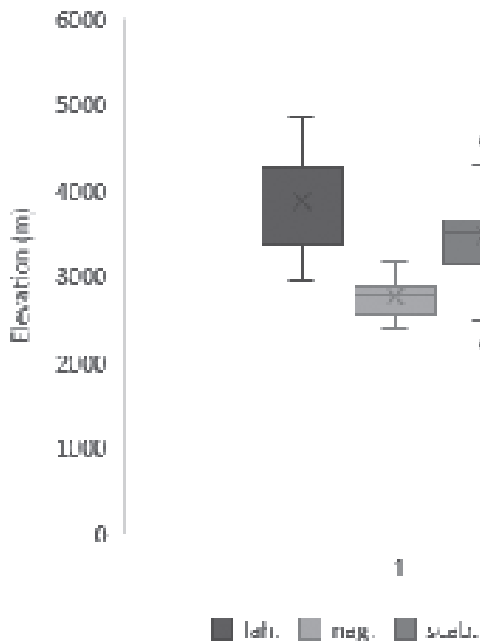


Figure 6. Box plot for vertical distribution of *C. lahulensis*, *C. nagarum* and *C. scabrescens*.

Taxonomic notes and allied species. *Calamagrostis nagarum* should be placed in *C. labulensis*-*C. scabrescens* complex because of its rachilla with penicillate hairs equal to longer than lemma, callus hairs shorter than half of the lemma and awn inserted at about middle to tip of the lemma. Within this complex, it should be recognized by the presence of pilose hairs on adaxial surface of leaf blade, widely spreading panicle branches, nerve prolongation of lemma (0.3–)0.4–0.7(–0.9) mm long and filiform awn within this complex (Figs 7, 8, 9). *Calamagrostis nagarum* is more similar to *C. labulensis* than to

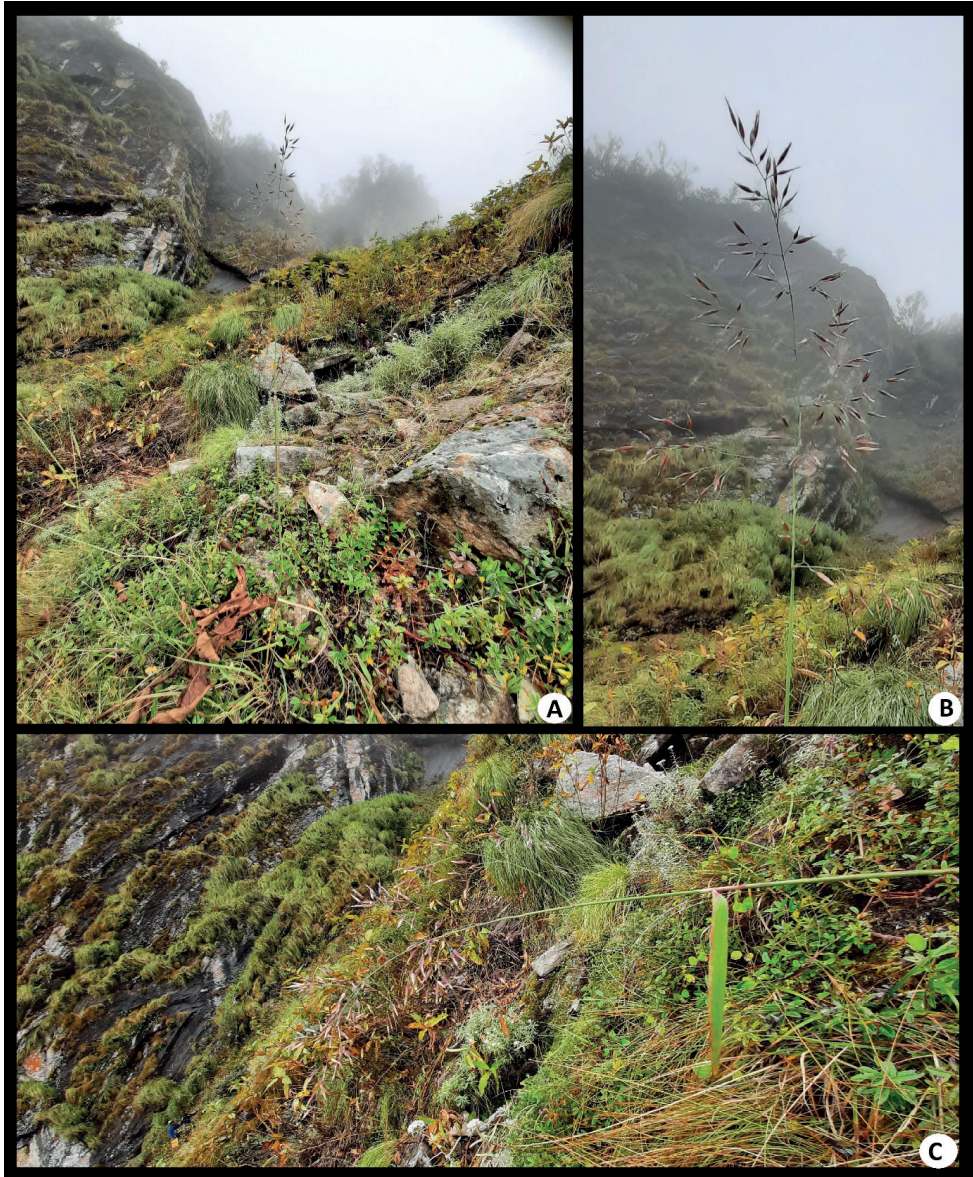


Figure 7. *Calamagrostis nagarum*: **A** habit **B** panicle **C** leaf blade and panicle. [Photos were taken through Samsung F41 by the first author, correspond to D. Prasad et al. 339372].

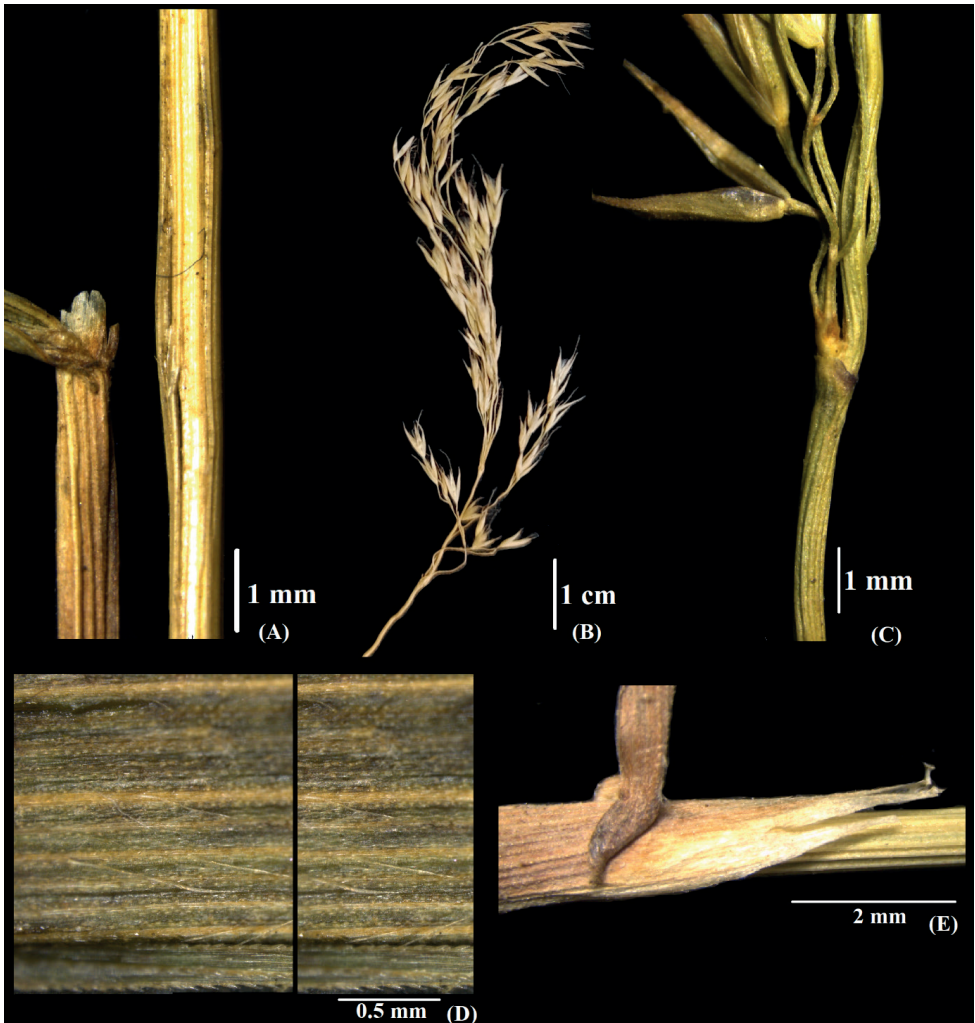


Figure 8. *Calamagrostis nagarum*: **A** culm and ligule **B** Panicle **C** lower panicle branch **D** leaf blade, adaxial view **E** ligules. [Photographs: **A–C** from Prasad et al. 339324 and **D–E** from D. Prasad et al. 339372].

C. scabrescens. It differs from *C. labulensis* in panicle length [(5–)8.1–12(–18) cm long vs. (1.5–)4–7(–9) cm long], lower branches of panicle [spreading with (1.0–)3–7(–8) cm long vs. ascending with (0.5–)1–3(–3.5) cm long] and, from the latter in culm (glabrous vs. scabrous), ligule length [(0.75–)0.83–1.2(–1.36) mm long vs. (3.6–)4.9–7.1(–8.84) mm long], lower glume width [(0.65–)0.81–1.1(–1.3) mm long vs. (1.1–) 1.3–1.5 (–1.7) mm long]) and awn length [(1.6–)2.3–3.2(–5.7) mm long vs. (3.3–)5.1–6.8(–7.9) mm long]. *Calamagrostis nagarum* is somewhat similar to another member of this complex, *C. nandadeviensis*, in having (5–)8.1–12(–17) mm long panicles, but differs from the latter in culm pubescence (glabrous vs. scabrous), ligule length [(0.75–)0.83–1.2(–1.36) mm long vs. (6.1–)6.5–7.5(–8.1) mm long], upper glume nervation (3-nerved vs. 1-nerved) and ratio of palea length to lemma length [(0.49–)0.54–0.62(–0.72) vs. (0.75–)0.77–

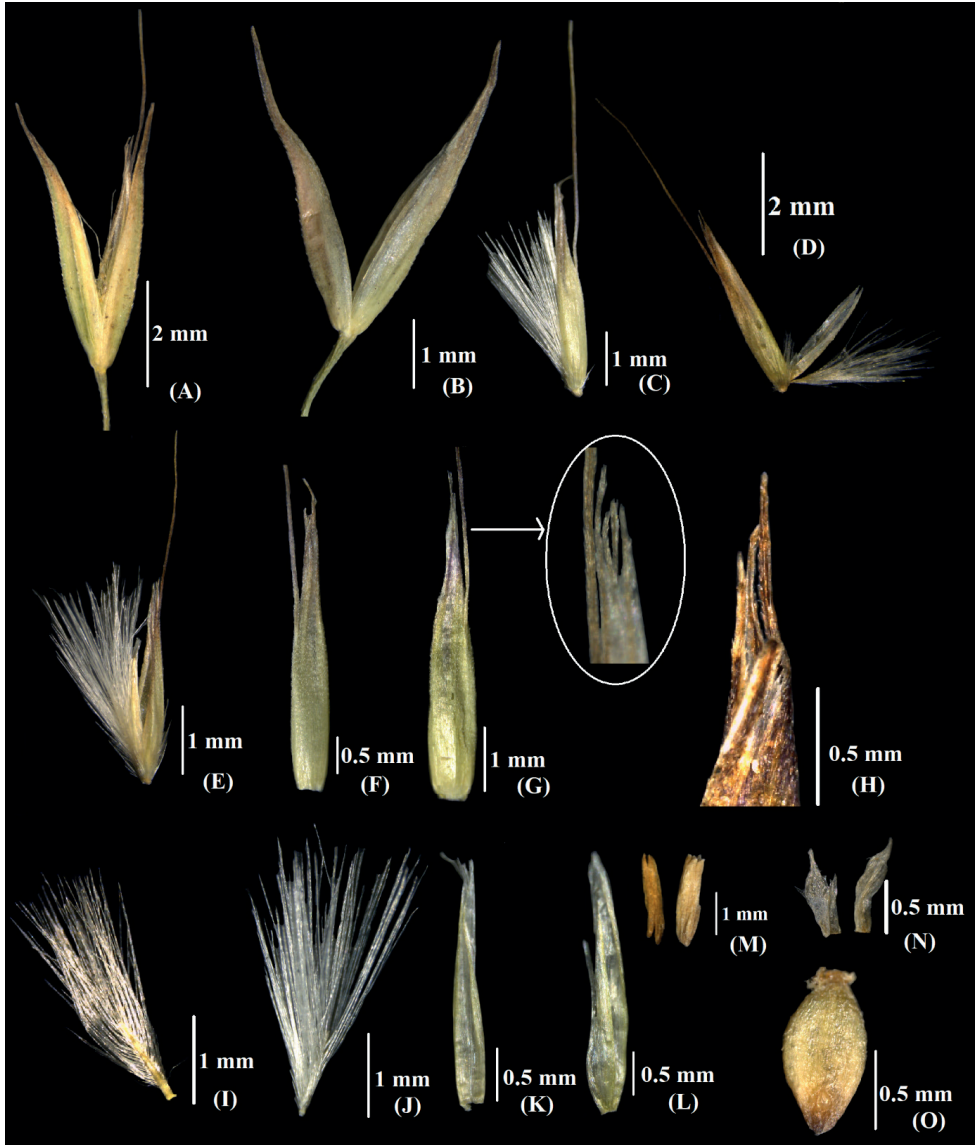


Figure 9. *Calamagrostis nagarum*: **A** spikelet **B** remove glumes **C** floret **D, E** Open floret **F, G** lemma, **H** lemma apex **I, J** rachilla, **K, L** palea **M** anthers **N** lodicules **O** caryopsis. [Photographs: **A–E, H–I** and **L–O** from D. Prasad et al. 339324 and **F–G** and **J–K** from D. Prasad et al. 339372].

0.85(–0.90)]. Along with this, *C. himalaica* (L.Liu ex Wen L.Chen) Paszko, reported from China and Myanmar, and *C. nyingchiensis* (P.C.Kuo & S.L.Lu) Paszko, restricted to China (Paszko 2015; Paszko 2016) are also members of the *C. lahulensis*–*C. scabrescens* complex. *C. nagarum* differs from *C. himalaica* in awn (2.8–5.1 mm long, straight and filiform vs. 4.5–10 mm long, strongly geniculate) and from *C. nyingchiensis* in anther length (1.5–2.3 mm long vs. 0.7–1.1 mm long). *Calamagrostis nagarum* differs from *C. elatior* by having callus hairs shorter than half of the length of lemma and, straight and filiform awn.

Taxonomic key to the *C. lahulensis*, *C. nagarum* and *C. scabrescens*

- 1 Leaf blades pilose on adaxial surface; panicle branches widely spreading; nerve prolongation of lemma conspicuous with (0.3–)0.4–0.7(–0.9) mm long *C. nagarum*
- Leaf blades without hairs on adaxial surface; panicle branched ascending; nerve prolongation of lemma usually absents, if present then < 0.4 mm long **2**
- 2 Leaf blades with prominent grooves and deep furrows; panicle (6–)11–18(–25) cm long; awns usually strongly geniculate, rarely straight with (3.3–)5.0–6.8(–7.8) mm long *C. scabrescens*
- Leaf blades without prominent grooves and deep furrows: panicles (1.5–)4–7(–9.0) cm long; awns not geniculate and straight with (1.6–)2.3–3.2(–4.5) mm long..... *C. lahulensis*

Typification of names

1. *Calamagrostis lahulensis* G.Singh, in *Taxon* 33 (1) 94 (1984)

Replaced name (typonym). *Calamagrostis pulchella* Griseb. Nachr. Ges. Wiss. Göttingen, Math. -Phys. Kl., 78 (1868), non Saut. ex Rchb. Fl. Germ. Excurs.: 26 (1830)

Lectotype (designated here).—INDIA. Sikkim, Guantong, 12,000 ft. [3657 m], 5 September 1849, [*Deyeuxia* 10], J.D. Hooker s.n. (K000032374; digital image!). (Image available at <https://plants.jstor.org/stable/10.5555/al.ap.specimen.k000032374>)

Note. *Calamagrostis lahulensis* was originally described by Grisebach (1868) as *C. pulchella*. Later, Hooker (1896) assigned *C. pulchella* to the genus *Deyeuxia*. Thereafter, Singh (1984) transferred the Indian species of *Deyeuxia* into *Calamagrostis* and proposed a new name *C. lahulensis* for *C. pulchella* Griseb. as the epithet “*pulchella*” was preoccupied in *Calamagrostis* by the name *C. pulchella* Saut. ex Rchb. Grisebach (1868) proposed the name *C. pulchella* based on the heterogenous collections of Hooker, covering the regions between Garhwal and Sikkim Himalaya of India. Although all specimens seen by Grisebach, were ‘sino numero’ (without collection number), he cited localities, altitude, date of collection, name of the collector, and annotation “10*Deyeuxia*” in the protologue. While searching for the original specimens in various herbaria (BM, CAL, DD, E, K and P), where most of the Hooker’s specimens are housed, we traced seven specimens at K (K000032374, K000032375, K000032376, K000032377, K000838345, K0000838346, and K0000838348), three specimens at CAL (CAL0000002397, CAL0000002398, and CAL0000002399), four specimens at W (W0026815, W1889-0241774, W1889-0038498, and W1916-00037771) and one specimen at E (E00394124). All the specimens have a label consisting of the collection details with the annotation ‘10*Deyeuxia*’ and matched well with the protologue. Therefore, they should have been considered as syntypes (Art. 9.6 of the ICN; Turland et al. 2018). The specimens housed at K have been verified by H.J.

Noltie as syntypes, while the specimens preserved at W and CAL have been verified by Beata Paszko, Polish Academy of Sciences Poland (KRAM) as type materials. In addition to these, L. Pignotti has also identified the specimens housed at W as syntypes. Another specimen housed at K (K000838347) was from East Nepal, and thus we have excluded it from type materials. We have also examined the type specimens of *C. lahulensis* housed at CAL, which has the same morphological characters, such as panicle short with about 3–4 cm long and congested and awn straight and shortly or not exerted from the spikelet as found in the typical form of *C. lahulensis*. Since Grisebach (1868) examined the grass specimens which were housed at Kew herbarium for the description of *C. lahulensis*, the nomenclatural type should be from the Kew specimens. The presence of rhizomes, culms, ligules, inflorescences, and spikelets and its good preservation makes the specimen K000032374 suitable to choose as the lectotype; the same has been designated here lectotype for the name *C. lahulensis* following Art. 9.3 of the ICN (Turland et al. 2018).

2. *Calamagrostis scabrescens* Griseb., Nachr. Königl. Ges. Wiss. Georg-Augusts-Univ. 3: 79. (1868)

C. scabrescens var. *humilis* Griseb. Nachr. Königl. Ges. Wiss. Georg-Augusts-Univ. 3: 79 (1868). Lectotype (designated here):—INDIA. Sikkim, Lachen, 11,000 ft. [3352.8 m], [D. nr. 9], 3 July 1849, *J.D. Hooker s.n.* (K: K000838368, digital image!). (Image available at <https://plants.jstor.org/stable/viewer/10.5555/al.ap.specimen.k000032368>).

Lectotype (designated here).—INDIA. Sikkim, Lachen, 12,000 ft [3600 m], [*Deyeuxia scabrescens* Munr.], 3 August 1849, *J.D. Hooker s.n.* (K: K000838333, digital image!). (Image available at <https://plants.jstor.org/stable/viewer/10.5555/al.ap.specimen.k000838333>)

Note. Grisebach (1868) described *Calamagrostis scabrescens* with three varieties viz. (α) var. *scabrescens* Griseb., (β) var. *elatior* Griseb. and (γ) var. *humilis* Griseb. based on Hooker's gatherings which were housed in Kew Herbarium. The name *C. scabrescens* (\equiv var. *scabrescens*) was given for H. [Hooker's]: *D. [Deyeuxia] scabrescens* Munr., characterized by ciliated glumes along the margin. The var. *elatior* was proposed for H. [Hooker's]: *D. [Deyeuxia]* nr. 7, in which glumes are not ciliated along the margin, panicle sub-violet and about 30 cm long. Var. *humilis* was proposed for the H. [Hooker's]: *D. [Deyeuxia]* nr. 9, which differs from the above by having non ciliated glumes, panicle narrow and greenish, and ligule short, truncate or obtuse. Later, var. *humilis* was synonymized with *C. scabrescens*, while var. *elatior* raised to rank of species as *C. elatior* (Griseb.) A. Camus (Camus 1928; Bor 1960).

While searching for Hooker's specimen(s) belonging to the name *C. scabrescens* in various herbaria we traced six specimens, two at K (K000838333 and K000838334), one specimen at BM (BM000573477), CAL (0000004002), MPU (MPU027066),

and W (W1889-0241775) each. All the specimens were collected from the different localities of Sikkim Himalaya and have the annotation “H.: *Deyeuxia scabrescens* Munr.” The specimens at K, W, and CAL were verified as type materials by Beata Paszko. We have examined all the specimens including those which are housed in MPU and BM and determined as type material of *C. scabrescens*.

At CAL, the specimen, CAL0000002402, was stored under the type materials of *C. scabrescens*, without annotation of “*Deyeuxia scabrescens* Munr.” on the sheet. This specimen was identified as the type of *Deyeuxia filiformis* sensu. Hook. f., but later identified as *C. scabrescens* by Sunanda Bhattacharya, Botanical Survey of India. According to Paszko (2012a), it belongs to *Deyeuxia filiformis* sensu. Hook. f. of *C. lahulensis*-*C. scabrescens* complex. Therefore, we excluded it from the type materials.

Since Grisebach examined Hooker’s specimens housed at K for his new species *C. scabrescens*, the specimen with barcode K000838333 (left-hand side) is designated here as lectotype for the name *C. scabrescens* as per Art. 9.3 of the ICN (Turland et al. 2018), because of its good preservation with complete plants including inflorescence and spikelet and illustration of ciliated glumes on the sheet.

In addition to this, for the var. *humilis* we have traced another two specimens at K (K000838352 and K000032368) and one specimen at W (W0026817) which belong to the type materials of var. *humilis*. All of them bear the annotation “H.: D. nr. 9”, and thus should be considered as syntypes (Art. 9.6 of the ICN; Turland et al. 2018). The specimen with barcode K000838368 is designated here as the lectotype for the name *C. scabrescens* var. *humilis* following Art. 9.3 of the ICN (Turland et al. 2018), as the specimen is well-preserved and also morphologically complete with roots, inflorescences, and spikelets.

Acknowledgements

The authors would like to thank the Prof. Saroj K. Barik, Director of the CSIR-National Botanical Research Institute, Lucknow, India, for providing facilities and encouragement; Dr. Tariq Husain, former chief scientist of the CSIR-National Botanical Research Institute, India, for his consistent guidance; Principal Chief Conservator of Forests (Wildlife) and Sikkim Biodiversity Board of Sikkim for permitting access to the grass diversity of East Sikkim; Principal Chief Conservator of Forests (Wildlife), Dehradun, Uttarakhand for giving the permission to collect voucher specimens from Kedarnath Wildlife Sanctuary (KWLS) and Valley of Flower’s National Park (VoFNP). We also thank the curators of the following herbaria: BSD, CAL, DD, KASH and LWG for allowing the examination of herbarium specimens, and staff of the Herbaria BM, E, K and P for making specimens and/or their images/photos available. Institutional manuscript number provided by ethical committees: CSIR-NBRI_MS/2022/05/05.

This work is a part of DP & RK PhD Thesis, co-funded by CSIR, New Delhi, India; and was also supported by SERB New Delhi under CRG scheme (grant: CRG/2021/000720).

References

- Aswal BS, Mehrotra BN (1994) Flora of Lahul Spiti (A Cold Desert in North-West Himalaya). Bishen Singh Mahendra Pal Singh, Dehradun, India, 761 pp.
- Bor NL (1938) A list of the grasses of Assam. Indian Forest Records. Botany 1(3): 100.
- Bor NL (1940) Gramineae vol. 5. In: Kanjilal UN, Kanjilal PC, Das A (Eds) Flora of Assam. Assam Government Press, Shillong, 480 pp.
- Bor NL (1960) Grasses of Burma, Ceylon, India and Pakistan (excluding Bambuseae). Pergamon Press, London, 767 pp.
- Camus A (1928) Quelques Graminées nouvelles pour la flore de l'Indo-Chine. Bulletin de la Société Botanique de France 75(3): 552–555. <https://doi.org/10.1080/00378941.1928.10836296>
- Chowdhary HJ, Wadhwa BM (1984) Flora of Himachal Pradesh: Analysis. Vols. 1–3. Botanical Survey of India. Calcutta, 860 pp.
- Doğan M (1988) A scanning electron microscope survey of the lemma in *Phleum*, *Pseudophleum* and *Rhizocephalus* (Gramineae). Notes from the Royal Botanic Garden Edinburgh 45: 177–124.
- Gaur RD (1999) Flora of the District Garhwal Northwest Himalaya. Transmedia, Srinagar U.P., India.
- Grisebach A (1868) Ueber die Gramineen Hochasiens. Nachrichten von der Königlichen Gesellschaft der Wissenschaften und von der Georg-Augusts-Universität 1868: 61–93.
- Hijmans RJ, Guarino L, Cruz M, Rojas E (2001) Computer tools for spatial analysis of plant genetic resources data: 1 DIVA-GIS. Plant Genetic Resources Newsletter (Rome, Italy) 127: 15–19. https://www.diva-gis.org/docs/pgr127_15-19.pdf
- Hooker JD (1896) The flora of British India 7. L. Reeve & Co., London, 842 pp. <https://doi.org/10.5962/bhl.title.678>
- Howard TG, Saarela JM, Paszko B, Peterson PM, Werier D (2009) New records and a taxonomic review of *Calamagrostis perplexa* (Poaceae: Poaeae: Agrostidinae), a New York state endemic grass. Rhodora 111(946): 155–170. <https://doi.org/10.3119/08-5.1>
- Kandwal M, Gupta BK (2009) An update on grass flora of Uttarakhand. Indian Journal of Forestry 32(4): 657–668. <https://doi.org/10.54207/bsmps1000-2009-WM8B5Q>
- Kellogg EA, Abbott JR, Bawa KS, Gandhi KN, Kailash BR, Ganeshiah KN, Shrestha UB, Raven P (2020) Checklist of the Grasses of India. PhytoKeys 163: 1–560. <https://doi.org/10.3897/phytokeys.163.38393>
- Lu SL, Phillips SM (2006) *Calamagrostis*. In: Wu, ZY, PH Raven, DY Hong (Eds) Flora of China—Poaceae 22. Science Press, Beijing & Missouri Botanical Garden Press, St. Louis, 359–361. http://www.efloras.org/florataxon.aspx?flora_id=2&taxon_id=105009
- Noltie HJ (2000) Flora of Bhutan, 3 (2)—the Grasses of Bhutan. Royal Botanic Garden Edinburgh & Royal Government of Bhutan, Edinburgh, 883 pp.
- Paszko B (2012a) Taxonomic revision of *Calamagrostis filiformis*, *C. tripilifera* and their allies (Poaceae: Agrostidinae). Polish Botanical Journal 57: 335–346.
- Paszko B (2012b) *Calamagrostis gamblei* sp. nov. (Poaceae) from the Western Himalayas, NW India. Polish Botanical Journal 57: 327–334.

- Paszko B (2013) The identity of *Calamagrostis emodensis* var. *brevisetata* (Poaceae, Agrostidinae). Phytotaxa 118(2): 35–42. <https://doi.org/10.11646/phytotaxa.118.2.2>
- Paszko B (2014a) *Deyeuxia himalaica* (Poaceae, Agrostidinae): Taxonomy and its first record from Myanmar. Phytotaxa 156(5): 285–290. <https://doi.org/10.11646/phytotaxa.156.5.4>
- Paszko B (2014b) Typification of Grisebach's name *Calamagrostis emodensis* (Poaceae, Agrostidinae). Phytotaxa 172(3): 297–300. <https://doi.org/10.11646/phytotaxa.172.3.13>
- Paszko B (2015) First record of the Sino-Himalayan species *Deyeuxia himalaica* in Yunnan province, SW China, and three new combinations in *Calamagrostis* (Poaceae, Agrostidinae). Polish Botanical Journal 60(2): 141–145. <https://doi.org/10.1515/pbj-2015-0029>
- Paszko B (2016) *Calamagrostis nyingchiensis*, a new combination for *Deyeuxia nyingchiensis* (Poaceae, Agrostidinae), and its first record from Yunnan Province, SW China. Polish Botanical Journal 61(1): 53–57. <https://doi.org/10.1515/pbj-2016-0011>
- Paszko B, Chen WL, Szczepaniak M (2013) *Deyeuxia debilis* (Poaceae, Agrostidinae): Typification, taxonomy and update of the Chinese distribution. Phytotaxa 135(1): 1–10. <https://doi.org/10.11646/phytotaxa.135.1.1>
- Paszko B, Liu B, Ma HY (2017) *Calamagrostis* (Poaceae, Agrostidinae) in Vietnam. Polish Botanical Journal 62(2): 213–228. <https://doi.org/10.1515/pbj-2017-0013>
- Paszko B, Ma HY (2011) Taxonomic revision of the *Calamagrostis epigeios* complex with particular reference to China. Journal of Systematics and Evolution 49(5): 495–504. <https://doi.org/10.1111/j.1759-6831.2011.00140.x>
- Paszko B, Nobis M (2010) The hybrid origin of *Calamagrostis* × *gracilescens* (Poaceae) in Poland inferred from morphology and AFLP data. Acta Societatis Botanicorum Poloniae 79(1): 51–61. <https://doi.org/10.5586/asbp.2010.008>
- Paszko B, Soreng RJ (2013) Species delimitation and name application in *Deyeuxia abnormis*, *Agrostis zenkeri*, *A. pleiophylla* and related taxa (Poaceae: Agrostidinae). Phytotaxa 111(1): 1–26. <https://doi.org/10.11646/phytotaxa.111.1.1>
- Peterson PM, Soreng RJ, Romaschenko K, Barberá P, Quintanar A, Aedo C (2019) New combinations and new names in American *Cinnagrostis*, *Peyritschia*, and *Deschampsia*, and three new genera: *Greeneochloa*, *Laegaardia*, and *Paramochloa* (Poaceae). Phytoneuron 2019–39: 1–23.
- Prasad D, Tripathi S, Jaiswal S, Yadav R, Agnihotri P (2021) *Calamagrostis nandadeviensis* (Poaceae, Agrostidinae), a new grass species from India. Phytotaxa 505(2): 221–228. <https://doi.org/10.11646/phytotaxa.505.2.8>
- Pusalkar PK, Singh Dk (2012) Flora of Gangotri National Park, Western Himalaya, India. Kolkata: Botanical Survey of India, 708 pp.
- Saarela JM, Bull RD, Paradis MJ, Ebata SN, Peterson PM, Soreng RJ, Paszko B (2017) Molecular phylogenetics of cool-season grasses in the subtribes Agrostidinae, Anthoxanthinae, Aveninae, Brizinae, Calothecinae, Koeleriinae and Phalaridinae (Poaceae, Pooideae, Poaceae, Poaceae chloroplast group 1). PhytoKeys 87: 1–139. <https://doi.org/10.3897/phytokeys.87.12774>
- Singh G (1984) Nomenclatural notes on Asiatic *Calamagrostis* (Poaceae). Taxon 33: 94–95. <https://doi.org/10.2307/1222039>
- Shukla U (1996) The Grasses of North-Eastern India. Scientific Publishers, Jodhpur, 404 pp.

- Soreng RJ, Peterson PM, Zuloaga FO, Romaschenko K, Clark LG, Teisher JK, Gillespie LJ, Barberá P, Welker CAD, Kellogg EA, Li D, Davidse G (2022) A worldwide phylogenetic classification of the Poaceae (Gramineae) III: An update. *Journal of Systematics and Evolution* 60(3): 476–521. <https://doi.org/10.1111/jse.12847>
- Turland NJ, Wiersema JH, Barrie FR, Greuter W, Hawksworth DL, Herendeen PS, Knapp S, Kusber WH, Li DZ, Marhold K, May TW, McNeill J, Monro AM, Prado J, Price MJ, Smith GF (Eds) (2018) International Code of Nomenclature for Algae, Fungi, and Plants (Shenzhen Code) adopted by the Nineteenth International Botanical Congress Shenzhen, China, July 2017. *Regnum Vegetabile* 159. Koeltz Botanical Books, Glashütten. <https://doi.org/10.12705/Code.2018>

Appendix I

C. labulensis: INDIA. **Himachal Pradesh**, Kullu, Manali, near bridge of Marhi, 32.348869N, 77.223234E, 3372 m, 7 August 2019, *D Prasad, R Yadav & P Rajput 326811* (LWG!); near bridge of Marhi, 32.348869N, 77.223234E, 3390 m, *D Prasad, R Yadav & P Rajput 326811* (LWG! ?); 10 km before from Rohtang Pass, 32.35789N, 77.21695E, 3635 m, 5 August 2019, *D Prasad, R Yadav & P Rajput 316253, 316250* (LWG!); Marhi, 32.341507N, 77.216715E, 3260 m, 5 August 2019, *D Prasad, R Yadav & P Rajput 316299* (LWG!); Manali, 1 km after Gulaba check post, on the way to Marhi, 32.319782N, 77.20379E, 2944 m, *D Prasad, R Yadav & P Rajput 326868* (LWG!); **Uttarakhand**, Chamoli, Valley of Flowers National Park, 30.711627N, 79.595142E, 3250 m, 23 August 2019, *D Prasad, R Yadav, S Jaiswal & P Agnihotri 326641* (LWG!); Valley of Flowers National Park, 30.711627N, 79.595142E, 3380 m, 23 August 2019, *D Prasad, R Yadav, S Jaiswal & P Agnihotri 326642* (LWG!); Valley of Flowers National Park, 2 km after Ghanghria, 30.7114N, 79.5962E, 3137 m, 23 August 2019, *D Prasad, S Jaiswal, R Yadav & P Agnihotri 326698* (LWG!); Valley of Flowers National Park, 30.711627N, 79.595142E, 3380 m, 23 August 2019, *D Prasad, S Jaiswal, R Yadav & P Agnihotri 326642* (LWG!); Valley of Flowers of National Park, 30.729139N, 79.596606E, 3567 m, 23 August 2019, *D Prasad, R Yadav, S Jaiswal & P Agnihotri 326628* (LWG!); **Sikkim**, Gangtok, 13000ft [3962.4 m], [9 *Deyeuxia*], 6 September 1849, *JD Hooker s.n.* (K, K000838352); no specific locality, 15000ft [4572 m], 12 August 1913, *GH Gave 975* (CAL!); no specific locality, 14500 ft [4419.6 m], 7 October 1869, [*Trisetum?*], *sc.l. s.n.* (CAL!); no specific locality, 13000ft [3962.4 m], September 1885, *G King s.n.* (CAL!); no specific locality, 16000ft [4876.8 m], 19 August 1892, *GA Gammie s.n.* (CAL!); **Meghalaya**, Shillong, Kamegh, Sangetsar lake road, on hill slope, 19 August 1976, *PK Hajra 68327* (CAL!) (Seen rosette spikelet); Pankensaw, Nahula road, 16 August 1976, *PK Hajra 68551* (CAL!). **Nagaland**, Khasia, Khasi Hills, 13 September 1883, *CB Clarke 40446* (CAL!); **NEPAL**, no specific locality, alpine habitat, 12–16000ft [3657.6–4876.8 m], [10 *Deyeuxia*], *JD Hooker s.n.*, (K, K000838347); East Nepal, Chaika Pahar, 13000ft [3962.4 m], 25 September 1954, *Stainton, Sykes & Williams 4583* (CAL!); Chaika Pa-

har, 15000ft [4572 m], 22 September 1954, *Stainton, Sykes & Williams 4546* (CAL!); Gyang, Kyangsin, 13,500ft [4114.8 m], August 1949, *O. Polunin 1682* (CAL!); Sauwla Khola, 12,500ft [3810 m], 23 July 1954, *Stainton, Sykes & Williams 3606* (CAL!); **BHUTAN**. GaFoola, upper Phu Chu, 14500ft [4419.6], July 1949, *F Ludlow, G Sheriff & JH Hicks 16761* (CAL!); without specific locality, 12000ft [3657.6 m], *sc.l. s.n.*, (CAL! ac. no. 56614), (intermix with *C. scabrescens*).

C. nagarum: INDIA. Uttarakhand, Bageshwar, Pindari Valley, Dwali, 30.1783N, 79.9958E, 2800 m, 28 September 2021, *D Prasad, S Sharma, K Yadav & P Dey 339324* (LWG!); same locality, 28 September 2021, *D Prasad, S Sharma, K Yadav & P Dey 339325* (LWG!); Phurkia, 30.2192N, 80.0002E, 3300 m, 30 September 2021, *D Prasad, S Sharma, K Yadav & P Dey 339372* (LWG!); same locality, 30 September 2021, *D Prasad, S Sharma, K Yadav & P Dey 339374* (LWG); Dhakuri top, 30.072219N, 79.920847E, 2900 m, 21 August 2022, *Ravindra Kumar 342005* (LWG!).

C. scabrescens: INDIA. **Jammu & Kashmir**, Hazara, 26 July 1899, *Inaiyat s.n.* (CAL!); **Himachal Pradesh**, Kullu, Manali, 12 km after Marhi, on the way to Rohtang pass, 32.356838N, 77.222554E, 3013 m, 7 August 2019, *D Prasad, R Yadav & P Rajput 326829*, (LWG!); 12 km after Marhi, on the way to Rohtang Pass, 32.356858N, 77.222554E, 7 August 2019, *D Prasad, R Yadav & P Rajput 326842* (LWG!); Marhi, on the way to Rohtang pass, 32.3568N, 77.2225E, 3528 m, 7 August 2019, *D Prasad, R Yadav & P Rajput 326843* (LWG!); Marhi, 32.34150N, 77.216715E, 3260 m, 5 August 2019, *D Prasad, R Yadav & P Rajput 326888* (LWG!); on the way to Marhi, 32.3565N, 77.2225E, 3528 m, 7 August 2019, *D Prasad, R Yadav & P Rajput 314813* (LWG!); Kinnaur, Nachar, upper Bahshar, 10,000ft [3048 m], 25 September 1858, *PC Nanda 1802* (CAL!); **Uttarakhand**, Garhwal, Sri Nagar, University Campus, 30.226388N, 78.5022E, 587 m, 22 September 2018, *S Tripathi 315803*, (LWG!); Chamoli, Valley of Flowers National Park, 30.711895N, 79.595247E, 3428 m, 23 August 2019, *D Prasad, R Yadav, S Jaiswal & P Agnihotri 326657*, (LWG!); Valley of Flowers National Park, 30.711077N, 79.596004E, 3417 m, 23 August 2019, *D Prasad, R Yadav, S Jaiswal & P Agnihotri 326657*, (LWG!); Chamoli, Ghanghria, on the way to Himkund, 30.70594N, 79.598963E, 3224 m, 22 August 2019, *D Prasad, R Yadav, S Jaiswal & P Agnihotri 326717*, (LWG!); Valley of Flowers National Park, 30.711896N, 79.59524E, 3296 m, 23 August 2019, *D Prasad, R Yadav, S Jaiswal & P Agnihotri 326651* (LWG!); Ghanghria, on the way to Himkund, 30.705944N, 79.59896E, 3224 m, 22 August 2019, *D Prasad, R Yadav, S Jaiswal & P Agnihotri 326729* (LWG!); Valley of Flowers National Park, 30.7059N, 79.6022E, 3438 m, 23 August 2019, *D Prasad, R Yadav, S Jaiswal & P Agnihotri 326683*, (LWG!); Valley of Flowers of National Park, 30.712096N, 79.592776E, 3417 m, 23 August 2019, *D Prasad, R Yadav, S Jaiswal & P Agnihotri 326863* (LWG!); 2 km after Ghanghria, on the way to Valley of Flowers, 30.71114N, 79.596208E, 3137 m, 23 August 2019, *D Prasad, R Yadav, S Jaiswal & P Agnihotri 326691* (LWG!); Valley of Flowers National Park, 30.712096N, 79.592776E, 3417 m, 23 August 2019, *D Prasad, R Yadav, S Jaiswal & P Agnihotri 326745* (LWG!); Pithoragarh, Kali Valley, 12000ft [3657.6 m],

15 September 1884, *JF Duthie 3584* (CAL!); Kumaon, Bageshwar, Dwali, 10-11000ft [3048-3352.8 m], 6 August 1886, *JF Duthie 6216* (CAL!); Pithoragarh, Malpa, 2200-2500 m, 12 June 1960, *TA Rao 1178* (CAL!); Tehri-Garhwal, Rhudaghara, 10-11000ft [3048- 3352.8 m], *JF Duthie 145* (CAL!); Garhwal, Jaunsar, 8500ft [2590.8 m], September 1898, *JS Gamble 27238* (CAL!); Kumaon, 4,300 m, 10 August 1972, *CM Arora 49828* (LWG!); Pithoragarh, Kali Valley, 12-13000ft [3657.6-3962.4 m], 27 July 1888, *JF Duthie 6223* (CAL!); Kumaon, 14-15000ft [4267.2-4572 m], 31 August 1884, *JF Duthie 3538* (CAL!); Sansal-Nala, Killar Valley, 13-14000ft [3962.4-4267.2 m], 31 July 1893, *JF Duthie 13349* (CAL!); Teyum, Haya, 4300 m, 10 August 1972, *CM Arora 49826*, (CAL!); BhojPass, 3600 m, 8 September 1972, *S. cl, 69* (CAL!); **Sikkim**, Kupup-Chango road, 13300ft [4114.8 m], 10 October 1928, *NL Bor 487* (CAL!); without precise locality, 12000ft [3657.6 m], 27 July 1910, *WW Smith 3875* (CAL!); Gangtong, 13000ft [3962.4 m], 21 September 1926, *NL Bor 153* (CAL!); **West Bengal**, Darjeeling, 11917ft [3632.3 m], 27 June 1960, *AB Chaoudhary 33* (CAL!); Darjeeling, 12000ft [3657.6 m], *JS Gamble s.n.*, (CAL!); Meghalaya, Shillong, Kamegh, Sangetsvar-ZImithang road, 20 August 1976, *PK Hajra 68351* (CAL!). **North-East**, 3600 m, 19 September 1962, *B. Safui 1781*, (CAL!); BHUTAN, without precise locality, *Griffith 6599* (CAL!); NEPAL. Muktinath, on open slope, 12,500ft [3810 m], 26 July 1954, *Stainton, Sykes & Williams 1429* (CAL!); Near Tara-kot, 10,000 m [3048 m], 10 July 1990, *O Polunin, WR Sykes & LHJ Williams 2426* (CAL!); North of Muktinath, Damoda Kund, 14,000ft [4267.2 m], 30 July 1954, *Stainton, Sykes & William 2102, 7371* (CAL!).

Supplementary material I

Quantitative data of morphological characters and elevation data of *Calamagrostis labulensis*, *C. nagarum*, and *C. scabrescens*

Author: Dileshwar Prasad

Data type: table

Explanation note: Morphological and Elevation (m).

Copyright notice: This dataset is made available under the Open Database License (<http://opendatacommons.org/licenses/odbl/1.0/>). The Open Database License (ODbL) is a license agreement intended to allow users to freely share, modify, and use this Dataset while maintaining this same freedom for others, provided that the original source and author(s) are credited.

Link: <https://doi.org/10.3897/phytokeys.212.89253.suppl1>

